Transcriptome analysis of adult neural stem cells and functional analysis of novel candidate genes TSP-4 and Uhrf1

PhD Thesis

Submitted to Graduate School of Systemic Neurosciences of the Ludwig-Maximilians-University Munich

Prepared in the group of Prof. Dr. Magdalena Götz at the Helmholtz Zentrum Munchen / Institute for Stem Cell Research

Efil Bayam

2014

Supervisor: Prof. Dr. Magdalena Götz

Second expertappraiser: Prof. Dr. Heinrich Leonhardt

Date of oral defense: 11.11.2014

For my grandmother

Acknowledgements

First and foremost I would like to deeply thank **Magdalena Götz** for giving me the opportunity to work in her laboratory. I am very grateful for her constant assistance as this work would not have been accomplished without her support. I thank her for many useful comments, all the time she spend to discuss my project and for creating a great scientific environment with outstanding scientists, intellectual exchange and extraordinary technical possibilities has been all been a great motivation throughout my work.

Very special thanks to **Silvia Cappello, Pia Johansson, Tessa Walcher, Ruth Beckervordersandforth-Bonk** and **Filippo Calzolari**, not only for the very fruitful scientific discussions but also for being very nice friends. I furthermore want to thank **Pratibha Tripathi** who carried out the screen that was the starting point of this study and **Vidya Ramesh** who took over the project to analyze my findings further in detail. I also thank **Dilek Colak** and **Marcos Costa** for the support to get established in the beginning of my time both in the lab and in Munich. Thanks to **Alex Lepier** for help with virus production, to **Sergio Gascon** for help with cloning, to **Felipe Ortega de la O** for help with the viral injections, to **Gregor Pilz** for help with all confocal problems and to **Christiane Simon** for sharing her injury sections with me. I am also truly glad to **Benedikt Berninger, Judith Fischer-Sternjak** and **Sven Falk** for being always available whenever I had something to discuss. Many thanks to **Angelika Waiser**, not only for providing great technical help but also for her "mother-like" smile, and also to **Andrea Steiner-Mezzadri, Emily Violette Baumgart** and **Detlef Franzen** for their excellent technical support. I want to also thank **Elsa Melo, Donna Thomson** and **Lana Polero** for all their help with administrative issues.

I want to say very special and deep thanks to **Engin Gumusel, Teoman Ogan, Levent Kent, Mehmet Can Isik, Alphan Savaryan, Esra Karakose, Mehtap Bakir, Ferhat Bakir** and **Konstantinos Kokkaliaris** without whom for sure life in Munich would not have been the same. Thanks for sharing all the happy and hard moments of my life in Munich and making Munich "home" for me.

Table of Contents

1. Abstract

Although the initial discovery of lifelong neurogenesis in the subependymal zone (SEZ) of the lateral ventricle and the subgranular zone (SGZ) of the hippocampus has been repeatedly confirmed in many species including humans and several following studies showed alterations in adult neurogenesis is a common pathological feature in several human neurodegenerative and psychiatric diseases, lack of full understanding of the mechanisms that allow neurogenesis only in these two restricted brain regions, hampered the further clinical applications of these endogenous stem cells. As unveiling the mechanisms that regulate the lineage progression from aNSCs to newborn neurons require direct analysis of aNSCs and their progeny, our lab developed a FACS based protocol for improved purification of aNSCs from the SEZ of the adult mouse brain. This approach not only allowed us to make a genome wide expression analysis of aNSCs, their progeny and ependymal cells from SEZ and non-neurogenic astrocytes from diencephalon but also revealed many genes that are differentially expressed in different populations. The major aim of this thesis was to confirm this microarray data and then to analyze some of the selected novel candidate genes functionally.

After successful confirmation of the reliability of the microarray analysis I selected 2 candidates for functional analysis. One, the extracellular matrix protein Thrombospondin 4 that is specifically highly enriched in the aNSCs, the other, the epigenetic factor Uhrf1 whose expression levels are elevated in the aNSCs and further increase in the neurogenic progeny. While Thrombospondin 4 analysis did not reveal functional effects on neurogenesis, supposedly due to Thrombospondin 4 having a function in different aspects on neurogenesis than we analyzed , conditional deletion of Uhrf1 in aNSCs using the GLAST^{CreERT2} line showed profound defects in neurogenesis. Detailed analysis revealed Uhrf1 as a critical regulator of adult neurogenesis in both regions where neurogenesis continues in the adult murine brain. Interesting, although in both regions loss of Uhrf1 resulted in decreased proliferation and decreased number of newborn neurons, additional defects in neuronal maturation or survival were observed in the region of the hippocampus where neurogenesis continues. These results therefore demonstrate that Uhrf1 has common and region-specific functions in adult neurogenesis.

As adult and embryonic neurogenesis has been shown to share many common hallmarks, in the second part of my thesis I extended the expression and functional analysis to neurogenesis during development. I showed that Uhrf1 is expressed in the apical progenitors of the cerebral cortex, the neural stem cells, but then is down regulated in transit amplifying progenitors and newborn neurons. Using conditional deletion at the onset of neurogenesis in the embryonic dorsal telencephalon I showed that Uhrf1 is not critical for proliferation at this stage in contrast to its role in adult neurogenesis. Rather it regulates maintenance of NSCs at the apical surface and its absence also results in massive cell death culminating in neuronal degeneration at postnatal stages. Genome-wide transcriptome analysis of control and Uhrf1 knock-out cortices shed some light on the possible molecular cause for this in derepression of Uhrf1 target genes.

In conclusion, my data suggest that, the genome wide expression analysis of prospectively isolated aNSCs, their progeny, ependymal cells and non-neurogenic diencephalic astrocytes enables identification of novel genes regulating neurogenesis and one such gene, Uhrf1, that was shown to be differentially expressed in this microarray, is a critical regulator of both adult and embryonic neurogenesis.

2. Introduction

2.1 Early Brain Development and Regionalization of the Telencephalon

During gastrulation three primary germ layers: endoderm, mesoderm and ectoderm that give rise to all of the organs are established. By a process called neuronal induction ectodermal cells that are lying above the mesoderm derivative notochord change their shape, elongate and become the neural plate in response to Bone Morphogenetic Protein (BMP) antagonists noggin, chordin and follistatin and molecules with anti-Wnt (Wingless-Type MMTV Integration Site Family) activity like cerberus, dickkopf and frzb secreted from the notochord (De Robertis, Larraín, Oelgeschläger, & Wessely, 2000; Levine & Brivanlou, 2007; Patthey & Gunhaga, 2014). The remainder of the ectoderm gives rise to the epidermis. Then by a series of events that involve cell shape changes and cell movements, the neural plate folds outward and forms the neural groove. The walls of the neural groove or the so called neural folds are brought together and form the neural tube in a process called neurulation. During this process some cells of the neural folds delaminate and form the neural crest cells which later generate the Peripheral Nervous System (PNS) and parts of the craniofacial skeleton whereas the neural tube generates the Central Nervous System (CNS) (Gilbert & Singer, 2006) (Fig.1A). During neurulation, closure of the neural tube does not take place simultaneously throughout the whole neural tube but it is rather well advanced at the rostral regions when the caudal regions are still at the gastrulation stage. So before the neural tube closes at the posterior end, at the anterior part of the neural tube which will form the brain, three primary vesicles called the prosencephalon (forebrain), mesencephalon (midbrain) and rhombencephalon (hindbrain) form by the actions of local organizers (Wurst and Bally-Cuif, 2001; Gilbert & Singer, 2006). As the posterior end of the neural tube which will form the spinal cord closes, two secondary vesicles balloon from each side of the forebrain and form the optic vesicle (Fig.1B). The prosencephalon is then further subdivided into telencephalon which will form the cerebrum, olfactory bulbs and hippocampus and diencephalon which will form the thalamus, hypothalamus and retina. The rhombencephalon further subdivides as well, forming the metencephalon that will form the cerebellum and pons and myelencephalon that will form medulla oblongata. Caudal to myelencephalon, the neural tube stays as a straight structure forming the spinal cord (Gilbert & Singer, 2000) (Fig.1B).
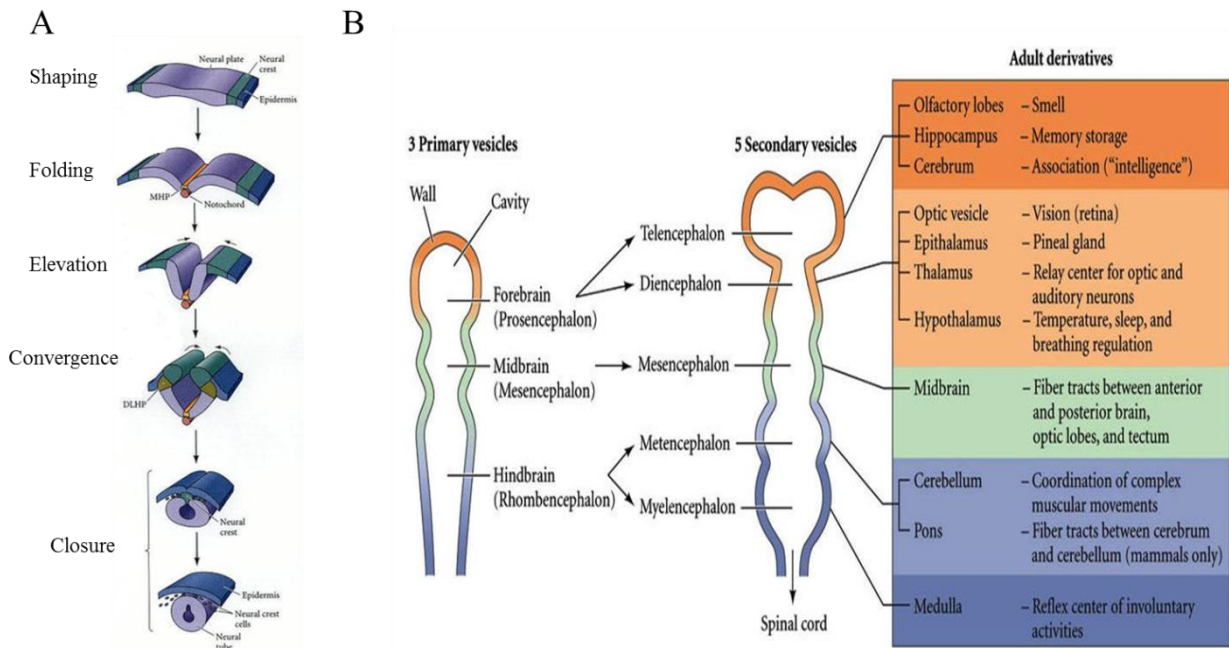
Figure 1: Schematic depiction of key steps in early brain development and the formation of primary and secondary brain vesicles (Modified from Nicholls, 2011).

(A) Cells of the neural plate can be distinguished as elongated cells in the dorsal region of the ectoderm. Folding begins as the medial neural hinge point (MHP) cells anchor to notochord and change their shape, while the presumptive epidermal cells move towards the center. The neural folds are elevated as presumptive epidermis continues to move toward the dorsal midline. Convergence of the neural folds occurs as the dorsolateral hinge point (DLHP) cells become wedge-shaped and epidermal cells push toward the center. The neural folds are brought into contact with one another, and the neural crest cells link the neural tube with the epidermis. The neural crest cells then disperse, leaving the neural tube separate from the epidermis. **(B)**The first structure to appear is the division of the embryonic brain into three primary brain vesicles, known as the forebrain (prosencephalon), midbrain (mesencephalon), and hindbrain (rhombencephalon). In the next step the brain becomes further subdivided: the forebrain generates the paired telencephalic vesicles and the diencephalon, while the rhombencephalon splits into the metencephalon and the myelencephalon.

In addition to being patterned in an anterior to posterior axis, the neural tube is also patterned in the dorsal to ventral (DV) and medial to lateral (ML) axis. Along the DV axis, the telencephalon is subdivided into pallium (cerebral cortex) that is located dorsally and subpallium (ganglionic eminences) that is located ventrally, with the pallialsubpallial boundary. The pallium is then further subdivided into medial pallium (MP), dorsal pallium (DP), lateral pallium (LP), and ventral pallium (VP), which will give rise to the archicortex (including the hippocampus), the neocortex, the olfactory/piriform cortex, and the claustroamygdaloid complex respectively (Puelles et al., 2000; Yun, Potter, & Rubenstein, 2001). The ganglionic eminences is also further subdivided into lateral- , medial- , and caudal-ganglionic eminences (LGE , MGE , CGE respectively) which will give rise to striatum and basal ganglia (Puelles et al., 2000). This patterning is mediated by coordinated actions of signaling molecules released from the patterning centers (Hoch, Rubenstein, & Pleasure, 2009; Rubenstein, 2011; H. Takahashi & Liu, 2006) (Fig.2A). Sonic Hedgehog (Shh) secreted from the prechordal plate mesoderm is responsible for ventralization of the telencephalon, and temporal changes of Shh competence and different levels of Retinoic Acid (RA) play roles in patterning of the ventral telencephalon along the ML axis (Hoch et al., 2009; Rubenstein, 2011; H. Takahashi & Liu, 2006). On the other hand, Wnts and BMPs secreted from the cortical hem, Fibroblast Growth Factor 7 (FGF7), Epidermal Growth Factor (EGF), Transforming Growth Factor-Alpha (TGF-alpha) and Neuregulins secreted from anti-hem and FGF8 and FGF17 secreted from the anterior neural ridge are responsible for dorsalization of telencephalon and its patterning along the ML axis (Hoch et al., 2009; Rubenstein, 2011; H. Takahashi & Liu, 2006). These different concentration gradients of secreted molecules are then translated into transcription factor codes that delineate different domains along the DV and ML axis of the telencephalon (Fig.2B). For example in the dorsal telencephalon, transcription factors Paired box gene 6 (Pax6), Neurogenin1/2 (Ngn1/2), and Empty spiracles homeobox 1/2 (Emx1/2) are important for inhibition of the ventral identity (Fode et al., 2000; Mallamaci, Muzio, Chan, Parnavelas, & Boncinelli, 2000; Stoykova, Treichel, Hallonet, & Gruss, 2000; Yoshida et al., 1997), whereas LIM homeobox 2 (Lhx2) is important to repress the spread of medial pallial fate (Bulchand, Grove, Porter, & Tole, 2001). However the boundaries between different cortical areas of the dorsal telencephalon are not always defined by the discrete gene expression patterns but rather with graded expression of transcription factors such that Pax6 is expressed in a rostral high to caudal low and laterally high to

medially low gradient whereas Emx2 shows just the opposing pattern (K M Bishop, 2000; Kathie M Bishop, Rubenstein, & O'Leary, 2002; Muzio & Mallamaci, 2003).
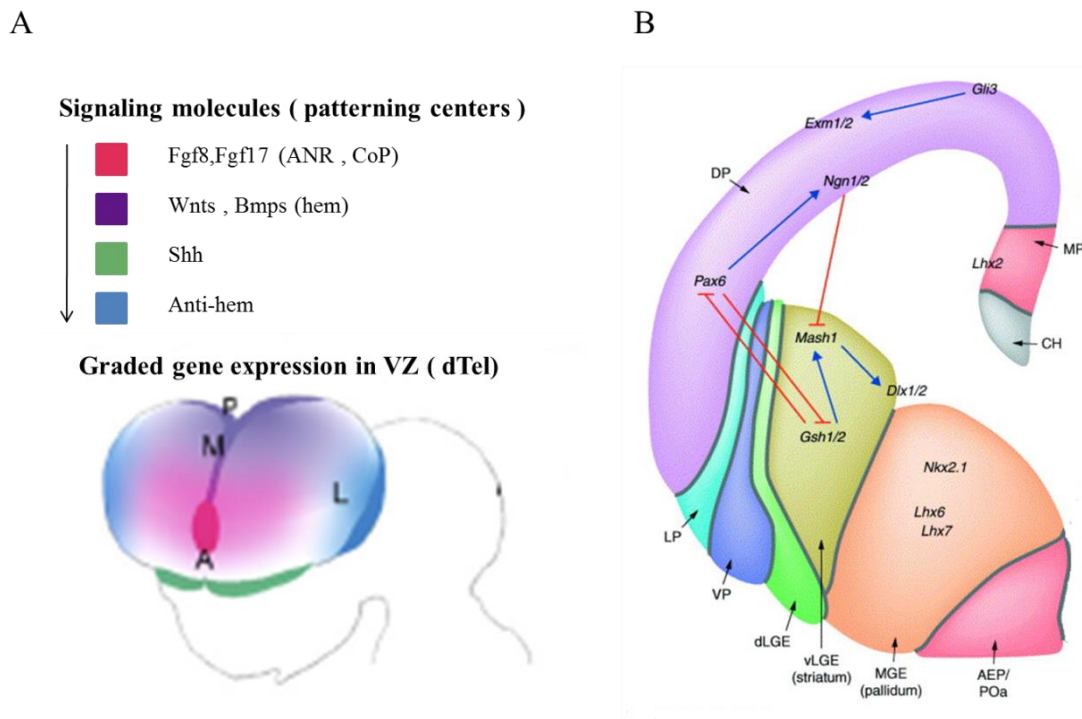
Figure 2: Schematic depiction of the main patterning centers and gradients of transcription along the telencephalon formed by signaling from the patterning centers.

(A) The initial, tangential axial gradients of transcription factors (TFs) in the ventricular zone (VZ) are likely established by signaling molecules or morphogens (or both) secreted from localized patterning centers. This figure illustrates four such patterning centers. *Fgf8* and *Fgf17* are secreted from the anterior patterning center, the anterior neural ridge (ANR), which later becomes the commissural plate (CoP). Wnts and Bmps are secreted from the posterior-medial-located cortical hem. Sonic hedgehog (Shh) is secreted from a ventral domain. In addition, a lateral putative patterning center, termed the anti-hem, also might contribute to graded TF expression. (Modified from O'Leary et al., 2007)**(B)** Schematic drawing of a coronal section through the telencephalon of an E12.5 mouse brain, showing dorsal and ventral subdomains, as defined by their unique patterns of gene expression. The dorsal telencephalon shows high expression levels of Pax6, Ngn1/2, Emx1, Emx2 and Lhx2. In contrast, high expression of Mash1, Gsh1/2 (Gsx1/2), Dlx1/2/5/6 is found in the lateral ganglionic eminence (LGE) of the ventral telencephalon whereas Lhx6, Lhx7 and Nkx2.1 are only found in the medial ganglionic eminence (MGE). The dorsal telencephalon can be further subdivided into different domains: medial pallium (MP), dorsal pallium (DP), lateral pallium (LP) and ventral pallium (VP). The LGE can be further subdivided into the dorsal LGE (dLGE) and ventral LGE (vLGE) compartments on the basis of higher levels of Pax6,

Gsx2, Mash1 and Dlx2 in the dLGE and exclusive expression of Gsx1 in the vLGE (Taken from Schuurmans & Guillemot, 2002).

On the other hand, in the ventral telencephalon NK2 homeobox 1 (Nkx2.1), Lhx6, Lhx7 and Lhx8 are important for specification of MGE and inhibition of LGE fates (Grigoriou, Tucker, Sharpe, & Pachnis, 1998; Mori et al., 2004; Sussel, Marin, Kimura, & Rubenstein, 1999; Zhao et al., 2003) whereas higher levels of Pax6, GS homeobox 2 (Gsx2), Mammalian achaete scute homolog 1 (Mash1) and Distal-less homeobox 2 (Dlx2) differentiate dLGE progenitors from the vLGE progenitors that express Gsx1(Corbin, Gaiano, Machold, Langston, & Fishell, 2000; Fode et al., 2000; Stoykova et al., 2000; Toresson, Potter, & Campbell, 2000).

2.2. Neural Stem and Progenitor Cells of Cerebral Cortex

Before the onset of neurogenesis, the neural plate and the neural tube is composed of a single layer of cells called "neuroepithelial (NE) cells" that divide symmetrically to increase their own pool and thereby increase the ventricular surface (Götz & Huttner, 2005; Murciano, Zamora, López-Sánchez, & Frade, 2002). These cells span the whole wall of the neural tube from basal (pial) to apical (ventricular) surface where they are attached to neighboring cells by adherens junctions (AJ), tight junctions (TJ) and gap junctions (GJ) (Aaku-Saraste, Hellwig, & Huttner, 1996; Aström & Webster, 1991; Götz & Huttner, 2005; Shoukimas & Hinds, 1978). They show the typical polarized nature of epithelial cells and express some proteins such as Prominin-1 (CD133) and receptors for basal lamina constituents such as integrin α6 selectively in the apical and basal plasma membranes respectively (Weigmann, Corbeil, Hellwig, & Huttner, 1997; Wodarz & Huttner, 2003). Although the neuroepithelium is a single cell layered structure, it looks stratified due to the characteristic movement of the nucleus, known as interkinetic nuclear migration (INM) from basal to apical positions as the cell cycle progresses from G1 to M phase (Murciano et al., 2002; T. Takahashi, Nowakowski, & Caviness, 1996). These earliest neural precursors switch their mode of division over time from symmetric proliferative to asymmetric and produce the first neurons that are destined to settle in the preplate (Casanova & Trippe, 2006; Pinto & Götz, 2007) (Fig.3). At around E9-10 in the mouse, NE cells down regulate some of their epithelial features (for example tight junctions) (Aaku-Saraste et al., 1996; Aaku-Saraste, Oback, Hellwig, & Huttner, 1997) and

progressively gain some astroglial hallmarks giving rise to a new but related cell type namely radial glia (RG) that then continuously replace the former (Campbell & Götz, 2002; Götz, 2003; A. R. Kriegstein & Götz, 2003). While gaining some astroglial features these cells do not lose all epithelial features, and like their former counterparts, RG cells are highly polarized and keep contact with both apical and the pial surfaces having a much longer basal process due to progressive thickening of the cortex (Aaku-Saraste et al., 1996; Aström & Webster, 1991; Møllgård, Balslev, Lauritzen, & Saunders, 1987; Shoukimas & Hinds, 1978) (Fig.3). These cells also maintain the expression of some intermediate filaments like Nestin and its derivative, the antigen recognized by the monoclonal antibody radial glial cell marker 2 (RC2)(Pinto & Götz, 2007). They also maintain the apical localization of prominin-1, junction proteins and proteins associated with the apical cell cortex like Par3, Par6 and aPKC and as well maintain the basal lamina contact (Aaku-Saraste et al., 1996; Halfter, Dong, Yip, Willem, & Mayer, 2002; Hartfuss, Galli, Heins, & Götz, 2001; Mori, Buffo, & Götz, 2005; Weigmann et al., 1997; Wodarz & Huttner, 2003). Although RG cells also show INM like the NE cells, their cell body does not span the whole cortical wall but instead remains in the VZ where the cell bodies of most progenitor cells are found (Götz & Huttner, 2005). However unlike the NE cells, as their name implies, RG cells also show several astroglial features like acquisition of glycogen granules (Brückner & Biesold, 1981; Gadisseux & Evrard, 1985), formation of specialized contacts with endothelial cells of the developing cerebral vasculature (T. Takahashi, Misson, & Caviness, 1990) and expression of glial markers such as the astrocyte specific glutamate transporter (GLAST), brain lipid binding protein (BLBP), Ca binding protein S100β , and intermediate filaments Vimentin and glial fibrillary acidic protein (GFAP) (Campbell & Götz, 2002).

These cells can also divide symmetrically to increase their own progenitor pool but around mid-neurogenesis (E13.5), the prominent mode of division of RG cells has already switched from symmetric self-renewal divisions (30%) to asymmetric neurogenic divisions generating daughter neurons either directly or indirectly (Huttner & Kosodo, 2005; Konno et al., 2008; Noctor, Martínez-Cerdeño, Ivic & Kriegstein, 2004). Although a small percentage of cortical glutamatergic neurons is generated directly from RG cells, most of them are generated via generation of a secondary progenitor the so called intermediate (basal) progenitor (IP or BP) (Haubensak, Attardo, Denk, & Huttner, 2004; Huttner & Kosodo, 2005; T Miyata, Kawaguchi, Okano, & Ogawa, 2001; Takaki Miyata et al., 2004; S C Noctor, Flint,

Weissman, Dammerman, & Kriegstein, 2001; Stephen C Noctor et al., 2004; Stephen C Noctor, Martínez-Cerdeño, & Kriegstein, 2007) (Fig.3).

IPs, generated from RG cells by apical mitosis, migrate upwards to undergo S phase and then retract their both apical and basal processes and undergo M phase in this more basal position forming a second proliferative layer, the so called subventricular zone (SVZ) (Takaki Miyata et al., 2004; Stephen C Noctor et al., 2004). As shown by time lapse imaging studies around 90% of IPs undergo symmetric terminal divisions generating two neurons and only 10% undergo symmetric proliferative divisions generating two IPs which then give rise to four neurons (Haubensak et al., 2004; Takaki Miyata et al., 2004; Stephen C Noctor et al., 2004, 2007).
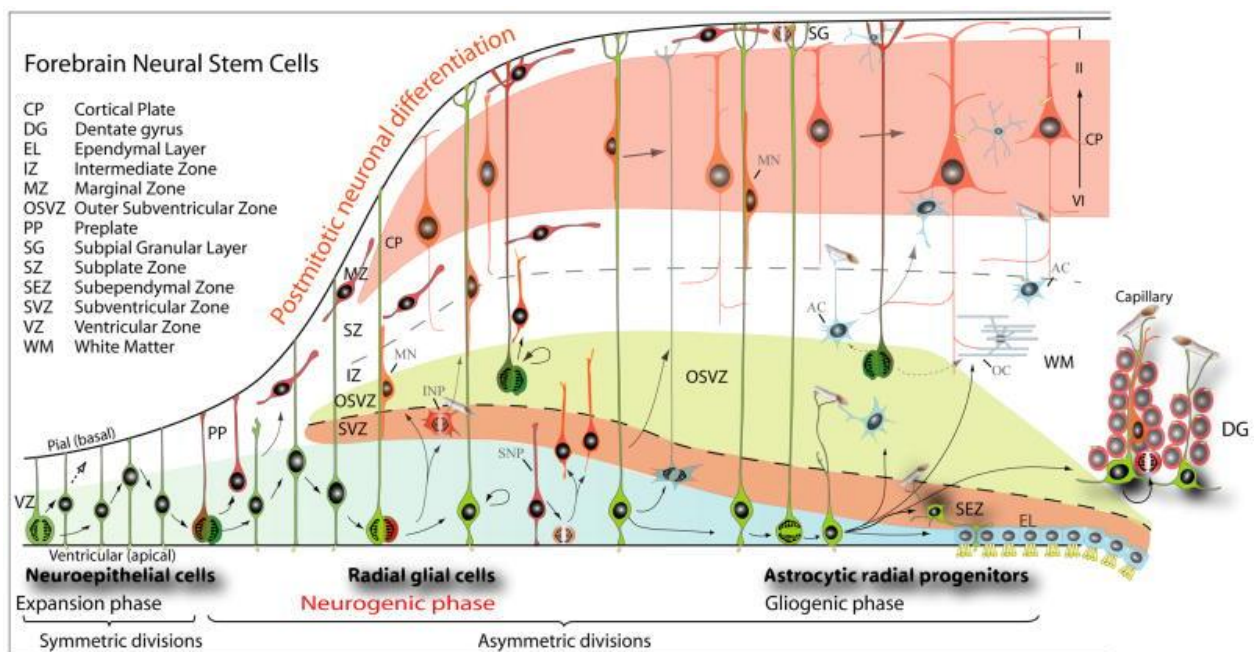
Figure 3: Schema of the heterogeneity of stem and progenitor cells in the mammalian forebrain (Modified from Breunig, Haydar, & Rakic, 2011).

Initially, neuroepithelial cells constitute the major class of neural stem cells. During the neurogenic phase, these cells give rise to radial glia (RG) which can self-renew or generate neurons directly or can generate classes of intermediate types such as intermediate neural progenitors (INP) which divide in the SVZ, short neural progenitors (SNP) which contact and divide at the VZ surface or outer radial glia (oRG) which contact only the basal surface and divide above the SVZ. RG transition into neurogenic SEZ astrocytes and SGZ radial astrocytes during the gliogenic phase. In addition, radial glia can give rise to ependymal (EL) cells, oligodendrocytes (OC) and astrocytes (AC) pre- and peri-natally and in the adjacent dentate gyrus (DG) into prolonged postnatal stage.

In addition to being identified by the location where they undergo mitosis, IPs can also be characterized by their specific gene expression pattern since unlike NE cells or RG cells, they do not express Pax6, but rather express T-box brain 2 (Tbr2), Ngn2, Cut-Like homeobox 1 (Cux1), Cut-Like homeobox 2 (Cux2) and Subventricular expressed transcript 1 (Svet1) (A. Kriegstein & Alvarez-Buylla, 2009).

Although in rodents IPs constitute 90 % of the secondary progenitors generated from the RG cells, recently two new types of progenitors namely short neural progenitors (SNPs) and outer radial glial (oRG) cells have been identified. Like RG cells, SNPs are found in the VZ, havean apical process and express Pax6. However SNPs can be distinguished from the RG cells by having a short basal process that is retracted during mitosis and by the expression of the Ta1 promoter. Moreover genetic fate mapping studies showed that SNPs do not self-renew and generate neurons directly rather than via generation of IPs (Fietz & Huttner, 2011; Gal et al., 2006; Stancik, Navarro-Quiroga, Sellke, & Haydar, 2010). On the other hand, oRG cells that are located in the vicinity of SVZ are unipolar cells having a radially oriented basal process, express Pax6 and undergo symmetric self-renewing divisions (Shitamukai, Konno, & Matsuzaki, 2011; X. Wang, Tsai, LaMonica, & Kriegstein, 2011). Taken together, although NE cells, RG cells, SNPs and oRG cells all contribute to production of neurons, IPs are the main source of neuronal output in the developing murine cortex.

At the end of neurogenesis, RG cells retract their processes and differentiate into post-mitotic ependymal cells and astrocytes some of which keep their neurogenic potential and serve as adult neural stem cells (aNSCs).

2.3 Layered Organization of Cerebral Cortex

The neocortex, which is the biggest part of the cerebral cortex, is a highly organized, 6 layered structure containing different types of neurons and glia. Of the two main classes of cortical neurons, GABAergic interneurons are generated from progenitors in the ventral telencephalon, migrate long distances to their final locations in the cerebral cortex and make local connections, whereas the glutamatergic projection neurons are generated from progenitors within the cerebral cortex, populate distinct cortical layers depending on the time they are generated and acquire distinct morphological features, gene expression profiles and projection patterns according to the layer they settle in (Molyneaux et al.,2007).

The earliest born projection neurons, generated directly from NE cells, appear around E10.5 in mouse cerebral cortex and together with the Cajal Retzius cells, generated from the cortical hem, form a transient structure called preplate underlying the meninges and basement membrane at the basal site of the neuroepithelium (Casanova & Trippe, 2006; Molyneaux et al., 2007). Then with the replacement of NE cells by RG, at around E12.5, newly generated neurons split the preplate into marginal zone (Layer I) and subplate and form the layers II-VI of cortical plate (Molyneaux et al., 2007). Cortical plate neurons settle in different cortical layers in an inside out manner with the latest generated neurons forming the most superficial layers such that the neurons that are born around E12.5 and E13.5 form the deep layers 6 and 5 respectively and the neurons born around E14.5 and E15.5 form the upper layers 4 and 2/3 respectively (Molyneaux et al., 2007) (Fig.4A). In addition to being generated at different time points, projection neurons settled at different layers also express different complements of genes. For example upper layers II, III and IV express Cux1, Cux2 and Svet1 in common whereas Rgs8, Cart and RorB are expressed specifically by layers II, III and IV respectively. Likewise, although at different levels, neurons in deep layers V and VI express Ctip2 and Fezf2 in common and can be differentiated by the expression of Er81 and Foxp2 in layers V and VI respectively (Molyneaux et al., 2007).

Moreover as already depicted in the drawings of Ramon y Cajal in 1899, the projection neurons that settle in different cortical layers also have different morphologies and different projection patterns (Fig.4B). Layer I, also called the molecular layer contains mainly the apical dendrites of the pyramidal cells from lower layers and has very few scattered neurons that are Cajal Retzius cells and other types of interneurons. Layer II and III, also called external granular and external pyramidal layers respectively, contains small, densely packed pyramidal neurons and medium sized pyramidal neurons respectively and are the main origin and termination of intercortical connections respectively. Layer IV, also called the internal granular layer, contains many spiny stellate (excitatory) interneurons as well as pyramidal neurons and receives the thalamocortical connections. Layer V and VI also called the internal pyramidal layer and multiform layer respectively, contain the largest pyramidal neurons forming long distance projections and send axons to the basal ganglia, brain stem and spinal cord and to the thalamus respectively (Molyneaux et al., 2007).
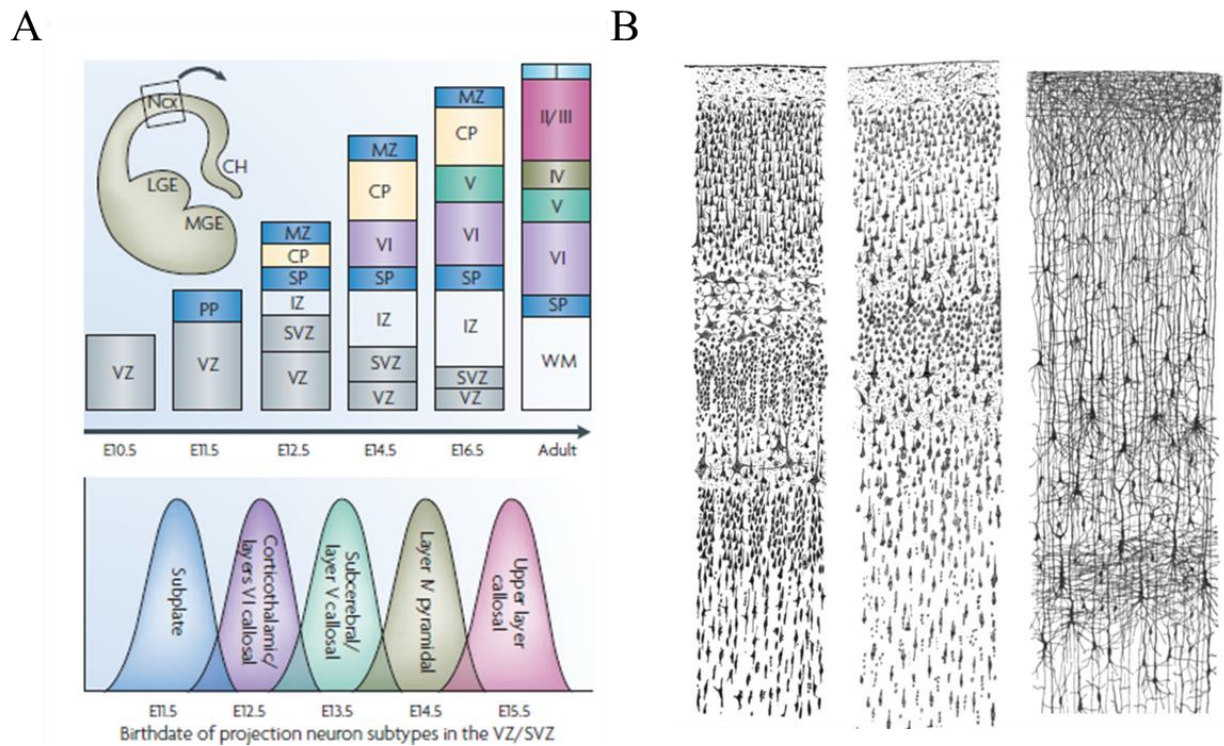
Figure 4: Six layered structure of the cortex

(A) Schematic drawings depicting how progenitors residing in the VZ and SVZ in mice produce projection neurons in an 'inside-out' fashion. The earliest born neurons form the preplate (PP), which is later split into the more superficial marginal zone (MZ) and the deeply located subplate (SP). The cortical plate (CP), which will give rise to the multilayered neocortex, develops in between these two layers, such that later born neurons arriving at the cortical plate migrate past earlier born neurons. Different classes of projection neuron are born in overlapping temporal waves. All times listed are approximations given the neurogenic gradients that exist across the cortex, where caudomedial neurogenesis lags behind rostro-lateral neurogenesis. CH, cortical hem; E, embryonic day; Ncx, neocortex; IZ, intermediate zone; LGE, lateral ganglionic eminence; MGE, medial ganglionic eminence; SVZ, subventricular zone; VZ, ventricular zone; WM, white matter (Taken from Molyneaux et al., 2007).**(B)**Layers of human cerebral cortex drawn by Ramon y Cajal.

2.4 History of adult neurogenesis

Although in early 1900s, neurogenesis was thought to occur only in embryonic and perinatal stages, with the advancements in autoradiographic labeling techniques, in the 1960s, Altman was able to present the first scientific evidence for ongoing postnatal neurogenesis in the rat brain (Altman, 1963, 1969). By combining injections of 3H – thymidine which is incorporated into the DNA during replication with morphological analysis, he could define the dentate gyrus (DG) of the hippocampus and the lateral ventricles as mitotically active regions that contain undifferentiated cells, which give rise to granule neurons in the DG and short axoned neurons in the olfactory bulb (OB) (Altman & Das, 1965; Altman, 1963, 1969). Since Altman's observation of newborn neurons depended on morphological identification of neurons but lacked immunohistochemical evidence due to lack of marker proteins at this time, many scientists claimed that these proliferating cells in the lateral ventricles were glial precursors and yet many other studies suggested that 3H – thymidine incorporation observed was mainly due to cell death or DNA repair (Crespel, Baldy-Moulinier, & Lerner Natoli, 2004; Gross, 2000). As Altman's reports of ongoing neurogenesis throughout life, contradicted the belief of the time, they were largely ignored until 1992 when two labs could isolate EGF responsive cells from the periventricular area of the adult mammalian brain that fulfill the stem cell properties: self-renewal and multipotentiality (Reynolds & Weiss, 1992; Richards, Kilpatrick, & Bartlett, 1992). This in vitro evidence was followed by in vivo studies that used new lineage tracing methods like administration of a thymidine analog bromodeoxyuridine (BrdU), retroviral vector labeling or transplantation in combination with immunofluorescence and confocal microscopy and showed presence of two germinal neurogenic zones in the adult rodent brain: subependymal zone (SEZ) of the lateral ventricles and subgranular zone (SGZ) of the hippocampus (Corotto, Henegar, & Maruniak, 1993; Kuhn, Dickinson-Anson, & Gage, 1996; Lois & Alvarez-Buylla, 1994; Luskin, 1993). These findings were then also further substantiated by studies that use Cre mediated fate mapping and electron microscopy (EM) to characterize the precise nature and character of adult neural stem cells (aNSCs) and their progeny (DeCarolis et al., 2013; Imayoshi et al., 2008; Kohwi et al., 2007; Ninkovic, Mori, & Götz, 2007; Ventura & Goldman, 2007; Willaime-Morawek et al., 2006; Young, Fogarty, Kessaris, & Richardson, 2007).

Although whether adult neurogenesis occurs in areas of mammalian brain other than SEZ and SGZ remains still controversial (Fig.5), it was shown to be conserved across many species

analyzed, including insects, non-mammalian vertebrates and more remarkably primates including also humans (Adolf et al., 2006; Cayre, Strambi, & Strambi, 1994; Curtis et al., 2007; Eriksson et al., 1998; Goldman & Nottebohm, 1983; Elizabeth Gould, Tanapat, McEwen, Flügge, & Fuchs, 1998; Kornack & Rakic, 1999). However, humans appear unique among mammals in that despite the substantial hippocampal neurogenesis (Knoth et al., 2010; Spalding et al., 2013), there is no detectable OB neurogenesis (Bergmann et al., 2012; Sanai et al., 2011) in spite of generation of neuronal precursors in the SEZ (Sanai et al., 2011; Congmin Wang et al., 2011). The recent identification of continuous generation of striatal neurons in humans suggest that newborn neurons in the SEZ migrate to striatum rather than OB in humans (Ernst et al., 2014).
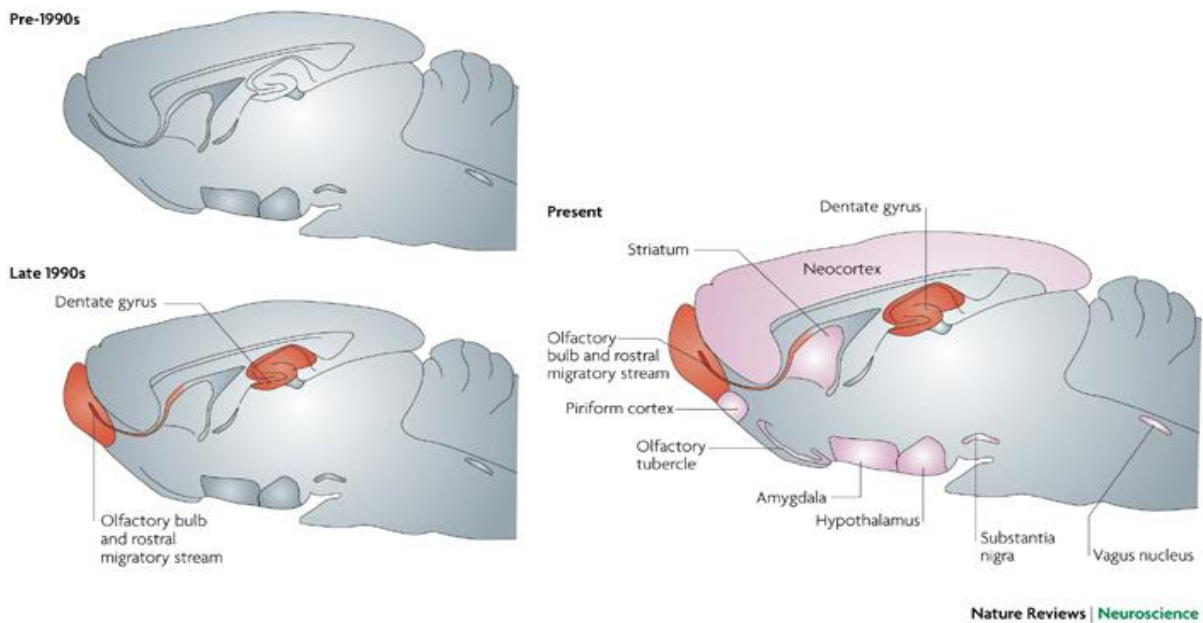
Figure 5: Schematic diagram of the adult rat brain showing the changes in the view of adult neurogenesis in the mammalian brain over the past 15 years (Taken from E Gould, 2007).

In the pre-1990s, all regions were categorized as 'non-neurogenic' (grey). In the late 1990s, only the dentate gyrus and olfactory bulb (as well as the subependymal zone, which gives rise to the rostral migratory stream) were categorized as 'neurogenic' (red). Today, the two known neurogenic regions are shown in red, and areas for which there is controversial evidence for low-level adult neurogenesis are shown in pink

2.5 Neurogenic Niche in the Adult Mammalian Brain

After the discovery that neurogenesis takes place also in the adult mammalian brain but only in two restricted regions, SEZ and SGZ, transplantation experiments of SEZ cells grafted either homotypically into SEZ of another mouse (Lois & Alvarez-Buylla, 1994) or heterotypically into nonneurogenic brain regions like striatum (Herrera, Garcia-Verdugo, & Alvarez-Buylla, 1999) showed that stem cells of SEZ, like stem cells of many other tissues, reside in a specialized microenvironment – or niche – that allows both self-renewal and differentiation of these cells. Since then, several lines of evidence indicated soluble factors secreted from endothelial cells, ependymal cells, microglia, mature neurons, astrocytes and the progeny of aNSCs as well as membrane bound molecules and extracellular matrix proteins as the major components that confer the unique permissive and instructive abilities of these niche (D. K. Ma, Bonaguidi, Ming, & Song, 2009; G. Ming & Song, 2005).

Although no neurogenesis takes place outside the germinal niches, two types of parenchymal glial cells, namely NG2 expressing cells and astrocytes, can also proliferate in the intact brain and upon injury respectively (Robel, Berninger, & Götz, 2011). More interestingly, these cells can give rise to multipotent stem cells under proper culturing conditions (Buffo et al., 2008; Sirko et al., 2013) or upon transplantation in a neurogenic environment (Shihabuddin, Horner, Ray, & Gage, 2000) raising the possibility that these cells also retain a stem cell capacity which is inhibited by the non-permissive environment. So understanding the cellular components that make SEZ and SGZ special in supporting proliferation and neurogenic differentiation of aNSCs is a very important area of research not only to understand the natural course of neurogenesis but also to explore the possibility of using these cells or other proliferating cells in the adult brain for therapeutic approaches after pathological conditions.

2.6 Neurogenesis in the Subependymal Zone

The SEZ is the largest germinal zone in the adult mammalian brain and is located at the lateral wall of the lateral ventricle. Thousands of new neurons that migrate through the rostral migratory stream (RMS) to the OB (Lois & Alvarez-Buylla, 1994; Luskin, 1993) as well as some glial cells destined to the corpus callosum (CC) (Michael A Hack et al., 2005; Menn et al., 2006) are generated in this region every day.

The first attempt to identify the different cell types residing in the SEZ was done in 1997 by Fiona Doetsch in an EM based study and depending on ultrastructural and immunocytochemical criteria she had identified four cells types, the so called type A, B, C and E cells (Doetsch et al.,1997) (Fig.6A). In this model proposed by Doetsch, Type B cells are slowly proliferating cells that have many astrocytic features and they correspond to aNSCs of the SEZ. These cells than give rise to type C cells that are the most actively proliferating cells in the SEZ with immature ultrastructural characteristics and correspond to transit amplifying progenitors (TAPs). Type C cells then give rise to type A cells that have the ultrastructure of migrating neuronal precursors and move long distances by means of chain migration to the OB. Type E cells are the ependymal cells that do not proliferate (Spassky et al., 2005). Recently, two studies that use whole mount preparations of SEZ and three dimensional imaging further defined the architecture of the SEZ (Fig.6B and C). One of these studies showed the presence of two different types of E cells one with multiple cilia and one with only 2 cilia (Mirzadeh, Merkle, Soriano-Navarro, Garcia-Verdugo, & Alvarez-Buylla, 2008) and another study proposed that type B cells are also divided into two types, one being apical and other being tangential (Shen et al., 2008) (Fig.6B and C). Despite these slight refinements in the original model proposed by Doetsch, today it is still accepted that Type B cells correspond to aNSCs of the SEZ which then give rise to type C cells that are fast proliferating transit amplifying cells that then give rise to either neuroblasts that migrate through the RMS to the OB where they differentiate into OB interneurons or to glial cells that migrate to the CC.
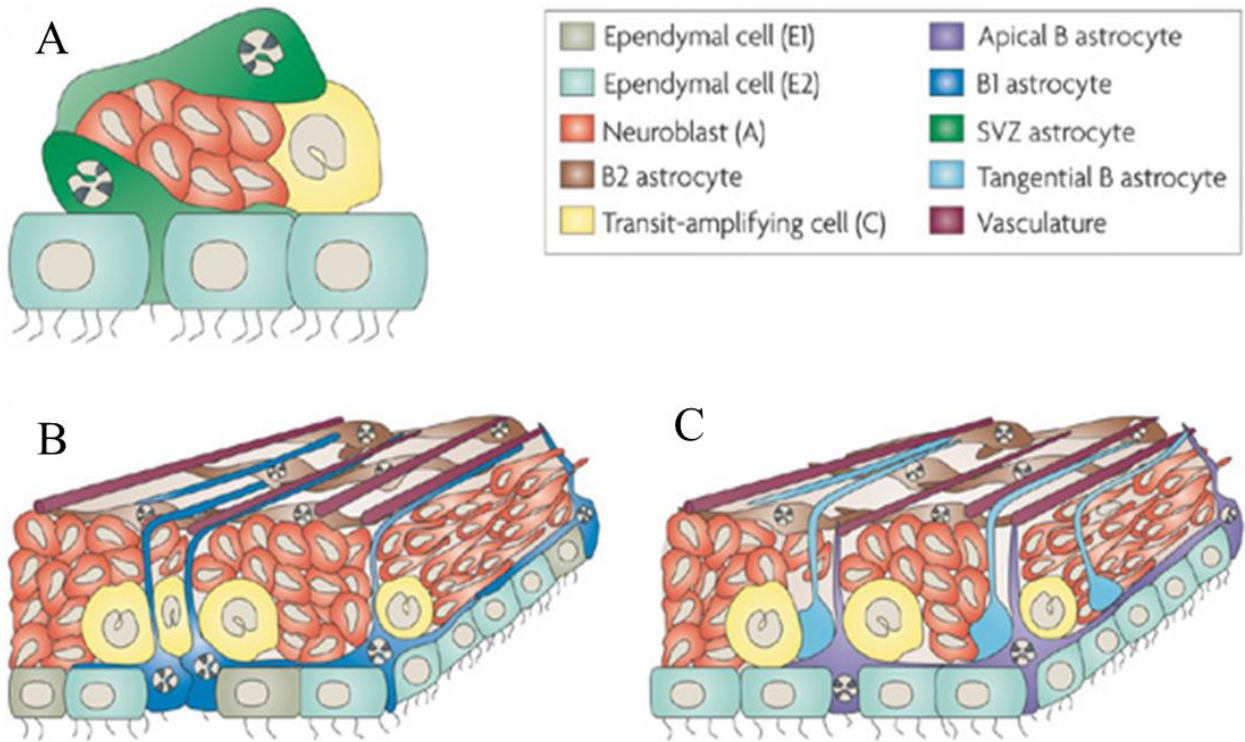
Figure 6: Schematic drawings of revised models for the cytoarchitecture of the adult periventricular area. (Modified from Chojnacki et al., 2009)
(A) In contrast to the original models of the adult periventricular area subependymal zone (SEZ) astrocytes were later found to contact the ventricular surface. They also frequently acquired a single cilium and possessed clumped chromatin after their activation. Use of whole-mount preparations of the adult periventricular area in conjunction with three-dimensional confocal microscopy resulted in the emergence of two different models of the resident cells in the adult periventricular area (represented in parts B and C). **(B)** Mirzadeh et al. (2008) observed that the type B1 astrocyte always contacted the ventricular surface, possessed a single cilium and had a long basal process that ran parallel to the ependymal layer and terminated on a blood vessel. A new cell type, the E2 ependymal cell, which possesses only two cilia, was also found to populate the ventricular wall. **(C)** Shen et al. (2008) observed that type B astrocytes could be subdivided into apical type B astrocytes, which frequently contacted the ventricular surface apically and also contacted a blood vessel basally, and tangential B astrocytes, which possessed a long basal process running parallel to the ependymal layer.

2.6.1 Neural Stem Cells

aNSCs, corresponding to a subpopulation of Type B cells, are slow-dividing cells that have many astrocytic features including light cytoplasm, expression of astroglial markers GFAP, Glast and BLBP and presence of glycogen granules (F Doetsch et al., 1997; A. Kriegstein & Alvarez-Buylla, 2009). In addition to these astrocytic features, aNSCs also share some characteristics with their embryonic counterparts, RG cells, such as expression of marker antigens Nestin and RC2 (A. Kriegstein & Alvarez-Buylla, 2009). Moreover two recent studies showed that aNSCs also have another very important hallmark of RG cells, namely apico-basal polarity. Using whole mount preparations of SEZ, aNSCs were shown to contact the ventricle with a small apical surfaces that contain a single cilium (Mirzadeh et al., 2008). These apical surfaces form clusters among themselves that are surrounded by ependymal cells that form a pinwheel like structure around the apical endings of aNSCs and junctional complexes found in these clusters seem similar to those that join RG whereas they appear different from those that join aNSCs with ependymal cells or ependymal cells with each other (Mirzadeh et al., 2008). Moreover aNSCs were shown to contact the blood vessels with their long basal process that allow them to be exposed to blood born molecules since astrocytic end feet are absent in these contact points (Shen et al., 2008; Tavazoie et al., 2008).

Although some studies suggested that ependymal cells were the NSCs of the SEZ and could give rise to self-renewing multipotent neurospheres, we now know that these results were rather misinterpreted because the markers used were not exclusive for ependymal cells and the Dil injected into the ventricle was also labeling the type B1 astrocytes that also contact the ventricle with their primary cilia (Chojnacki et al., 2009). On the other hand astrocytic nature of NSCs could be shown by many studies. An initial study used infusion of anti-mitotic drug cytosine-β-D-arabinofuranoside(Ara-C) into the ventricle to eliminate TAPs and neuroblasts. Authors could then see that twelve hours after removal of Ara-C, SEZ astrocytes started to proliferate and within 10 days the entire SEZ regenerated whereas there was no sign of ependymal proliferation at any time point analyzed (F Doetsch, Caillé, Lim, García-Verdugo, & Alvarez-Buylla, 1999). The same group also made use of a transgenic mouse line that expresses the receptor for an avian retrovirus under the control of an astrocytic promoter, GFAP, and injected a replication competent avian leukosis (RCAS) retrovirus carrying a reporter gene into the ventricle and observed that RCAS labeled SEZ astrocytes gave rise to olfactory bulb neurons (F Doetsch et al., 1999). Further evidence for the astrocytic nature of

aNSCs came from inducible Cre mediated fate mapping using astrocytic promoters like Glast or GFAP (A. D. R. Garcia, Doan, Imura, Bush, & Sofroniew, 2004; Ninkovic et al., 2007) and more recently our group could show using a split-Cre technology that, astrocytes that have coincident activity of both hGFAP and prominin1 promoters are the aNSCs in vivo (Beckervordersandforth et al., 2010).

Although first studies that used injection of retroviruses carrying LacZ reporter into different rostro-caudal levels of subependymal zone suggested that neurogenesis was taking place only at the anterior part of the lateral ventricle (Luskin, 1993), following studies showed that progenitors located throughout the entire lateral ventricular wall, as well as the ones in the dorsal and anterior medial wall of lateral ventricle and RMS can produce neurons although they are not homogenously distributed in these regions but rather more concentrated in two hot spots one in the anterior-ventral and other in the posterior-dorsal region (Michael A Hack et al., 2005; Kohwi et al., 2007; Merkle, Mirzadeh, & Alvarez-Buylla, 2007; Mirzadeh et al., 2008). However lineage tracing experiments using Cre recombinase under the control of TFs expressed in different locations of the developing brain together with viral injections at different locations in the postnatal SEZ showed that adult SEZ is regionally specified along the dorsoventral and rostocaudal axis like the embryonic cortex and progenitors residing in different regions have different transcription factor profiles and hence give rise to different types of OB neurons (Weinandy et al., 2011). For example calbindin (CB) + periglomerular cells (PGCs) in the OB are mainly derived from Gsx2 expressing progenitors derived from the LGE/MGE whereas dopaminergic and some calretinin (CR) + PGCs are coming from the dorsally located Emx1 expressing progenitors. At the dorsal SEZ, Pax6 was shown to cooperate with Dlx2 to regulate dopaminergic PGC identity and with Ngn2 and Tbr2 to regulate generation of a small fraction of glutamatergic interneurons (Brill et al., 2008, 2009). More recently the medial septal wall and RMS were also identified to be the main source of CR + interneurons and dopaminergic PGCs respectively (Weinandy et al., 2011). In addition to being restricted spatially, aNSCs are also restricted temporally in their ability to generate different types of OB neurons such that CB+ and parvalbumin (PV) + interneurons of the OB are generated mainly at embryogenesis or early postnatal stages whereas CR+ and dopaminergic PGNs continue to be generated in the adult mouse (Batista-Brito, Close, Machold, & Fishell, 2008; De Marchis et al., 2007). Moreover as shown by homotopic and heterotopic grafting experiments , this spatial and temporal restriction is rather cell-

autonomous suggesting further that SEZ NSCs are a regionally heterogeneous population (De Marchis et al., 2007; Merkle et al., 2007).
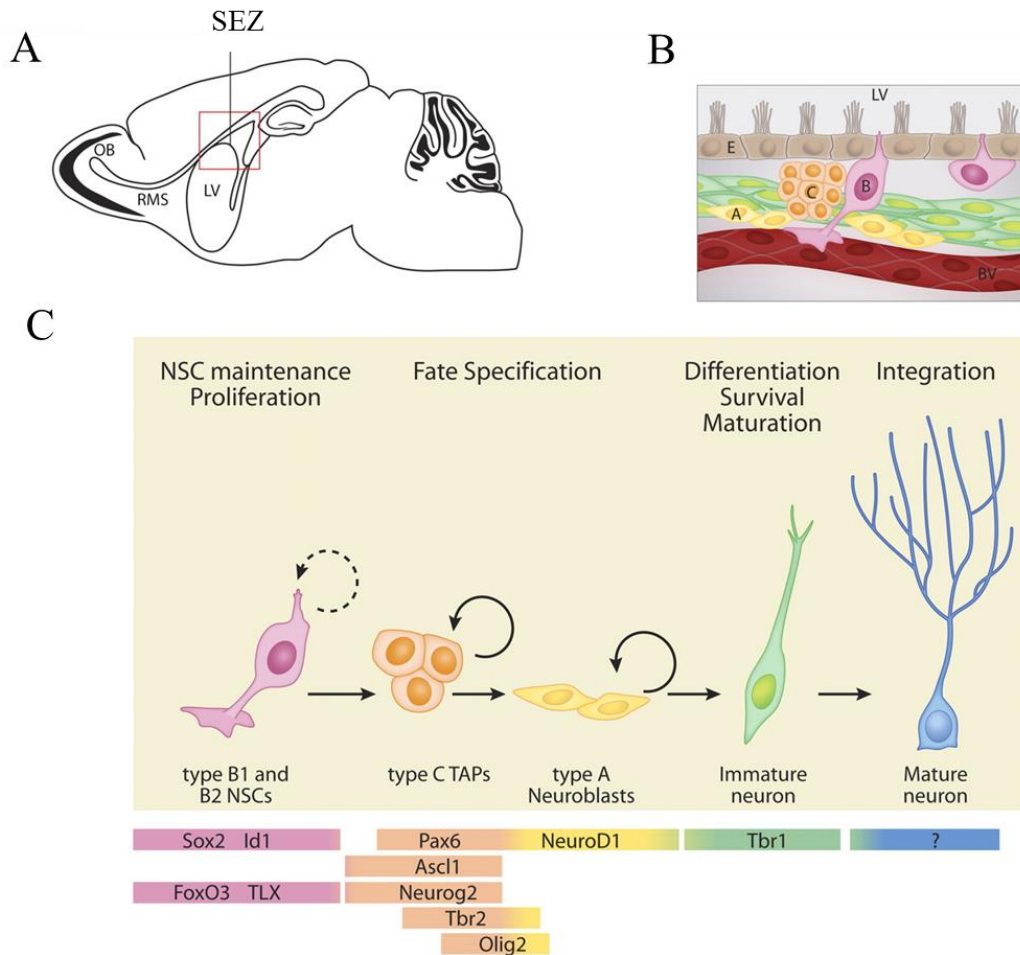
Figure 7: Adult neurogenesis in the SEZ and RMS.(Modified from Hsieh et al., 2012)

(A) Sagittal view of the rodent brain, with the boxed region outlining the SEZ region next to the lateral ventricle (LV). *(B)* Schematic of the SEZ with ependymal cells (E), blood vessel cells (BV), and distinct stem/progenitor cell types (types B, C, and A). *(C)* The SEZ niche is comprised of astrocyte-like type B1 and B2 NSCs (pink), type C TAPs (orange), type A neuroblasts (yellow), immature neurons (green), and mature neurons (blue). The progression from type B NSCs to mature neurons in the adult SEZ is a multistep process with distinct stages (labeled on *top*) and is controlled by the sequential expression of transcription factors (bottom colored panels).

2.6.2 Transit amplifying progenitors

Transit amplifying progenitors corresponding to the Type C cells are the immediate progeny of aNSCs and have a very fast cell cycle as demonstrated by labeling with a short pulse BrdU (F Doetsch et al., 1999; Fiona Doetsch, Petreanu, Caille, Garcia-Verdugo, & Alvarez-Buylla, 2002). These cells are usually found in clusters intermingled within the Type A cells along the SEZ and RMS and proliferate close to blood vessels that are devoid of pericytes and astrocytic end feet, allowing them to be exposed to blood born molecules (F Doetsch et al., 1997; Tavazoie et al., 2008). Two subpopulation of TAPs have been described, one expressing different combinations of neurogenic TFs like Dlx1, Dlx2, Pax6 and Ngn2 and giving rise to neuroblasts and the other expressing Oligodendrocyte lineage transcription factor 2 (Olig2) and giving rise to oligodentrocytes (Brill et al., 2008; Colak et al., 2008; Doetsch et al., 2002; Hack et al., 2005; Menn et al., 2006). Until recently, it was not known whether this heterogeneity is coming from heterogeneity at the stage of aNSC such that two separate pools of aNSCs give rise to either neurogenic or oligodentrocytic TAPs or at the stage of TAPs such that a common bi-/tri-potent aNSC gives rise to two separate pools of TAPs. However, in 2013, Ortega et al. showed that oligodentrogliogenic and neurogenic aNSCs in the adult SEZ constitute two distinct lineages such that aNSCs exclusively generate oligodendroglia or neurons, but never both within a single lineage (Ortega et al., 2013). Many studies that manipulate either the intrinsic fate determinants or extrinsic regulators could show that TAPs represent a population with high lineage plasticity. For example interference with an intrinsic fate determinant Olig2 was shown to cause decreased oligodendrogenesis and increased neurogenesis whereas interference with Pax6 function was shown to lead to increased oligodendrogenesis at the expense of neurogenesis (Michael A Hack et al., 2005; Ninkovic et al., 2013). Moreover infusion of an extrinsic regulator, the BMP inhibitor Noggin, was shown to promote oligodendrogenesis (Colak et al., 2008).

2.6.3 Neuroblasts

Neuroblasts, corresponding to type A cells, are constantly generated through the entire lateral and dorsal wall of the lateral ventricle forming interconnected chains that then converge at the anterior SEZ to form the rostral migratory stream that is ensheathed by astrocytes. They then migrate tangentially through the RMS by a novel mechanism called "chain migration" towards the olfactory bulb where they leave the RMS and migrate radially to populate the granule or glomerular cell layers of the OB (Lois, García-Verdugo, & Alvarez-Buylla, 1996).

Although these young neuroblasts can be identified by expression of molecules like double cortin (DCX), PSA-NCAM and CD24 (Calaora, Chazal, Nielsen, Rougon, & Moreau, 1996; F Doetsch et al., 1997; Gleeson, Lin, Flanagan, & Walsh, 1999), they are known to be heterogeneous. For example only the population giving rise to dopaminergic PGCs and subpopulation of superficial granule cells (GCs) express Pax6 (Michael A Hack et al., 2005; Kohwi, Osumi, Rubenstein, & Alvarez-Buylla, 2005), whereas only a very small subpopulation giving rise to glutamatergic neurons express Tbr2 (Brill et al., 2009).

In mice, neuroblasts migrate a distance of up to 5mm through a very restricted path to reach the OB and the highly directed nature of this process is mediated by many molecules including chomorepellents, chemoattractants, extracellular matrix proteins and cell surface proteins (Hagg, 2005). It was shown that chemorepellants Slit1 and Slit2 are highly expressed in the cerebrospinal fluid (CSF) and septum and beating of cilia generates a gradient of these molecules which is required for proper neuroblast migration. Upon defective cilia this gradient cannot be established and migration of neuroblasts is impaired (Nguyen-Ba-Charvet et al., 2004; Sawamoto et al., 2006). Many groups also showed that chemoattractant molecules including Netrin-1 (Murase & Horwitz, 2002), Prokineticin-2 (Ng et al., 2005), Glial cell-derived neurotrophic factor (GDNF) (Paratcha, Ibáñez, & Ledda, 2006) and Hepatocyte growth factor (HGF)(Garzotto, Giacobini, Crepaldi, Fasolo, & De Marchis, 2008) are expressed in the OB and can attract neuroblasts in vitro. However since surgical removal of OB does not inhibit this migration, these chemoattractant molecules from OB are probably not so crucial for the directionality (Kirschenbaum, Doetsch, Lois, & Alvarez-Buylla, 1999). Neuroblasts themselves also express many cell surface molecules that mediate this chain migration. For example inhibition of α6β1 integrin expressed by neuroblasts disrupts the cohesive nature of the RMS (Emsley & Hagg, 2003). Moreover neuroblasts were shown to be rerouted to different locations by infusing α6β1 integrin ligand laminin. Laminin is known to be expressed in the basement membrane of blood vessels and since blood vessels create a special network around the RMS, they are also thought to be important to inhibit deviation of neuroblasts out of this restricted route (Mercier, Kitasako, & Hatton, 2002; Snapyan et al., 2009). In addition, disruption of EphB2/Ephrin-B2 and neurogulin/ErbB4 signaling pathways was shown to lead to defects in chain migration (Anton et al., 2004; Conover et al., 2000). As mentioned above, migrating chains of neuroblasts are ensheathed by astrocytes and although astrocytes were not shown to have a role in chain migration, they were shown to have a negative effect on the speed and proliferation of neuroblasts by modulating γ-Aminobutyric

acid (GABA) levels (Bolteus & Bordey, 2004; Liu, Wang, Haydar, & Bordey, 2005; Nguyen et al., 2003). This tangential mode of migration changes upon reaching the OB, neuroblasts detach from the RMS and migrate radially to populate different OB layers and the extracellular matrix protein Tenasin C and the glycoprotein Reelin were shown to be important for this radial migration and detachment of neuroblasts from RMS (I. Hack, Bancila, Loulier, Carroll, & Cremer, 2002; Saghatelyan, De Chevigny, Schachner, & Lledo, 2004).

2.6.4 Ependymal Cells

Ependymal cells are mainly derived from RG cells and their production starts at around E12, peaks at E14 and continues till P0 in a decreasing manner (Spassky et al., 2005).

These cells line the ventricles and separate the cerebrospinal fluid from the brain tissues by forming tight-junctions. Although many studies described ependymal cells as having multiple cilia and very large apical surfaces, a recent study identified a new type of ependymal cell that is biciliated and has a smaller apical surface (Mirzadeh et al., 2008). Analysis of neurogenic and non-neurogenic ventricular walls using whole mount preparations showed that the apical surfaces of ependymal cells are regularly shaped in non-neurogenic ventricles whereas they form special pinwheel like structures around the apical surfaces of type B1 cells in the neurogenic ventricle (Mirzadeh et al., 2008). Disruption of this ependymal organization/assembly was shown to impair production of new neurons, highlighting the importance of this niche structure in controlling neurogenesis (Paez-Gonzalez et al., 2011).

Despite their quiescence in vivo under normal physiological conditions (Spassky et al., 2005), some recent work revealed a very surprising lineage relationship between the aNSCs and ependymal cells showing that ependymal cells re-enter the cell cycle and produce striatal neurons and astrocytes in response to stroke (Carlén et al., 2009). Moreover other studies showed that upon distention of ependymal layer either due to aging or due to genetic deletion of Numb/Numblike SEZ astrocytes incorporate within the ependymal layer and take characteristics of ependymal cells over time (Kuo et al., 2006; Luo, Shook, Daniels, & Conover, 2008).

In addition to this lineage plasticity between ependymal cells and type B1 astrocytes, ependymal cells are known to synthesize molecules like BMP inhibitor Noggin and Pigment epithelium derived factor (PEDF) to regulate the proliferation and differentiation of aNSCs

(Lim et al., 2000; Ramírez-Castillejo et al., 2006). Moreover the motile cilia of the ependymal cells was shown to regulate the flow of CSF and to create a Slit gradient to guide the migration of neuroblasts from the SEZ to the OB (Sawamoto et al., 2006). These motile cilia might also have functions in receiving signals like Wnts, Hedgehogs and platelet-derived growth factor (PDGF) from the CSF.

2.7 Neurogenesis in the Dentate Gyrus

The second neurogenic zone in the adult brain is the Dentate Gyrus of the hippocampus and unlike the progenitors of the SEZ, progenitors of the DG are separated from the ventricle and the ependymal cells and reside in the Subgranular Zone (SGZ) that is lying between the granule cell layer (GCL) and the hilus (Fig.8A and B).

Recent studies that use retroviral labeling or genetic fate mapping to label the aNSCs, showed the presence of two morphologically distinct NSC populations, one having a radial process penetrating through the GCL and branching in the molecular layer (ML) (Type 1 radial astrocytes) (Lugert et al., 2010) and another having branched processes parallel to the SGZ (Type 1 horizontal astrocytes) (Lugert et al., 2010; Suh et al., 2007) (Fig.8C). Although these distinct aNSCs share some common features such as expression of markers like GFAP, Vimentin, BLBP, SRY- related HMG transcription factor 2 (Sox2) and Hairy and enhancer of split 5 (Hes5), they differ in their mitotic activity (radial ones are more quiescent and horizontal ones are more mitotically active) and in their response to physiological and pathological stimuli in such a way that physical exercise activates the radial population whereas seizures induce expansion of horizontal population (Hsieh, 2012; Lugert et al., 2010). When Type 1 cells become activated, they give rise to Type2a cells that continue to express Sox2, lose the expression of GFAP, down regulate Nestin and BLBP and up regulate Mash1 (Seri, García-Verdugo, McEwen, & Alvarez-Buylla, 2001; Suh et al., 2007) (Fig.8C). As recently shown, contrary to previous belief, this Mash1 high population is not an amplifying intermediate but instead by a single division gives rise to Type2b cells (also called early neuroblasts) which are Tbr2 and DCX positive (Lugert et al., 2012) (Fig.8C). These Type2b cells then undergo multiple rounds of divisions and act as the main transit amplifying progenitor population of the DG and give rise to Type3 cells (neuroblasts) before they exit the cell cycle (Lugert et al., 2012) (Fig.8C). Type3 cells (neuroblasts) are DCX+, Prospero homeobox protein 1 (Prox1) + and Neurogenic differentiation 1 (NeuroD1) + and over a

period of 4-7 weeks these cells pass first to a NeuN+, CR+ stage and then to a NeuN+ and CB+ stage and acquire a fully mature granular cell identity and integrate into the hippocampal circuitry functionally.
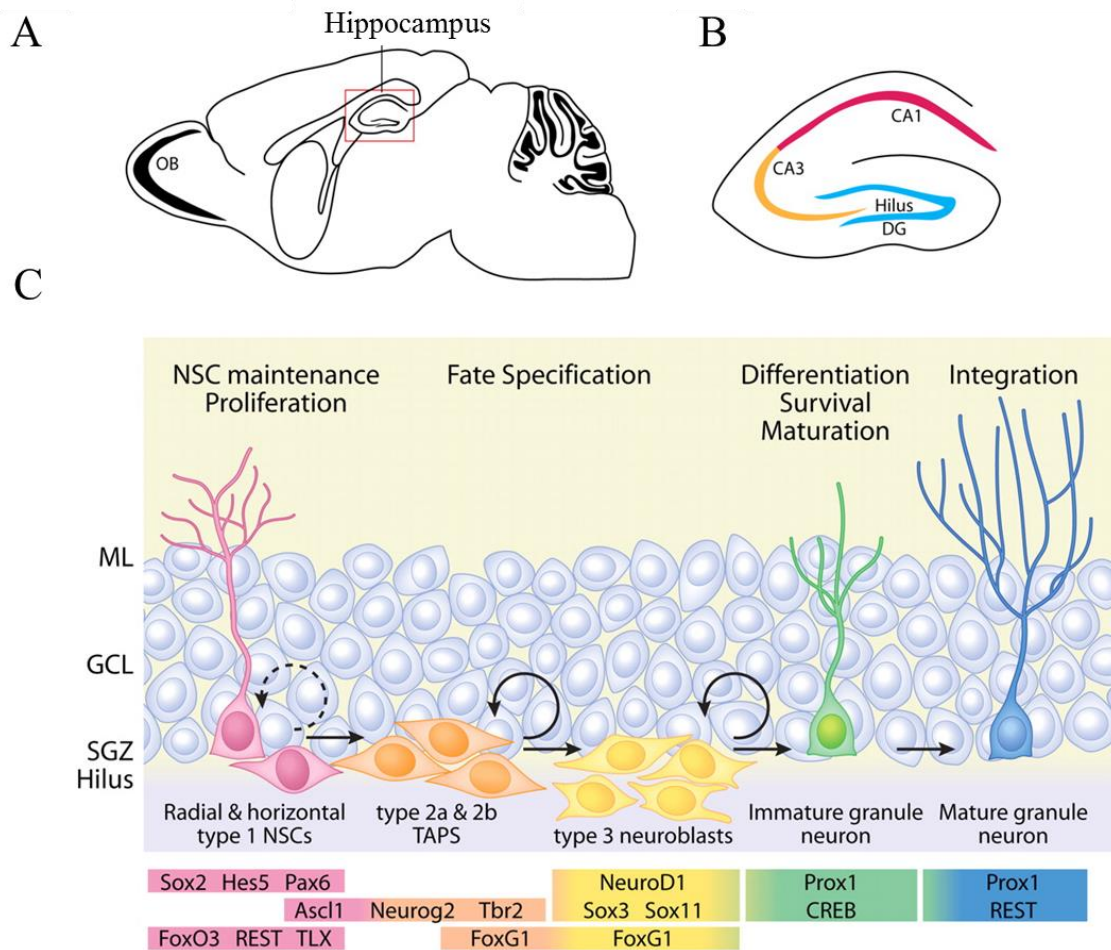
Figure 8: Adult Neurogenesis in the SGZ (Taken from Hsieh et al., 2012)

(A) The DG is part of the hippocampal formation (red box). **(B)** Schematic diagram of the hippocampal formation outlined in the red box in A. Granule neurons in the DG receive inputs from the perforant pathway, and in turn, send axonal projections via the mossy fiber pathway to the CA3 field. The tri-synaptic hippocampal circuitry is completed by Schaffer collateral projections from CA3 to CA1, which sends reciprocal axonal projections to entorhinal cortex. **(C)** The SGZ neurogenic niche is made up of radial and horizontal type-1 NSCs (green), early stage type-2a and -2b INPs (yellow), and late-stage type-3 INPs. These progenitor cells are located along the base of the granule cell layer (GCL), adjacent to the dentate hilus. This progenitor pool gives rise to immature granule neuroblasts (orange), which, if they survive, integrate into the existing GCL circuitry (pink, mature neurons). The progression from NSC to mature granule neuron is indicated by expression of a number of

stage-specific cellular markers (upper colored panels corresponding to individual cell types) and transcription factors (lower colored panels). Color gradients indicate overlap of transcription factor expression into multiple cell types.

2.8 Prospective Isolation of aNSCs and the progeny

Since the initial discovery of adult neurogenesis and aNSCs in rodents was followed by studies that suggest presence of lifelong neurogenesis and aNSCs also in human, these cells gained more attention due to their potential to be utilized as endogenous sources for repair. As this would require understanding the molecular mechanisms regulating the unique ability of aNSCs to generate neurons throughout life, many groups attempted to prospectively isolate these cells and their progeny to achieve a full understanding of the molecular signature of aNSCs. Some groups used in vitro culturing methods to enrich for aNSCs (Azari et al., 2011; Barraud, Thompson, Kirik, Björklund, & Parmar, 2005; Costa et al., 2011; Gabay, Lowell, Rubin, & Anderson, 2003; M A Hack, Sugimori, Lundberg, Nakafuku, & Götz, 2004), however these methods involve treatment with growth factors and long culturing times which are known to alter gene expression pattern and behavior of these cells. Yet, some other groups used transgenic mouse lines such as Nestin-GFP and hGFAP-GFP or cell surface antigens including Prominin1 (CD133), Lewis X (LeX), peanut agglutinin/heat-stable antigen (PNA/HAS) and epidermal growth factor receptor (EGFR) to be able to enrich for acutely isolated aNSCs using fluorescence activated cell sorting (FACS), however in all of these studies either the purification was below 35% or the isolated fraction contained only a proportion of the aNSCs (Capela & Temple, 2002; Corti et al., 2007; Hamanoue et al., 2009; Kawaguchi et al., 2001; Pastrana, Cheng, & Doetsch, 2009; Rietze et al., 2001).

To solve these limitations, our lab developed a FACS based dual labeling method that utilizes the knowledge about glial identity and ciliated nature of aNSCs for improved purification of aNSCs from the SEZ (Beckervordersandforth et al., 2010; Fischer et al., 2011)(Fig.9). In this study, hGFAP-eGFP mouse line in which the expression of enhanced GFP is under the control of the human GFAP promoter was used to identify the cells with astrocyte identity in combination with a cilia marker Prominin1. Sorting of cells from the SEZ based on their expression of GFAP and Prominin1 showed that only hGFAP-GFP+/Prominin1+ cells form neurospheres with a very high efficiency (72%) that can self-renew for more than six passages and that can give rise to all three cell types (astrocytes, oligodentrocytes, and neurons) indicating their multi-potent nature, whereas neurospheres obtained from Prominin1+ only or

hGFAP-GFP+ only cells were unipotent and could not self-renew. Then by using a very elegant in vivo fate mapping technique that allow following the progeny of cells co-expressing two markers ('split-Cre'') (Hirrlinger et al., 2009) and combining it with many different markers to identify different cell types residing in the SEZ, hGFAP-GFP/ Prominin1 co-expressing cells were shown to be the neural stem cells also in vivo, whereas Prominin1+ only cells were shown to be ependymal cells and hGFAP-GFP+ only cells were shown to be a mixed population of cells comprising the progeny of stem cells as well as niche astrocytes (Beckervordersandforth et al., 2010). So our group developed a method that allows prospective isolation of all self-renewing, multipotent stem cells at high purity without the need for in vitro amplification and this method was further used for mRNA profiling of different populations.
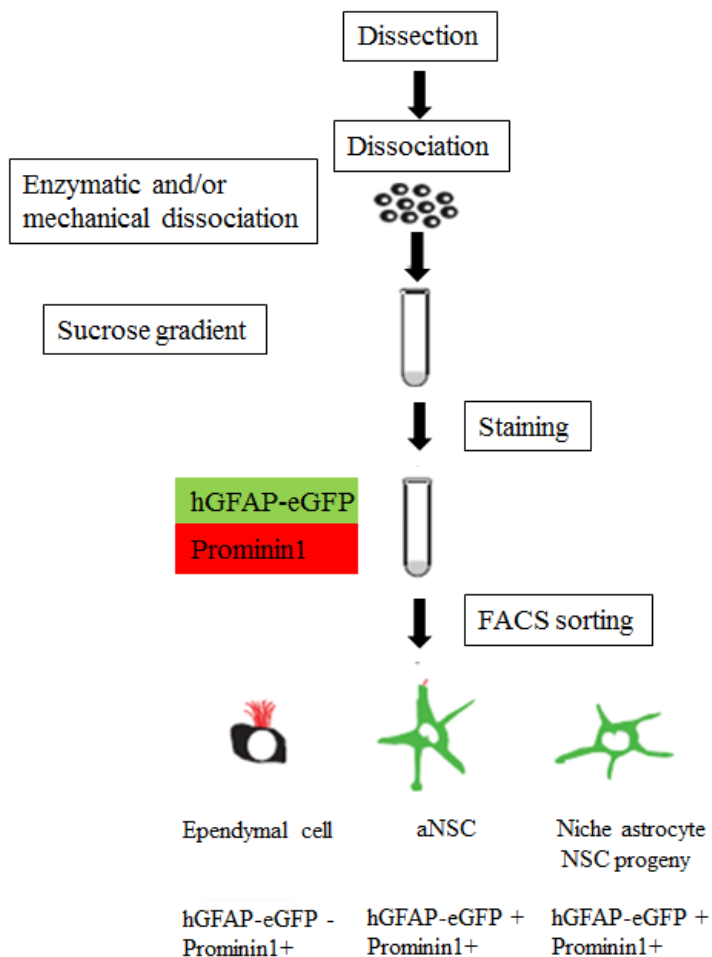
Figure 9: Flow diagram depicting the major steps of isolation of different cell types in the adult SEZ using a FACS based dual labeling protocol (Modified from Fischer et al., 2011).

3. Aims of the thesis

Using this FACS based dual labeling approach our lab was able to reliably discriminate between aNSCs, niche astrocytes and progeny of aNSCs, ependymal cells and parenchymal astrocytes from diencephalon. In order to gain more insights into the molecular signature of neural stem cells and to see how similar/different they are to/from other cells in this niche and non-neurogenic astrocytes, transcriptome analysis of all these different populations was performed (Beckervordersandforth et al., 2010). Comparing the expression profiles of aNSCs with non-neurogenic astrocytes from the brain parenchyma showed increased mRNA level of neurogenic regulators already at the aNSC stage, although the proteins for these neurogenic factors are only detected in the progeny of aNSCs suggesting that aNSCs in the SEZ are already ''primed'' for neurogenesis. On the other hand comparing the expression profiles of aNSCs with all other cell types revealed the importance of specific cilia- and Ca-dependent signaling pathways as unique aNSC characteristics (Beckervordersandforth et al., 2010). Since this work identified many genes that are differentially regulated between aNSCs and other cell types, I first aimed at confirming this transcriptome data with different methods and then to choose some candidate factors that are differentially regulated in the neurogenic lineage to analyze their role in adult neurogenesis. In the second part of my thesis, I extended the functional analysis to neurogenesis during development to elucidate the extent of similarities and differences in regulating neurogenesis in the adult or embryonic brain.

4. Results

4.1 Confirmation of the transcriptome data

Before I select some candidate genes for functional analysis, I chose some genes that had an average expression level > 100 in at least one population and were statistically significantly 4 fold or more differentially expressed to validate the differences in gene expression using Real Time PCR (RT-PCR), in situ hybridization (ISH) and immunohistochemistry.

Towards this aim, total RNA was prepared from different populations isolated by FACS. For this, SEZ and diencephalon of adult hGFAP-GFP mice was microdissected and single cell suspension of adult tissue was prepared according to the protocol described by Beckervordersandforth et al., 2010 (Fig.9). Then dissociated cells from the SEZ were incubated with the Prominin1 antibody and hGFAP-GFP+/Prominin1+ cells (aNSCs), Prominin1+ cells (ependymal cells) and hGFAP-GFP+ cells (aNSC progeny and niche astrocytes) from SEZ and hGFAP-GFP+ cells from diencephalon (non-neurogenic astrocytes) were sorted. As we required around 100.000 cells to have a good RNA quality, cells coming from several rounds of FACS were combined to obtain sufficient amounts for RNA isolation. Then the total RNA was isolated from different populations and RNA quality was assessed at the Agilent 2100 Bioanalyzer. Only high quality RNA (RIN>7) samples were used to generate cDNA, which was then used for RT-PCR. First, transcriptome of hGFAP-GFP+/Prominin1+ cells (aNSCs) was compared to transcriptome of hGFAP-GFP+ cells from diencephalon (non-neurogenic astrocytes). This comparison identified 213 genes that were at least 4 fold enriched with a FDR<1% in hGFAP-GFP+/Prominin1+ cells (aNSCs). Then RT-PCR was performed for 10 genes predicted to be differentially expressed by microarray and for 7 of them up regulation of their mRNA in hGFAP-GFP+/Prominin1+ cells (aNSCs) compared to hGFAP-GFP+ cells from diencephalon (non-neurogenic astrocytes) was confirmed by RT-PCR (Fig.10A).Transcriptome of hGFAP-GFP+/Prominin1+ cells (aNSCs) was then further compared with transcriptomes of Prominin1+ cells (ependymal cells) and hGFAP-GFP+ cells (aNSC progeny and niche astrocytes). In the comparison of hGFAP-GFP+/Prominin1+ cells (aNSCs) with SEZ Prominin1+ cells (ependymal cells) and with SEZ hGFAP-GFP+ cells (aNSC progeny and niche astrocytes), 74 and 257 genes that were at least 4 fold enriched with a FDR<1% in hGFAP-GFP+/Prominin1+ cells (aNSCs), were detected respectively. RT-PCR analysis confirmed the differential expression of 9 genes out of 10 selected genes in the comparison of hGFAP-GFP+/Prominin1+ cells (aNSCs) with SEZ

Prominin1+ cells (ependymal cells) (Fig.10B) and of 6 genes out of 9 selected genes in the comparison of hGFAP-GFP+/Prominin1+ cells (aNSCs) with SEZ hGFAP-GFP+ cells (aNSC progeny and niche astrocytes) (Fig.10C). Thus, reliability of gene expression differences predicted by the fold change analysis of the microarray data was supported by RT-PCR analysis as in total 22 genes out of 29 selected genes were confirmed to be differentially expressed.

Further validation of the transcriptome data was done by ISH to determine the localization of severaldifferentially expressed mRNAs. ISH probes were generated using the cDNA obtained from total SEZ and several genes selected as being enriched in aNSCs and their progeny in comparison to parenchymal astrocytes were indeed shown to be expressed in the SEZ and absent in the diencephalon (Fig.11). For example mRNAs of two novel genes, Ifitm3 and TSP-4, with higher expression in hGFAP-GFP+/Prominin1+ cells (aNSCs) compared to all other populations according to the microarray, was strongly expressed in the SEZ in accordance with the microarray data (Fig.11A-B'). Moreover mRNAs of two known neurogenic genes, Sox11 and Hes6, as well as mRNAs of two genes that have not been implicated in neurogenesis before, Uhrf1 and Whsc1, were strongly expressed in the SEZ-RMS path in agreement with their high expression level in hGFAP-GFP+/Prominin1+ cells (aNSCs) which becomes even higher in the SEZ GFP+ only cells (aNSC progeny and niche astrocytes) according to the microarray data (Fig.11C-F'). In addition, mRNA of Brunol5 was shown to be present in the ependymal layer as would be expected from its highest expression in the Prominin1+ only cells (ependymal cells) (Fig.11G-G') and mRNA of Igsf1 was shown to be present in diencephalon but absent in SEZ, in agreement with its highest expression in the hGFAP-GFP+ only cells of diencephalon (non-neurogenic astrocytes) (Fig.11H-H') according to the microarray data.

A

High in SEZ hGFAP-GFP+/Prom+ (aNSCs), Low in Dien hGFAP-GFP+ only (non-neurogenic, diencephalic astrocytes)
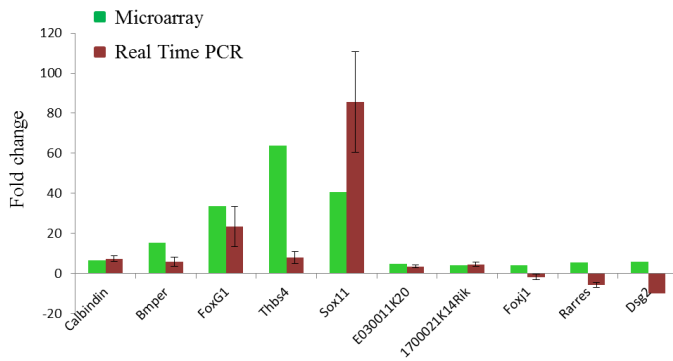
B

High in SEZ hGFAP-GFP+/Prom+ (aNSCs), Low in SEZ Prom+ only (SEZ ependymal cells)
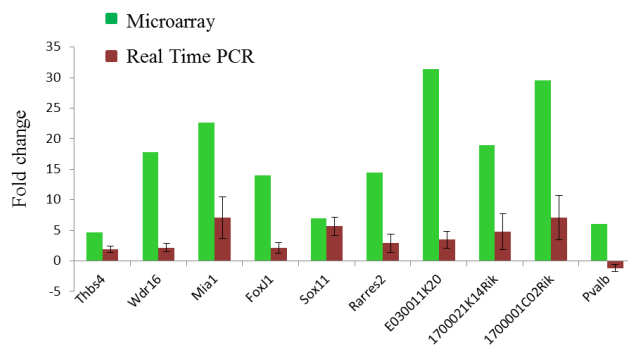
C

High in SEZ hGFAP-GFP+/Prom+ (aNSCs), Low in SEZ hGFAP-GFP+ only (aNSC progeny and niche astrocytes)
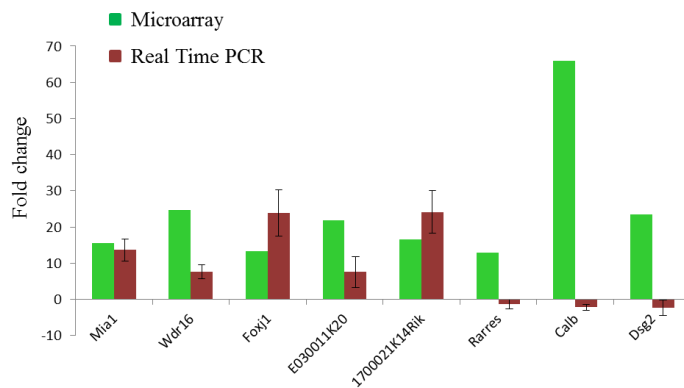
Figure 10: Confirmation of differentially expressed genes with Real Time PCR

(A-C) Histograms depicting the linear ratio of gene expression levels between SEZ hGFAP-GFP+/Prom+ cells (aNSCs) and (A) hGFAP-GFP+ only cells from diencephalon (non-neurogenic astrocytes), (B) SEZ Prom+ only cells (ependymal cells) and (C) SEZ hGFAP-GFP+ only cells (aNSC progeny and niche astrocytes) as measured by Affymetrix array analysis or quantitative RT-PCR. Data are shown as mean ± SEM
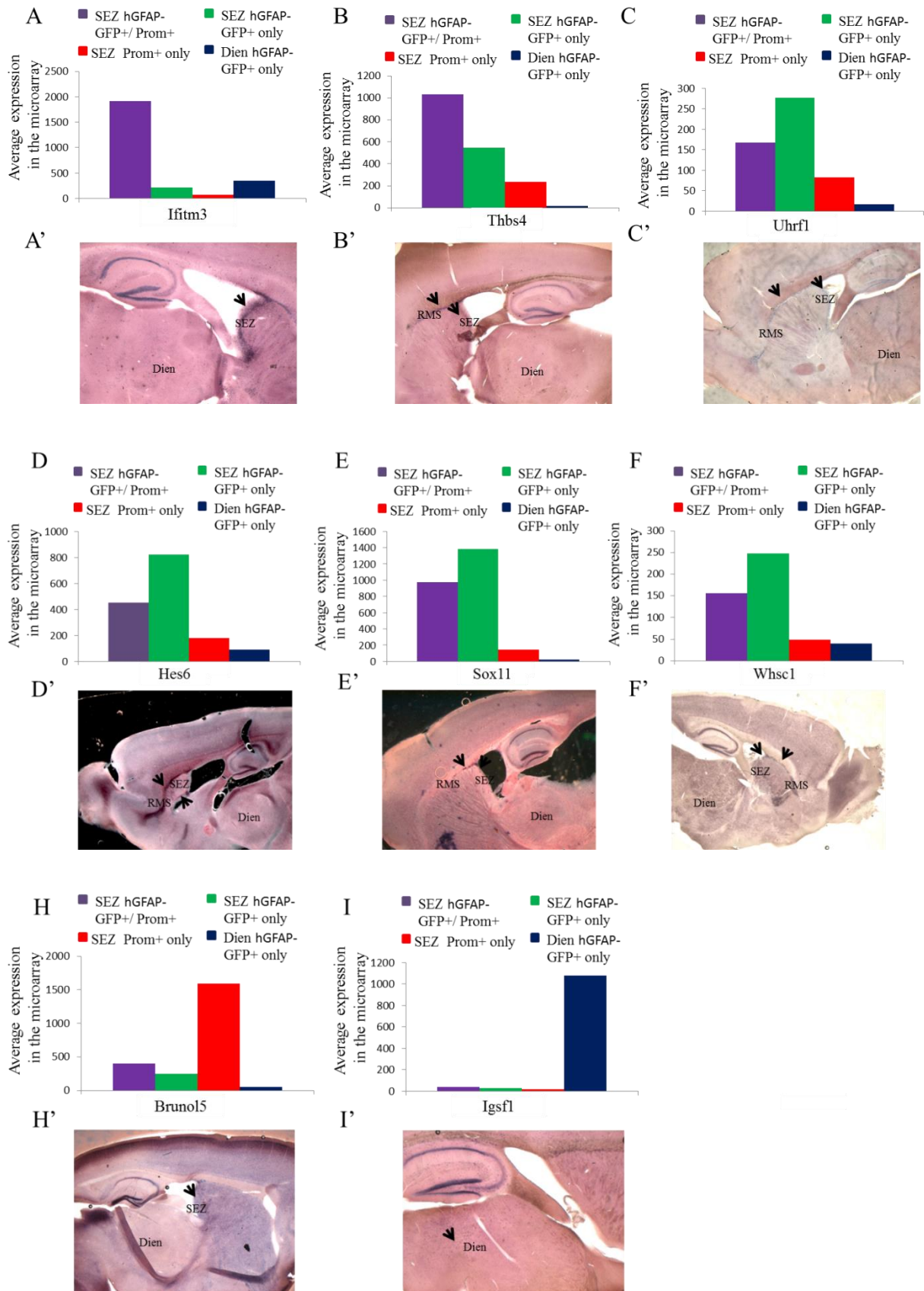
Figure 11: Confirmation of differentially expressed genes with *in situ* hybridization.

(A-B') Histograms depicting the average expression of genes that are high in SEZ hGFAP-GFP+/Prom+ population (aNSCs) compared to all other populations and *in situ* hybridizations for these genes on adult sections. **(C-F')** Histograms depicting the average expression of genes that are high in SEZ hGFAP-GFP+/Prom+ population (aNSCs) and become even higher in SEZ hGFAP-GFP+ only population (aNSC progeny and niche astrocytes) and *in situ* hybridizations for these genes on adult sections. **(G-G')** Histogram depicting the average expression of Brunol5 that is high in SEZ Prom+ only population (ependymal cells) compared to all other populations and *in situ* hybridizations for that gene on adult sections. **(H-H')** Histogram depicting the average expression of Igsf1 that is high in hGFAP-GFP+ only population from diencephalon (non-neurogenic astrocytes) compared to all other populations and *in situ* hybridizations for that gene on adult sections. Abbreviations: Dien= diencephalon; RMS= rostral migratory stream; SEZ=subependymal zone.

Moreover, we performed immunohistochemistry for two genes, Whsc1 and Foxg1 that has not been implicated to have a role in adult neurogenesis before, and could show that these genes are expressed by the hGFAP-GFP+ cells in the SEZ of hGFAP-eGFP mice as we would expect from our microarray data (Fig.12). This observation confirms that the differential mRNA levels detected in our arrays translate into differences in protein levels amongst the isolated populations.

4.2 Selection of the candidate genes

Comparison of the transcriptome of aNSCs with the transcriptome of non-neurogenic astrocytes from the diencephalon as well as with other cell types in the SEZ and analysis of Gene Ontology (GO) terms associated with the genes enriched in aNSCs, revealed very interesting properties of aNSCs.

When expression profiles of aNSCs were compared to non-neurogenic astrocytes from diencephalon, interestingly one significantly enriched GO category was ''nervous system development and differentiation''. Moreover the GO term "regulation of transcription" which was also highly enriched, contained many known neurogenic fate determinants like Sox4, Sox11 and Meis2. Although the expression level of these TFs was already up regulated in aNSCs compared to diencephalic astrocytes, their expression level was even higher in the hGFAP-eGFP + population that contain the progeny of aNSCs. More interestingly, at the

protein level these TFs were detectable only in the progeny of aNSCs suggesting a "neurogenic priming" already at the aNSC level. Since this expression pattern was also shared by other neurogenic TFs like Pax6 and Dlx2 that failed the stringent criteria of differential expression, we selected genes that have the same expression pattern and have so far not been implicated in neurogenesis as new neurogenic candidate factors.
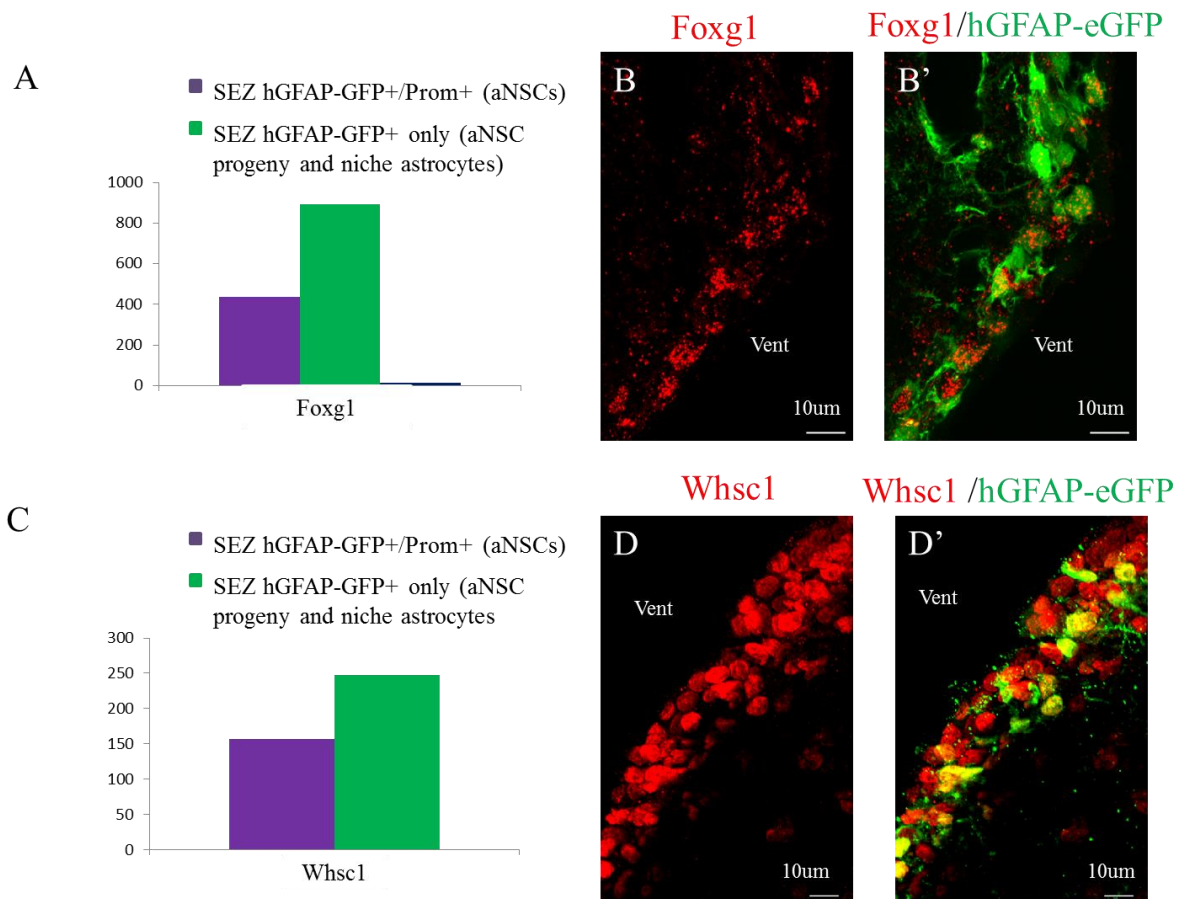
Figure 12: Confirmation of differentially expressed genes with immunohistochemistry

(A) Histogram depicting the average expression of Foxg1, as measured by Affymetrix array analysis, that is high in SEZ hGFAP-GFP+/Prom+ (aNSC) population and become even higher in SEZ hGFAP-GFP+ only population containing the progeny of aNSCs and some niche astrocytes. (B-B') Micrographs depicting the immunoreactivity for Foxg1 in sagittal sections of SEZ of adult hGFAP-eGFP mice. Note the Foxg1 immunoreactivity in hGFAP-GFP+ cells.(C) Histogram depicting the average expression of Whsc1, as measured by Affymetrix array analysis, that is high in SEZ hGFAP-GFP+/Prom+ population and becomes even higher in the SEZ hGFAP-GFP+ only population. (D-D') Micrographs depicting the immunoreactivity for Whsc1 in sagittal sections of the SEZ of adult hGFAP-eGFP mice. Note the Whsc1 immunoreactivity in hGFAP-GFP+ cells. Abbreviations: Vent= ventricle

On the other hand, in order to identify the unique molecular hallmarks of aNSCs, transcriptome of aNSCs was compared to all other populations and expression profile of aNSCs was depleted for genes expressed in other sorted populations. In this analysis the most enriched GO terms were associated with cilia function, Ca signaling, cell adhesion and extracellular matrix (ECM), highlighting the importance of niche and interaction/communication with other cells in order to maintain a unique stem cell signature.

As we thought selecting a candidate from the comparison of aNSCs to diencephalic astrocytes could give us new neurogenic candidates whereas selecting another candidate from the comparison of aNSCs to all other populations could help us to understand the unique hallmarks of stem cells, we selected two different candidates each coming from these comparisons.

4.2.1 First Candidate: Thrombospondin 4

Since cell to cell adhesion and ECM were two GO terms that were highly enriched in aNSCs compared to all other populations of isolated cells and since ECM components were shown to play a role in neurogenesis before (Kazanis & ffrench-Constant, 2011; Purushothaman, Sugahara, & Faissner, 2012; Wojcik-Stanaszek, Gregor, & Zalewska, 2011), we choose Thrombospondin 4 (TSP-4) that belongs to Thrombospondin (TSP) family of secreted glycoproteins, as candidate to study its role in adult neurogenesis.

TSP are a family of evolutionarily conserved, secreted, glycoproteins that function as part of the ECM. They are divided into 2 subgroups organized by oligomerization state and domain structure. TSP-1 and TSP-2 comprise subgroup A that forms homo and heterotrimers whereas TSP-3, TSP-4 and TSP-5 constitute subgroup B that forms homo- and heteropentamers (Adams & Lawler, 2011). They have a complex domain architecture that modulate their oligomerization and interaction with other ECM proteins and cell surface receptors (Fig.13A). The invariant carboxy-terminal regions contain EGF like domains, calcium binding type 3 repeats and a carboxy terminal domain homologous to the L-type lectin domain and the much more varied amino terminal half comprise laminin-G like amino terminal domain, alpha helical coiled coil domain, von Willebrand type C domain and thrombospondin type1 domain (Fig.3A) (Kazerounian, Yee, & Lawler, 2008; Stenina, Topol, & Plow, 2007). These distinct domains of the protein serve to bind different cell surface receptors and ECM proteins

including CD36, CD47, heparin, HSPG, integrin, TGF-B, LRP-1, Notch, Neuroligin, VLDLR, α2δ-1 and ApoER2 to mediate cell-cell and cell-matrix interactions unlike other extracellular matrix proteins like collagen and laminin that rather play structural roles in ECM (Risher & Eroglu, 2012). All members of the TSP family were shown to have a low-level of ubiquitous expression in diverse tissues including the bones, the muscles, the heart and the brain (O'Shea, Liu, Kinnunen, & Dixit, 1990; Tucker, Adams, & Lawler, 1995) and their expression is dramatically induced by injury, stress or acute remodeling events (Kazerounian et al., 2008; Risher & Eroglu, 2012). TSP1-4 have all been found in the brain and they are mainly expressed by the astrocytes, the most common non-neuronal cell type in the CNS (Eroglu, 2009; Lawler et al., 1993; O'Shea, Rheinheimer, & Dixit, 1990). TSP-1 and 2 were shown to promote excitatory synapse formation in the CNS and participate in synaptic repair after brain injury (Eroglu, 2009; Liauw et al., 2008). TSP-1 was also found to becrucial for migration of neuronal precursor cells *in vivo* in early postnatal brain (Blake et al., 2008) and important for proliferation and differentiation of neural progenitor cells (NPCs) (Lu & Kipnis, 2010). Recently, TSP-4, which is known to be differentially expressed in human vs. nonhuman primates, (Cáceres, Suwyn, Maddox, Thomas, & Preuss, 2007) was shown to have a role in cortical injury induced protective astrogenesis (Benner et al., 2013). Moreover decreased TSP expression is observed in many neurological disorders including Down Sydrome and Alzheimer's disease (Buée et al., 1992; O. Garcia, Torres, Helguera, Coskun, & Busciglio, 2010) further highlighting their role in CNS.
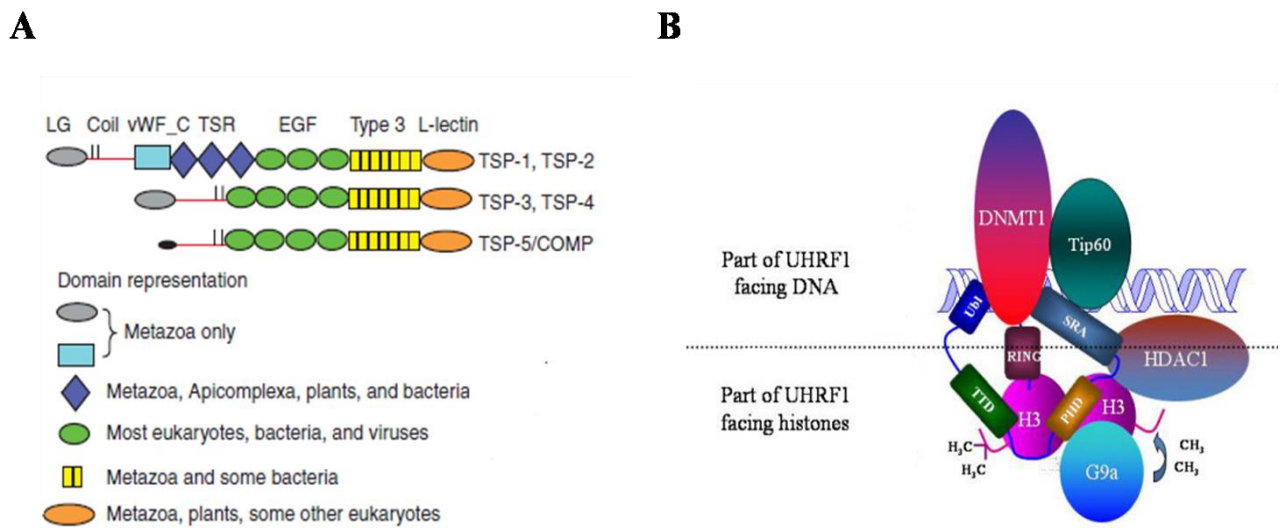
Figure 13: Schematic representation of domains of Thrombospondin family members and Uhrf1.

(A) Schematic diagram of the domain architectures of thrombospondin family members. Abbreviations: LG=laminin G-like amino terminal domain; vWF_C = von Willebrand type C domain; TSR= thrombospondin type 1 domains; EGF= epidermal growth factor like domains; Type 3= thrombospondin type 3 repeats; L-lectin= L-type lectin like domain (Modified from Adams and Lawler, 2011)**(B)** Schematic representation of Uhrf1 with the structural domains facing other DNA or histones. Abbreviations: UBL= Ubiquitin like domain; TTD= cryptic Tandem Tudor Domain; PHD=Plant Homeo Domain; SRA=Set and Ring Associated; RING=Really Interesting New Gene. The major partners of Uhrf1, namely Tat-Interactive Protein of 60kDA (Tip60), DNA methyltransferase 1 (DNMT1), histone methyltransferase G9a(G9a) and Histone deacetylase (HDAC1) are also depicted (Modified from Alhosin et al., 2011)

4.2.2 Second Candidate: Uhrf1

Since many known neurogenic genes showed a very unique expression pattern at mRNA level such that they were high in aNSCs compared to diencephalic astrocytes and become even higher at the progeny of aNSCs, we thought Uhrf1 which showed the same expression pattern (Fig.11C) but was not being implicated in neurogenesis before, could also be a neurogenic fate determinant.

Uhrf1 (ubiquitin-like, PHD and RING finger containing 1, also known as ICBP90 in humans and NP95 in mouse) was identified as a factor that binds the inverted CCAAT box in the

topoisomerase 2a promoter and regulates its expression (R Hopfner et al., 2000; Raphael Hopfner, Mousli, Oudet, & Bronner, 2002). However subsequent studies showed that Uhrf1 functions rather as an important epigenetic regulator connecting DNA methylation and histone modifications (Bostick et al., 2007; Citterio et al., 2004; J. K. Kim, Estève, Jacobsen, & Pradhan, 2009; Sharif et al., 2007; Motoko Unoki, Nishidate, & Nakamura, 2004; J. Zhang et al., 2011). Uhrf1 is a multidomain protein that contains: (i) N-terminal ubiquitin-like domain, (ii) a tandem tudor domain (TTD), (iii) a plant homeodomain (PHD), (iv) a SET and RING-associated (SRA) domain, and (v) a C-terminal RING (really interesting new gene) domain (Fig.13B). These five distinct domains of the protein serve different functions. The SRA domain binds hemi-methylated CpG dinucleotides during the semi-conservative replication of DNA in S-phase and recruits DNA methyltransferase 1 (Dnmt1) to copy the methylation pattern on the daughter strand (Bostick et al., 2007; Sharif et al., 2007). Via the SRA domain, Uhrf1 also constitutes a complex with Hdac1 and binds to methylated promoter regions of various tumor suppressor genes, including pRb, Brca1, Mdr1, p16INK4A and p14ARF in cancer cells (Jeanblanc et al., 2005; Jin, Chen, et al., 2010; Jin, Liu, et al., 2010; Motoko Unoki et al., 2004). Apart from binding to hemi-methylated DNA sequences, recently the SRA domain of Uhrf1 was also found to bind to substrates containing 5-hydroxy-methylcytosine (5hmC), a newly identified modification of genomic DNA, with same affinity as methylated substrates (Frauer et al., 2011). The TTD domain recognizes H3 tail peptides and binds to di- and trimethylated lysine 9 (H3K9me2/3) (Nady et al., 2011; Scott B Rothbart et al., 2012; Xie, Jean, & Qian, 2012). This binding mediates its localization to pericentromeric heterochromatin (PCH) and also is thought to have a role in formation of heterochromatin. The PHD domain specifically binds unmodified H3R2 and this binding is thought to represent an important mechanism for targeting Uhrf1 to euchromatic regions (Hu, Li, Wang, Lin, & Xu, 2011; Rajakumara et al., 2011; Chengkun Wang et al., 2011). Moreover, it is also known to function in the reorganization of PCH (Papait et al., 2008). The RING domain possesses E3 ligase activity with autoubiquitination activity, and has a role in ubiquitination of histone H3 and Dnmt1 (Citterio et al., 2004; Du et al., 2010; Jenkins et al., 2005; Qin et al., 2011). Besides Dnmt1 and Hdac1, Uhrf1 also interacts with Dnmt3a, Dnmt3b, PCNA, USP7 (also known as HAUSP), H3K9 methyltransferases (Suv39H1, G9a), and histone acetyltransferase (Tip60) to form multicomponent complex, termed the epigenetic code replication machinery, to regulate DNA replication and mediate regulation of gene

expression (Achour et al., 2009; Babbio et al., 2012; Bronner, 2011; Felle et al., 2011; Kim et al., 2009; Meilinger et al., 2009).

Uhrf1 itself is a cell cycle regulated protein with expression peaking at late G1 and G2/M phase. and this expression is tightly regulated by key cell cycle regulators including Rb/E2F complex, p53/p21Cip1, the E1A transcription factor and Ccna2/Cdk2 (Abbady et al., 2003; Arima et al., 2004; Bonapace et al., 2002; Chu et al., 2012). However, in various cancer cells including breast, prostate, lung and colorectal cancer, cell cycle dependent expression is abolished and up regulation of Uhrf1 is observed (Daskalos et al., 2011; Jin et al., 2010a, 2010b; Mousli et al., 2003; Sabatino et al., 2012; Unoki et al., 2009, 2010; Wang et al., 2012; Yan et al., 2011). Since Uhrf1 deletion was shown to cause cell cycle arrest at G2/M and G1/S transitions (Bonapace et al., 2002; Tien et al., 2011), hypersensitivity to DNA damage and chemotherapeutic agents (Arima et al., 2004; Muto et al., 2002) or apoptosis (Abbady et al., 2003; Tien et al., 2011; Tittle et al., 2011) , it is a potential target for cancer therapy.

4.3 Expression Pattern and Functional Analysis of TSP-4 in Adult Neurogenesis

4.3.1 Expression Pattern of Thrombospondins (TSPs)

4.3.1.1 TSP-4 is expressed in the SEZ and in neurosphere cultures

After seeing by in situ hybridization that TSP-4 mRNA is very strongly expressed in the SEZ but is not expressed in non-neurogenic areas like diencephalon (Fig 11A) and confirming by RT-PCR that TSP-4 mRNA is 8-fold enriched in aNSCs compared to non-neurogenic astrocytes from Diencephalon (Fig.10A), I aimed to determine the localization of TSP-4 in the SEZ by immunostainings (Fig.14). In accordance with the expression of the TSP-4 mRNA, we observed a very strong TSP-4 staining that was restricted to a layer in the SEZ delineating its borders with the striatum but not anywhere else in non-neurogenic areas like cortex. Moreover as expected from a member of a family of secreted glycoproteins that functions as part of the ECM, TSP-4 staining was in the ECM and was closely associated with GFP+ cells that contain the aNSCs and their progeny in the SEZ of hGFAP-eGFP mice (Fig.14A-C').

The localization of TSP-4 protein in aNSCs was further examined in vitro by immunocytochemical analysis of neurosphere cultures. Neurospheres are aggregates of cells

composed of a mixture of the stem and precursor cells that derive from a single NSC when cells dissociated from the SEZ are grown at clonal density (F Doetsch et al., 1999). In accordance with the expression of TSP-4 in vivo, TSP-4 immunoreactivity was also detected in these neurospheres when these cells were passaged 5 times and then fixed 2 hours after plating.
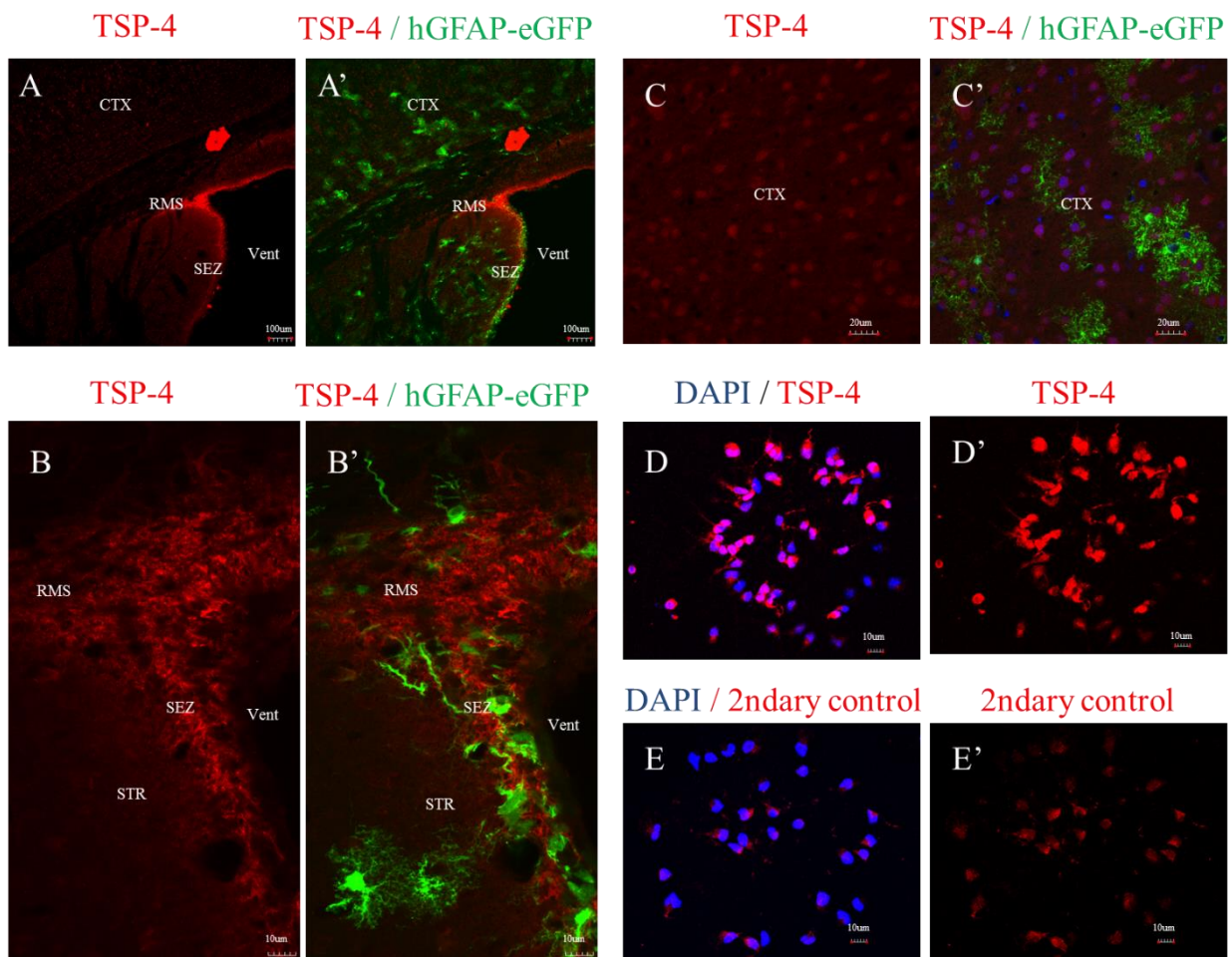
Figure 14: Expression analysis of TSP-4 in adult mouse brain and in neurosphere cultures

(A-C') Micrographs depicting the immunoreactivity for TSP-4 in sagittal sections of the SEZ of adult hGFAP-eGFP mice. Note the TSP-4 immunoreactivity around the GFP+ cells in the adult neurogenic niche SEZ but not in the cortex. **(D-E')** Micrographs depicting the immunoreactivity for TSP-4 in neurospheres that were fixed 2h after plating. Abbreviations: CTX= cortex; STR= striatum; Vent= ventricle; SEZ= subependymal zone; RMS= rostral migratory stream

4.3.1.2 Expression of other TSP family members in the adult brain.

Although according to our microarray, TSP-4 was the only member of the TSPs family that was differentially expressed between aNSCs and non-neurogenic astrocytes from diencephalon, as TSP-4 belongs to TSP family of ECM proteins; I set out to determine if other TSP members are also expressed in the SEZ. First I checked the expression using Allan Brain Atlas database and by RT-PCR (Fig.15). In situ data from Allen Brain Atlas clearly showed that TSP-4 is the strongest expressed family member, but in accordance with the previous data showing the role of TSP-1 in adult SEZ (Lu & Kipnis, 2010),TSP-1 was also expressed along the SEZ-RMS-OB path (Fig.15A). Moreover, RT-PCR using SEZ tissue also showed TSP-1 and TSP-3 expression in the SEZ although at lower levels compared to TSP-4 (Fig.15B). However, when we compared the expression of different TSP members in the SEZ with their expression in diencephalon, in accordance with our microarray data, TSP-4 was the only one that was enriched in the SEZ (Fig.15C).
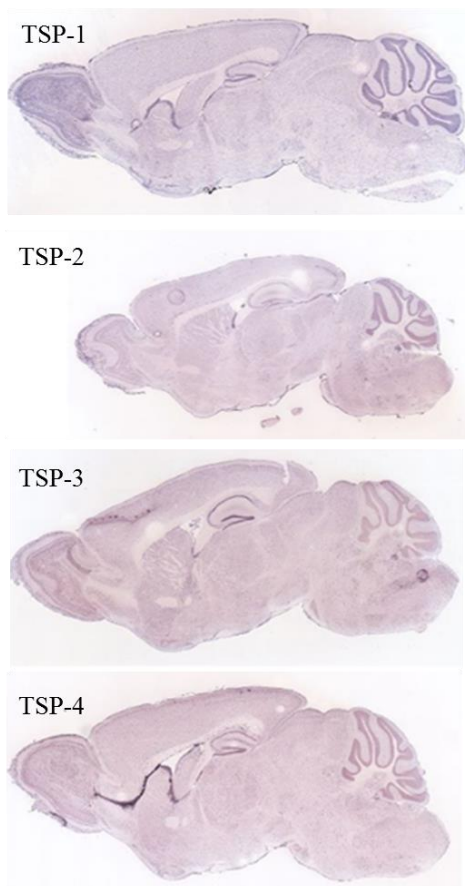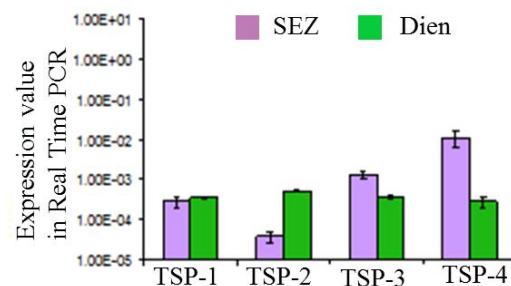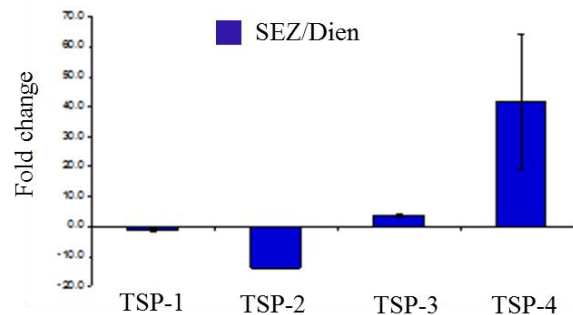
Figure 15: Expression analysis of other members of TSP family

(A) Expression patterns of TSP family members taken from the Allen Brain Atlas. Note the TSP-1 expression along the SEZ-RMS-OB path in addition to TSP-4 expression. **(B)** Histograms depicting the expression of TSP members in total SEZ and diencephalon tissue as measured by RT-PCR. **(C)** Histogram depicting the fold changes of TSP members in SEZ tissue compared to diencephalon.

4.3.2 Analysis of TSP-4 Knock Out mice

Next, in order to investigate a possible role of TSP-4 in adult neurogenesis, we collaborated with Asst.Prof.Dr.Cagla Eroglu to examine brains from TSP-4 heterozygous and null mice (Frolova et al., 2011) and analyzed the structure and cellular composition of the SEZ in these mice.

Since according to our microarray, aNSCs were the major source of TSP-4 in the SEZ, we first assessed whether they were affected by the absence of TSP-4. To evaluate the numbers of aNSCs we took advantage of their relative quiescence (Doetsch et al., 1999a) and used a BrdU label retention protocol (Fig.16A). Heterozygous or null mice were given BrdU in drinking water for two weeks followed by two weeks chase period. Addition of BrdU into the drinking water for two weeks allows for labeling of slowly diving stem cells, fast proliferating TAPs and newly generated neuroblasts. However in the next two weeks during which animals receive normal drinking water, fast proliferating cells and neuroblasts dilute the BrdU label or migrate away from the SEZ so the cells that still keep the BrdU after this chase period are the slowly dividing stem cells and the neuroblasts that left the cell cycle shortly after incorporating BrdU. So combining this protocol with doublecortin (DCX) staining to exclude the neuroblasts allows identification of NSCs. When we applied this protocol, few labeled (i.e., slowly dividing) cells could be detected in the SEZ, however there were no differences in the number or positioning of these label retaining cells between the TSP-4 null and heterozygous animals (Fig.16B-F) indicating that deletion of TSP-4 does not affect the number or proliferation of NSCs.
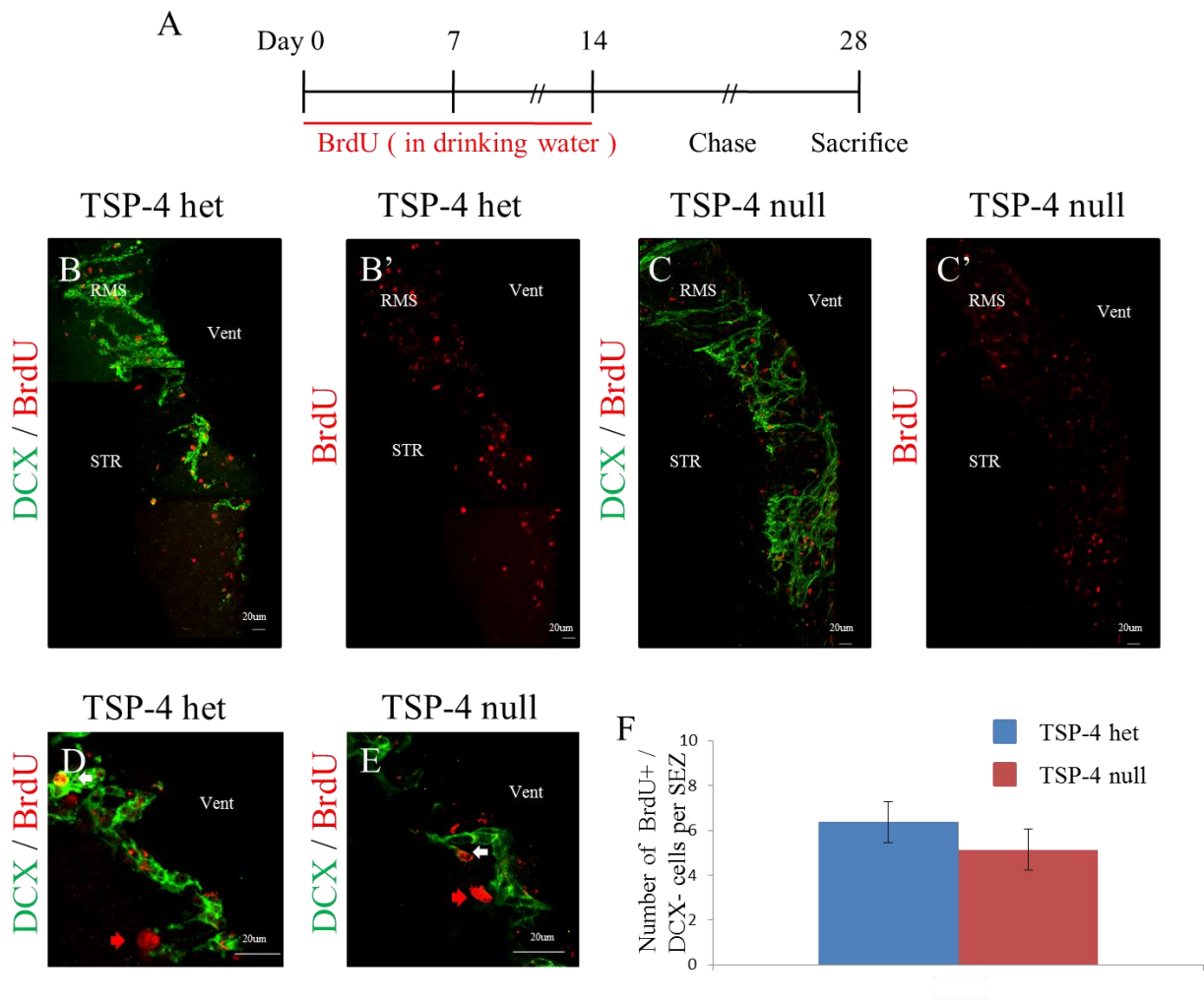
Figure 16: Deletion of TSP-4 does not affect neural stem cell numbers in vivo

(**A**) Scheme of BrdU application for detection of label retaining neural stem cells in vivo. (**B-E**) In D and E red arrows indicate neural stem cells that are only labeled by BrdU and white arrows indicate neuroblasts that are labeled by both BrdU and DCX. Note that these BrdU+/DCX+ cells are excluded from the countings. (**F**) Histogram depicting the quantification of label retaining neural stem cells (BrdU+ / DCX-) in the SEZ of adult TSP-4 heterozygous or null mice. Data are shown as mean ± SEM, n (animals analyzed) = 3 Note that the number of label retaining cells is not changed between TSP-4 heterozygous and null SEZ. Abbreviations: RMS= rostral migratory stream; STR= striatum; Vent= ventricle

As an ECM protein, TSP-4 could also affect other cell types in the SEZ. In order to see how other cell types are affected from the absence of TSP-4, we used GFAP as a marker of astrocytes and DCX as a marker of neuroblasts; however we could not detect any difference in the abundance of the respective labeling between the TSP-4 heterozygous and null mice (Fig.17).
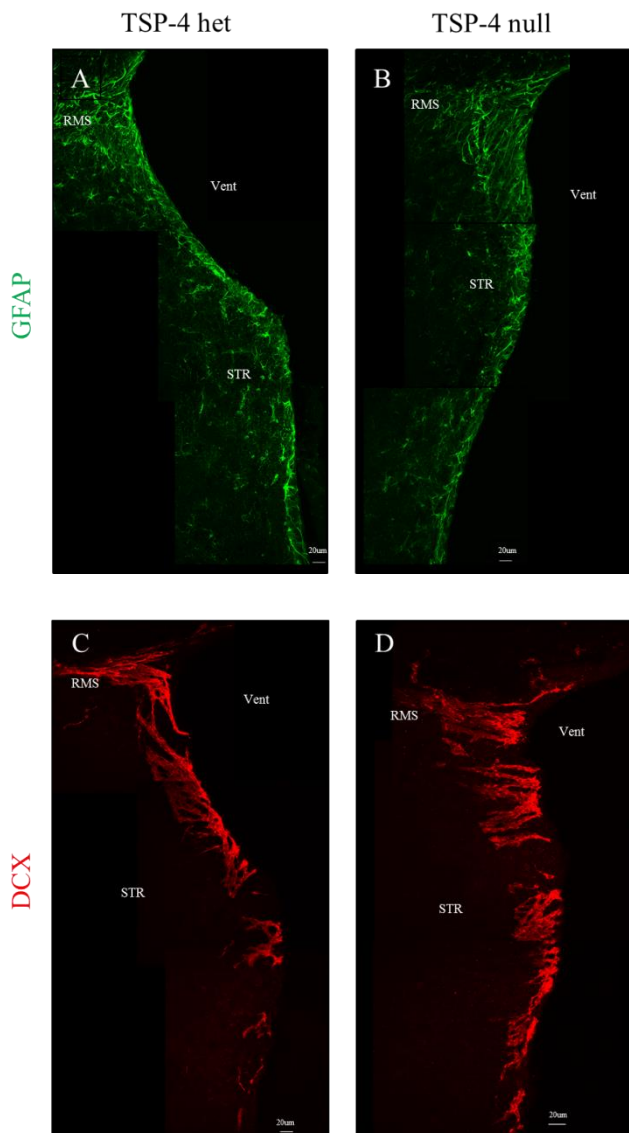
Figure 17: Deletion of TSP-4 does not affect astrocytes and neuroblasts in vivo

(A-D) Micrographs depicting GFAP immunoreactivity for astrocytes (A-B) and DCX immunoreactivity for neuroblasts (C-D) in sagittal sections of the SEZ of adult TSP-4 heterozygous and null mice. Abbreviations: RMS= rostral migratory stream; STR= striatum; Vent= ventricle

Yet, another cell type that could be affected by TSP-4 deletion is transit amplifying progenitors (TAPs), that can be labeled by a 1 hour BrdU pulse which is incorporated into the DNA at the S phase of the cell cycle allowing to label the actively dividing TAPs and some neuroblasts that are still proliferating. So to see if deletion of TSP-4 affected the proliferative activity of these cells, we injected the animals with BrdU and analyzed them 1h later by immunolabeling for BrdU and DCX to distinguish between BrdU+/DCX- TAPs and BrdU+/DCX+ proliferating neuroblasts and quantified the number of each population per field of view (Fig.18). However, similar to number of stem cells, no significant change was observed in the numbers of proliferating TAPs or neuroblasts in TSP-4 null mice compared to heterozygous controls (Fig.18E).
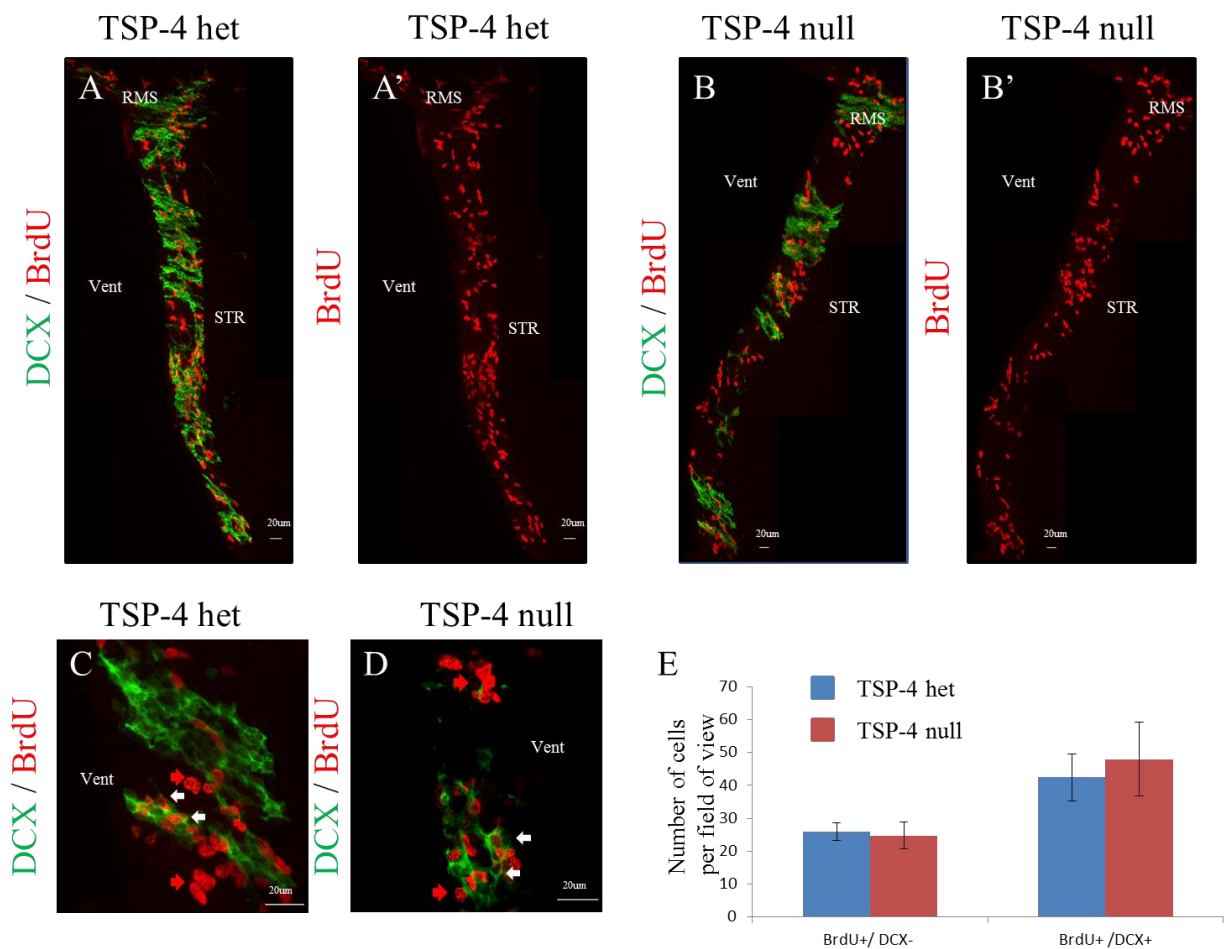
Figure 18: Deletion of TSP-4 does not affect proliferating TAPs or neuroblasts in vivo

(A-D) Micrographs depicting the immunoreactivity for DCX and 1h BrdU labeling in sagittal sections of the SEZ of adult TSP-4 heterozygous or null mice. Red arrows indicate TAPs that are only labeled by BrdU and white arrows indicate neuroblasts that are labeled by both BrdU and DCX. **(E)** Histogram depicting the number of TAPs (BrdU+ / DCX -) and neuroblasts (BrdU+ / DCX +) labeled with BrdU 1h prior to sacrifice. Data are shown as mean ± SEM, n (animals analyzed) = 3. Note that number of TAPs or neuroblasts is not changed between TSP-4 heterozygous and null conditions. Abbreviations: RMS= rostral migratory stream; STR= striatum; Vent= ventricle

4.3.3 Addition of exogenous TSP-4 does not alter neurogenesis

4.3.3.1 Addition of exogenous TSP-4 to the SEZ primary culture does not change clone size or composition

Since the mice we analyzed were full TSP-4 knockout mice, we thought the absence of any change in neurogenesis upon loss of TSP-4 could be due to compensation by other TSP family members. As an alternative approach, we performed gain of function experiments and analyzed the influence of exogenous TSP-4 on adult primary SEZ cultures.

WT mice were used to prepare the non-expanded SEZ primary cultures in the absence of EGF and FGF as described in Ortega et al., 2011. 2 hours after plating the cells, the culture was infected with retroviral vectors encoding GFP which allowed us to follow the progeny of single transduced cells that had divided at the time of transduction. Experimental wells were treated with 5 ug/ml of recombinant TSP-4 (R&D Systems) every second day and coverslips were fixed seven days after viral transduction. All coverslips were then stained for GFP, DCX and GFAP to identify the transduced cells, neurons and astrocytes respectively and only the ones that have less than 40 clones were analyzed (Fig.19A). During the analysis, the clones were classified into three types - a group of GFP+ cells that were all DCX+ were considered a neuronal clone, if all the cells were DCX- and GFAP+ they were considered as glial clone and a group of GFP+ cells that contained at least one DCX+ cell and at least one GFAP+ cell was considered a mixed clone. Consistent with previous observations (Costa et al., 2011; Ortega et al., 2013), most of the clones were of neuronal identity both in the control cultures and in the ones treated with TSP-4 (Fig.19F) suggesting that TSP-4 addition does not have an effect on identity of the clones.
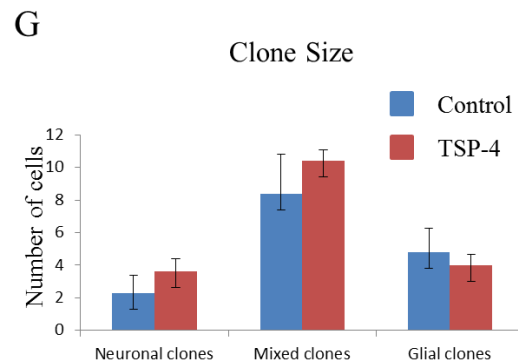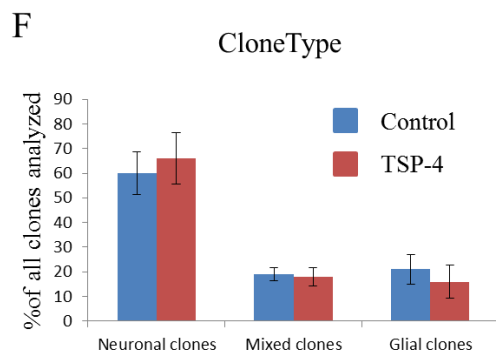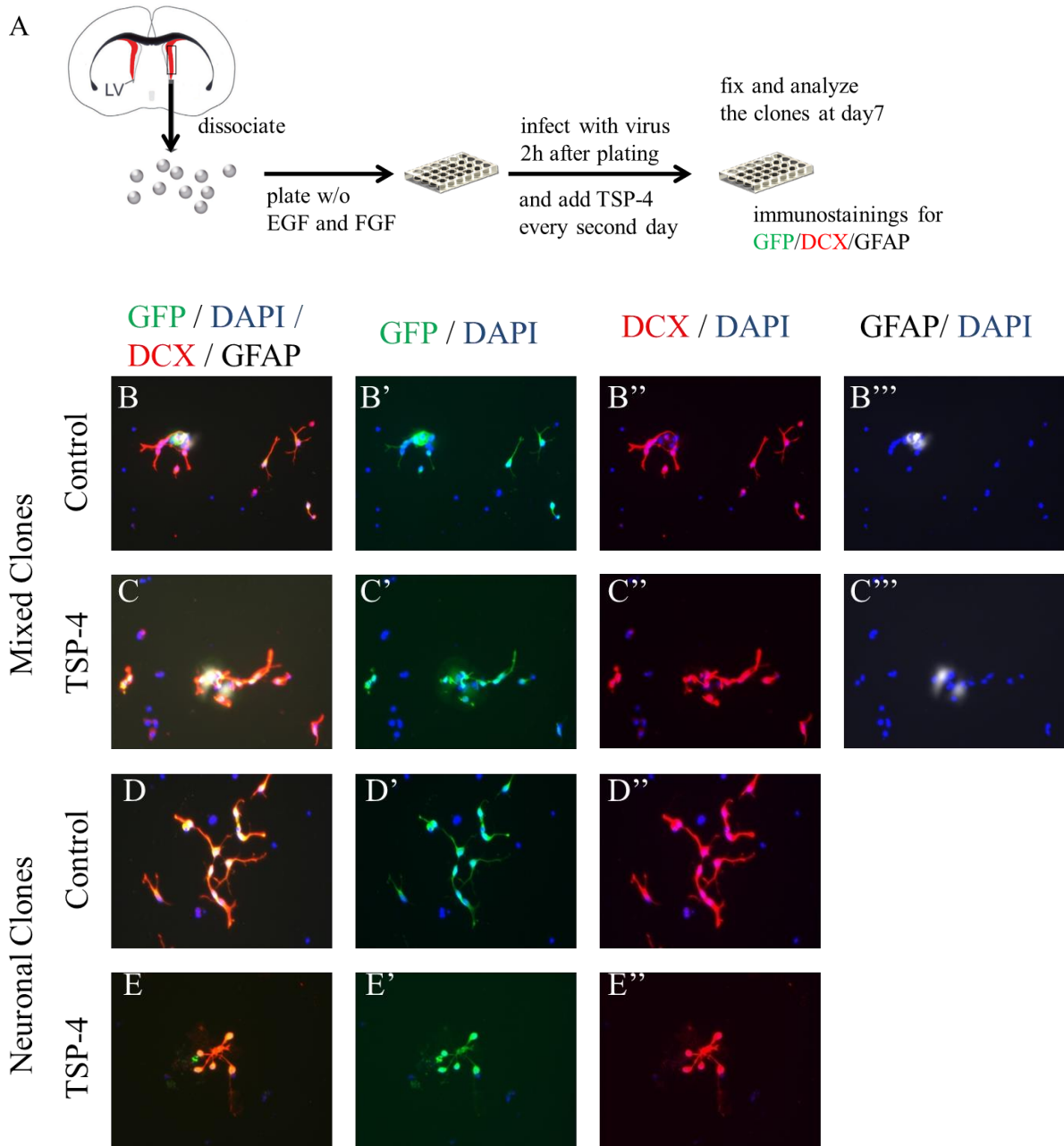
Figure 19: Addition of exogenous TSP-4 to the SEZ primary culture does not have any effect in clone type, size and composition.

(A) Scheme of experimental design to analyze the effect of addition of TSP-4 to the SEZ primary cultures. **(B-E''')** Examples of mixed and neuronal clones in control conditions and upon addition of TSP-4. **(F)** Histogram depicting the percentage of neuronal, mixed and glial clones in control and TSP-4 added conditions. Data are shown as mean ± SEM, n (experiments) = 3. Note that most clones are of neuronal type and this is not affected from TSP-4 addition. **(G)** Histogram depicting the size of each clone type in control and TSP-4 added conditions. Data are shown as mean ± SEM, n (experiments) = 3. Note that neuronal clones have a smaller size whereas mixed clones are larger and this is not affected by TSP-4 addition.

Next I analyzed the size of each type of clone. Again consistent with previous data (Costa et al., 2011; Ortega et al., 2013), neuronal clones and glial clones were rather small in size whereas the mixed clones were larger. However no change in the size of these clones was detected upon TSP-4 addition (Fig.19G), indicating that TSP-4 also does not affect the proliferative behavior of the cells. Moreover, since we also analyzed the composition of mixed clones and saw that in both control and TSP-4 treated coverslips, most of the cells in the mixed clones were neurons whereas there were only 1-2 glial cells (Fig 19B-C'''), we concluded that TSP-4 addition does not affect the clone composition, identity or proliferation at least under those in vitro conditions.

4.3.3.2 Infusion of exogenous TSP-4 into the ventricle does not cause any change in adult neurogenesis

As we did not observe any influence of adding TSP-4 in vitro, we hypothesized that cell grown under these artificial conditions could be missing other ECM or growth factor components required to mediate the TSP-4 effect. Therefore, we decided to examine the effect of TSP-4 addition in vivo and infused exogenous TSP-4 into the lateral ventricle of hGFAP-eGFP mice for 7 days using osmotic minipumps. Then we used our FACS based approach to determine how different populations found in the SEZ are affected (Fig.20A-B). However also in vivo, infusion of TSP-4 did not have any effect on the composition of SEZ with a comparable proportion of NSCs (GFP+/Prom+), their progeny (GFP+ only) and ependymal cells (Prom+ only) as analyzed by FACS (Fig.20C).

Thus, neither genetic deletion nor exogenous addition of TSP-4 had any detectable effect on neurogenesis. This can be due to compensation in the case of knock-out mice and ceiling effect in the case of TSP-4 addition. It is also conceivable that TSP-4 affects other parameters not covered by our read out and /or is particularly relevant after a challenge of the system such as injury.
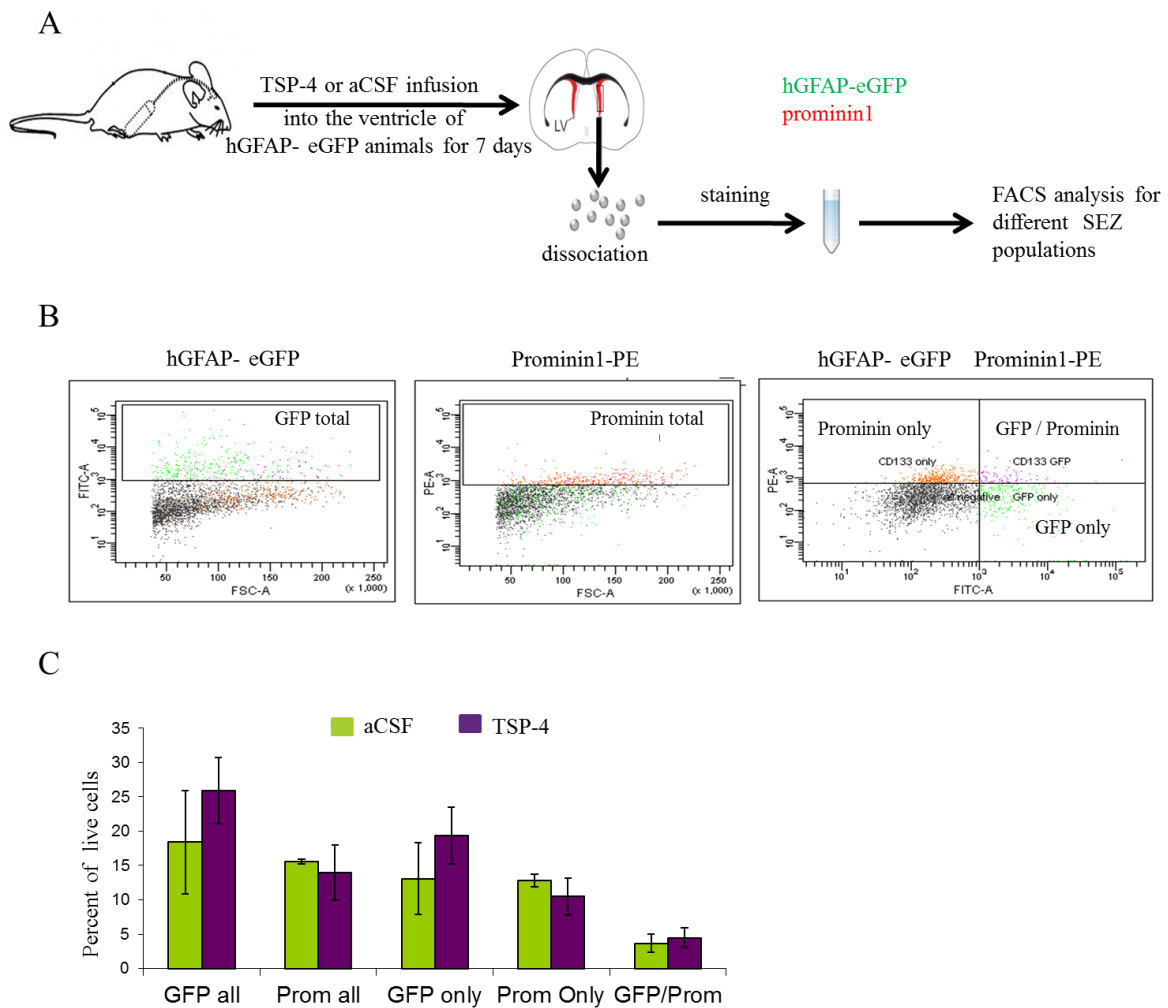
Figure 20: Infusion of exogenous TSP-4 into the ventricle does not alter cell composition of SEZ.

(A) Scheme of experimental design to analyze the effect of infusion of exogenous TSP-4 into the ventricle, on cell types in the SEZ of hGFAP-eGFP mice. **(B)** Dot plots depict GFP +, Prominin + and GFP/Prominin double + cells that correspond to progeny of aNSCs, ependymal cells and aNSCs respectively. **(C)** Histograms depicting the number of aNSCs (GFP+/Prom+), their progeny and niche astrocytes (GFP+ only) and ependymal cells (Prom+ only). Data are shown as mean ± SEM, n (animals) = 3. Note that there is no significant change in any of the populations upon TSP-4 infusion.

4.4 Expression Pattern of Uhrf1 in Adult Mouse Brain and its Functional Analysis in Adult Neurogenesis

4.4.1 Analysis of Uhrf1 expression in adult neurogenic zones

After seeing by ISH that Uhrf1 mRNA is expressed in the SEZ and RMS (Fig.11C), we wanted to analyze the protein localization in more detail in the adult neurogenic zones. So we performed immunostainings for Uhrf1 and combined it with different markers to label different cell types found in the SEZ and DG.

In order to analyze if the Uhrf1 immunoreactivity is present in the aNSCs in the adult neurogenic zones, we used the BrdU label retaining protocol explained in section 4.3.2 and depicted in Figure 16A. When we applied the label retaining protocol and did a triple immunostaining for Uhrf1, BrdU and DCX, we saw that only 10-15 % of BrdU +/DCX – cells expressed Uhrf1 in SEZ (Fig.21A-A'') whereas none of the BrdU+ cells expressed Uhrf1 in the DG (Fig.22A-A'') suggesting that Uhrf1 is not expressed by DG NSCs while a significant fraction of SEZ NSCs contain Uhrf1 protein.
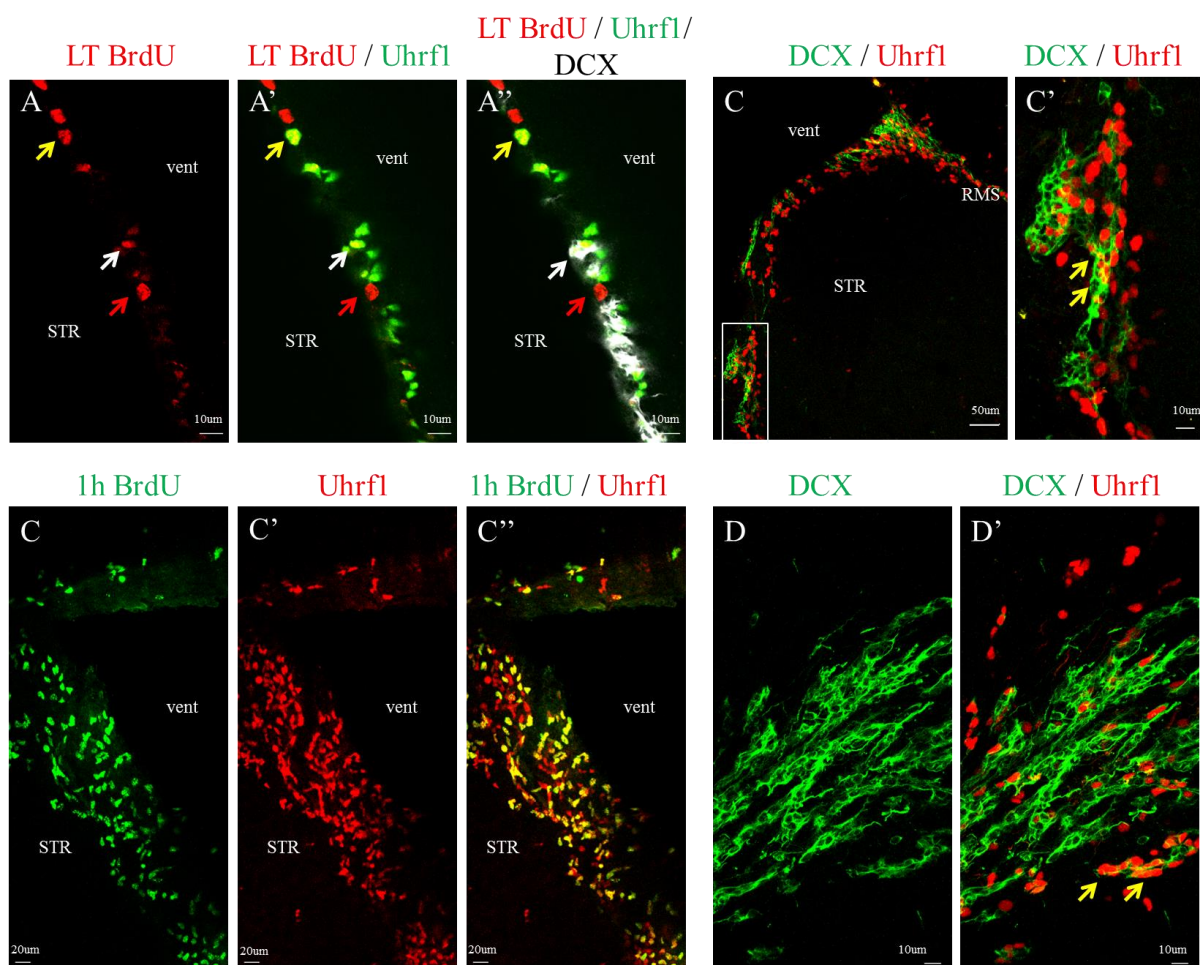
Figure 21: Expression analysis of Uhrf1 in adult SEZ

(A-A'') Micrographs depicting the immunoreactivity for Uhrf1, BrdU and DCX in sagittal sections of the SEZ of adult mice treated with BrdU label retaining protocol. Note the colocolization of Uhrf1 with some BrdU label retaining cells that are DCX- (yellow arrow). Red arrow indicates label retaining cells that do not express Uhrf1 and white arrow indicates the neuroblasts that express Uhrf1, BrdU and DCX. **(B-B'')** Micrographs depicting the immunoreactivity for Uhrf1 and BrdU in sagittal sections of the SEZ of adult mice treated with a short BrdU pulse. Note that all BrdU+ cells are co-labeled with Uhrf1. **(C-D')** Micrographs depicting the immunoreactivity for Uhrf1 and DCX in sagittal sections of the SEZ (C-C') and RMS (D-D') of adult mice. Note that in both SEZ and RMS some of DCX+ cells are colabeled with Uhrf1 (yellow arrows). Abbreviations: RMS= rostral migratory stream; STR= striatum; vent= ventricle

As Uhrf1 may be contained in the activated aNSCs and its expression should increase in their progeny according to the microarray data, we next examined proliferating cells including TAPs and proliferating neuroblasts. In order to label the proliferating cells, we applied a short BrdU pulse 1h prior to sacrifice. Since combining BrdU staining with DCX staining in this protocol allows identification of BrdU+/DCX- cells as TAPs and BrdU+/DCX+ cells as proliferating neuroblasts, triple immunostaining for Uhrf1, BrdU and DCX was performed. Virtually all the BrdU+ cells in the SEZ (Fig.21B-B'') and DG (Fig.22B-B'') were Uhrf1 positive. Although expression of Uhrf1 by all BrdU+ cells suggested that Uhrf1 is also expressed by neuroblasts, not all neuroblasts in the SEZ were expressing Uhrf1 (Fig.21C-C'). Moreover, in the DG, Uhrf1 expression was strong in horizontal DCX + neuroblasts that are very immature whereas its expression was either very weak or completely absent in vertical ones that are more mature (Fig.22C-C'').

In the SEZ upon maturation neuroblasts migrate along the lateral wall of the lateral ventricle and form the rostral migratory stream before entering the olfactory bulb. Notably Uhrf1 was still present in the neuroblasts entering the RMS, as well as the ones that are at the end of the RMS where they just start to detach from the stream to populate the OB (Fig 21 D-D'). However Uhrf1 expression was completely absent in the young neurons that down regulate DCX and reach the OB (data not shown).
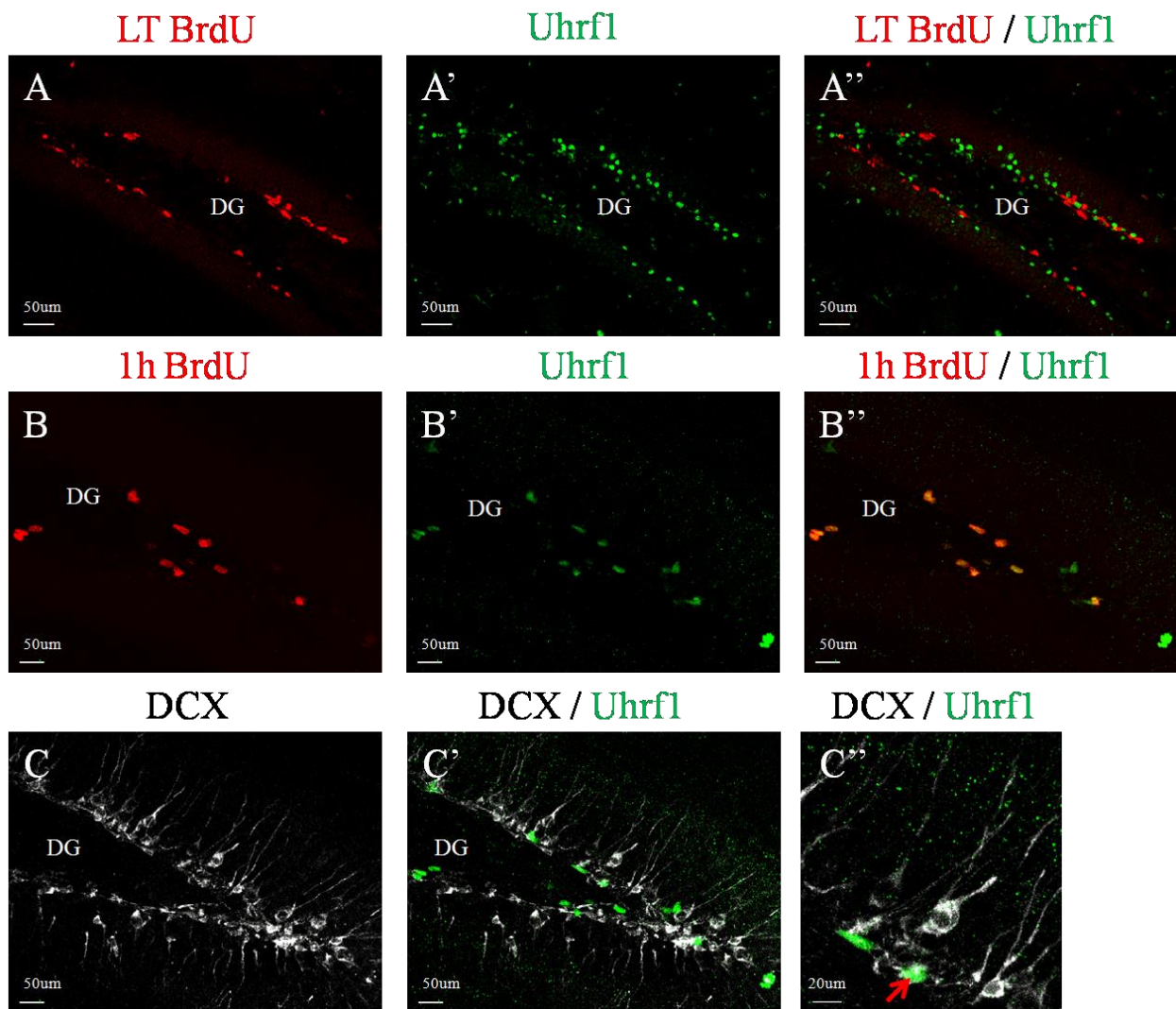
Figure 22: Expression analysis of Uhrf1 in adult DG

(A-A'') Micrographs depicting the immunoreactivity for Uhrf1 and BrdU in sagittal sections of the DG of adult mice that was treated with BrdU label retaining protocol. Note that none of the cells labeled with LT BrdU pulse are Uhrf1+. **(B-B'')** Micrographs depicting the immunoreactivity for Uhrf1 and BrdU in sagittal sections of the DG of adult mice that was treated with BrdU pulse 1h before sacrifice. Note that all BrdU+ cells are co-labeled with Uhrf1. **(C-C'')** Micrographs depicting the immunoreactivity for Uhrf1 and DCX in sagittal sections of the DG of adult mice. Note that very few DCX+ cells express Uhrf1 and these are mainly horizontal cells that are very immature (red arrow) whereas most of the vertical DCX positive cells do not express Uhrf1. Abbreviations: DG= Dentate Gyrus

4.4.2 Analysis of Uhrf1 expression outside the neurogenic zones and after stab wound injury.

In the adult brain there are also non-neurogenic proliferating cells, namely oligodendrocyte progenitors (OPCs) that are located in the cortical white and grey matter and are the progenitors of the oligodendrocyte lineage (Dimou, Simon, Kirchhoff, Takebayashi, & Götz, 2008).In order to see if Uhrf1 is also expressed by the OPCs, we also checked for Uhrf1 expression outside the neurogenic regions in the brains of the animals that were injected with a 1h BrdU pulse. Since these cells have a very long cell cycle, a short pulse of BrdU labels only very few of these cells. However to our surprise, all the cells that were BrdU + in the cortex were also Uhrf1+, showing that Uhrf1 is not only expressed by the neurogenic progenitors but also by the OPCs (Fig.23A-A').

Moreover upon injury to the cortex, in addition to OPCs that fasten their cell cycle, some astrocytes and microglia that normally do not proliferate, re-enter the cell cycle and start to proliferate (Simon, Götz, & Dimou, 2011). To see if Uhrf1 is also up regulated in these proliferating cells upon injury, we made a stab wound injury to the cortex (see e.g. Buffo et al., 2008; Simon et al., 2011), gave BrdU in drinking water to label the proliferating cells and sacrificed the animal 3 days after injury. We then checked for Uhrf1 and BrdU immunoreactivity and saw that Uhrf1 was strongly up regulated in the BrdU+ cells upon injury (Fig.23B-B'). Since different cell populations respond to injury, to understand which cells up regulate Uhrf1, coimmunostainings with CD45 to label the microglia and with PDGFRαto label the OPCs were performed. Interestingly, despite their active proliferation microglia were not Uhrf1+ (Fig.23C-C'). Conversely, Uhrf1 was strongly up regulated in proliferating OPCs (Fig.23D-D'). To further understand if Uhrf1 is also up regulated by astrocytes that respond a few days later than OPCs and microglia (Simon et al., 2011), we also analyzed the Uhrf1 immunoreactivity 7 days post-injury. Co immunostainings with S100β to label the astrocytes showed that Uhrf1 is also up regulated in astrocytes upon injury (Fig.23E).
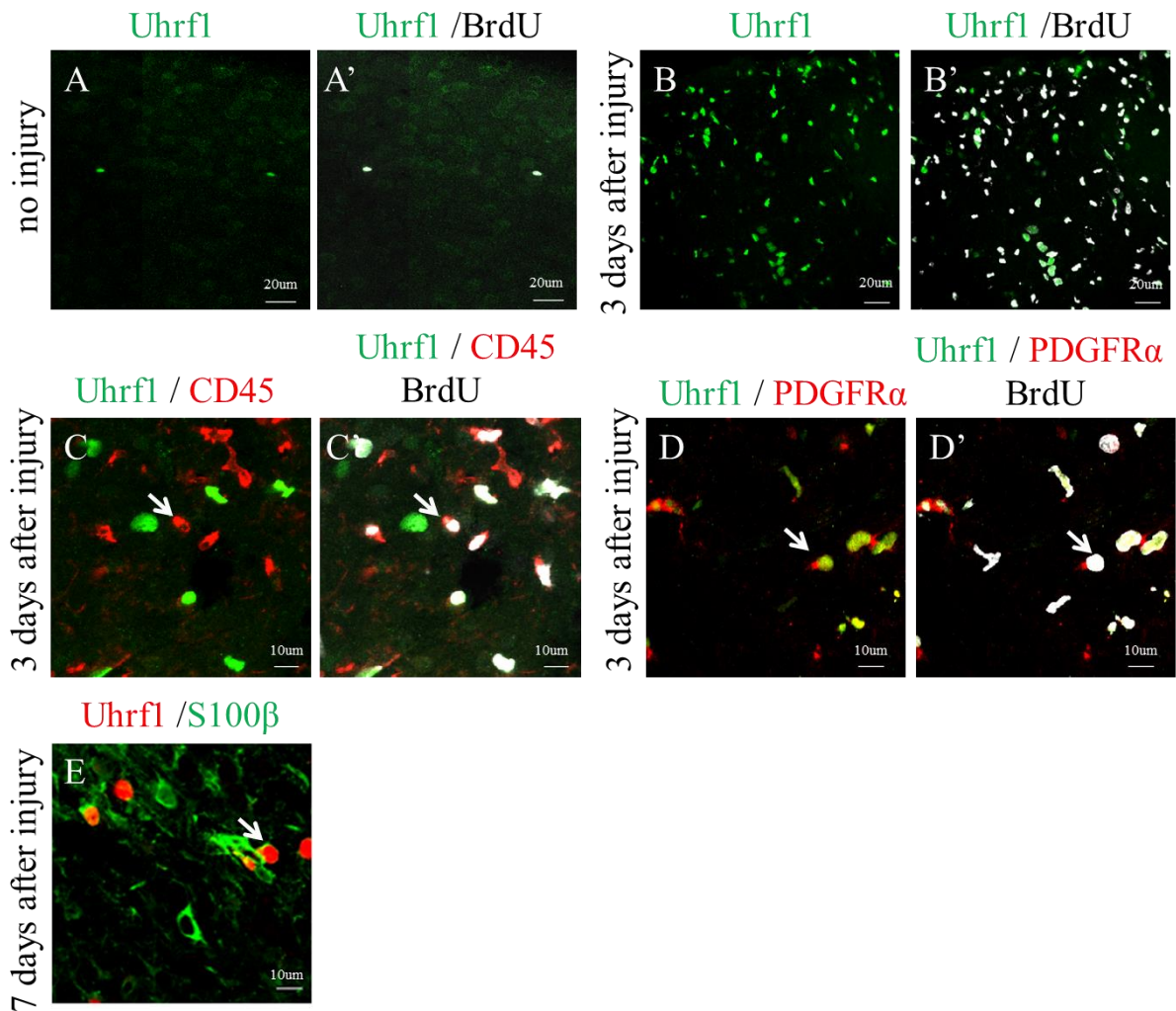
Figure 23: Expression analysis of Uhrf1 in adult cortex in normal physiological conditions and upon injury.

(A-A'') Micrographs depicting the immunoreactivity for Uhrf1 and BrdU in coronal sections of the cortex of adult mice treated with BrdU 1h before sacrifice. Note that all of the cells labeled with BrdU are also Uhrf1+. **(B-B'')** Micrographs depicting the immunoreactivity for Uhrf1 and BrdU in coronal sections of the cortex of adult mice that had a stab wound injury in the cortex and received BrdU pulse immediately after lesion for 3 days. **(C-D')** Micrographs depicting the immunoreactivity for Uhrf1, BrdU and CD45 (C-C') or PDGFRα (D-D') in coronal sections of the cortex of adult mice that had a stab wound injury in the cortex and received BrdU immediately after for 3 days. Note that Uhrf1 is not up regulated by proliferating microglia whereas it is strongly up regulated in proliferating OPCs. **(E)** Micrograph depicting the immunoreactivity for Uhrf1 and S100β in coronal sections of the cortex of adult mice 7 days after stab wound injury.

4.4.3 Conditional Deletion of Uhrf1 in adult NSCs

4.4.3.1 Conditional deletion strategy of Uhrf1 in aNSCs

After showing that Uhrf1 is expressed by some aNSCs and most of their progeny, we used the GLAST^{CreERT2} mouse line (Mori et al., 2006)to achieve conditional deletion of Uhrf1 specifically in aNSCs using Cre/loxP system. In the GLAST^{CreERT2} mouse line, the Cre recombinase, which mediates site specific recombination between loxP sites, is fused to the ligand binding domain of the modified estrogen receptor (ERT2) and is expressed in the locus of the astrocyte and NSC specific glutamate transporter (GLAST). ERT2 cannot bind to its natural ligand (17β- estradiol) at physiological concentrations, but will bind the synthetic estrogen receptor ligand tamoxifen upon treatment with tamoxifen and hence translocate from cytoplasm to nucleus where Cre then can mediate recombination (Fig.24A). For deletion of Uhrf1 using the Cre/loxP system, we took advantage of the Uhrf1 Knockout-first allele line which was generated by the EUCOMM by using promoterless targeting cassettes for the generation of knockout-first alleles (Skarnes et al., 2011). This strategy relies on the identification of a 'critical exon' common to all transcript variants that, when deleted, creates a frame-shift mutation triggering nonsense mediated decay of the deleted transcript (Fig.24B). KO-first allele is flexible and can produce reporter knockouts, conditional knockouts, and null alleles following exposure to site-specific recombinases Cre and Flp. In order to convert the knock out first allele to a conditional Uhrf1 allele, we crossed this mouse line with the FLPeR mouse line (Farley et al., 2000). Then we crossed the progeny of this cross, with the Glast^{CreERT2}mouse line to delete the floxed exon of the conditional allele (Fig.24B). In order to monitor the recombined cells, Uhrf1 floxed/ floxed mice were crossed with the CAG CAT eGFP reporter line (Nakamura, Colbert, & Robbins, 2006). In this line, expression of the enhanced Green Fluorescent Protein (eGFP) is blocked by a loxP-flanked stop cassette. Upon excision by Cre, eGFP is expressed by achicken beta-actin promoter resulting in constitutive expression of eGFP in all recombined cells.
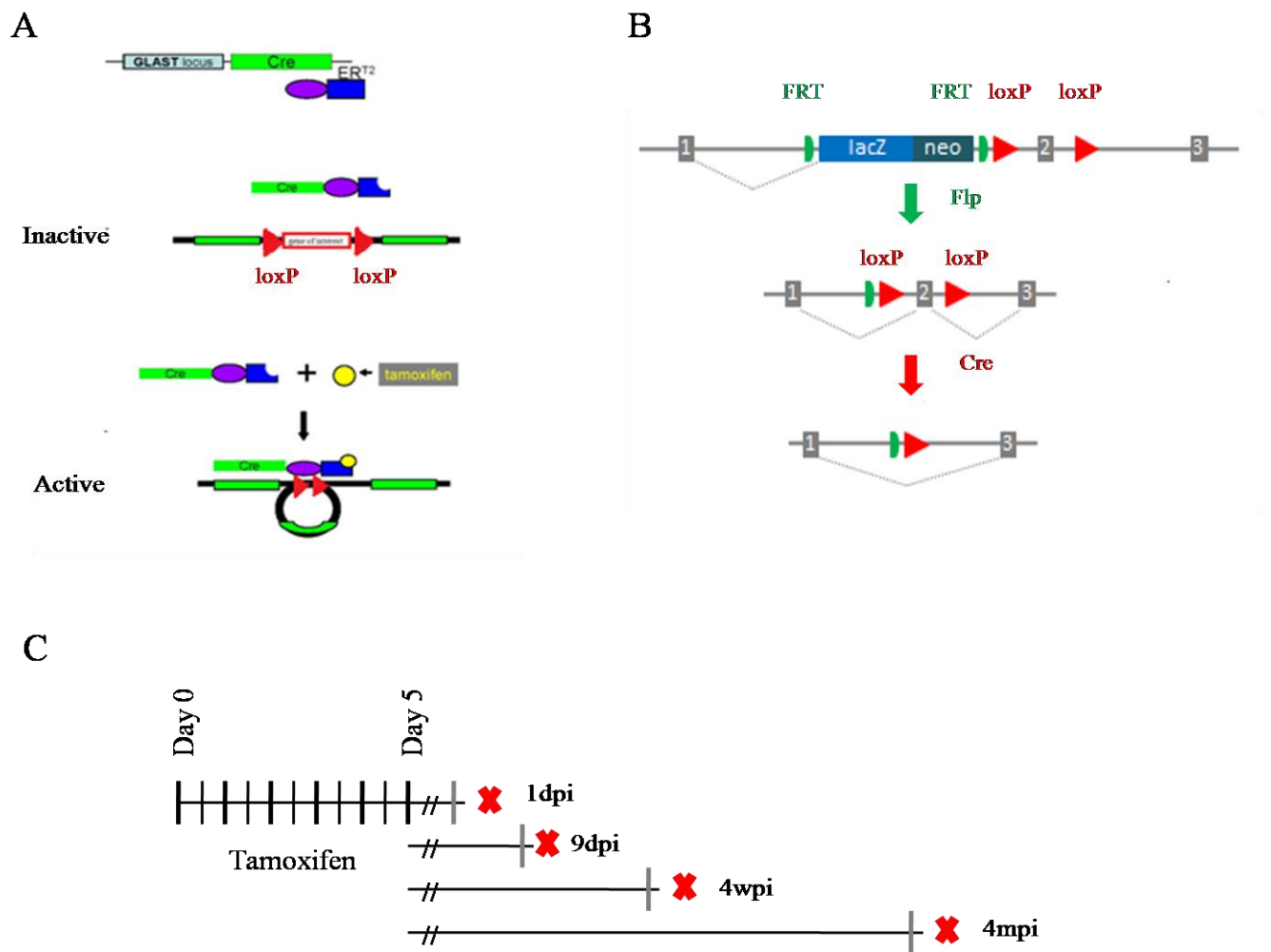
Figure 24: Experimental outline for conditional deletion of Uhrf1 in the adult murine brain

(**A**)Schematic drawing of tamoxifen based inducible Cre/loxP system. CreERT2 encodes a Cre recombinase (Cre) fused to a mutant estrogen ligand-binding domain (ERT2) that can only bind to estrogen analog tamoxifen but not estrogen. In the absence of tamoxifen CreERT2 stays in the cytoplasm whereas upon tamoxifen administration the CreERT2 is able to penetrate the nucleus and induce recombination in the loxP sites. (**B**) Scheme of generation of conditional knockout mice from the knock out first allele line. Uhrf1 knockout first allele line was first crossed with FLPeR mice to convert it to a conditional Uhrf1 line and then conditional Uhrf1 line was crossed with a line that carries Cre (it is GLAST^{CreERT2} line in our case) to delete the floxed exon. Modified from Skarnes et al., 2011)(**C**) Experimental design. Tamoxifen was injected two times a day for 5 days to transgenic mice being heterozygous for GLAST^{CreERT2} and carrying one or two floxed allele of Uhrf1 at the age of 8-10 weeks. Mice were killed one day (1dpi), nine days (9dpi), four weeks (4wpi) or four months (4mpi) after the end of tamoxifen induction.

All the in vivo experiments that will be presented in the following chapters were performed with 8-10 weeks old animals heterozygous for the GLAST^{CreERT2} allele and the CAG-eGFP reporter. While control animals carried only a single allele of Uhrf1 floxed allele (GLAST^{CreERT2}; Uhrf1$^{fl/wt}$, in graphics shown as Uhrf1 het), experimental animals were homozygous for the Uhrf1 floxed allele (GLAST^{CreERT2}; Uhrf1$^{fl/fl}$, in graphics shown as cKO). Since tamoxifen itself as an estrogen analogue could also have effects on neurogenesis, all the animals were treated with same amount of tamoxifen. This also ensured that the same amount of Cre translocate to the nucleus of control and experimental animals and excluded the possibility that the observed phenotypes could be due to differential Cre activity that was reported to cause cell death due to mis-recombination and DNA damage (Forni et al., 2006; Schmidt-Supprian & Rajewsky, 2007). All animals used in the experiments were treated with tamoxifen two times a day for five days and sacrificed at different time points after the end of tamoxifen treatment (Fig.24C).

4.4.3.2 Uhrf1 is lost in aNSCs and their progeny 9 days after the last tamoxifen injection in the SEZ

First, the efficiency of the recombination in the triple-transgenic animals was examined by performing immunostaining against GFP immediately 1 day post induction (1dpi). Reporter activity was seen along the dorsal, medial and lateral wall of the lateral ventricle and the amount of reporter signal was comparable in animals carrying one or two Uhrf1 floxed alleles suggesting a similar recombination rate in both heterozygous and homozygous animals (Fig.25).

Next, we examined the protein levels of Uhrf1 by immunostainings for Uhrf1 at 1, 5 and 9 days post induction (1, 5 and 9 dpi). Although there was a strong reduction in the Uhrf1 protein 5 days after the last tamoxifen injection (data not shown) since the Uhrf1 protein was almost completely gone by 9 dpi (Fig.26), we decided to do further analysis earliest at this time point.
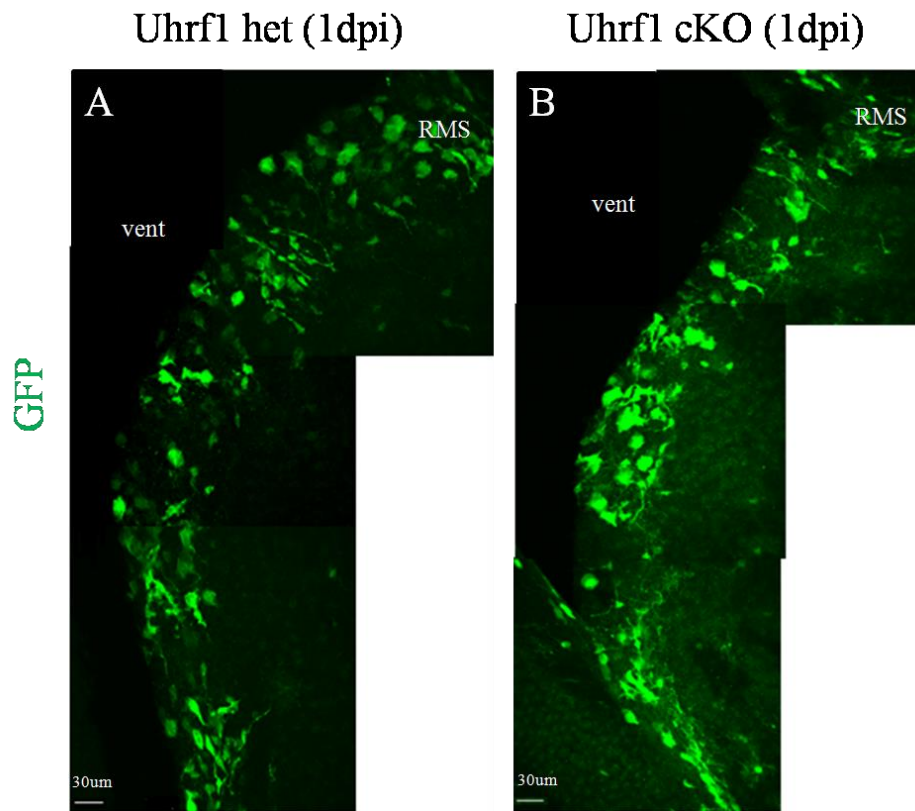
Figure 25: Similar recombination is seen in Uhrf1 heterozygous and cKO animals immediately after the end of induction

(A-B) Micrographs depicting the immunoreactivity for GFP in sagittal sections of the SEZ of adult mice 1 day after the end of tamoxifen treatment. Note that reporter signal is comparable in both animals suggesting a similar recombination rate. Abbreviations: RMS= rostral migratory stream; vent= ventricle
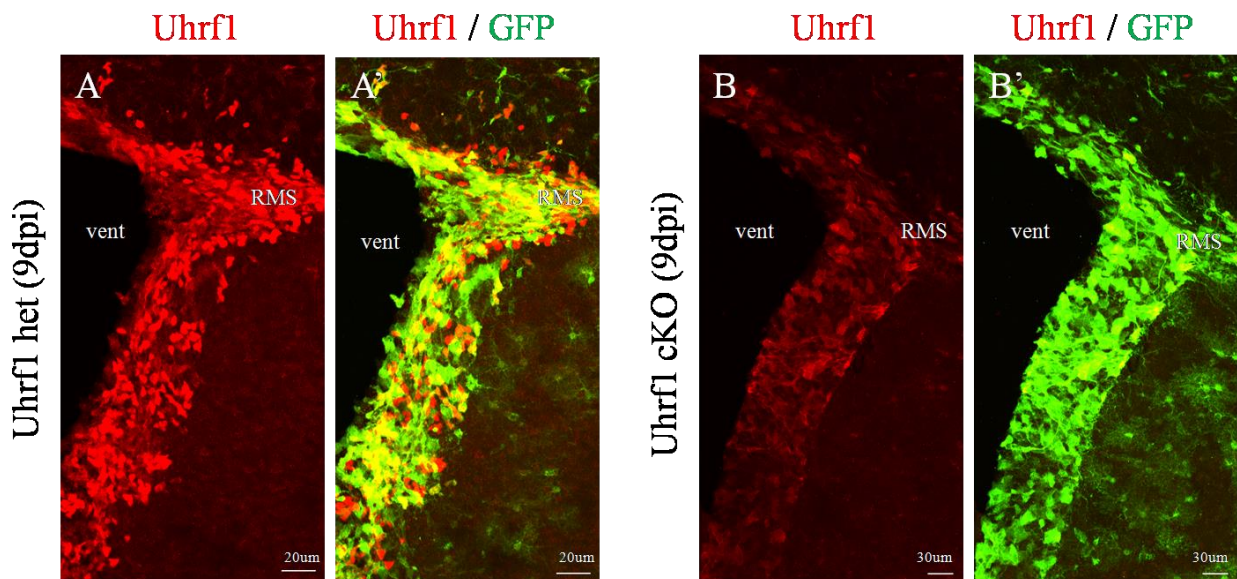
Figure 26: Uhrf1 immunoreactivity 9 days post induction

(A-B') Micrographs depicting the immunoreactivity for Uhrf1 and GFP in sagittal sections of the SEZ of adult mice heterozygous for GLAST^{CreERT2} and carrying one or two floxed allele of Uhrf1, 9 days after the end of tamoxifen induction (9 dpi). Note that Uhrf1 immunostaining is largely absent in GFP+ cells in cKOs. Abbreviations: RMS= rostral migratory stream; vent= ventricle

4.4.4 Analysis of adult SEZ neurogenesis after Uhrf1 deletion

4.4.4.1 Number of proliferating cells is decreased 9 days after Uhrf1 deletion

Since Uhrf1 is expressed by all cells labeled with a short BrdU pulse (Fig.21B), we first determined how this proliferating population is affected upon Uhrf1 deletion. Therefore at 9dpi, I injected the animals with BrdU 1h prior to their sacrifice and counted the number of GFP+ and GFP/BrdU double + cells per SEZ area. Quantification of GFP+ cells, although not significant, showed a slight decrease in the number of GFP+ cells per area in the cKO mice versus heterozygous controls (Fig.27A -C). Since we had observed similar recombination rates in heterozygous and cKO animals immediately after the end of tamoxifen application, this decrease in GFP+ cells may indicate proliferation defects. Indeed, the number of BrdU/ GFP double + cells was significantly decreased in cKO mice compared to heterozygous controls (Fig.27A, B and D).
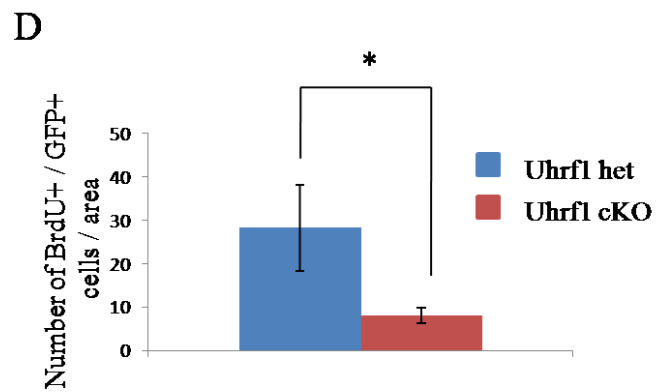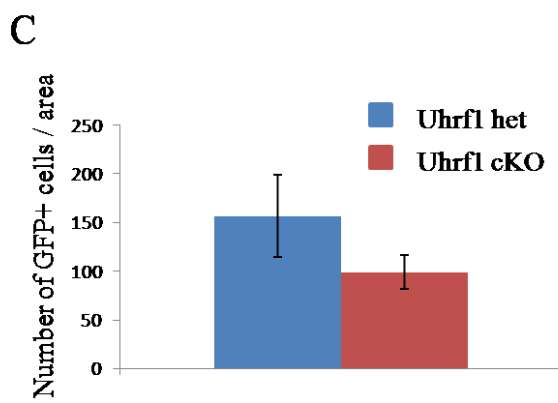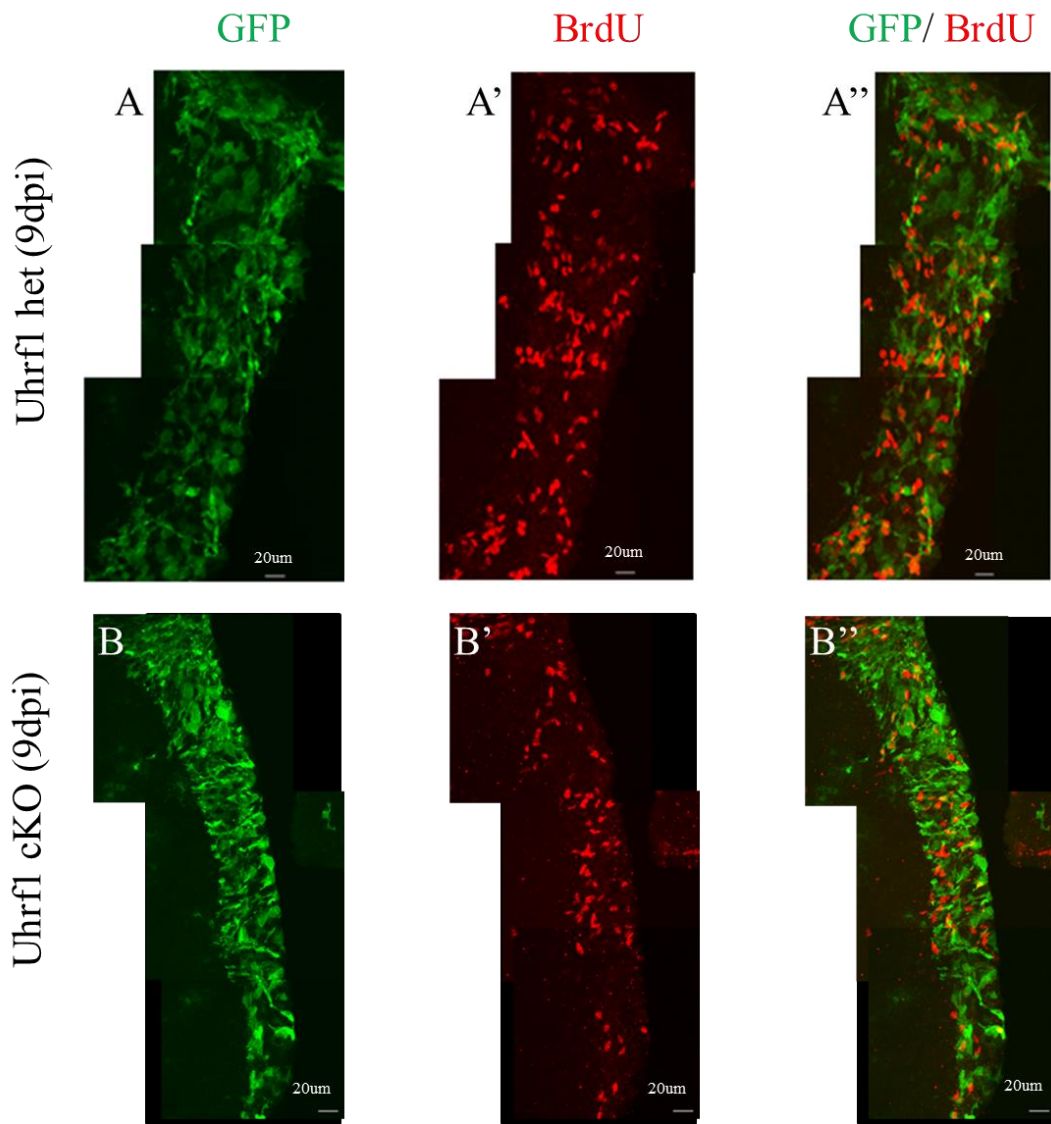
Figure 27: Decrease in BrdU incorporation in SEZ after Uhrf1 deletion
(A-B'') Micrographs depicting the immunoreactivity for BrdU and GFP in sagittal sections of the SEZ of adult mice being heterozygous or knock-out for Uhrf1 9 days after the end of tamoxifen (9dpi). **(C-D)** Histograms depicting the number of GFP+ (C) and GFP/BrdU double + cells (D) per area in the SEZ of Uhrf1 heterozygous and cKO mice 9dpi. Data are shown as mean ± SEM, n (animals analyzed) = 3; *p<0.05. Note the decrease in the number of BrdU positive cells in cKOs.

4.4.4.2 Number of proliferating cells remains low 4 weeks after Uhrf1 deletion

To further follow the phenotype upon Uhrf1 deletion at later stages, I analyzed the Uhrf1 cKO and heterozygous mice 4 weeks after Uhrf1 was gone. In accordance with what was observed 9 dpi, the number of GFP+ cells per area was still reduced at this later time point (Fig.28A-C). As BrdU is incorporated into the DNA during S phase, 1h BrdU pulse labels only cells in S phase of the cell cycle. In order to see if the decrease in the number of GFP+ cells is due to overall proliferation defects, I examined Ki67 that labels cells in all phases of the cell cycle except G0. In the SEZ, TAPs and neuroblasts constitute the two main populations that proliferate so to further understand if deletion of Uhrf1 affects one of these populations specifically or if its deletion causes a more general proliferation defect, Ki67 and DCX staining was combined and DCX-/Ki67+/GFP+ cells (proliferating TAPs) and DCX+/Ki67+/GFP+ cells (proliferating neuroblasts) were quantified. These first quantifications showed a decrease in both of these populations in the cKO SEZ compared to heterozygous controls (Fig.28D) suggesting that deletion of Uhrf1 leads to a more general proliferation defect rather than affecting a certain population.
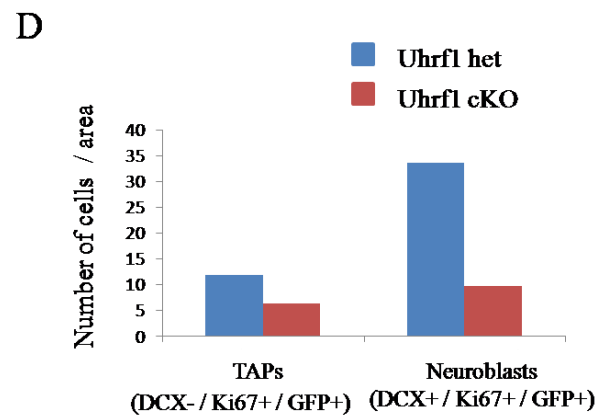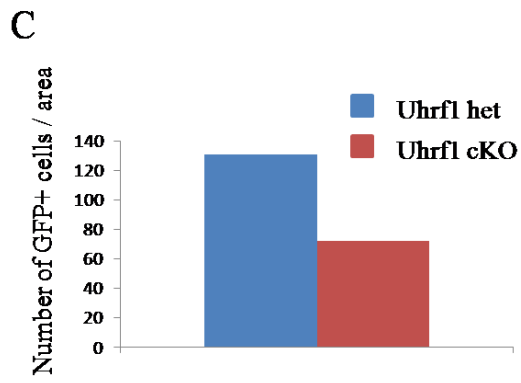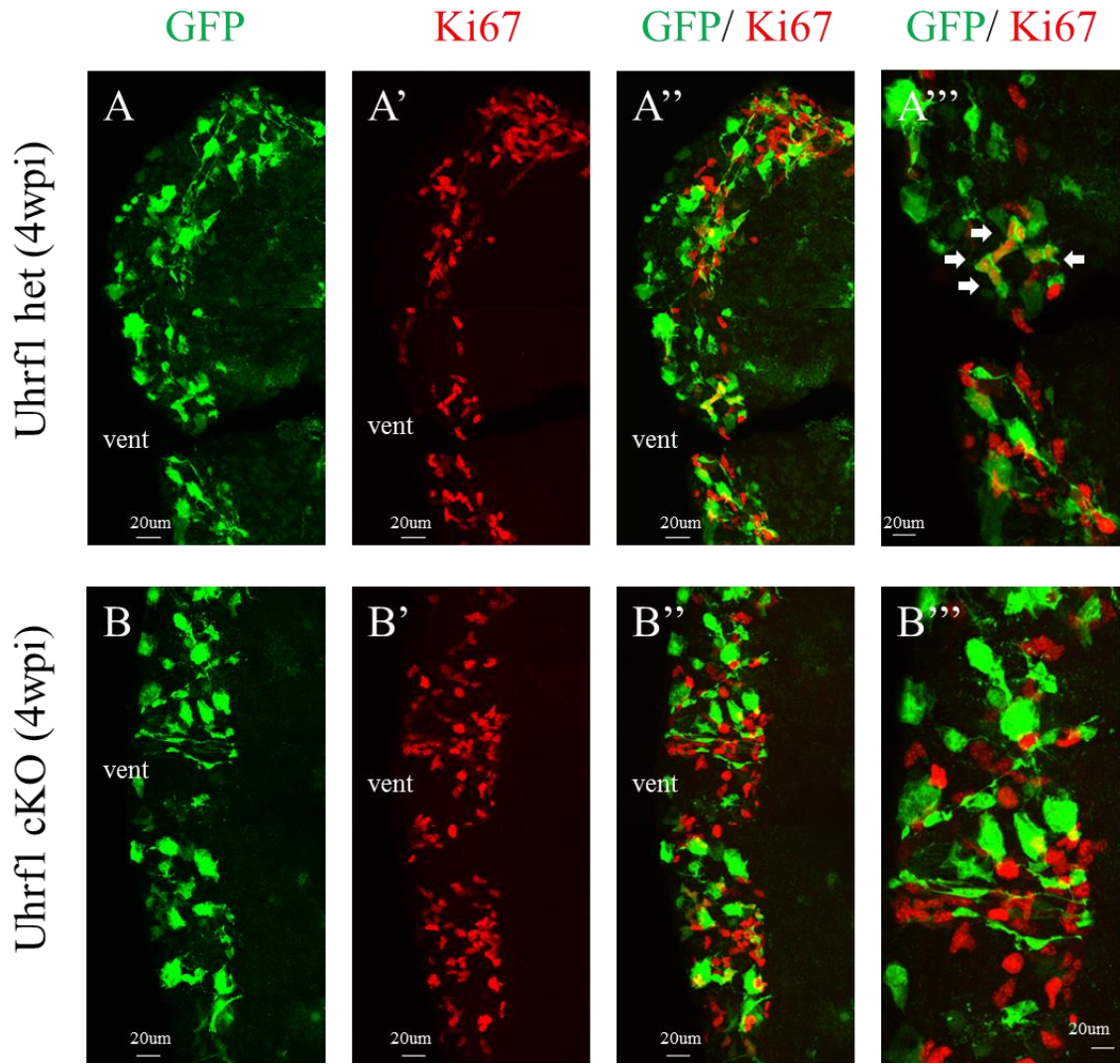
Figure 28: Number of proliferating TAPs and neuroblasts is decreased 4 weeks after Uhrf1 deletion
(A-B''') Micrographs depicting the immunoreactivity for Ki67 and GFP in sagittal sections of the SEZ of adult mice heterozygous or knock-out for Uhrf1 4 weeks after the end of tamoxifen treatment (4 wpi). Note that although Ki67 staining does not seem to be lower overall in cKOs, when one looks at a higher magnification one can see that most of these cells are not recombined and GFP+. **(C-D)** Histograms depicting the number of GFP+ cells (C) and GFP+/Ki67+/DCX- proliferating TAPs and GFP+/Ki67+/DCX+ proliferating neuroblasts (D) per area in the SEZ of Uhrf1 heterozygous and cKO mice 4wpi. n (animals analyzed) = 1

4.4.4.3 Neurogenesis in SEZ is impaired after Uhrf1 deletion

After examining the proliferation of NSC progeny, I also examined how the observed defects in proliferation are reflected in neurogenesis and counted the number of DCX+/GFP+ neuroblasts in the SEZ. As expected 4 weeks after deletion of Uhrf1, preliminary quantification of the number of recombined neuroblasts in the SEZ, showed a strong reduction in neuroblasts in the Uhrf1 cKOs to around half of the Uhrf1 heterozygous controls (Fig.29).

4.4.4.4 Impaired neurogenesis in the SEZ seems to result in reduced numbers of neurons reaching the OB

Neuroblasts that are born in the SEZ migrate through the RMS to the OB where they differentiate into OB interneurons (F Doetsch et al., 1997). Since our preliminary quantification showed a decrease in the number of neuroblasts in the SEZ upon Uhrf1 deletion, we wanted to see if this decrease causes a decrease in the number of neurons reaching the OB. Immunostainings for GFP and DCX showed to obvious decrease in the GFP+ cells in the OB 4 wpi (Fig.30A-B''). However at this time point many GFP+ cells may still derive from cells prior to Uhrf1 deletion (1-9 days). Indeed when we analyzed the OBs 4 mpi, a decrease in the GFP+ cells in the OB was detectable as well as a decrease in the DCX+ newly arriving neuroblasts (Fig.30C-D'').
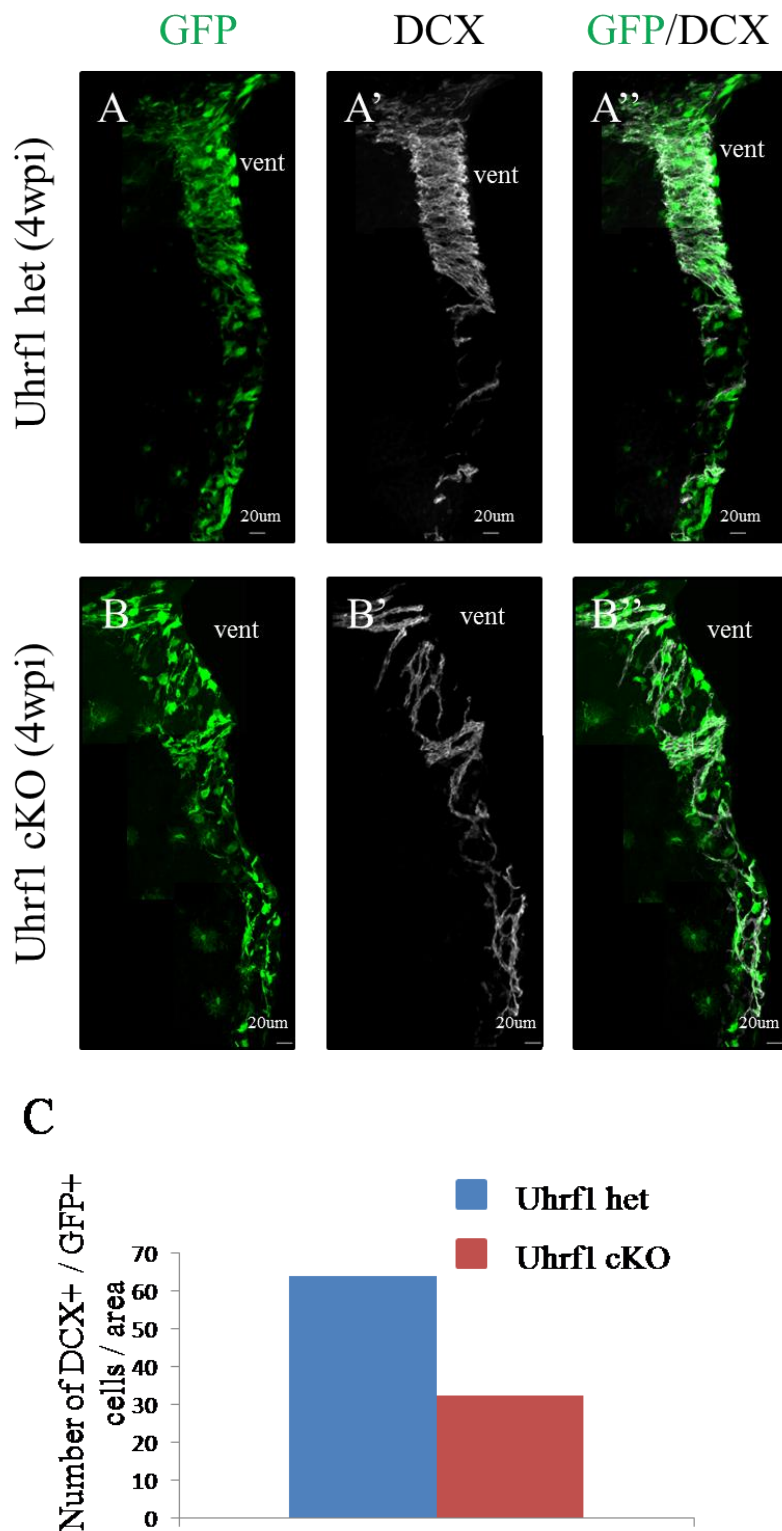
Figure 29: Number of neuroblasts is decreased in the SEZ 4 weeks after Uhrf1 deletion
(A-B''') Micrographs depicting the immunoreactivity for DCX and GFP in sagittal sections of the SEZ of adult mice heterozygous or knock-out for Uhrf1 4 wpi. **(C)** Histogram depicting the number of GFP+/DCX+ positive cells per area in the SEZ of Uhrf1 heterozygous and cKO mice 4wpi. n (animals analyzed) = 1 from each genotype.
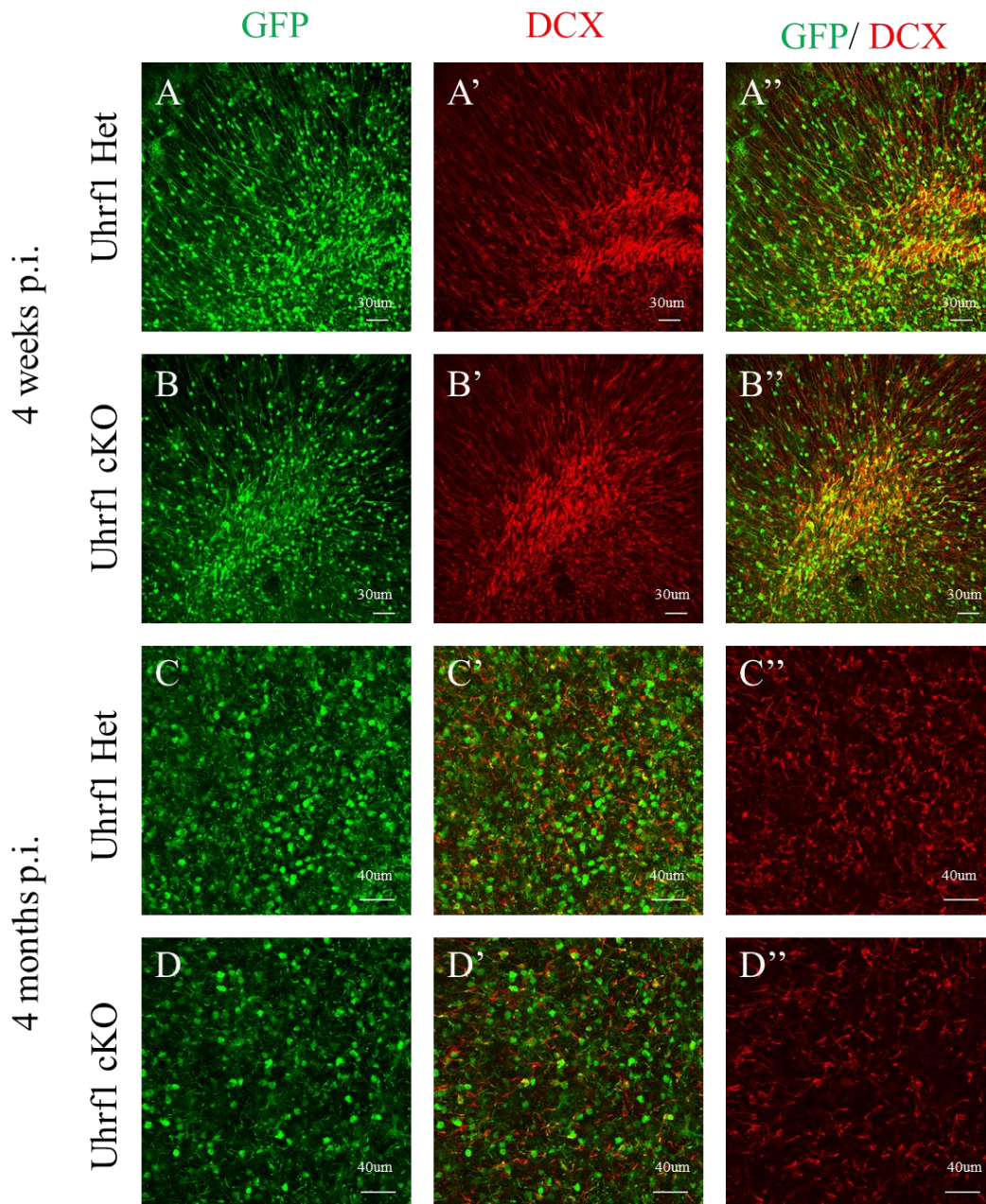
Figure 30: Number of neuroblasts in the OB is decreased 4 months after Uhrf1 deletion

(A-D''') Micrographs depicting the immunoreactivity for DCX and GFP in sagittal sections of the OB of adult mice heterozygous or knock-out for Uhrf1 4 weeks (A-B'') or 4 months (C-D'') after the end of tamoxifen treatment.

4.4.5 Analysis of adult DG neurogenesis after Uhrf1 deletion

Since we showed that Uhrf1 was also expressed in the DG, the second neurogenic region of the adult brain (Fig.22), we also examined the effect of Uhrf1 deletion in this region using the same conditional knock out strategy (Fig.24).

4.4.5.1 Number of proliferating cells decreased 9 days after Uhrf1 deletion

In the DG, Uhrf1 was strongly expressed by the proliferating cells labeled by 1h BrdU pulse whereas its expressing was going down in neuroblasts (Fig.22). In light of the expression pattern of Uhrf1, we first examined proliferation in the DG upon loss of Uhrf1. The number of GFP+ recombined cells in the adult DG 9 dpi was significantly decreased in cKO mice compared to heterozygous controls (Fig.31A, B and C) similar to the SEZ. Ki67 immunostainings of recombined cells (Ki67+/GFP+) also revealed their decrease in number in Uhrf1 cKO mice compared to heterozygous controls 9dpi (Fig.31A, B and D) in accordance with what was observed in the SEZ. Thus, Uhrf1 is required for proliferation in both adult neurogenic niches.
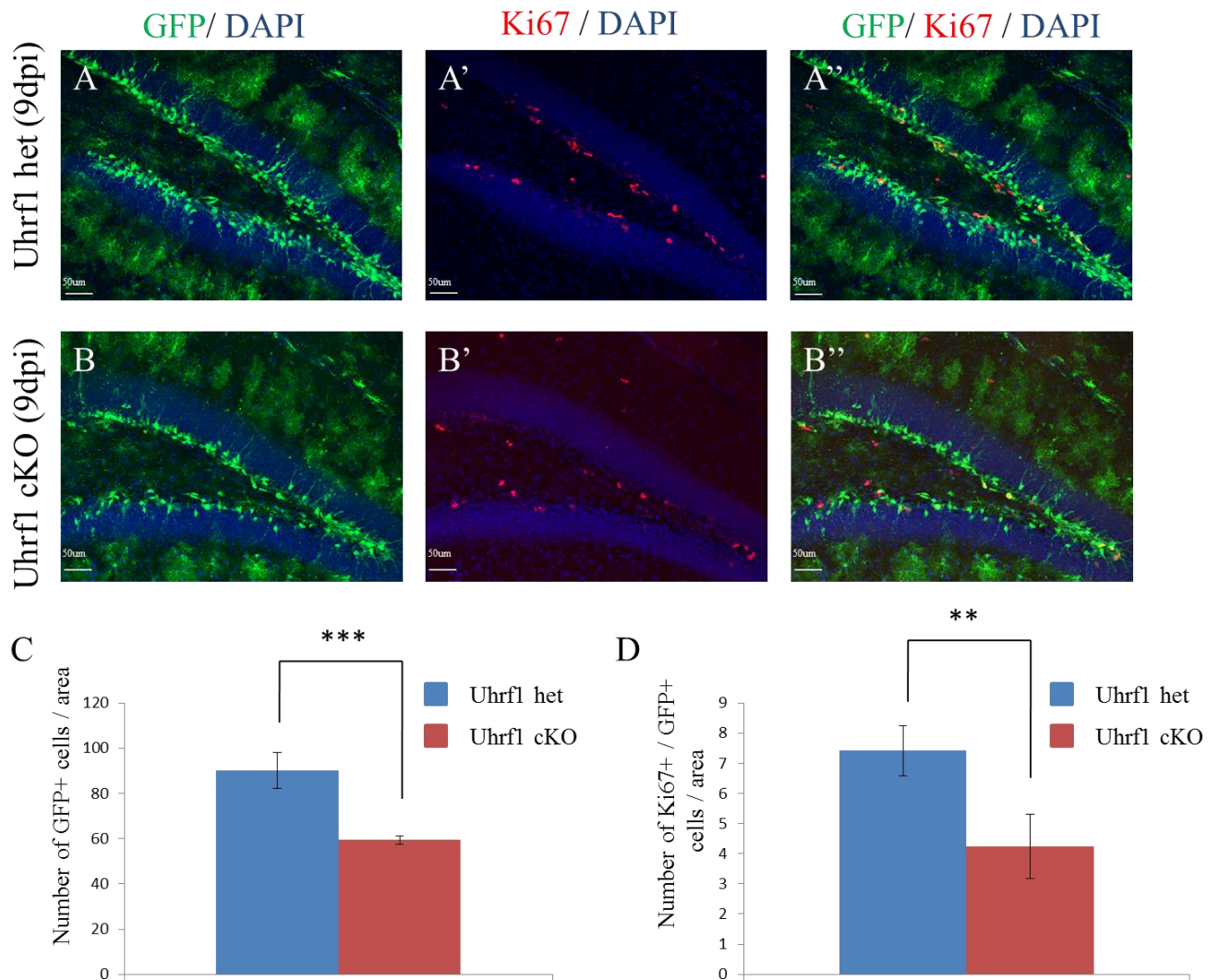
Figure 31: Loss of Uhrf1 leads to proliferation defects in the DG 9 days post injection
(A-B'') Micrographs depicting the immunoreactivity for GFP and Ki67 in sagittal sections of the DG of adult mice 9 days after the last injection of 5 days tamoxifen in Uhrf1 heterozygous (A) and Uhrf1 cKO mice (B). **(C)** Histograms depicting the number of GFP+ cells (C) and GFP/Ki67 double + cells (D) per area in the DG of Uhrf1 heterozygous and cKO mice 9dpi. Data are shown as mean ± SEM, n (animals analyzed) = 3; **p<0.01, ***p<0.001. Note the decrease in the number of GFP+ cells and Ki67+/ GFP+ cells in cKO DG compared to heterozygous controls 9dpi.

4.4.5.2 Number of proliferating cells remains low 4 weeks after Uhrf1 deletion

To further follow the phenotype at later stages, I also analyzed the DG in Uhrf1 cKO and heterozygous mice 4 weeks after Uhrf1 immunostaining is largely gone (Fig.32). Quantification of the number of GFP+ cells showed that the decrease in the number of GFP+ cells became even more severe reaching 50% of the heterozygous mice 4 weeks after Uhrf1 is lost (Fig.32A-D).

To determine if both TAPs and neuroblasts (the two main proliferating populations) are affected after deletion of Uhrf1, Ki67 and DCX stainings were combined and Ki67+/DCX-cells (proliferating TAPs) and Ki67+/ DCX+ cells (proliferating neuroblasts) were quantified. While proliferating TAPs were not yet significantly decreased (Fig.32E), proliferating neuroblasts showed a strong decrease in Uhrf1 cKO animals compared to heterozygous mice 4 weeks post induction (4wpi) (Fig.32E). Therefore we concluded that similar to its role in SEZ, Uhrf1 is also required for proliferation in the DG and proliferating neuroblasts are most affected.
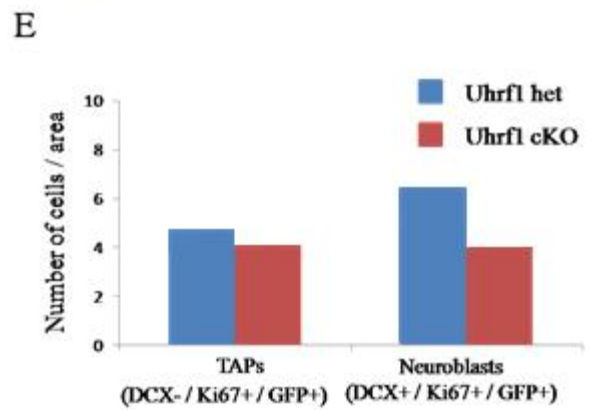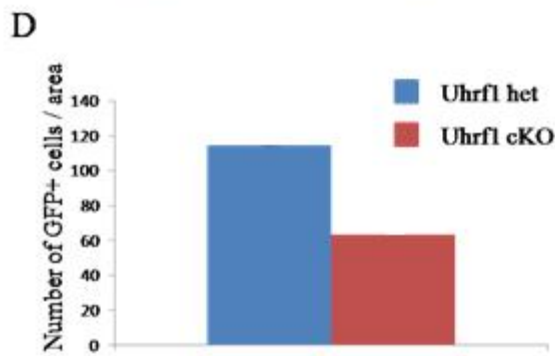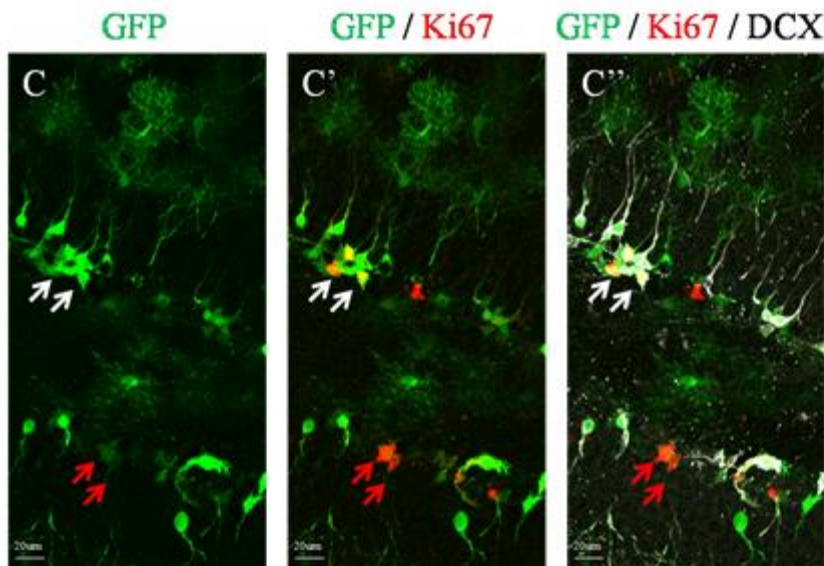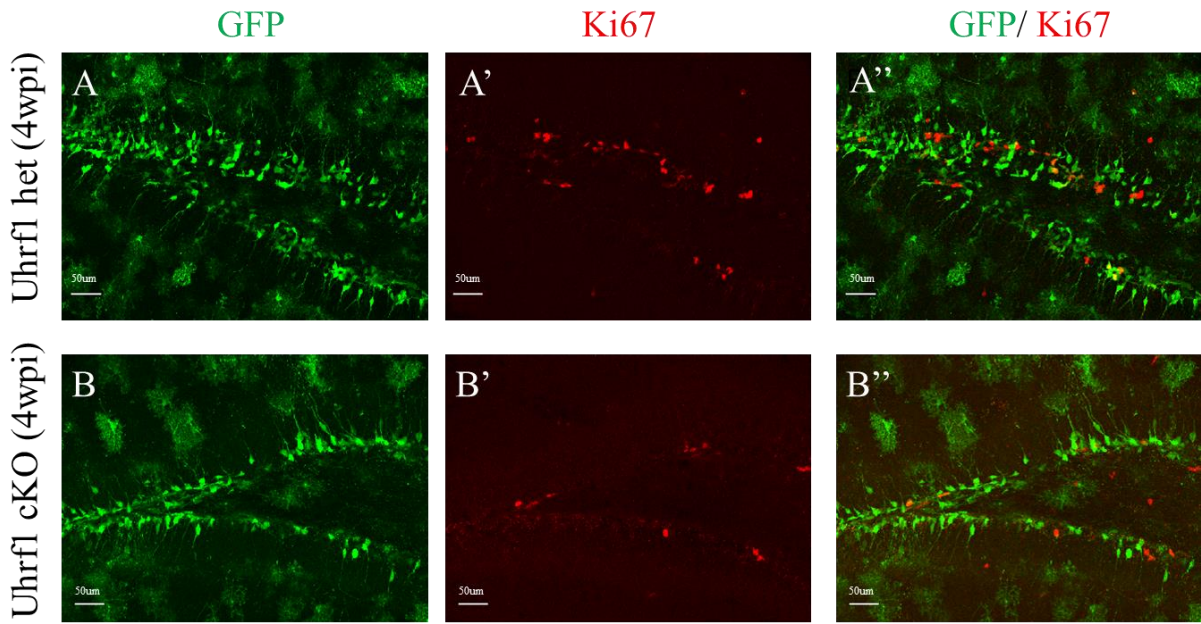
Figure 32: Proliferation defects observed upon Uhrf1 deletion in the DG persist 4 weeks post induction

(A-B'') Micrographs depicting the immunoreactivity for GFP and Ki67 in sagittal sections of the DG of adult mice 4 weeks after the loss of Uhrf1 in Uhrf1 heterozygous (A) and Uhrf1 cKO mice (B). **(C)** Histograms depicting the number of GFP+ cells (C) and GFP/Ki67 double + cells (D) per area in the DG of Uhrf1 heterozygous and cKO mice. Data are shown as mean ± SEM, n (animals analyzed) = 2. Note the decrease in the GFP+ cells and DCX+/Ki67+/GFP+ cells 4wpi.

4.4.5.3 Neurogenesis is strongly impaired in the DG upon Uhrf1 deletion

In order to determine if these defects in proliferation further manifest in a reduced number of newborn neurons, I stained for DCX (Fig.33). Indeed, GFP+/DCX+ cells were remarkably decreased 4wpi (Fig.33A, B and E) and this decrease in the number of GFP+/DCX+ cells became even more severe 4 months post induction (4mpi) with very few newborn neurons remaining in the cKO DG (Fig.33C, D and F). These data suggest that in addition to defects in proliferation, further defects in neuronal maturation and/or survival occur in the DG after Uhrf1 deletion resulting in more severe defects in neurogenesis compared to the SEZ phenotype. Consistent with defects in neuronal maturation, higher magnification of single DCX+ cells revealed an aberrant morphology in the Uhrf1cKOs with sorter dendrites and reduced size of the dendritic tree (Fig.34).
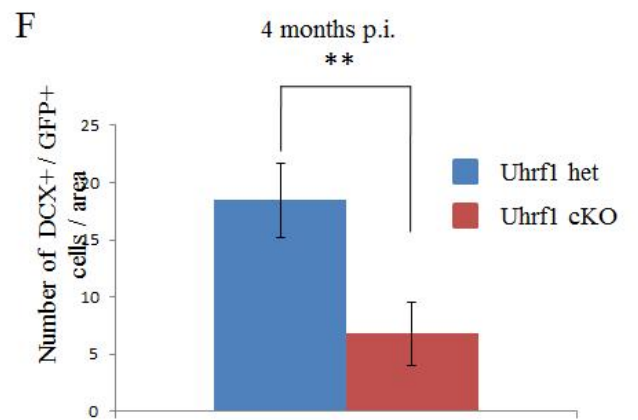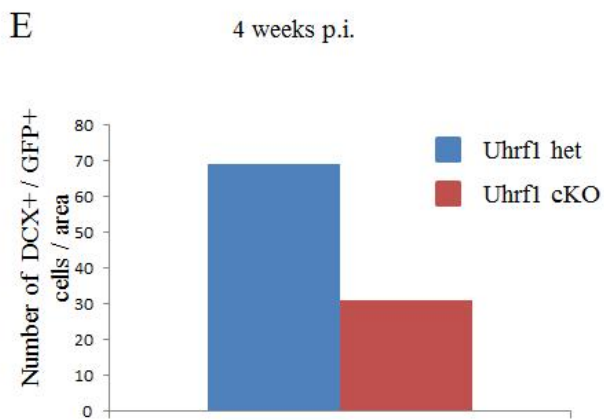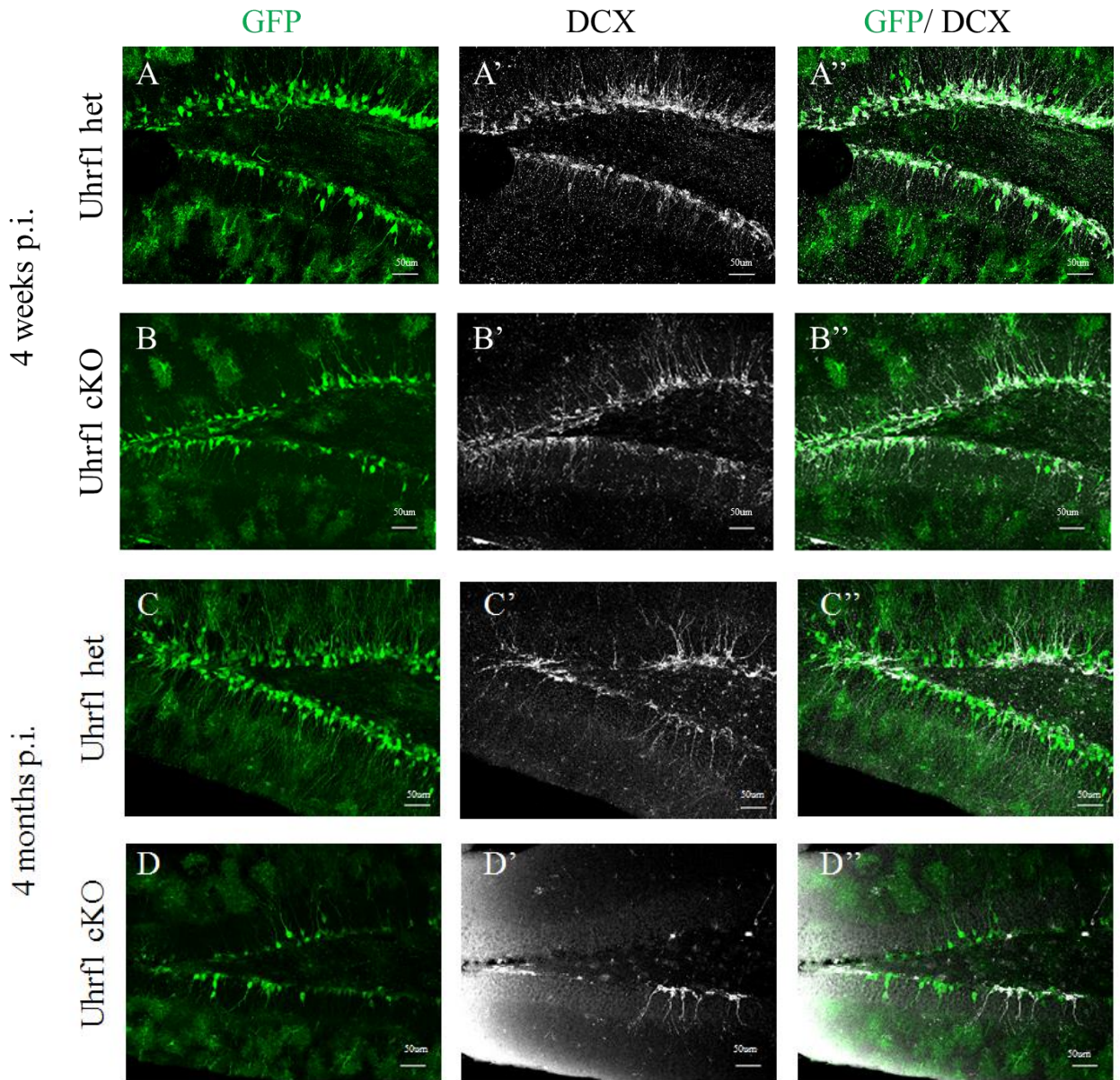
Figure 33: Deletion of Uhrf1 impairs neurogenesis in the DG

(A-D'') Micrographs depicting the immunoreactivity for GFP and DCX in sagittal sections of the DG of adult mice 4 weeks (A-B'') and 4 months (C-D'') after induction in Uhrf1 heterozygous (A-A'' and C-C'') and Uhrf1 cKO mice (B-B''and D-D''). **(G)** Histogram depicting the number of GFP/DCX double + cells per area 4 weeks (E) and 4 months (F) after induction in the DG of Uhrf1 heterozygous and cKO mice. Data are shown as mean ± SEM, n (animals analyzed) = 2 for 4 wpi and n=3 for 4mpi; **p<0.01. Note the decrease in the number of DCX+ cells both 4 wpi and 4mpi.
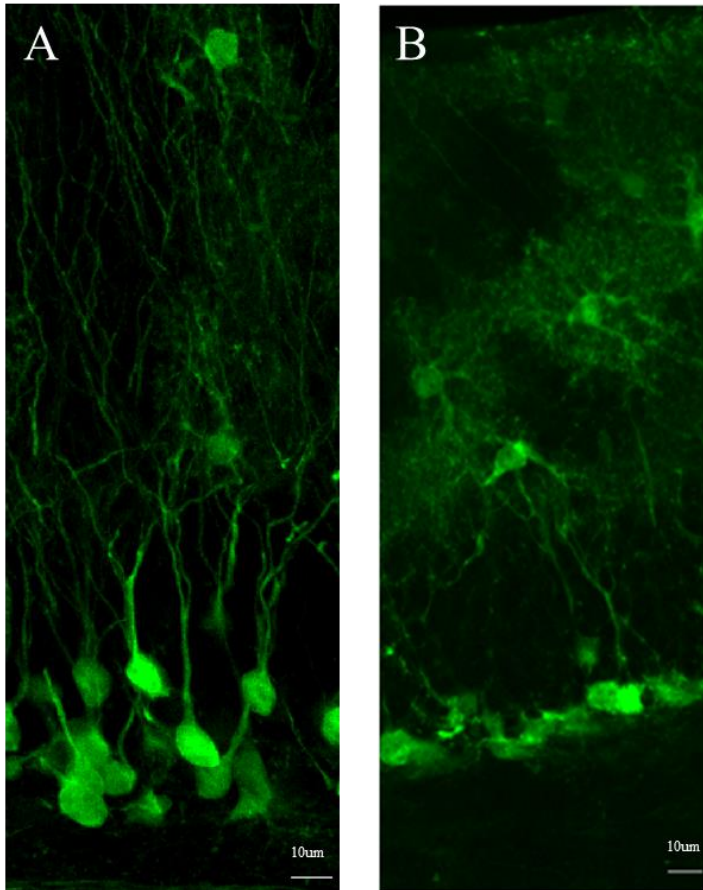
Figure 34: Deletion of Uhrf1 causes aberrations in dendrite morphology

(A-B'') Micrographs depicting the immunoreactivity for GFP in Uhrf1 heterozygous (A) and Uhrf1 cKO mice (B) 4 months after induction. Note that the dendritic tree of the heterozygous mice looks much more developed compared to the dendritic tree of the cKO mice.

4.5 Expression Pattern of Uhrf1 in Embryonic Mouse Brain and Its Functional Analysis in Embryonic Neurogenesis

Previous studies revealed that factors affecting adult neurogenesis often also play a role in development. Hence after observing strong impairment of adult neurogenesis in both SEZ and DG upon deletion of Uhrf1, we examined the role of Uhrf1 in the developing cerebral cortex.

4.5.1 Analysis of Uhrf1 expression during forebrain development

In order to understand the possible function of Uhrf1 during brain development, the expression pattern of Uhrf1 at different developmental stages of the murine forebrain was first analyzed. At all developmental stages analyzed, Uhrf1 expression was nuclear consistent with its location described above and previous functional analysis. From the beginning of neurogenesis at E12 to the end of neurogenesis at E16, it was highly expressed in virtually all apical progenitors lining the ventricle both in the dorsal and the ventral telencephalon (Fig.35).
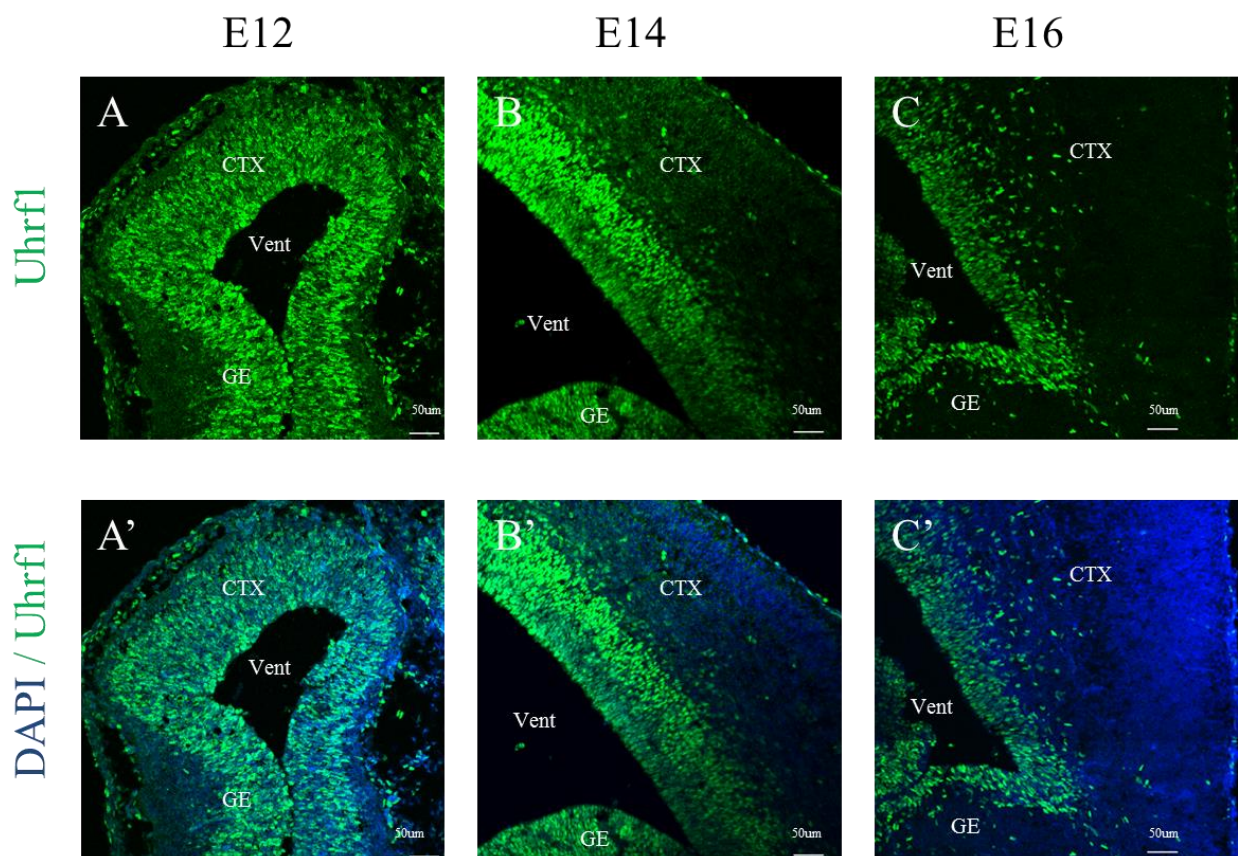
Figure 35: Expression analysis of Uhrf1 protein at different stages of forebrain development

(A-C') Micrographs of coronal sections of the developing telencephalon at different developmental stages (E12-E16) labeled for Uhrf1 and DAPI. Note that Uhrf1 is expressed in apical progenitors close to the ventricle both in the cerebral cortex and in the ganglionic eminence. Abbreviations: CTX= cortex; GE= ganglionic eminence; Vent= ventricle

4.5.2 Detailed expression analysis at mid-neurogenesis

To better identify the cell type expressing Uhrf1 at mid neurogenesis (E14), immunohistochemicalstainings for Pax6 (labeling apical stem and progenitor cells), Tbr2 (labeling basal progenitors) and βIII-tubulin (labeling newborn neurons) was performed (Fig.36). Double immunostainings with anti-Uhrf1 antibody showed that at mid neurogenesis, Uhrf1 is highly expressed by the Pax6+ apical progenitors (Fig.36A-A') whereas its expression is very low or absent in the Tbr2 + basal progenitors (Fig.36B-B'). Moreover some cells that are Uhrf1 and Pax6 double + were found above the basal progenitor layer. These could be outer radial glial cells which are another progenitor type that was recently described (Shitamukai et al., 2011; X. Wang et al., 2011) (Fig.36A-A'). There were no βIII-tubulin/Uhrf1 double + cells indicating that Uhrf1 is strongly down regulated upon neuronal commitment (Fig.36C-C').Taken together, this expression pattern suggested a role of Uhrf1 in the regulation of different subsets of progenitor cells during cortical neurogenesis.

Since Uhrf1 was not only found to be expressed in the dorsal but also in the ventral part of the telencephalon (ganglionic eminence), the ventral progenitor specific transcription factors (TF) Mash1 (also called Ascl1) and Olig2 was utilized for further analysis. Double immunostainings showed that all Mash1+ and Olig2+ progenitors were also Uhrf1+ suggesting a role of Uhrf1 not only in dorsal but also in the ventral telencephalic progenitors (Fig.36D-E').
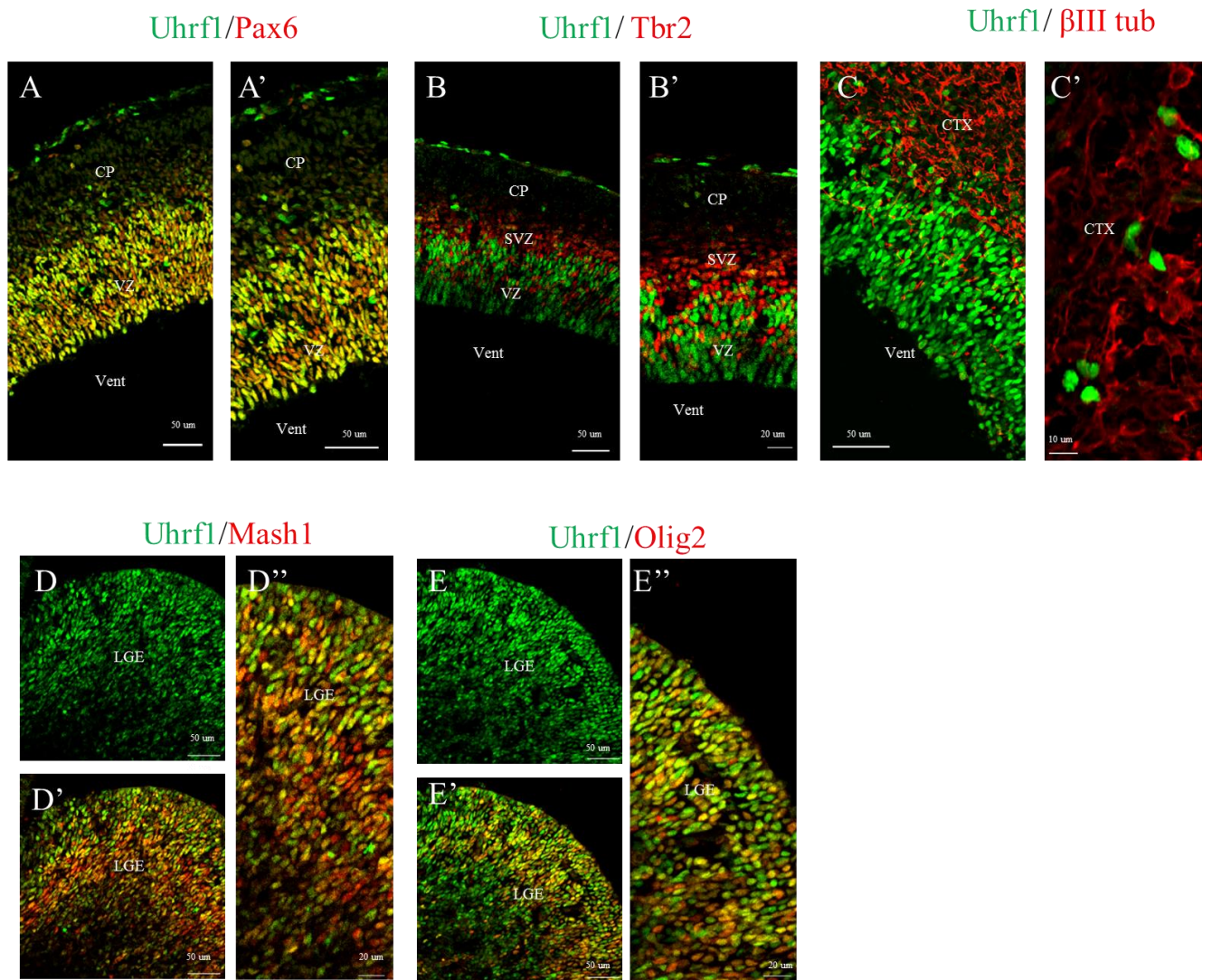
Figure 36: Detailed expression analysis of Uhrf1 at mid neurogenesis

(A-C') Micrographs depicting the co-expression analysis of Uhrf1 together with the radial glial transcription factor (TF) Pax6 (A-A'), the basal progenitor TF Tbr2 (B-B'), the neuronal marker βIII-tubulin (C-C') in coronal sections of the developing cerebral cortex at E14. Note that Uhrf1 is expressed by all Pax6+ apical progenitors and that most of the Tbr2+ basal progenitors and βIII-tubulin+ neurons are Uhrf1-. **(D-E'')** Micrographs depicting the co-expression analysis of Uhrf1 together with the TFs Mash1 (D-D'') and Olig2 (E-E'') in coronal sections of the lateral ganglionic eminence (LGE) at E14. Note that Uhrf1 is expressed by almost all Mash1+ and Olig2+ progenitors in the LGE. Abbreviations: CTX= cortex; CP= cortical plate, SVZ= subventricular zone; LGE= lateral ganglionic eminence; Vent= ventricle; VZ= ventricular zone

4.5.3 Deletion of Uhrf1 at the onset of neurogenesis

Since the above described expression pattern suggested a potential role of Uhrf1 in progenitor cells of the embryonic telencephalon, we wanted to study its function by conditional deletion of Uhrf1.

In order to delete Uhrf1 selectively in the dorsal telencephalon, the Emx1^{Cre} line which expresses Cre recombinase in the locus of Emx1 and therefore in the progenitors of the developing dorsal telencephalon from E9.5 onwards, was used (Iwasato et al., 2000). Consistent with the previous data (Cappello et al., 2006, 2012), Cre expression effectively deleted Uhrf1 in the neocortex, the hippocampal anlage and the cortical hem and Uhrf1 immunoreactivity was no longer detectable at E11 whereas Uhrf1 could still be nicely detected in the ventral telencephalon (GE) where Cre is not expressed (Fig.37).
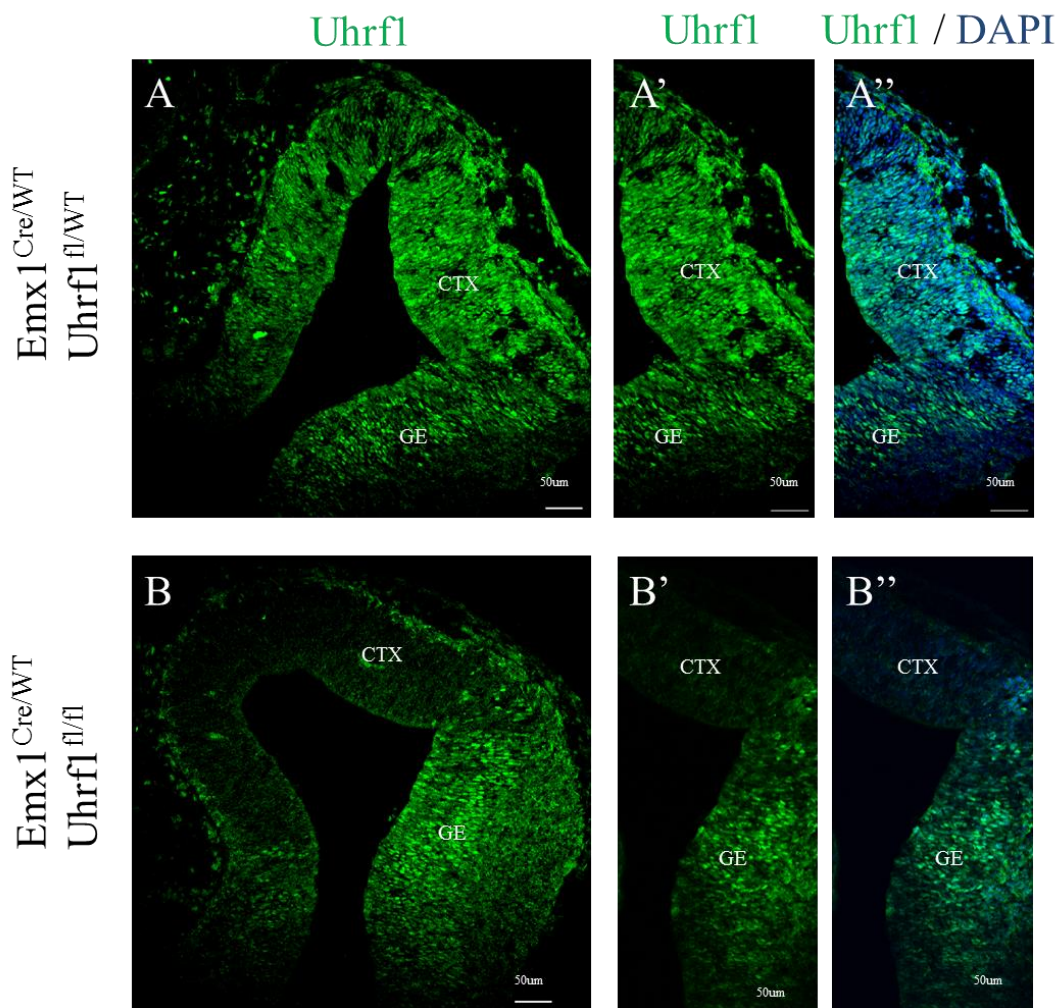
Figure 37: Deletion of Uhrf1 by Emx1$^{Cre/WT}$ at mid neurogenesis

(A-B'') Micrographs depicting the immunoreactivity for Uhrf1 in coronal sections of Emx1$^{Cre/WT}$; Uhrf1 $^{fl/WT}$ (A-A'') or Uhrf1 $^{fl/fl}$ (B-B'') mice at E11. Note that Uhrf1 expression is lost in the cerebral cortex including the cortical hem whereas it is still detected in the ganglionic eminence where Cre activity is not observed. Abbreviations: CTX= cortex; GE= ganglionic eminence

4.5.4 Survival of Uhrf1 mutants and gross morphological analysis

Emx1$^{Cre/WT}$; Uhrf1$^{fl/fl}$ animals were born at the expected Mendelian distribution and they survived normally into adulthood (data not shown). They did not show overall growth retardations compared to Emx1$^{Cre/WT}$;Uhrf1$^{fl/WT}$ or Uhrf1$^{WT/WT}$ animals however they had striking degeneration in the cerebral cortex at early postnatal stages (Fig.38A). Although only a moderate decrease in cortical thickness was observed in mutant brains at postnatal day 0 (P0), severely reduced cortical and hippocampal size was observed at P27 (Fig.38A, C-F). Quantitative measurements of cortical length and width indicate, as a percentage of control, a reduction of 30% and 20% respectively in P27 mutants whereas no change in the length or width of cerebellum where Uhrf1 is not deleted was observed (Fig.38B).Immunostaining for the post-mitotic neuronal marker NeuN confirmed that the mutant cortex contained fewer neurons than heterozygous littermate controls (Fig.38C-D). Moreover NeuN staining showed that the hippocampus is severely reduced and the DG had not formed in the mutants at P27 (Fig.38 E-F).

A

Emx1^{Cre/WT}
Uhrf1^{fl/WT}

Emx1^{Cre/WT}
Uhrf1^{fl/fl}

P0

CTX

CB   OB

CTX

CB   OB

P27

CTX

CB   OB

CTX

CB   OB

B

Emx1^{Cre/WT}; Uhrf1^{fl/WT}
Emx1^{Cre/WT}; Uhrf1^{fl/fl}

**   **

Length (cm)

CTX length   CTX width   CB length   CB width

Emx1^{Cre/WT}
Uhrf1^{fl/WT}

C

NeuN

CTX

WM

50um

Emx1^{Cre/WT}
Uhrf1^{fl/fl}

D

CTX

WM

50um

NeuN

E

Emx1^{Cre/WT}
Uhrf1^{fl/WT}

Hippo

DG

100um

F

Emx1^{Cre/WT}
Uhrf1^{fl/fl}

CTX

Hippo

100um
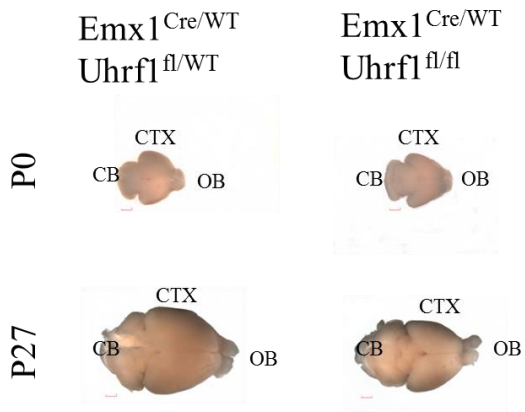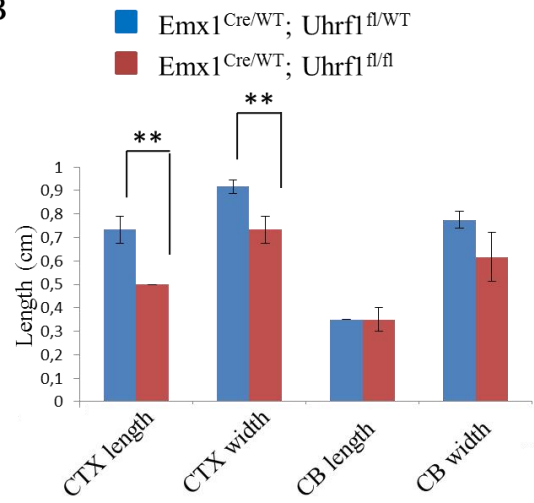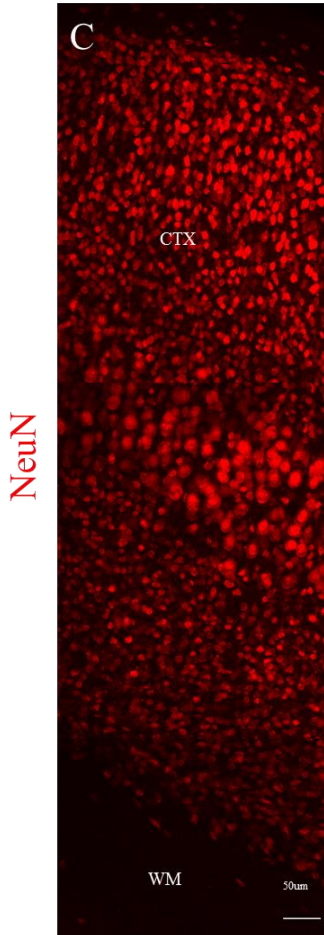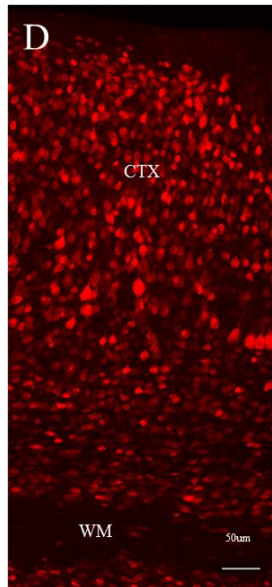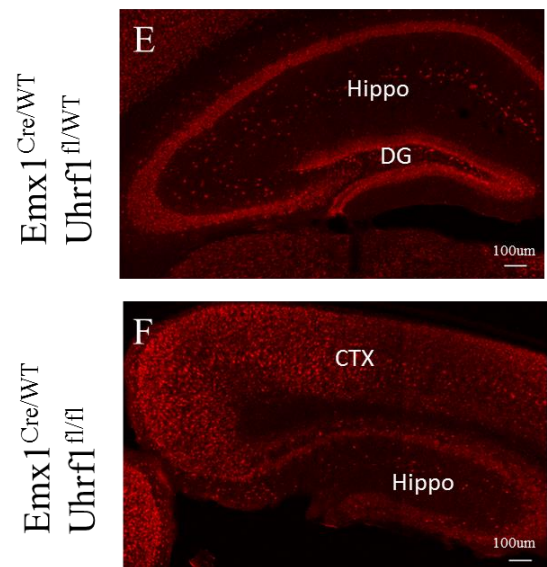
Figure 38: Severe cerebral cortex degeneration is observed after deletion of Uhrf1 in this region

(**A**) Images of brains of Emx1$^{Cre/WT}$; Uhrf1$^{fl/WT}$ and Uhrf1$^{fl/fl}$animals at P0 and P27. Note the reduction in cerebral cortex size in Uhrf1 mutants. (**B**) Histogram depicting the length and width of cerebral cortex and cerebellum of Emx1$^{Cre/WT}$; Uhrf1$^{fl/WT}$ and Uhrf1$^{fl/fl}$animals. Data are shown as mean ± SEM, n (embryos analyzed) ≥ 3; **p<0.01. Note that the cerebral cortex has a smaller length and width in the mutants whereas cerebellum is not affected. (**C-F**)Micrographs depicting the immunoreactivity for NeuN in coronal sections of Emx1$^{Cre/WT}$; Uhrf1$^{fl/WT}$ and Uhrf1$^{fl/fl}$mice at P27. Note that NeuN immunohistochemistry reveals a strong decrease in neuron number in thecerebralcortex of the mutant (C-D). The hippocampus is severely reduced and dentate gyrus did not form in the mutant (E-F). Abbreviations: CB=cerebellum; CTX=cortex; DG= dentate gyrus; Hippo=hippocampus; OB=olfactory bulb; WM=white matter

4.5.5 Proliferation of progenitors is affected in the Uhrf1 mutants

As Uhrf1 is expressed in the progenitors in the developing cerebral cortex, we thought alterations in the proliferation of progenitors could account for the reduction of cortical thickness observed in mutants at prenatal stages. In order to analyze proliferation of progenitors, immunostainings for phospho- Histone H3 (PH3) was used to detect cells in the G2/M phase of the cell cycle was used (Fig.39). Since different progenitors divide at different positions, PH3 allowed discriminating between apical progenitors that divide at the ventricular zone and the non-apical progenitors that divide at more basal positions in the tissue. Dividing progenitor were quantified in several sections from rostral to caudal levels at three developmental stages – at E12, immediately after the Uhrf1 protein is lost and when the first non-apically dividing cells begin to appear, at E14 which is the peak of neurogenesis and at E16. Although there was not a significant change in the total number of proliferating cells at any time points analyzed (Fig.39G,H and I)from E14 onwards, we observed an increase in the percentage of cells dividing at non apical positions and a decrease in the percentage of cells dividing at apical positions (Fig.39G',H' and I').
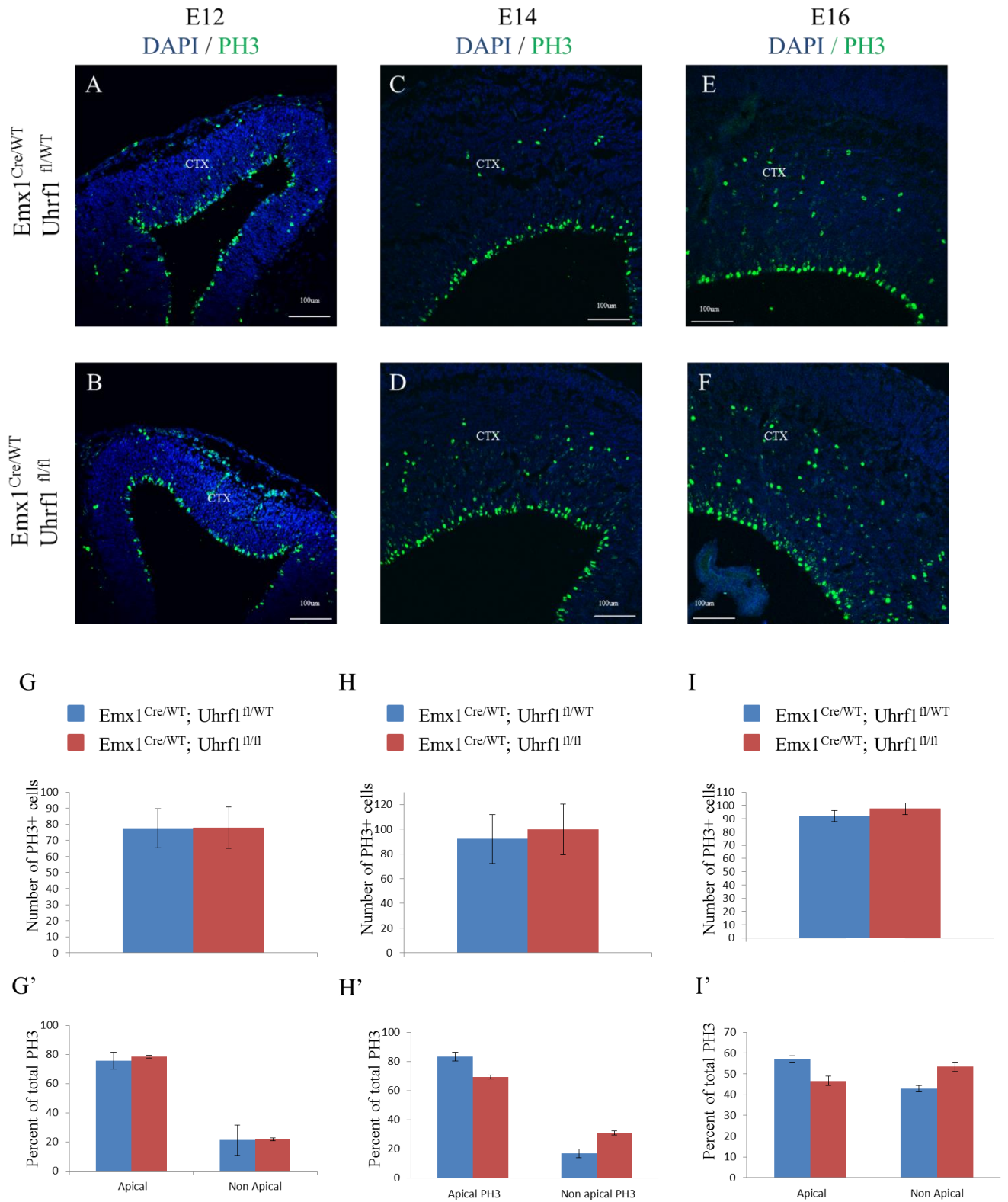
Figure 39: Proliferation of progenitors in the developing cerebral cortex is affected upon Uhrf1 deletion

(A-F) Micrographs depicting the immunoreactivity for PH3 in coronal sections of Emx1$^{Cre/WT}$; Uhrf1$^{fl/WT}$ or Uhrf1$^{fl/fl}$ mice at E12 (A-B), E14 (C-D) and E16 (E-F). Note the increase in non-apically dividing cells from E14 on upon deletion of Uhrf1. **(G-I')** Histograms depicting the total number of PH3+ cells or percentages of apical and non-apical PH3 cells among the total PH3+ cells in coronal sections of Emx1$^{Cre/WT}$; Uhrf1 $^{fl/WT}$ or Uhrf1 $^{fl/fl}$mice at E12 (G-G'), E14 (H-H') and E16 (I-I'). Data are shown as mean ± SEM, n (embryos analyzed) ≥ 3; **p<0.01.Abbreviations: CTX= cortex

4.5.6 Progenitor identity in the Uhrf1 mutants

As described in the introduction, apically and non-apically dividing cells present different types of progenitors that can be characterized by expression of different transcription factors. Radial glial cells that divide apically are characterized by expression of Pax6 whereas intermediate progenitors that divide non-apically in the SVZ are characterized by expression of Tbr2. Yet a more recently identified type of progenitor cells namely oRG cells are also characterized by expression of Pax6 but they undergo mitosis at non-apical positions above the SVZ. Thus immunohistochemistry against Pax6 and Tbr2 allowed us to examine the molecular identity of progenitors in order to understand if the changes in the position of proliferating cells observed in the Uhrf1 mutant cerebral cortices are accompanied by changes in their identity upon Uhrf1 deletion.

Remarkably, the expression of Tbr2 was maintained in the mutant cortices at their proper localization at both time points analyzed (Fig.40) while the distribution of Pax6 was significantly altered in the mutant cortices such that more Pax6+ cells were observed in ectopic locations outside the Pax6 dense band while there was no change in the total number of Pax6+ cells at both time points analyzed (Fig.41). Moreover when we had a closer look at the nuclei at higher magnifications, we saw that in contrast to the elongated shape of the nuclei of apical progenitors found in the control animals, nuclei in the mutants lost their characteristic elongated shape and became less elongated (Fig.42). As the elongated shape of the nuclei was shown to be lost upon inhibition of the interkinetic nuclear migration (INM) (Liu, Hashimoto-Torii, Torii, Ding, & Rakic, 2010), changes in nuclear shape upon Uhrf1 deletion may indicate defective INM.
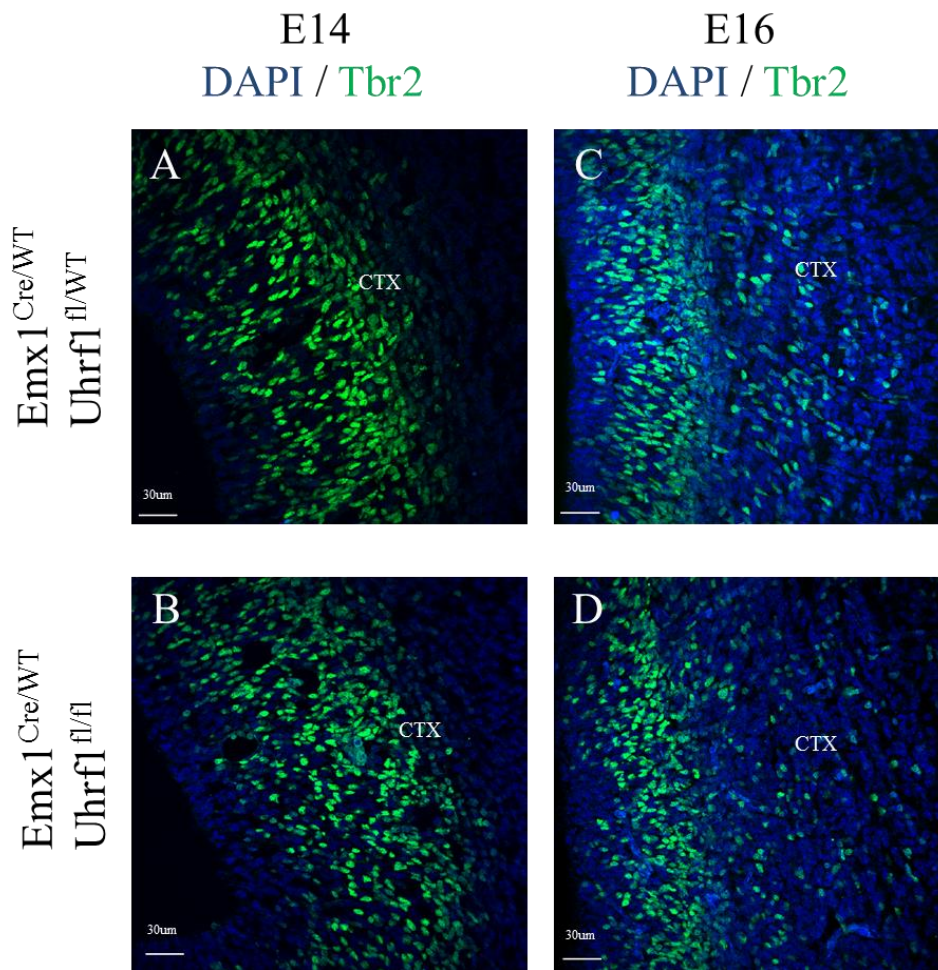
Figure 40: Tbr2 positive non apical progenitors are not affected by deletion of Uhrf1

(A-D) Micrographs depicting the immunoreactivity for Tbr2 in coronal sections of Emx1$^{Cre/WT}$; Uhrf1$^{fl/WT}$ or Uhrf1$^{fl/fl}$ mice at E14 (A-B) and E16 (C-D). Note that neither the distribution nor the apparent density and number of Tbr2 positive cells seem to be altered upon Uhrf1 deletion.
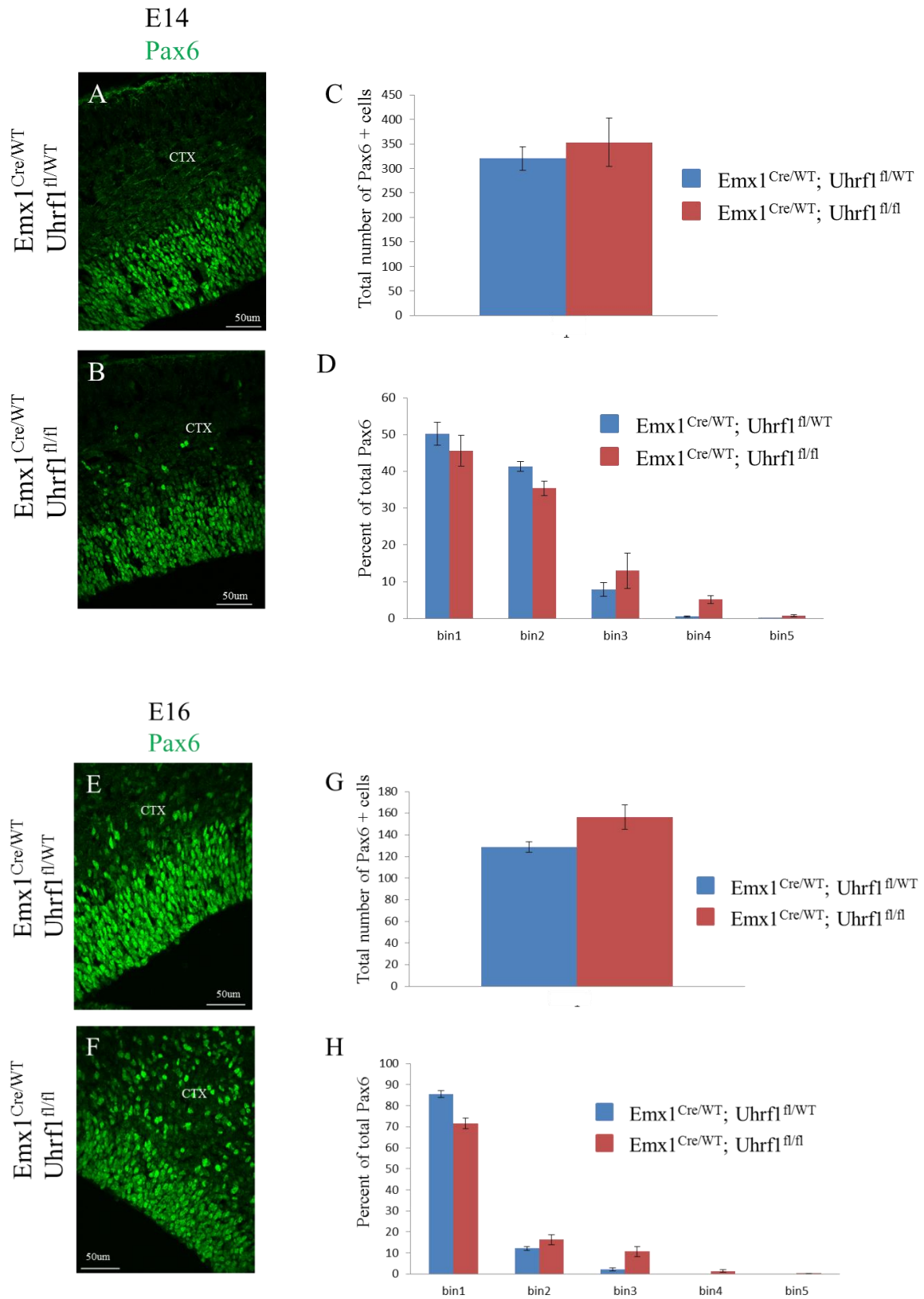
Figure 41: Distribution of Pax6 positive cells is altered upon Uhrf1 deletion

(A-B and E-F) Micrographs depicting the immunoreactivity for Pax6 in coronal sections of Emx1$^{Cre/WT}$; Uhrf1$^{fl/WT}$ or Uhrf1$^{fl/fl}$ mice at E14 (A-B) and E16 (E-F). **(C and G)** Histograms depicting the total number of Pax6+ cells per area in coronal sections of Emx1$^{Cre/WT}$; Uhrf1$^{fl/WT}$ or Uhrf1$^{fl/fl}$ mice at E14 (C) and E16 (G). **(D and H)** Histograms depicting the percentage of Pax6 found in each bin of the cerebral cortex divided into five equally sized bins in coronal sections of Emx1$^{Cre/WT}$; Uhrf1$^{fl/WT}$ or Uhrf1$^{fl/fl}$ mice at E14 (D) and E16 (H). Data are shown as mean ± SEM, n (embryos analyzed) ≥ 3; *p<0.05, **p<0.01. Note the increase of Pax6+ cells in upper bins at both time points analyzed. Abbreviations: CTX= cortex
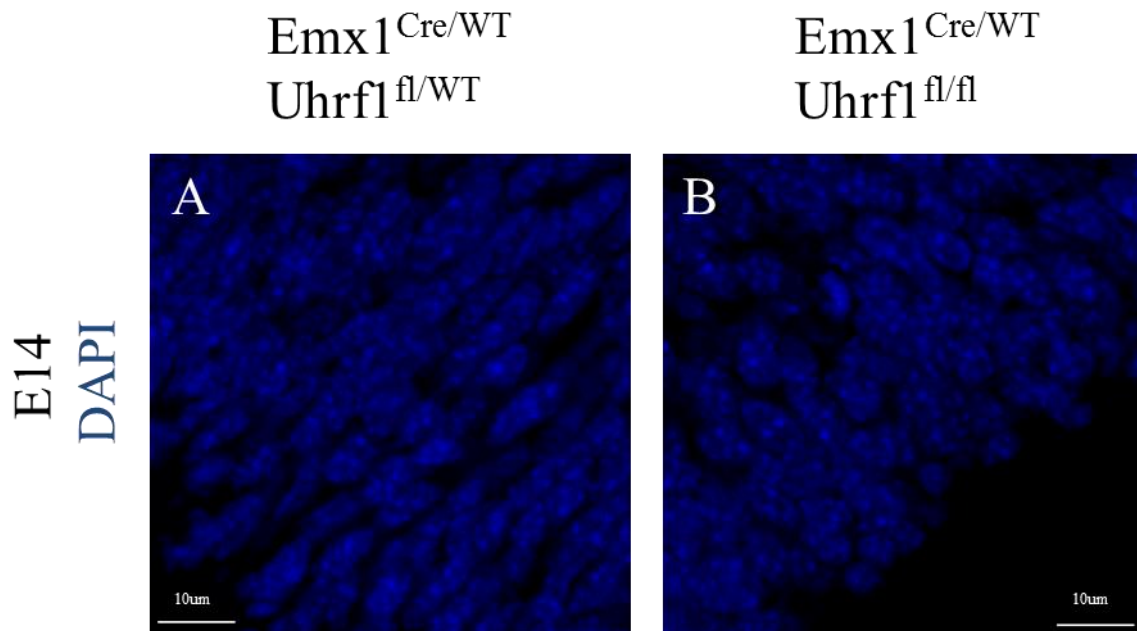
Figure 42: Apical progenitors seem to lose their elongated shape upon Uhrf1 deletion

(A-B) Micrographs depicting the DAPI in coronal sections of Emx1$^{Cre/WT}$; Uhrf1$^{fl/WT}$ or Uhrf1$^{fl/fl}$ cerebral cortex at E14. Note that nuclei of apical progenitors in the cerebral cortex of Uhrf1$^{fl/fl}$ animals appear less elongated in contrast to the nuclei of progenitors in the Uhrf1$^{fl/WT}$ animals.

4.5.7 Layering of the cerebral cortex is not affected in the Uhrf1 mutants

During embryonic neurogenesis specific neurons are generated at different developmental stages as described in the introduction. These neurons settle at different layers in an inside-out manner such that the early born neurons settle in deeper layers and the later born neurons settle in upper layers which then leads to the laminated structure of the cerebral cortex (Molyneaux et al., 2007) (Fig.4). The observations that the proliferative behavior of mutant progenitors was changed and the cortex of Uhrf1 mutants was considerably smaller compared to WT littermates raised the question whether specific neuronal subtypes were lost in the mutant embryos. To examine if the laminated structure of the cortex was preserved in the Uhrf1 mutants and if different neuronal subtypes are generated, the identity of neurons was examined using antibodies specific for certain neuronal subtypes. Early born neurons that settle in the deep layers of the cortex were identified by immunostainings for Tbr1, Foxp2 and Ctip2 (Fig.43A-F) and later born neurons that settle in upper layers were identified by Cux2 staining (Fig.43G-H). Although an overall decrease in the density of all neuronal subtypes was observed, the strongest decrease was in the number of Cux2+ cells (Fig.43A-H) which could be explained by the high number of cell death observed after E14 (Fig.44) which probably leads to a strong decrease in the number of progenitors that form the upper layers. Moreover some cells that are labeled by Ctip2 and settle in layers V and IV had very large nuclei which was also observed in the Dnmt1 mutants (Hutnick et al., 2009a). However despite these changes in the neuronal density and nuclear morphology, all of the different neuronal subtypes were found at their proper locations suggesting that Uhrf1 deletion does not cause major defects in neuronal migration.
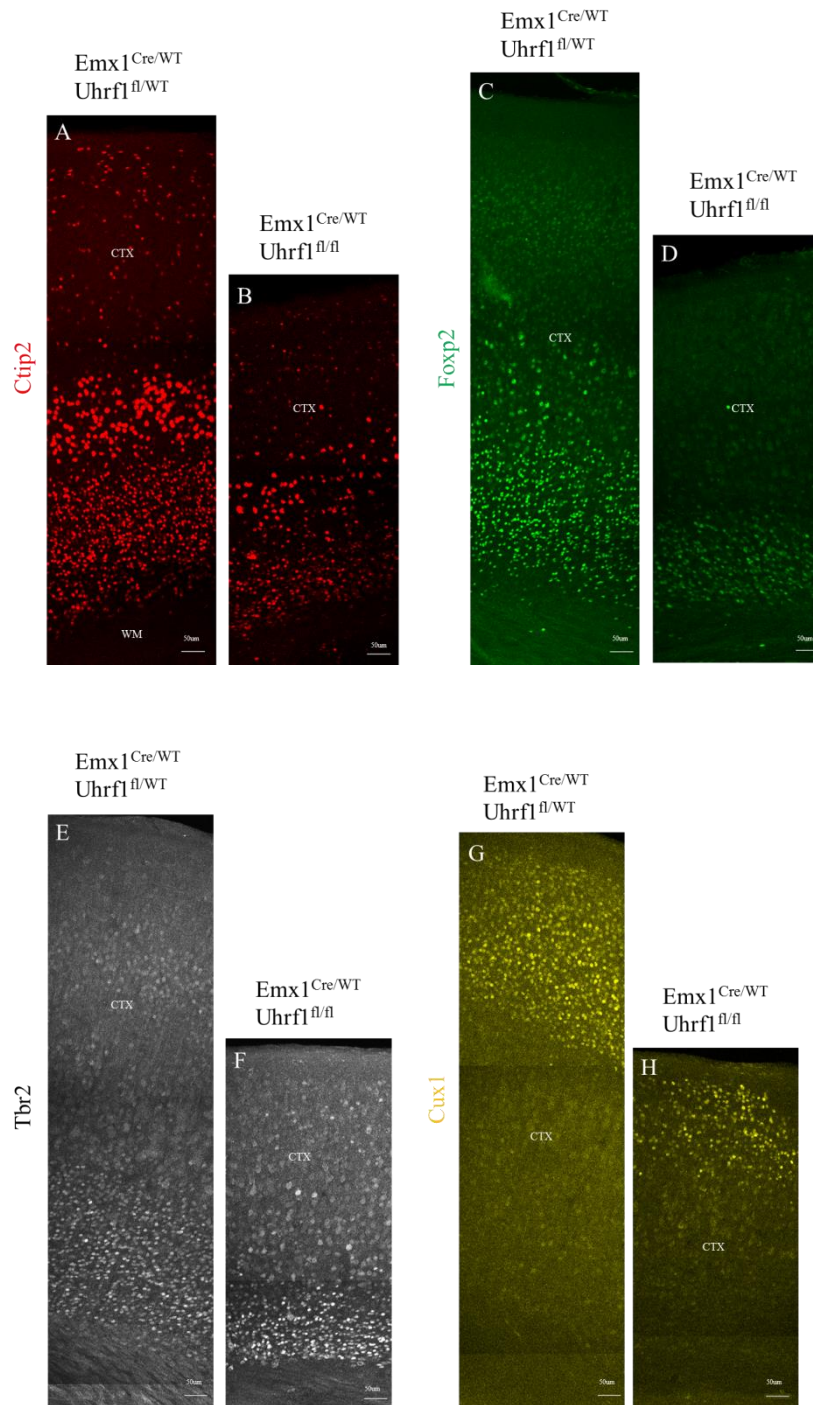
Figure 43: Layering of the cerebral cortex is not affected upon Uhrf1 deletion

(A-H) Micrographs depicting the immunoreactivity for Ctip2 (A-B), Foxp2(C-D), Tbr2 (E-F) and Cux1 (G-H) in coronal sections of the cerebral cortex of Emx1$^{Cre/WT}$; Uhrf1$^{fl/WT}$ and Uhrf1$^{fl/fl}$mice at P27. Note that all the layer markers analyzed seem to be localized at their proper location.

4.5.8 Cell death is increased in the developing cerebral cortex after Uhrf1 deletion

Uhrf1 was reported to interact with Dnmt1 (Sharif et al., 2007) and deletion of Dnmt1 with the Emx1[Cre] was shown to cause hypomethylation induced apoptotic cell death in the mutants (Hutnick et al., 2009a). Therefore, we used the TUNEL assay at E14 and E16 to understand if cell death contributed to the extensive reduction in the cerebral cortical size observed in the Uhrf1 mutants (Fig.44A-D). At both time points analyzed, number of TUNEL+ cells were significantly increased in the mutant cortical plate and ventricular zone (Fig 44E-F). Thus, severe cortical degeneration observed in Uhrf1 mutants is possibly in part mediated by apoptotic cell death.
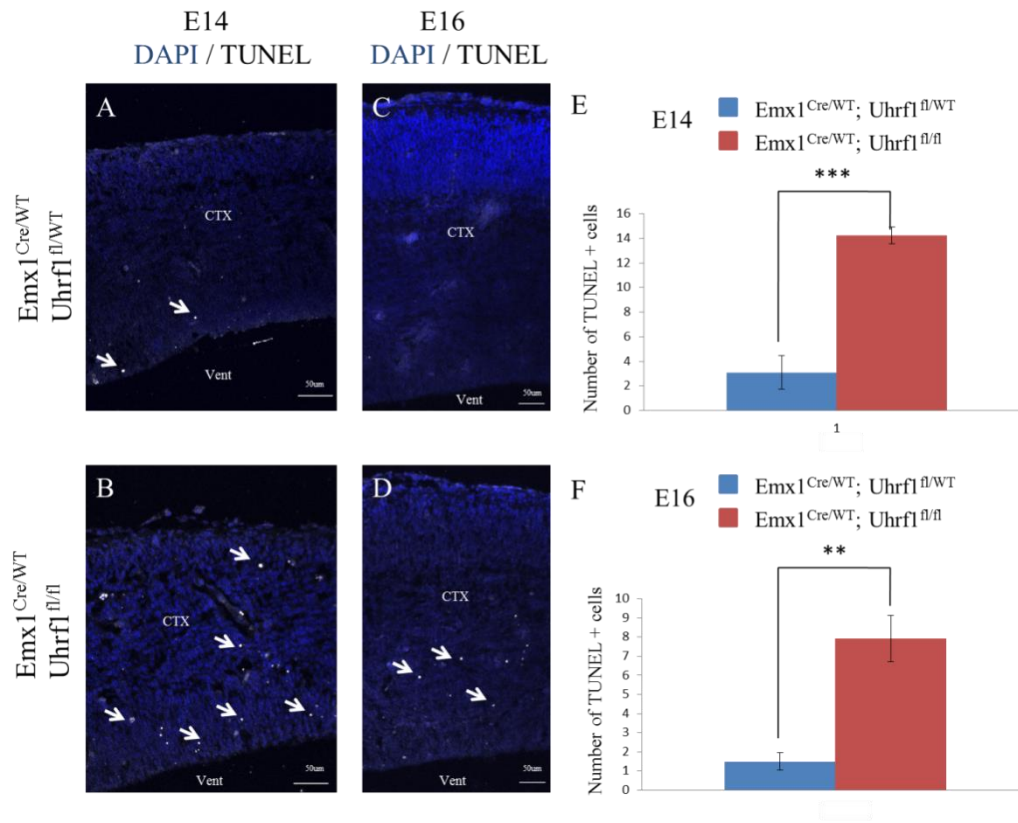
Figure 44: Cell death is increased upon Uhrf1 deletion in the developing cerebral cortex

(A-D) Micrographs depicting the TUNEL immunoreactivity in coronal sections of Emx1[Cre/WT]; Uhrf1[fl/WT] or Uhrf1^{fl/fl} mice at E14 (A-B) and E16 (C-D). **(E-F)** Histograms depicting the number of TUNEL+ cells per area at E14 (E) and at E16 (F). Data are shown as mean ± SEM, n (embryos analyzed) ≥ 3; **$p<0.01$, ***$p<0.001$. Note the increase in apoptotic cells at both stages analyzed upon deletion of Uhrf1. Abbreviations: CTX= cortex; Vent= ventricle

4.5.9 Apical junctional contacts are maintained after deletion of Uhrf1 in the cerebral cortex

The observation that many ectopic PH3 and Pax6 + cells were present in the Uhrf1 mutant cerebral cortex raised the question whether these progenitors delaminated due to the defects in apical anchoring. Since disintegration of adherence junctions (AJs) was also shown to induce changes in nuclear shape (Schmid, 2007)which is another observed phenotype observed in the mutant cerebral cortex, we wanted to see if the AJs are formed properly in the Uhrf1 mutants. To examine AJs, I stained for β-catenin which is an essential component of AJs (Fig.45). Although normal β-catenin staining was observed in the mutant cerebral cortices at the apical ventricular surface at both E14 and E16, more detailed analysis of AJs at the ultrastructural level is needed to ascertain normal junctional complexes.
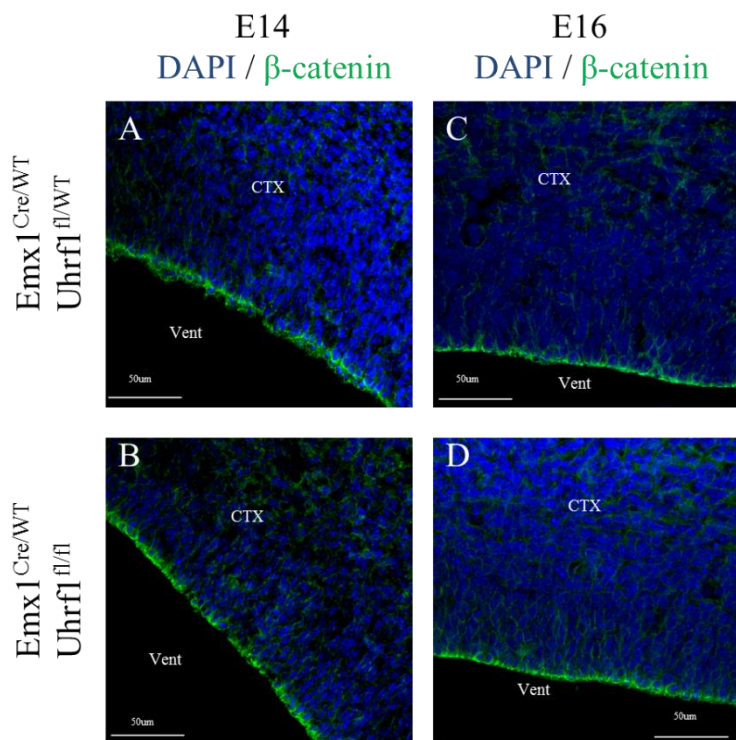
Figure 45: Deletion of Uhrf1 does not alter cell-cell contact
(A-D) Micrographs depicting the immunoreactivity for B catenin in coronal sections of Emx1$^{Cre/WT}$; Uhrf1$^{fl/WT}$ (A) or Uhrf1$^{fl/fl}$ (B) mice at E14 and Emx1$^{Cre/WT}$; Uhrf1$^{fl/WT}$ (C) or Uhrf1$^{fl/fl}$(D) mice at E16. Note that at both stages analyzed, B catenin staining does not seem to be different. Abbreviations: CTX= cortex; Vent= ventricle

4.5.10 Dorso-ventral patterning is not affected in the developing telencephalon after Uhrf1 deletion

The proliferation behavior observed after the loss of Uhrf1, with an increase in the percentage of basally dividing cells resembles the distribution of proliferating cells in the ventral telencephalon that has particularly high number of progenitors proliferating at basal locations (Bhide, 1996; Pilz et al., 2013). In order to examine if the proliferation phenotype and the reduced cortical thickness observed in the Uhrf1 mutants results from misspecification of dorsal progenitors to a more ventral identity, the transcription factors Mash1 and Olig2 normally expressed by the progenitors of the ventral telencephalon, were analyzed by immunohistochemistry at E14 and E16 upon Uhrf1 deletion (Fig.46). At none of the developmental stages analyzed, spread of Mash1 or Olig2 expression into the dorsal telencephalon was observed. The very few Mash1+ or Olig2+ cells present in the dorsal telencephalon of the mutants were consistent with Mash1+ interneuron progenitors or Olig2+ oligodendrocyte progenitors respectively that normally migrate from ventral telencephalon to populate the dorsal telencephalon. These data suggest that dorso-ventral patterning of the telencephalon is not majorly affected in the Uhrf1 mutants and hence appears not to be the reason for the observed phenotype in the cerebral cortex.
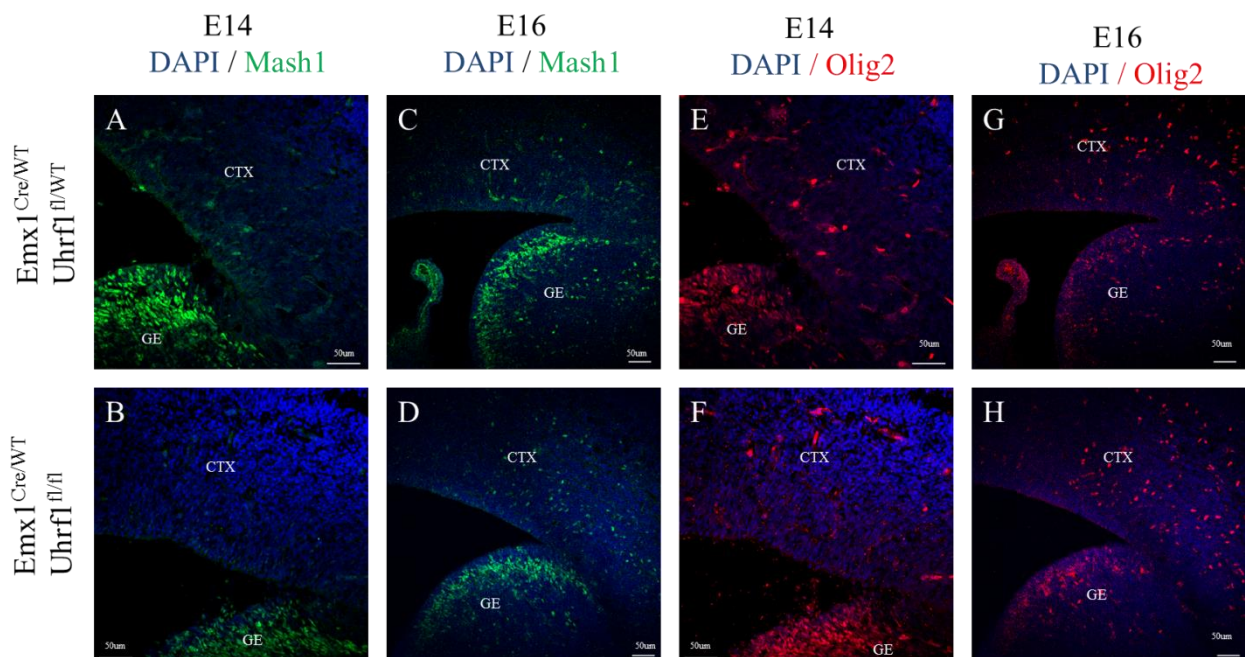
Figure 46: Deletion of Uhrf1 does not cause ventralization of the cerebral cortex.

(A-H) Micrographs depicting the immunoreactivity for Mash1 (A-D) and Olig2 (E-H) in coronal sections of Emx1$^{Cre/WT}$; Uhrf1$^{fl/WT}$ or Uhrf1$^{fl/fl}$mice at E14 (A-B and E-F) and at E16(C-D and G-H). Note that at both stages analyzed, both Mash1 and Olig2 staining seem not to be changed upon Uhrf1 deletion. Abbreviations: CTX= cortex; GE= ganglionic eminence; Vent= ventricle

4.5.11 Genome-wide expression analysis in the Uhrf1 mutant cerebral cortex

Since the proliferation behavior and localization of progenitors was altered and a strong cortical degeneration was observed in the Uhrf1 mutants, we aimed to determine the molecular mechanisms leading to the observed cellular defects. Towards this aim we performed a genome-wide expression analysis of E14 Uhrf1 heterozygous and mutant cerebral cortices. The time point E14 was chosen since this is the first time the phenotype becomes apparent and cDNA from 6 control and 6 mutant embryos was hybridized on Affymetrix Gene ST 1.0 arrays (containing about 770.000 probes for 29.000 genes) and gene expression differences between control and mutant cortices were determined. Gene expression differences between controls and mutants were assessed by a filter consisting of statistical significance (p<0.05) in the limma *t*-test and Benjamini-Hochberg multiple testing correction. In order to access the reliability of the transcriptome data, first the hierarchical divisive clustering of samples was performed. Apart from one control sample that clustered rather with the mutant samples, all other samples in clustering showed high reproducibility between biological replicates with control and mutant samples clustering together. (Fig.47A). Then the expression level for the Uhrf1 probe set was checked and one mutant samples where the probe set for Uhrf1 did not show a significant down regulation was excluded from the rest of the analysis (Fig.47B) . So further analysis was carried with the datasets from 5 control and 5 mutants by filtering for average expression levels > 50 in at least one group (mutant or control) and for a linear ratio difference of > 1.2-fold.

This analysis revealed 597 probe sets with significantly altered expression, of which 384 (64%) showed an increased expression level (Fig.47C-D). When we analyzed the data, we saw that among the up regulated genes there were many X-linked genes (Rhox2a, Rhox2e, Rhox5, Xist, Xlr3a, Xlr3b, Xlr3c, Xlr4b, Xlr4c) which is consistent with the fact that X-

linked genes are repressed by DNA methylation in both somatic cells and embryonic stem cells (Fouse et al., 2008) and since Uhrf1 interacts with Dnmt1, deletion of Uhrf1 could also lead to demethylation of these genes resulting with the observed increase in their expression levels (Table 1). Moreover genes involved in senescence and cell cycle arrest (Cdkn1a) and negative regulation of apoptosis (Prnp, Atf5, Crlf1, Hsph1, Lgmn and Ucp2) as well as genes involved in neurodegeneration (ApoE and Clu) were also among the up regulated genes suggesting that cells are up regulating their protective mechanisms to protect themselves from the detrimental effects of Uhrf1 loss (Table 1). Interestingly although only Pcdhb17 could pass our stringent criteria of expression >50 while selecting the genes to analyze, many other members of the procadherin family (Pcdhb3, Pcdhb4, Pcdhb8, Pcdhb10, Pcdhb11, Pcdhb14 and Pcdhb16) that have roles in synapse assemble and synaptic transmission were also up regulated upon Uhrf1 deletion when we set our selection criteria to average expression >20 (Table 1). Remarkably, genes down regulated upon loss of Uhrf1 function comprised many genes involved in neuronal migration (Cxcl12, Dab1, Robo1, Robo2, Sema3A, Sema5A, Eph3A, Eph5A and Netrin4) and cerebral cortex development/maturation (Bcl11b, Pou3f3, NeuroD4, Sox5, Satb2 and Meis2) (Table 2).Taken together, these data suggest that Uhrf1 is involved in regulation of many genes involved in neuronal development and survival and more specifically acts in transcriptional inhibition in agreement with its role in bridging DNA methylation with repressive histone modifications (Bostick et al., 2007; J. K. Kim et al., 2009; Sharif et al., 2007; Motoko Unoki et al., 2004; J. Zhang et al., 2011).
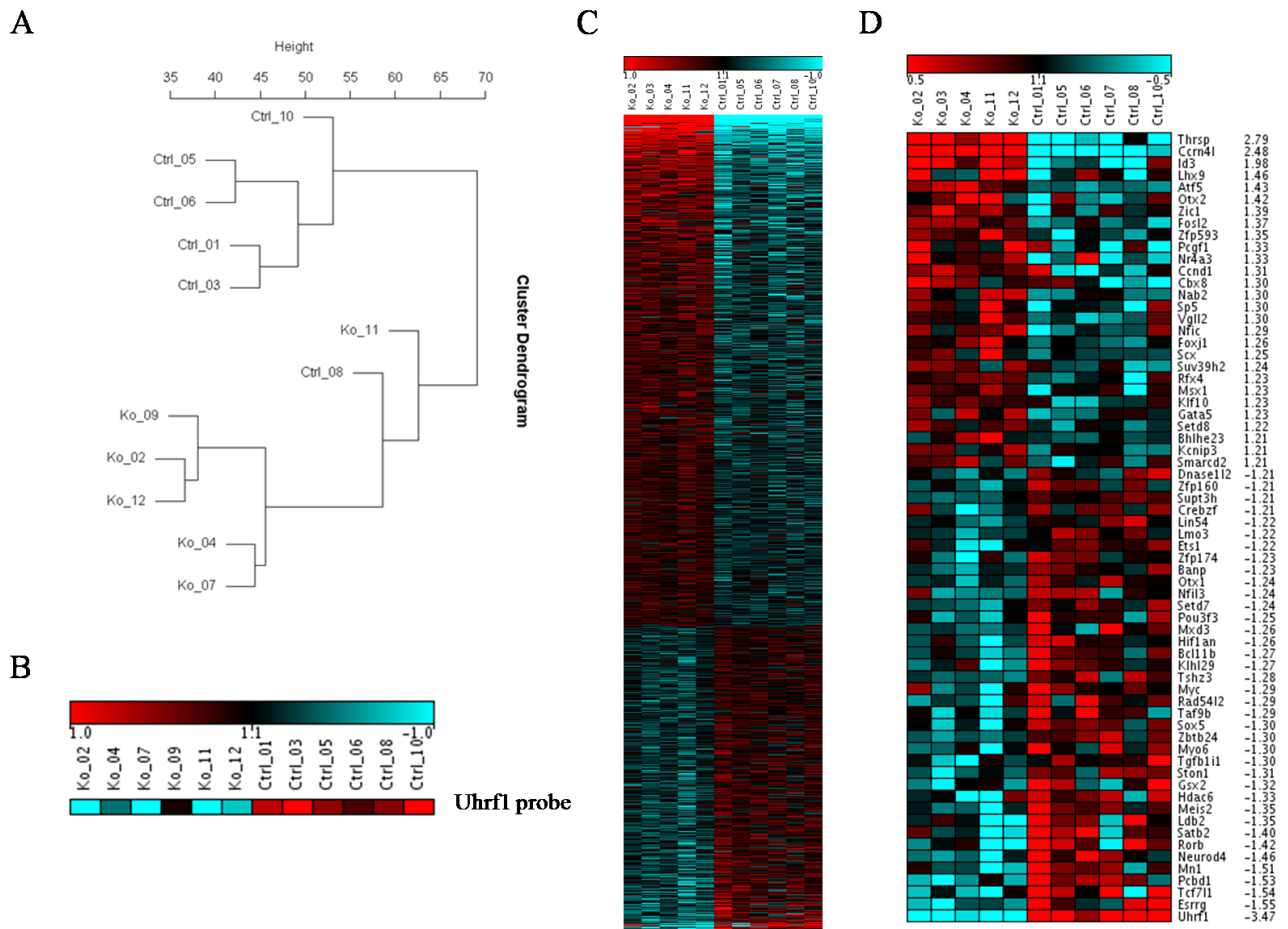
Figure 47: Transcriptome analysis at E14 upon Uhrf1 deletion in the developing cerebral cortex

(**A**) Hierarchical clustering of samples show that apart from one control sample (Ctrl_08) all the controls cluster with each other and all the knockouts cluster with each other. (**B**) Analysis of *Uhrf1*-mRNA levels of upon Uhrf1 deletion. Note that in one knock out sample (Ko_09) Uhrf1 expression seems to be in between controls and knockouts. This sample was omitted from further analyses. (**C**) Heatmap showing differentially expressed genes between controls versus knockouts with p<0.05, average expression >20 and ratio difference >1.2x. Red indicates higher expression levels, green indicates lower expression levels. Genes are shown from up regulated to down regulated Note that more genes are overall up regulated upon Uhrf1 deletion. (**D**) Heatmaps showing transcription (co)factors among the differentially expressed genes with p<0.05, average expression >20 and ratio difference >1.2x. Gene symbols and fold changes are shown. Red indicates higher expression levels, green indicates lower expression levels.

Table 1. Up-regulation of genes involving in senescence, cell death, neurodegeneration, synapse assemble and other functions in dorsal cortex in E14 Emx1$^{Cre/WT}$; Uhrf1$^{fl/fl}$ mice

Gene symbol	Genebank	Gene name	Fold change
X linked genes			
Xlr4c	NM_183094	X-linked lymphocyte-regulated 4C	14.21
Xlr4b	NM_021365	X-linked lymphocyte-regulated 4B	12.16
Xlr3c	NM_011727	X-linked lymphocyte-regulated 3C	9.63
Xlr3b	NM_001081643	X-linked lymphocyte-regulated 3B	8.77
Rhox5	NM_008818	reproductive homeobox 5	7.30
Xlr3a	NM_001110784	X-linked lymphocyte-regulated 3A	7.14
Rhox2e	NM_001085348	reproductive homeobox 2E	5.00
Xist	NR_001463	inactive X specific transcripts	4.59
Rhox2a	NM_029203	reproductive homeobox 2A	4.14
Negative regulation of apoptosis			
Ucp2	NM_011671	uncoupling protein 2	1.46
Prnp	NM_011170	prion protein	1.26
Atf5	NM_030693	activating transcription factor 5	1.43
Crlf1	NM_018827	cytokine receptor-like factor 1	1.54
Hsph1	NM_013559	heat shock 105kDa/110kDa protein 1	1.26
Lgmn	NM_011175	legumain	1.34
Cell cycle arrest and senescence			
Cdkn1a	NM_007669	cyclin-dependent kinase inhibitor 1A	1.61
Neurodegeneration			
Clu	NM_013492	clusterin	1.32
Apoe	NM_009696	apolipoprotein E	1.38
Pro-cadherins			
Pcdhb3	NM_053128	protocadherin beta 3	1.95
Pcdhb5	NM_053130	protocadherin beta 5	1.41
Pcdhb6	NM_053131	protocadherin beta 6	1.72
Pcdhb7	NM_053132	protocadherin beta 7	1.33
Pcdhb10	NM_053135	protocadherin beta 10	1.61
Pcdh11x	NM_001081385	protocadherin 11 X-linked	1.24
Pcdhb13	NM_053138	protocadherin beta 13	1.33
Pcdhb14	NM_053139	protocadherin beta 14	1.62
Pcdhb15	NM_053140	protocadherin beta 15	1.48
Pcdhb16	NM_053141	protocadherin beta 16	1.40
Pcdhb17	NM_053142	protocadherin beta 17	2.60
Pcdhb18	NM_053143	protocadherin beta 18	1.61
Pcdhb19	NM_053144	protocadherin beta 19	1.49
Pcdhb20	NM_053145	protocadherin beta 20	1.78
Pcdhb22	NM_053147	protocadherin beta 22	1.58

Table 2. Down-regulation of genes involving in neuronal migration and cerebral cortex

Gene symbol	Genebank	Gene name	Fold change
Neuronal migration			
Epha3	NM_010140	Eph receptor A3	-1.36
Robo2	NM_175549	roundabout homolog 2	-1.37
Sema3a	NM_009152	semaphorin 3A	-1.40
Epha5	NM_007937	Eph receptor A5	-1.23
Dab1	NM_177259	disabled 1	-1.23
Ntn4	NM_021320	netrin 4	-1.26
Sema5a	NM_009154	semaphorin 5A	-1.50
Cxcl12	NM_001012477	chemokine (C-X-C motif) ligand 12	-1.60
Cerebral cortex development and maturation			
Meis2	NM_001136072	Meis homeobox 2	-1.35
Satb2	NM_139146	special AT-rich sequence binding protein 2	-1.40
Neurod4	NM_007501	neurogenic differentiation 4	-1.46
Pou3f3	NM_008900	POU domain, class 3, transcription factor 3	-1.25
Bcl11b	NM_001079883	B cell leukemia/lymphoma 11B	-1.27
Sox5	NM_006940	SRY-box containing gene 5	-1.30

development and maturation in dorsal cortex in E14 Emx1$^{Cre/WT}$; Uhrf1$^{fl/fl}$ mice

5. Discussion

5.1 Confirmation of the transcriptome data and selection of candidate genes

Transcriptome analysis of aNSCs, their progeny, ependymal cells and non-neurogenic astrocytes from diencephalon gave very important insights into the mechanisms that confer unique stem cell hallmarks, self-renewal and multi-lineage differentiation potential, to aNSCs and the mechanisms that promote their neurogenic capacity over other cell fates. Comparison of the transcriptome of aNSCs with all other sorted populations showed enrichment of many factors involved in extracellular matrix, cilia and Calcium signaling in aNSCs, pointing to the importance of signaling and interactions within the neurogenic zone for the unique properties of aNSCs (Beckervordersandforth et al., 2010). On the other hand comparison of the transcriptome of aNSCs with that of diencephalic astrocytes revealed a very interesting expression pattern shared by many known neurogenic fate determinants such that their mRNA was already up regulated in the aNSCs compared to diencephalic astrocytes although their protein could only be detected in the progeny of aNSCs which coincided with even higher increased mRNA levels in the population comprising the progeny of aNSCs (Beckervordersandforth et al., 2010). As these two transcriptome comparisons enlightened two different aspects of aNSC regulation, I decided to select two candidate genes coming from different transcriptome comparisons to analyze their role in adult neurogenesis.

Before selecting the candidate genes to analyze functionally in adult neurogenesis, I first validated the differences in gene expression shown by the microarray data, either by qPCR using lysates of sorted aNSCs, their progeny, and ependymal cells from SEZ and non-neurogenic astrocytes from diencephalon of adult hGFAP-GFP mice or by in situ hybridization that allowed determining the localization of several differentially expressed mRNAs. This analysis not only confirmed the reliability of the approach used for the isolation of different populations but also revealed many interesting candidate genes that have not been implicated in adult neurogenesis before. For example among the confirmed mRNAs, interferon-induced transmembrane protein 3 (Ifitm3) mRNA was located strictly in the SEZ whereas it was absent from the RMS and the diencephalon, in agreement with the microarray data showing Ifitm3 mRNA being high in aNSCs and low in all other populations. Ifitm3 is an interferon induced transmembrane protein that was shown to plays an important role in glioma cell growth and migration (Zhao et al., 2013). More interestingly, interferon α that was shown to induce Ifitm3, but not interferon ɣ that was shown to indice Ifitm1 (Lau et al., 2012)

was shown to suppress proliferation in the DG, the other known neurogenic region in the adult brain, resulting in decreased neurogenesis (Kaneko et al., 2006). Although Ifitm3 has not been implicated in neurogenesis before, its expression pattern together with the previously published data showing its role in proliferation of other stem cell populations suggest a possible role in adult SEZ neurogenesis. Moreover, since it is a transmembrane protein, it can also potentially be used in FACS as a cell surface marker to identify aNSCs which will eliminate the need to use transgenic animals as in the method developed by our lab.

Another very interesting candidate gene that was confirmed by qPCR to be enriched in aNSCs compared to non-neurogenic astrocytes from diencephalon, and has not been implicated in neurogenesis before, is BMP binding endothelial regulator (BMPER). BMPER is a secreted protein that was shown to inhibit BMP-2 and BMP-4 dependent differentiation of endothelial cells (Moser et al., 2003). Since BMPs are well known regulators of fate choices in the SEZ (Colak et al., 2008), and since several BMP antagonists have been shown to be important for the induction of neural fate (Bond, Bhalala, & Kessler, 2012), it is highly conceivable that BMPER could also acts to regulate BMP levels in the adult SEZ, to create a niche suitable for neurogenesis, similar to the function of Noggin, another known BMP regulator secreted by ependymal cells (Lim et al., 2000). Yet another very interesting candidate gene shown to be differentially expressed by in situ hybridization and immunostainings is Whsc1. Whsc1 has been shown to be up regulated in many cancers including glioblastomas and neuroblastomas and promote cancer cell proliferation and survival by acting as a strong coactivator of NF-κB (J. Li et al., 2008; Yang et al., 2012). As NF-κB is also a well-known regulator of adult and embryonic neurogenesis (Y. Zhang & Hu, 2012), its expression pattern raises the possibility that Whsc1 might also have a similar function in promoting progenitor proliferation in the adult neurogenic zone SEZ. In addition to suggesting some genes that have not been implicated in any aspect of neurogenesis before as potential regulators of adult neurogenesis, confirmation of the transcriptome data also suggested that genes such as Hes6 (Jhas et al., 2006; Methot et al., 2013) and Foxg1 (Hanashima et al., 2004; Siegenthaler et al., 2008) that are known regulators of embryonic neurogenesis, might also have important roles in adult neurogenesis as their mRNA was shown to be enriched in the progeny of aNSCs.

Moreover, when we threshold the microarray data by an absolute expression level of 100 and sort the genes that are at least 2 fold higher with FDR<5% in the progeny of aNSCs compared to aNSCs, 77 genes are shown to up regulated in the progeny of aNSCs compared to aNSCs.

Among these genes, many genes that have not been implicated in neurogenesis before, show a very strong expression in the SEZ-RMS route according to the in situ data from Allen Brain Atlas (Fig.48), further suggesting that our transcriptome data is reliable and therefore can be used to select novel genes that may give new insights into the molecular mechanisms regulating adult neurogenesis.
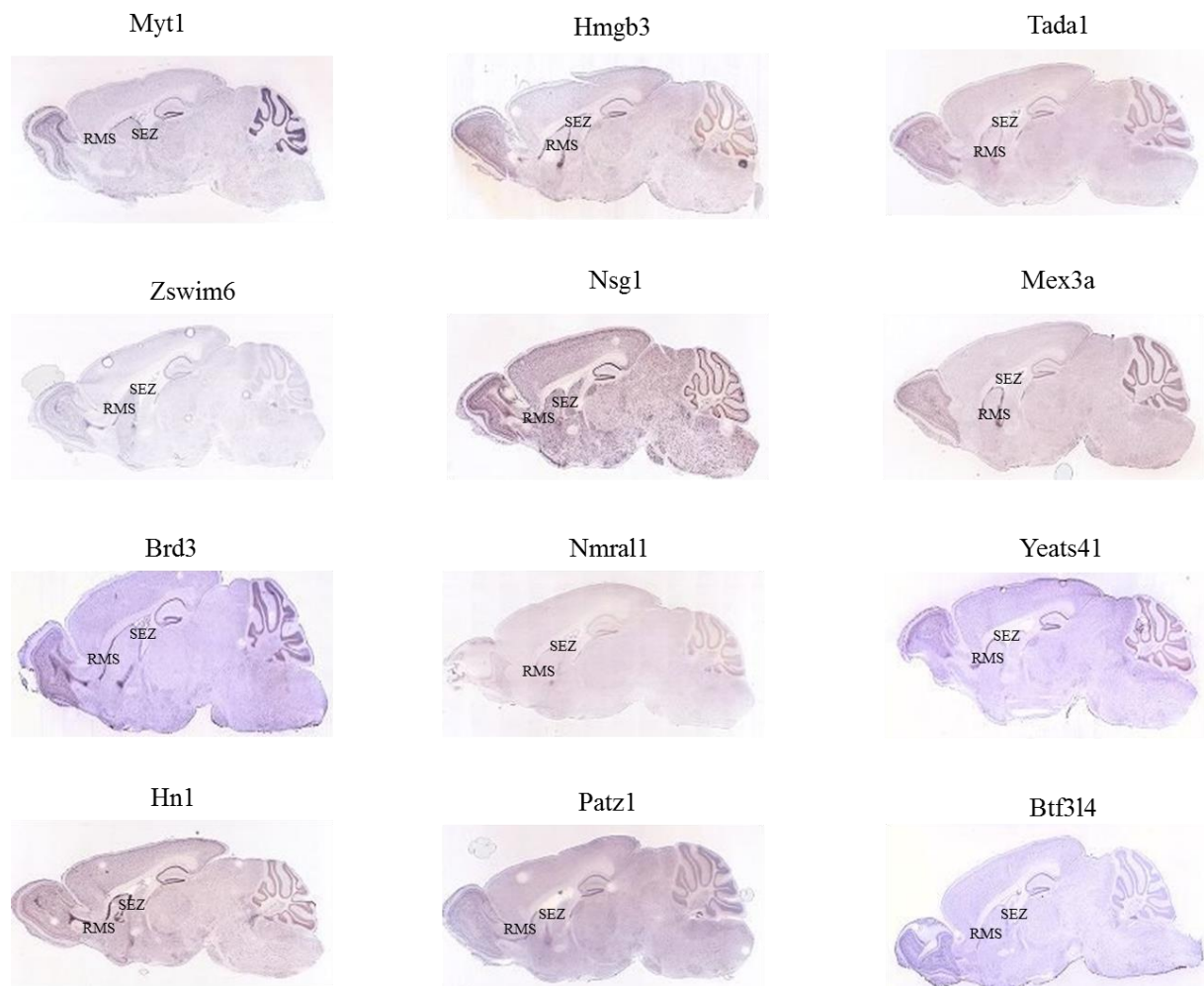
Figure 48: In situ hybridization data taken from Allen Brain Atlas for some of the genes that are at least 2 fold higher with FDR<5% in the progeny of aNSCs compared to aNSCs

As the GO term analysis of highly enriched genes in aNSCs compared to all other sorted cell populations revealed "extracellular matrix (ECM)" one of the most significantly enriched GO category (Beckervordersandforth et al., 2010), an extracellular matrix protein TSP-4 that showed enrichment in aNSCs compared to all other populations was selected as one of the candidate genes to study its function in adult neurogenesis. On the other hand, as many known neurogenic fate determinants shared a common expression pattern, with mRNA levels that are high in aNSCs compared to diencephalic astrocytes which become even higher in the progeny of aNSCs (Beckervordersandforth et al., 2010), we thought such an expression pattern could be indicative of a role in neurogenesis and hence selected Uhrf1 that shows the same expression pattern as second candidate gene for further functional analysis.

5.2 Expression and function of TSP-4 in the adult murine brain

The stem cell niche is defined as a microenvironment that facilitates the self-renewing capacity of the stem cells, as well as their multi-lineage differentiation potential. As explained in the introduction, in the adult murine brain there are two highly specialized areas – stem cell niches- where neurogenesis persist into adulthood: the subependymal zone (SEZ) of the lateral walls of the lateral ventricles and the subgranular zone (SGZ) of the dentate gyrus (Ma et al., 2009; Ming & Song, 2011). It was shown by heterotypic transplantation experiments where SEZ cells are grafted into a non-neurogenic brain region like striatum, that the neurogenic capacity of aNSCs is not only regulated by intrinsic mechanisms but also depend on the presence extrinsic factors present in the permissive environment of SEZ (Herrera et al., 1999). Extrinsic factors can regulate the behavior of NPCs via diffusible signals and/or molecules that mediate cell to cell and cell to ECM interactions (Kazanis & ffrench-Constant, 2011; Wojcik-Stanaszek et al., 2011). Interestingly, ECM of the SEZ seems to be significantly different from that of the surrounding tissue such that many ECM molecules that are expressed during embryonic development or after injury and then are down regulated during early post-natal life resulting in the formation of the classic brain parenchymal ECM, are persistently present in the adult SEZ. Matrix metalloproteinases, brevican, tenascin-C and chondroitin/dermatan sulfate proteoglycans are among the ECM molecules shown to be present in the adult SEZ (Bandtlow & Zimmermann, 2000; Kazanis & ffrench-Constant, 2011; Wojcik-Stanaszek et al., 2011; Zimmermann & Dours-Zimmermann, 2008) and for chondroitin sulfate glycosaminoglycans (Sirko et al., 2010) and chondroitin/dermatan

sulfotransferases (Akita et al., 2008) functional data suggestive of a role in NSC/progenitor behavior, is present. Moreover, recently extensions of the vessel basal lamina, that is rich in laminin and collagen I, were described to intrude the SEZ, branch around NSCs and progenitors and regulate growth factor concentrations and activity in the SEZ (Kerever et al., 2007; Mercier et al., 2002). These protrusions have been named fractones (Mercier et al., 2002). As our transcriptome comparison of aNSCs with that of all other sorted cell types revealed ECM as one of the most significantly enriched GO term in aNSCs (Beckervordersandforth et al., 2010), this lends further support to the key function of ECM in this context and prompted us to select TSP-4 as an interesting candidate for key functions in the NSC niche.

Confirming our transcriptome data, although all TSP members were detected in the SEZ and diencephalon with the qPCR, TSP-4 was the only one shown to be up regulated in the SEZ compared to diencephalon. Therefore, to further elucidate the role of TSP-4 in adult neurogenesis, we analyzed how neurogenesis is affected in the TSP-4 null mice. To our surprise, we did not observe any change in the aNSCs (as determined by BrdU label retaining protocol), TAPs or neuroblasts (as determined by a short BrdU pulse and DCX staining) in TSP-4 null mice compared to the heterozygous ones. Moreover, we also did not observe any influence of exogenous TSP-4 addition in neurogenesis neither in vivo nor in vitro. As deletion of another member of the TSP family, TSP-1 was shown to decrease proliferation and differentiation of neural progenitor cells both in vivo and in vitro (Lu & Kipnis, 2010), the lack of any effect in the case of TSP-4 deletion is unlikely to be explained by a compensatory mechanism taking place in the SEZ upon deletion of one member of the TSP family. Therefore lack of any effect of genetic TSP-4 deletion and exogenous TSP-4 addition on neurogenesis despite its very specific expression pattern along the SEZ-RMS route, raises the possibility that it affects some other parameters that are not covered by our read outs and are particulary relevant after challenging the system. Accordingly, a recent study in 2013 from J. Benner et al showed that TSP-4 is rather involved in Notch dependent astrogliogenesis from the SEZ upon injury in the adjacent brain region, the cerebral cortex(Benner et al., 2013).

5.3 Expression of Uhrf1 in the adult murine brain

After seeing in the transcriptome analysis of aNSCs (GFP+/Prom+ cells), their progeny (GFP+ cells) and non-neurogenic astrocytes from diencephalon (GFP+ cells) that Uhrf1 mRNA is highly enriched in aNSCs compared to non-neurogenic astrocytes from diencephalon and its expression further increases in the progeny of aNSCs, a detailed localization analysis of Uhrf1 protein was carried in the adult murine brain in this study. In agreement with our transcriptome data and with the expression pattern of Uhrf1 mRNA as elucidated by in situ hybridization, Uhrf1 protein was identified in a small percentage of aNSCs (identified by BrdU label retaining assay), in all TAPs (identified by a short BrdU pulse) and in some of the neuroblasts in the SEZ and RMS. An intriguing difference in the appearance of the Uhrf1 protein was found in the other neurogenic region, DG, in the adult brain. Unlike SEZ, Uhrf1 protein was not detected in aNSCs in this region, whereas similar to SEZ, Uhrf1 was shown to be highly present in all TAPs and at lower levels in some neuroblasts. As some recent studies showed presence of distinct aNSC pools some being quiescent and some being more activated (Hsieh, 2012; Lugert et al., 2010), whether the small percentage of Uhrf1 positive cells among the label retaining population in the SEZ belongs to the activated pool of aNSCs still remains to be elucidated. Furthermore as the BrdU label retaining protocol labels more quiescent cells, using a different approach to label the activated aNSCs could also better elucidate if activated aNSCs also express Uhrf1 in the DG or if the differential expression of Uhrf1 between the aNSCs of SEZ and DG result from intrinsic differences of these cells as described previously (G.-L. Ming & Song, 2011). The general presence of Uhrf1 protein mainly in proliferating cells of the SEZ and DG and its down regulation upon differentiation, is in accordance with a previous study that showed Uhrf1 is expressed in basal layer of human epidermal tissue where epidermal progenitors are located, while it is absent in outer layers with differentiated cells (Sen, Reuter, Webster, Zhu, & Khavari, 2010). Notably, several studies showed that Uhrf1 is required for cell cycle progression (Bonapace et al., 2002; Jeanblanc et al., 2005; Tien et al., 2011; Tittle et al., 2011), consistent with its expression in proliferating cells. Our study also showed that in addition to being expressed in neurogenic progenitors, Uhrf1 is present also in non-neurogenic progenitors in the adult cerebral cortex as all the cells labeled with a short BrdU pulse in the cerebral cortex were Uhrf1 positive. Since previous reports showed that in physiological conditions the only cells that proliferate in the adult murine cortex are OPCs (Dimou et al., 2008), our results strongly suggest that Uhrf1 is not expressed only by the

neurogenic progenitors but also by the OPCs in the adult murine brain. Interestingly, when examining cells proliferating after brain injury, Uhrf1 protein is not detectable in proliferating microglia whereas reactive and proliferating OPCs and astrocytes are highly Uhrf1+. As previous reports showed that Uhrf1 binds to the hemimetyhlated DNA and recruits Dnmt1 that is required for maintenance of DNA methylation during replication (Bostick et al., 2007; Sharif et al., 2007), absence of Uhrf1 in proliferating microglia suggest that different cell types may use different mechanisms for recruiting the epigenetic machinery for maintenance of DNA methylation during DNA replication. In summary, our results show that in the adult murine brain Uhrf1 is found in proliferating cells but strikingly not in all proliferating cells. Therefore, this may indicate a role beyond proliferation probably also involving fate specification.

5.4 Function of Uhrf1 in adult neurogenesis

Adult neurogenesis, which is a of generating functional neural cell types from aNSCs, is composed of a cascade of genetic programs that precisely control stage specific gene expression required for progenitor proliferation, fate decision, migration and neuronal connectivity. Recent studies showed that the temporally and spatially controlled gene expression in the nervous system is not only regulated by transcriptional machinery but also by epigenetic mechanisms such as DNA methylation, histone modifications, nucleosome and chromatin remodeling, and non-coding RNA-mediated posttranslational regulation (Feng et al., 2007; Gonzales-Roybal & Lim, 2013; H.-J. Kim & Rosenfeld, 2010; Ma et al., 2010; Singh et al., 2009). Although previous studies identified Uhrf1 as a key molecule that bridges the DNA with the chromatin to regulate gene expression (Alhosin et al., 2011; Bronner et al., 2007), its role in CNS has not been studied so far. Given the very interesting expression pattern of Uhrf1 in both of the two adult neurogenic zones, the function of Uhrf1 was analyzed in this study using conditional deletion of Uhrf1 in the aNSCs and their progeny. In accordance with the previous studies that showed Uhrf1 is required for the proper progression of the cell cycle in non-cancerous cells (Arima et al., 2004; Bonapace et al., 2002; Sadler, Krahn, Gaur, & Ukomadu, 2007; Tittle et al., 2011), my results showed that upon deletion of Uhrf1, proliferation of progenitors is decreased in both neurogenic regions. Consistent with the decreased proliferation, less neuroblasts reaching the OB and in the DG was observed. In addition to the proliferation defects, neuroblasts in the DG were also observed to have additional defects in neuronal maturation or survival unlike the ones in the SEZ. Moreover

upon deletion of Uhrf1, proliferating cells and neuroblasts decreased from 80% of reporter+ cells to 65% and from 66% to 50% in the SEZ and DG respectively raising the possibility that deletion of Uhrf1 could also cause to a fate conversion preventing part of the recombined cells from reaching the TAP or neuroblasts stage. Although our first impression of having more astrocytes in the DG and more ependymal cell in the SEZ supports this view, further analysis is required with additional markers labeling other cell types in the SEZ and DG to confirm such a fate conversion.

As mentioned above Uhrf1 binds to hemimethylated DNA and histones with different methylation status and recruit many different epigenetic regulators (Frauer et al., 2011; Karagianni et al., 2008a; Lallous et al., 2011; Papait et al., 2008; Rajakumara et al., 2011; Rothbart et al., 2013; Sharif et al., 2007; Unoki et al., 2004; Xie et al., 2012). One such interaction partner of Uhrf1 is Dnmt1 (Bostick et al., 2007; Sharif et al., 2007) which methylates cytosines on CpG islands of hemimethylatedDNA to mediate transcriptional repression (Hermann, Gowher, & Jeltsch, 2004). Uhrf1 binds to hemimethylated DNA via its SRA domain and flips out the methyl cytosine of the parent strand allowing Dnmt1 to access the unmethylated cytosine on the daughter strand (Arita, Ariyoshi, Tochio, Nakamura, & Shirakawa, 2008; Avvakumov et al., 2008; Hashimoto et al., 2008). As depletion of Uhrf1 prevents the association of Dnmt1 with chromatin leading to the hypomethylation of many genes (Sharif et al., 2007), it is highly probable that the phenotype that we observe upon Uhrf1 deletion at least in part result from the hypomethylation of genes important for adult neurogenesis.

Indeed, in the adult mouse brain, Uhrf1 and Dnmt1 show an overlapping but distinct expression pattern such that in addition to the proliferating cells and immature neurons, Dnmt1 is also expressed by mature neurons (Cushman et al., 2012; G Fan et al., 2001; Guoping Fan et al., 2005; Feng et al., 2010; Goto et al., 1994; Hutnick et al., 2009b). In accordance with this overlapping expression pattern and their known interaction, Cushmann et al showed that deletion of Dnmt1 in early postnatal stages in stem and progenitor cells using mGFAP[Cre] line severely decreases the number of cells incorporating BrdU and diminishes the generation of newborn neurons in both SEZ and DG (Cushman et al., 2012) similar to the phenotype that we observe upon deletion of Uhrf1 in aNSCs. Moreover, deletion of Dnmt1 in neural progenitor cells during development using Nestin[Cre] or Emx1[Cre]

lines caused passive demetylation of CpG islands in the promoter of many genes including the astrocytic gene GFAP and genes essential for JAK-STAT signaling, resulting with elevation of STAT activity that causes a premature fate switch of neural precursor cells to astrogliogenesis (Fan et al., 2005; Hutnick et al., 2009). Such a role of Uhrf1 though its interaction with Dnmt1, in repressing the promotors of certain lineage specific genes could also be taking place in the adult neurogenic zones and hence explain the decrease in the percentage of proliferating cells and neuroblasts which could result from a glial fate switch upon Uhrf1 deletion. Moreover, Uhrf1 and Dnmt1 were also shown to be necessary to maintain proliferation of epidermal progenitors in humans (Sen et al., 2010) and lens epithelial cells in zebrafish (Tittle et al., 2011) suggesting that regulation of proliferation maybe a general function of Uhrf1. Interestingly, another study showed deletion of Dnmt1 in neural progenitor cells of the retina does not cause a significant change in the total number of proliferating progenitors but instead alters the cell cycle progression leading to abnormal accumulation of cells in the G1 phase at the expense of the ones in the G2/M phase (Rhee et al., 2012). Dnmt1 deletion in these progenitors caused defective cell cycle exit and altered the initial steps in becoming postmitotic neurons such that horizontal cells, one of the cell types generated from the retinal progenitors, exhibited abnormally exuberant dendritic arbors and Dnmt1 defective photoreceptors, failed to differentiate properly as genes that mark progenitor cells remained to be expressed in cells that already up regulated genes that mark more differentiated cells (Rhee et al., 2012). This differential role of Dnmt1 in regulating different phases of neuronal maturation in different systems, could also explain the additional neuronal maturation defects that we observe in the DG upon Uhrf1 deletion.

In addition to interacting with the maintenance methytransferase Dnmt1, Uhrf1 was also shown to interact with the de novo methytransferases Dnmt3a and Dnmt3b (Meilinger et al., 2009) that can catalyze cytosine methylation at new genomic locations (Hermann et al., 2004). Consistent with such an interaction taking place also in vivo in the adult neurogenic zones, Dnmt3a has been shown to be present in the SEZ and DG of postnatal animals (Feng et al., 2005, 2010; Wu et al., 2010). More interestingly Dnmt3a null mice have severely diminished SEZ and DG neurogenesis as Dnmt3a promotes transcription of neurogenic targets by methylating non-promoter DNA regions of the neurogenic genes and represses glial differentiation genes by methylating proximal promoters of gliogenic genes (Wu et al., 2010). Therefore the defects observed in the maturation of new born neurons in the DG of Uhrf1

mutants could be resulting from the inability of Dnmt3a to initiate the neuronal maturation program upon Uhrf1 deletion as this could be inhibiting its recruitment to the DNA. Moreover our impression of increased percentage of recombined astrocytes in the DG could also be due to the derepression of gliogenic promoters upon Uhrf1 deletion.

Yet, another molecule that interacts with Uhrf1 is HDAC1 (Motoko Unoki et al., 2004) that catalyzes histone deactylation, a further chromatin modification associated with transcriptional silencing (Shahbazian & Grunstein, 2007). HDAC1 belongs to the class I HDACs together with HDAC2, 3 and 8 and participates in diverse repressory complexes via interaction with different cofactors such as Sin3A,Nurd, CoRest and Uhrf1(Kretsovali, Hadjimichael, &Charmpilas, 2012). In postnatal mice, HDAC1 is expressed in the GFAP+ cells – presumably including aNSCs – and HDAC2 is expressed in the TAPs and neuroblasts (Foti et al., 2013; Jawerka et al., 2010; MacDonald & Roskams, 2008; Montgomery et al., 2009). As inhibition of class I and II HDACs reduced neurosphere formation of the NSCs from adult SEZ grown in proliferative conditions (Zhou et al., 2011), the reduced proliferation observed upon Uhrf1 deletion can also result in part from the inability of HDAC1 to interact with Uhrf1 and perform its function. Moreover treatment of postnatal mice with class I/II HDAC inhibitors strongly perturbs postnatal neurogenesis causing a significant and differential decrease in the production and differentiation of progeny of aNSCs in the DG, RMS, and OB (Foti et al., 2013). A similar problem in differentiation and maturation of aNSCs in DG was also observed in the HDAC2 deficient mice due to aberrant maintenance of proteins normally expressed only in progenitors, such as Sox2, also into some differentiating neurons (Jawerka et al., 2010). The resemblance of the phenotype observed upon loss of HDAC activity or function to the phenotype that we observe upon Uhrf1 deletion in some aspects, suggest that HDAC1 and Uhrf1 might act cooperatively in regulating cell cycle progression and silencing the progenitor transcripts during neuronal differentiation of adult generated neurons.

5.5 Expression of Uhrf1 in the embryonic murine brain

In addition to elucidating the localization and function of Uhrf1 protein in adult murine brain, in this study the expression pattern and role of Uhrf1 was also studied during forebrain development. Similar to its cellular localization in the adult brain and in agreement with its role in bridging the chromatin modifications with histone and DNA methylation (Alhosin et

al., 2011; Bronner et al., 2007), Uhrf1 protein was shown to be localized to nucleus in all time points analyzed from the beginning of neurogenesis at E12 till the end of neurogenesis at E16. Characterization of different cell types at mid-neurogenesis revealed that Uhrf1 is expressed in apical neural stem and progenitor cells, whereas it is absent in basal progenitors and newborn neurons. Interestingly Uhrf1 was also detected in some Pax6+ cells located above the basal progenitor cell layer. These cells could be outer radial glial cells which are another progenitor type that was described recently and is particularly prominent in the developing cerebral cortex of the species with enlarged and folded cerebral cortex(Shitamukai et al., 2011; X. Wang et al., 2011). As apical progenitors and outer radial glial cells in the cerebral cortex can self-renew whereas the basal progenitors are more restricted in fate and directly give rise to neurons (Breunig et al., 2011), this expression pattern suggest that Uhrf1 is probably not only important for cell cycle progression but also is involved in self-renewal and fate specification in the developing cerebral cortex. In contrast to its expression in the developing cerebral cortex, Uhrf1 was detectable in both apical and Mash1+ basal progenitors in the developing GE. This expression pattern is in accordance with the expression of Uhrf1 in stem cells but also in TAPs in the adult SEZ that is developmentally derived from the GE. However whether Uhrf1 is expressed in newborn neurons in the GE similar to its adult derivative SEZ remains to be elucidated. All together the identification of Uhrf1 protein in proliferating progenitors of the telencephalon is in agreement with our data from the adult neurogenic zones as well as the data from previous studies showing Uhrf1 in proliferating progenitors and its down regulation later in the lineage upon differentiation (Sen et al., 2010; Tittle et al., 2011).

5.6 Function of Uhrf1 in the developing cerebral cortex

As our study showed that Uhrf1 is expressed in the stem and progenitor cells of both the dorsal and the ventral embryonic telencephalon, we crossed the Uhrf1 conditional mice with the Emx1^{Cre} line which allows deletion selectively in the dorsal telencephalon based on Cre expression selectively in this region from E9.5 onwards (Iwasato et al., 2000). Consistent with the previous data, Cre expression effectively deleted Uhrf1 in the neocortex, hippocampal anlage and the cortical hem and Uhrf1 immunoreactivity could no longer be detected in these regions at E11 whereas it could still be detected in the ventral telencephalon (GE) where Cre is not expressed (Cappello et al., 2006, 2012). After examining the brain morphology of control and mutant littermates, we found striking degeneration of the cerebral cortex in the

Uhrf1 mutants. Although only a moderate decrease was observed in cortical thickness at postnatal day 0 (P0), at P27 the cortical size was severely reduced and DG was entirely lacking in the mutants. This strong cortical degeneration phenotype is reminiscent of the phenotype observed after deletion of the maintenance methytransferase, Dnmt1 with Emx1[Cre] line (Hutnick et al., 2009b), in agreement with the known role of Uhrf1 in recruiting Dnmt1 to the replication foci via physical interaction (Bostick et al., 2007; Sharif et al., 2007). Despite the massive degeneration of the cerebral cortex, similar to Dnmt1 mutants (Hutnick et al., 2009b), the Uhrf1 mutant mice were born in the expected Mendelian ratios and had a normal lifespan in the laboratory environment in accordance with the previously published data that reported that even complete loss of dorsal forebrain is not directly incompatible with the viability of the mutant mice in laboratory environment (H. S. Li et al., 2003).

Since many previous studies suggested that Uhrf1 is required for proper cell cycle progression (Arima et al., 2004; Bonapace et al., 2002; Tien et al., 2011; Tittle et al., 2011) and since we observed a decrease in progenitor proliferation upon Uhrf1 deletion in the adult neurogenic zones, to understand if the defects in proliferation of progenitors in the mutant embryos account for the reduced cortical thickness, we used immunostainings for PH3 to mark the cells in the G2/M phase of the cell cycle. Surprisingly and in contrast to the decreased proliferation of progenitors in the adult neurogenic zones upon Uhrf1 deletion, Uhrf1 deletion in the dorsal telencephalon of embryos did not result in a significant change in the total number of PH3+ cells. Although one can argue that these differences could be due to use of different markers to identify proliferating cells – BrdU and Ki67 to label the S phase cells and all cycling cells respectively in the adults and PH3 to label the G2/M phase in embryos – preliminary data showing immunostainings for BrdU and Ki67 in the mutant embryos did not either reveal a visible change in proliferation as well (data not shown).

Interestingly although total proliferation did not seem to be affected upon Uhrf1 deletion, the percentage of cells dividing at non apical positions was significantly increased at the expense of the percentage of apically dividing cells. As described in the introduction, cortical development is characterized by the presence of two distinct types of progenitor cells that can be distinguished by their location during mitosis. While apical stem and progenitors that originate from the neuroepithelium exclusively undergo mitosis at the ventricular surface, basal progenitors that arise from apical progenitors divide only in the subventricular zone in non-apical positions (Breunig et al., 2011; A. Kriegstein & Alvarez-Buylla, 2009). So

106

considering also that Uhrf1 is not expressed in basal progenitors that divide non-apically, we thought deletion of Uhrf1 could cause a fate change in the apical progenitors and this fate change could explain the increased proportion of non-apically dividing cells, as basal progenitors divide in non-apical positions. However to our surprise when we did immunostainings for Tbr2 and Pax6 to identify basal and apical progenitors respectively, we did not observe any change in the band of Tbr2+ or Pax6+ cells suggesting that changes in the position of proliferating cells are not accompanied by changes in these markers. Remarkably while the Tbr2 positive cells were found in their proper localization, the distribution of Pax6 positive cells was significantly altered such that more Pax6 positive cells were observed in ectopic positions above the Pax6 dense band.

The observation that many ectopic Pax6+ and PH3+ cells were present in the Uhrf1 mutant cerebral cortex then raised the question whether these progenitors delaminated from the ventricular surface due to defects in apical anchoring. At mid neurogenesis, apical progenitor cells are connected to each other via cadherin based adherens junctions (AJ) (Aaku-Saraste et al., 1996). Cadherin adhesion receptors form homophilic complexes with their extracellular domain in a Ca^{+2} dependent manner to mediate cell to cell contacts (Gumbiner, 2000). At their intracellular side, cadherinshave two different domains binding to β-catenin and p120-catenin (Castaño et al., 2002; Gumbiner, 1996). By interactions between β-catenin and α-catenin, cadherin clusters in AJ become connected to the F-actin cytoskeleton (Drees, Pokutta, Yamada, Nelson, & Weis, 2005; Yamada, Pokutta, Drees, Weis, & Nelson, 2005). Deletion of two essential components of AJs, β-catenin and α-catenin, with the Emx1^{Cre} or Nestin^{Cre} lines were shown to cause a strong cortical disorganization with many ectopic PH3+ and Pax6+ cells (Lien et al., 2006; Machon et al., 2003; Schmid, 2007). Moreover in both mutant cortices, cortical cells were shown to have round shape nuclei in contrast to the elongated nuclei of the WT cells (Schmid, 2007) which is another phenotype that we observe upon Uhrf1 deletion. Although in the Uhrf1 mutants, β-catenin levels appeared normal, a more detailed analysis of AJs at the ultra-structural level is required to ascertain that normal structure of the AJs is maintained upon Uhrf1 deletion.

Another possible explanation for the increased proportion of basally dividing cells could be the misspecification of dorsal progenitors to a more ventral identity, as ventral telencephalon was shown to have particularly high number of progenitors dividing at basal locations (Bhide, 1996; Pilz et al., 2013). For example, Pax6 mutation or deletion results in increased

proliferation of basally dividing cells which correlates with spread of ventral telencephalic progenitor markers to the dorsal telencephalon (Heins et al., 2002; Haubst et al., 2004; Stoykova et al., 2000; Toresson et al., 2000; Yun et al., 2001; Walcher et al. 2013). Conversely, in the Uhrf1 mutants, the transcription factors Mash1 and Olig2 were normally expressed by the progenitors of the ventral telencephalon and did not spread into the mutant cerebral cortex. The very few Mash1+ and Olig2+ cells present in the dorsal telencephalon of the mutants were consistent with the Mash1+ interneurons and Olig2+ oligodentrocyte progenitors that normally migrate from ventral telencephalon to dorsal telencephalon suggesting that dorso-ventral patterning is not affected in the Uhrf1 mutants and hence appears not to be the reason for the observed phenotype in the cerebral cortex.

Another possible reason for the presence of ectopic Pax6+ cells could be the aberrant maintenance of Pax6 in basal progenitors. Such defects in down regulation of progenitor proteins in more differentiated progeny was also observed upon deletion of Dnmt1, a known interaction partner of Uhrf1, in retinal progenitors (Rhee et al., 2012) as well as upon loss of Hdac2 function (Jawerka et al., 2010a), a member of class I HDACs that also comprise Hdac1 another interaction partner of Uhrf1, in adult neural stem cells. Therefore it still remains to be elucidated by Tbr2 and Pax6 co-immunostaining if the ectopic expression of Pax6 is due to defects in down regulation of apical progenitor markers in basal progenitors.

In addition to interacting with the epigenetic regulators through its TTD and PHD domains, Uhrf1 also has ubiquitin ligase activity mediated through its Ring finger domain that has recently shown to be responsible for ubiquitination dependent degradation of promyelocytic leukemia protein (PML)(Guan, Factor, Liu, Wang, & Kao, 2013). PML is a tumor suppressor that limits the proliferation of RG cells and hence promotes the generation of committed neural progenitors (Regad, Bellodi, Nicotera, & Salomoni, 2009).Deletion of PML in the developing cerebral cortex showed increased percentage of apically dividing cells at the expense of the ones dividing non apically (Regad et al., 2009). As this is exactly the opposite of what we observe upon deletion of Uhrf1 in terms of division behavior of progenitors, it is also possible that deletion of Uhrf1 inhibits ubiquitination dependent degradation of PML and accumulation of PML is in part responsible for the observed decrese in the apically dividing cells.

In addition to defects in cell cycle progression, another possible mechanism that can lead to decreased cortical size is cell death. In agreement with the previously published data that

showed Uhrf1 depletion causes apoptosis in many tissues (Abbady et al., 2003, 2005; Dai, Shi, & Gu, 2013; Tien et al., 2011; Tittle et al., 2011), TUNEL assay showed that apoptosis is increased in the Uhrf1 mutant cortices and hence mediates at least in part the severe cortical degeneration observed upon Uhrf1 deletion. Given the ability of Uhrf1 to induce degradation-independent ubiquitination of TIP60 which suppresses the ability of TIP60 to acetylate p53 at K120 and mediate apoptosis (Dai et al., 2013), increased apoptosis observed in the Uhrf1 mutants could be resulting from the increased TIP60 mediated acetylation of p53 at K120 which is crucial for p53-dependent apoptotic responses. However another study also showed that Uhrf1 depletion in cancer cells causes caspase-8 dependent apoptosis in p53 containing and deficient cells (Tien et al., 2011) suggesting that cell death in observed response to Uhrf1 deletion could also act via p53 independent pathways. Moreover deletion of both Dnmt1 and G9a,a histone H3 lysine 9 (H3K9) methyltransferase that has also been shown to interact with Uhrf1 (Jin et al., 2010; Kim at al., 2009), cause increased apoptosis in dorsal forebrain and retinal progenitors respectively (Hutnick et al., 2009b; Katoh et al., 2012), further suggesting that the phenotype observed upon Uhrf1 loss could be caused by the disruption of the complex interactions that Uhrf1 has with the other epigenetic modifiers.

5.7 Regulatory function of Uhrf1 on gene expression in the developing cerebral cortex

Since deletion of Uhrf1 caused a dramatic phenotype with altered proliferation and localization of progenitors and strong degeneration of the cerebral cortex, I performed a genome wide transcriptome analysis of Uhrf1 heterozygous and mutant cerebral cortices to understand the molecular mechanisms leading to the observed defects. Although the Uhrf1 was lost from progenitor at around E11, as the first effects on proliferation was observed at E14, this time point was chosen for the analysis. In accordance with the role of Uhrf1 in maintaining repressed chromatin states and with its colocalization with heterochromatin (Karagianni, Amazit, Qin, & Wong, 2008b; Papait et al., 2007, 2008; Sharif et al., 2007), more genes (64 %) were up regulated upon loss of Uhrf1. Among the up regulated genes, similar to the loss of Dnmt1 in dorsal forebrain progenitors (Hutnick et al., 2009a), there were many X-linked genes which is consistent with the role of Uhrf1 in recruiting Dnmt1 to repress these genes in somatic and embryonic stem cells (Fouse et al., 2008). Consistent with the striking cortical degeneration observed in the mutants, ApoE and Clu genes that have been

implicated in neurodegeneration, were also among the up-regulated genes. However, although we observed an increase in apoptosis at this stage upon Uhrf1 deletion, genes implicated in apoptotic pathway were not found to be increased in our transcriptome data. Instead many genes involved in "negative regulation of apoptosis" were up regulated upon Uhrf1 deletion suggesting that we observe some secondary effects such that at this stage cells are already up regulating their protective mechanisms to fight against the detrimental effects of Uhrf1 loss. Indeed in agreement with this idea, another Ph.D student Vidya Ramesh from our laboratory showed that unlike the proliferation phenotype, apoptosis starts earlier at E12 in mutant cerebral cortices (unpublished data).

Interestingly several members of the procadherin family, that have homophilic/heterophilic cell-cell adhesion properties and been implicated to play tightly regulated roles in circuit formation and maintenance (Kim et al., 2011), were also up regulated upon Uhrf1 deletion. Among the up regulated procadherins, Pcdh16, also known as Dachsous1 (Dchs1) was very recently shown to be an important regulator for the proliferation of progenitor cells (Cappello et al., 2013) and Pcdh18 was shown to interact with Disabled-1 (Dab1), an intracellular adapter protein mediating the effect of Reelin on neuronal migration and cell positioning during mammalian brain development (Homayouni, Rice, & Curran, 2001). Yet another up regulated gene that further highlights the importance of tight gene regulation via Uhrf1 during cerebral cortical development is thyroid hormone responsive (Thrsp) (also known as Spot14) that was recently shown to be required for maintenance of quiescence in the adult neural stem cells (Knobloch et al., 2013). On the other hand, the list of down regulated genes contained many genes involved in the development of cerebral cortex such as NeuroD4, Sox5, Satb2, Meis2, Pou3f3 and Bcl11b. Among these genes Sox5 and Bcl11b are mainly expressed in the deep layer neurons whereas Satb2 and Pou3f3 are expressed by the upper layer neurons (Molyneaux et al., 2007). As cortical degeneration was not observed and thickness of mutant and control cerebral cortices seem similar at this stage, down regulation of these genes can not be attributed to the overall cortical degeneration but probably rather results from defects in differentiation. Moreover many genes involved in axon guidance and neuronal migration such as Cxcl12, Dab1, Robo1, Robo2, Sema3A, Sema5A, Eph3A, Eph5A and Netrin4 (Andrews, Barber, & Parnavelas, 2007; Chen et al., 2008; Chivatakarn, 2008; Lysko, Putt, & Golden, 2011; Marín, Yaron, Bagri, Tessier-Lavigne, & Rubenstein, 2001) were also down regulated upon Uhrf1 deletion. As these molecules are also known regulators of corticothalamic axon

guidance and neuronal migration, their down regulation is also probably attributed to the defects in neuronal migration and differentiation. In summary, our gene expression analysis showed that Uhrf1 deletion has highly specific effects on gene expression some of which is probably directly caused by its role in gene repression whereas some of which probably results via secondary effects.

5.8 Conclusion and Future Prospects

Confirmation of the microarray data obtained from aNSCs, their progeny, ependymal cells and diencephalic astrocytes, enabled identification of many genes that have not been implicated in neurogenesis before as potential regulators of neurogenesis. Conditional deletion of one of the selected candidate genes, Uhrf1, in both adult and embryonic neural stem cells had a striking phenotype, further suggesting that this data set can be utilized for further functional studies to understand the contribution of individual genes in the context of neural stem cell biology. Although in this study, the effect of Uhrf1 deletion on both embryonic and adult neurogenesis was studied in detail, further studies that will enable us to identify the molecular mechanisms leading to the observed phenotypes is still required. Uhrf1 was shown to interact with many different proteins in different tissues and it is very plausible that it can regulate different aspects of neural development through its interaction with different partners. Therefore, mass-spectrometric analyses of UHRF1 pull-down complexes will further enable us to identify the UHRF1-associated nuclear proteins in the adult and embryonic neurogenic regions. Moreover in this study a genome wide expression analysis was performed in order to identify the genes that are deregulated upon Uhrf1 deletion. Although some of the up regulated genes are probably direct targets of Uhrf1, it is also very probable that some of these genes are up regulated upon derepression of retrotransposons such as intracisternal A particle (IAP), long interspersed nuclear element 1 (LINE-1) and short interspersed nuclear element 1 (SINE-1) which are normally silenced by Uhrf1 (Sharif et al., 2007). Similarly, deletion of a histone H3 Lys9 (H3K9) methyltransferase ESET in neural progenitor cells, that is also involved in repression of retrotransposons, caused up regulation of many genes located near the retrotransposons due to the formation of chimeric transcripts (Tan et al., 2012). Therefore, further deep sequencing analysis is required to identify if some of the up regulated genes are influenced by nearby retrotransposons in the absence of Uhrf1. Moreover genome wide ChIP sequencing experiments to identify the promoters that are bound by Uhrf1, will also be very helpful to identify genes that are directly regulated by

Uhrf1. Uhrf1 associated protein complexes identified in different tissues, suggest that Uhrf1 is involved in the regulation of local and global epigenome. So further experiments to analyze how the methylation levels of the promoters or different modifications of the chromatin, change upon Uhrf1 deletion, may also shed light on gene regulation by DNA and histone modifications mediated via Uhrf1. As Uhrf1 up regulation is observed in many different cancers including glioblastomas, understanding gene regulatory mechanism mediated via Uhrf1 will also contribute to the development of better treatment strategies.

6. Materials and Methods

6.1 Materials

6.1.1 Chemicals

Chemical	Company
Acetic Acid	Merck
Agarose	Biozym
Ampicillin	Roth
Aqua Poly / Mount	Polyscience Inc.
Boric Acid	Roth
Bovine Serum	Sigma
BrdU (5'-bromo-2'-deoxyuridine)	Sigma
DAPI (4,6-dasmindino-2-phenylindol)	AppliChem
Deinhardt's solution	Gibco (Invitrogen)
Dextran sulfate	Sigma
Diethyl ether	Merck
Difco LB-Agar	Hartenstein Labor.
DNA Ladder (Generuler 1kb)	Fermentas
EDTA	Merck
Ethanol	Merck
Ethidium bromide	Roth

Ethyleneglycol	Merck
Formamide	Merck
Glycerol	Sigma
Glycine	AppliChem
HEPES	Roth
Hydrochloric acid	Merck
Hydrogen peroxides	Roth
Isopropanol	Merck
Maleic Acid	Sigma
Mercaptoethanol	Merck
Normal goat serum (NGS)	Vector Lab.
Orange G	Sigma
Paraformaldehyde (PFA)	Merck
PCR buffer (10X Taq Buffer)	Fermentas
PCR dNTP Mix (25mM each)	Fermentas
PCR reagent: $MgCl_2$ (25mM)	Fermentas
Potassium chloride	Merck
Potassium dihydrogen phosphate (KH_2PO4)	Merck
Proteinase K	Roth
Sodium azide	Merck
Sodium chloride	Fisher Bioreagents

Sodium citrate	Merck
Sodium dodecyl sulphate (SDS)	Roth
Sodium hydroxide	Roth
Sodium phosphate (Na$_2$HPO4•7H$_2$O)	Merck
Taq DNA Polymerase	Fermentas
Tissue Tek	Hartenstein Labor.
Tris Base	Sigma
Tris-HCl	Roth
Triton-X 100	Roth
Tween-20	Sigma

6.1.2 Tissue Culture Reagents

Chemical	Company
B-27 Serum-Free Supplement	Gibco (Invitrogen)
Sodium bicarbonate	Gibco (Invitrogen)
Bovine serum albumin (BSA)	Sigma
D-Glucose (Stock 45%)	Sigma
DMEM:F12 (Dulbecco's Modified Eagel Medium:Nutrient Mixture F12)+ GlutaMAX	Gibco (Invitrogen)
DMSO	Sigma

EBSS (Earle's Balanced Salt Solution)	Gibco (Invitrogen)
EGF (Epidermal Growth Factor)	Roche
FCS (Fetal Calf Serum)	Pan
FGF2 (Fibroblast Growth Factor-2)	Roche
HBSS 1X (Hank's balanced salt solution)	Gibco (Invitrogen)
HBSS 10X	Gibco (Invitrogen)
HEPES (1M)	Gibco (Invitrogen)
Hyaluronidase	Sigma
L-Glutamine (200mM)	Gibco (Invitrogen)
Penicillin/Streptomycin (Pen/Strep)	Gibco (Invitrogen)
Poly-D-Lysine (PDL)	Sigma
Tris-HCl (1M)	Rockland
Trypan Blue	Gibco (Invitrogen)
Trypsin	Sigma
Trypsin (EDTA), 0.05%	Gibco (Invitrogen)

6.1.3 Standard Solutions and Buffers

6.1.3.1 Phosphate Buffer Saline (PBS) (0.15M)

137mM NaCl

27mM KCl
83mM Na_2HPO_4
15mM KH_2PO_4

A 10X stock solution of PBS was prepared by dissolving 400g NaCl, 10g KCl, 10g KH$_2$PO$_4$and 58.75g Na$_2$HPO$_4$ x 2 H$_2$O in 5 liter Millipore water and the pH was adjusted to 6.8. After autoclaving, this stock solution was diluted 1:10 with autoclaved Millipore water to have 0.15M 1X PBS with a pH of 7.4.

6.1.3.2 Paraformaldehyde (PFA) 4%

40g of PFA was dissolved in 800ml MilliQ water by gentle heating during stirring and 3 NaOH pellets were added to enable and facilitate complete dissolvent. The solution was then cooled down to room temperature and HCl was added slowly till the pH drops dramatically between pH 1-3. The pH was then adjusted to 7.2 -7.3 with 100ml of 10X PBS and the solution was filled to 1l with MilliQ water. The solution was then filtered through a paper filter and stored at 4 C.

6.1.3.3 Lysis Buffer for tail DNA extraction

100mM Tris, pH 8.0-8.5

200mM NaCl

5mM EDTA, pH8.0

2% SDS

1l of lysis buffer was prepared by mixing 100ml 1M Tris HCl, 10ml 0,5M EDTA, 20ml 10% SDS, 200ml 1M NaCl and 660ml autoclaved H$_2$O. Before lysis 10μl/ml of Proteinase K (10mg/ml) of lysis solution were added freshly.

6.1.3.4 Storing Solution

30ml Glycerol, 30ml Ethylenglycol, 30ml autoclaved H$_2$O, and 10ml 10X phosphate buffer (0.25M, pH 7.4, 13.8g NaH$_2$PO$_4$xH$_2$0, 3.0g NaOH dissolved in 40ml H$_2$0) was mixed, the solution was sterile filtered and stored in fridge.

6.1.3.5 50X Tris Acetate EDTA (TAE) Buffer

2M Tris Acetate

50mM EDTA

Adjust pH 8.0 with Acetic Acid

1l of 50X TAE-buffer was prepared by dissolving 242g Tris Base, 57.1ml Acetic Acid and 100ml 0.5M EDTA in 800ml autoclaved H_2O. The pH was then adjusted to 8.0 with Acetic Acid and the solution was filled to 1l with autoclaved H_2O.

6.1.4 In situ Hybridization (ISH) Buffers

6.1.4.1 20X SSC (1L)

175.3g NaCl and 88.23g Sodium Citrate (100.5g Sodium citrate dihydrate) was dissolved in 1l dd H_2O and the pH was adjusted to 7.0.

6.1.4.2 Hybridization Buffer

5ml Formamid, 1ml 20X SSC, 200µl 50X Deinhardt's solution, 2ml Dextran sulfate and 1ml t-RNA (10mg/ml) was mixed and the solution was filled to 10ml with ddH_2O

6.1.4.3 Washing Solution

25ml Formamide, 2.5ml 20X SSC and 0.5ml 10 % Tween-20 was mixed and filled to 50ml with 22ml ddH_2O.

6.1.4.4 5X MABT

116.08g Maleic acid (500mM end concentration) was dissolved in 1980ml ddH_2O and the pH was adjusted to 7.5 by adding 70g NaOH. Then 87.7g NaCl (750mM end concentration) and 20ml 10% Tween20 was also added and dissolved in this solution.

6.1.4.5 Blocking Solution

2ml 5X MABT, 2ml Bovine Serum, 2ml 10 % Blocking Reagent was mixed and filled to 10ml with 4ml ddH_2O

6.1.4.6 AP Staining Buffer

5ml 1M Tris pH 9.5, 2.5ml 1M $MgCl_2$, 1ml 5M NaCl, 0.5ml 10 % Tween-20 was mixed and filled to 50ml with 41ml ddH_2O

6.1.5 Cell Culture Solutions

6.1.5.1 Dissection medium

Add 5ml of HEPES 1M (final concentration 10mM) to 500ml of HBSS 1X

6.1.5.2 Solution I

50ml 10X HBSS

9ml D-Glucose (final concentration 0.81%)

7.5ml HEPES

Fill up to 500ml with ddH$_2$O and adjust the pH to 7.5 using 7.5 % (wt/vol) sodium bicarbonate

6.1.5.3 Solution II

25ml 10X HBSS

154g Sucrose

Fill up to 500ml with ddH$_2$O and adjust the pH to 7.5 using 7.5% (wt/vol) sodium bicarbonate.

6.1.5.4 Solution III

10ml HEPES (1M)

20g BSA

Fill up to 500ml with EBSS and adjust the pH to 7.5 using 7.5% (wt/vol) sodium bicarbonate

6.1.5.5 Staining Solution

Add 200μl of 1% (wt/vol) sodium azide solution (final concentration 0.02%, wt/vol) and 1ml of FBS (final concentration 10%, vol/vol) to 10ml of PBS.

6.1.5.6 Neurosphere Media

1ml B27 supplement

0.5ml Penicillin/Streptomycin (100X)

0.4ml HEPES (1M)

50μl EGF2 (20μg/ml)

50μl FGF (10μg/ml)

Fill up to 50ml with DMEM/F12 + Glutamax

6.1.6 Kits

Name	Company
RNeasy Mini Kit	Qiagen
RNeasy Micro Kit	Qiagen
QIAprep MaxiPrep	Qiagen
QIAEX II Gel Extraction Kit	Qiagen
DyeEX 2,0 Spin columns	Qiagen
QIAquick PCR Purification kit	Qiagen
SuperScript™ III Reverse Transcriptase kit	Invitrogen
StrataClone PCR Kit	Stratagene
Tyramide Signal Amplification Kit	Perkin Elmer
Ovation PicoSL WTA System V2	Nugen
Encore Biotin Module	Nugen

6.1.7 Antibodies

6.1.7.1 Primary Antibodies

Antigen (species)	Working Dilution / Pretreatment	Company
Anti-β-Catenin (mouse, IgG)	1:200	BD Transd. Lab
Anti-β- tubulin-III (mouse, IgG2b)	1:500	Sigma Aldrich
Anti-BrdU (rat)	1:200 / HCl treatment	Abcam
Anti-Cd45 (rat)	1:100	BD Pharmingen

Anti-Ctip2 (rat)	1:200	Abcam
Anti-Cux1 (rabbit)	1:200	Santa Cruz
Anti-DCX (guineapig)	1:1000	Chemicon
Anti-Foxg1 (rabbit)	1:250	Abcam
Anti-Foxp2 (rabbit)	1:200	Abcam
Anti-GFAP (rabbit)	1:200	DAKO
Anti-GFAP (mouse, IgG1)	1:200	Sigma
Anti-GFP (chicken)	1:800	Aves Labs
Anti-Ki67 (rabbit)	1:200 / Citrate buffer boiling	Thermo Scientific
Anti-Mash1 (mouse, IgG1)	1:200	Kind gift from O.Raineteau
Anti-NeuN (mouse, IgG1)	1:100	Millipore
Anti-Olig2 (rabbit)	1:500	Millipore
Anti -Pax6 (rabbit)	1:500	Millipore
Anti-PH3 (rabbit)	1:500	Millipore
Anti Prominin1 (rat)	1:100	eBioscience
Anti PDGFRα (rat)	1:200	BD Pharmingen
Anti-S100 β (mouse, IgG1)	1:500	Sigma
Anti –Tbr2 (rabbit)	1:200	Abcam
Anti TSP-4 (guinea pig)	1:250	Kind gift from F. Zaucke

Anti Uhrf1 (rabbit)	1:1000	Kind gift from I.M. Bonapace
Anti Whsc1 (rabbit)	1:250	Abcam

6.1.7.2 Secondary Antibodies

Antigen (species)	Working Dilution	Company
Anti rabbit Alexa488, 546,633	1:1000	Invitrogen
Anti chick Alexa 488	1:1000	Invitrogen
Anti rat Cy5	1:1000	Jackson Laboratory
Anti guinea pig Alexa546, 633	1:1000	Invitrogen
Anti-mouse IgG1 Alexa 488,546,633	1:1000	Invitrogen
Anti-mouse IgG2b Alexa546, 633	1:1000	Invitrogen

6.1.8 Primers

6.1.8.1 Genotyping Primers

Name	Sequence 5´-3´
Glast for	GAGGCACTTGGTAGGCTCTGAGGA
Glast rev	GAGGAGATCCTGACCGATCAGTTGG
CER1(CreERT2 specific)	GGTGTACGGTCAGTAAATTGGACAT
hGFAP for	ACTCCTTCATAAAGCCCTCG
GFP rev	AAGTCATGCCCTTCAGCTC

Emx1 for	GTGAGTGCATGTGCCAGGCTTG
Emx1 rev	TGGGGTGAGGATAGTTGAGCGC
Cre	GCGGCATAACCAGTGAAACAGC
Uhrf1 for	ACCACATCACTCTTGATCTGTGCC
Uhrf1 rev	GGATGTTAGGTGTGAGCCACCATG
LAR3	CAACGGGTTCTTCTGTTAGGCC
CAG for	CTGCTAACCATGTTCATGCC
CAG rev	GGTACATTGAGCAACTGACTG

6.1.8.2 Cloning Primers

Name	Sequence 5´-3´
Hes6 for	ACTGTCTCAGCTGAACTCCT
Hes6 rev	CTCTCCAAAAGTCTCCTGTC
Hes6 nested	ATCCAGAGCTCTAGGGTCC
Whsc1 for	TGAGGAAGCTGCCAGCATGT
Whsc1 rev	TCTGGCCGTTTTGTCGGTGA
Whsc1 nested1	GGACCAATTGCACCTCAACCCT
Whsc1 nested2	TTTTCCTGGGCGCGTCTTCA
Uhrf1 for	ACCACCGTGTGTCAGCACAA
Uhrf1 rev	TGAAGAAGTGGCCAGCCCAA
Uhrf1 nested	ATCATGTCAGTGAATGGCGCGG

Brunol5 for	TCAACAAGCAGCAGTCAG
Brunol5 rev	TAAACAGGTTACAGCCTTCG
Brunol5 nested1	AAGTTTTCTTCCCACACAGA
Brunol5 nested2	GGATACATGGCTGTGTACTG

6.1.8.3 Real Time PCR Primers

Name	Sequence 5´-3´
Thbs4 for	CTTAGAAACTCCATCCTTGG
Thbs4 rev	TCCAGGGCTCTCTAGTGTAT
Foxg1 for	CCACAGGGAAATAGAGAGAG
Foxg1 rev	CAAAATCCTAGGGACAAAAG
Rarres for	ACTGTCTCAGCTGAACTCCT
Rarres rev	CTCTCCAAAAGTCTCCTGTC
Foxj1 for	TCGCAGCAAGCTTCAAGACG
Foxj1 rev	ATAGCCAGGCAGCCATGGAACT
Fech for	TGAGGAAGCTGCCAGCATGT
Fech rev	TCTGGCCGTTTTGTCGGTGA
Mia1 for	ACCACCGTGTGTCAGCACAA
Mia1 rev	TGAAGAAGTGGCCAGCCCAA
Bmper for	GCATGTCCTGCACTGAAGTC
Bmper rev	AAACGTAGATGGCCCCTAGC

Sox11 for	ATCATGTCAGTGAATGGCGCGG
Sox11 rev	TCAACAAGCAGCAGTCAG
Wdr16 for	GGAGGGCACTTTGTTACAGG
Wdr16 rev	CACGAAGCAAATGGGTATTTC
CyclinD2 for	CGCTCGCCCACCTTCCACTC
CyclinD2 rev	CCAGCCGGCCACCACTCG
Rere for	TGGCTTCCTTTTGGACTTTG
Rere rev	AGTGAGACGTGAAGCCCAAC
Creb1 for	AGCCCCTGCCATCACCACT
Creb1rev	ACCCATCCGTACCATTGTTAGC
1700021K14 for	CTACAGGCACCAAGCAAACC
1700021K14 rev	CCGTGAGTGTGTTGAACAGG
E030011K20 for	CACAGCTGGATCACTTGTGC
E030011K20 rev	AAGTGGACATCCCAGAATGC
1700001C02Rik for	GACCTACCAGACCTTCCCATC
1700001C02Rik rev	GGTCAACCACCTGGTTTCAG

6.2 Methods

6.2.1 In vivo Methods

6.2.1.1 Mouse lines

All the animals used for the experiments were kept at the animal facility of the Helmholtz Zentrum München on a 12h light-dark cycle. All the animal procedures were performed in accordance with German and European Union guidelines. Adult animals were used at the age of 2-3 months and embryonic animals were used at the indicated embryonic day where day of vaginal plug was considered to be embryonic day 0 (E0).

Strain	Characteristics	Producer
Emx1[Cre]	Emx1[Cre] line expresses Cre recombinase from the endogenous *Emx1* locus.	Iwasato et al.2000
CAG CAT eGFP	The CAG CAT GFP reporter line contained CMV-β actin promoter and loxP flanked CAT gene upstream of the enhanced green fluorescent protein (eGFP) cassette so only after successful Cre excision eGFP is expressed	Nakamura et al 2006
hGFAP-GFP	The hGFAP-GFP line labels astrocytes by the enhanced green fluorescent protein (eGFP) that is expressed under the control of the human glial fibrillary acidic protein (GFAP) promoter.	Nolte et al 2001
GLAST[CreERT2]	The GLAST[CreERT2] mouse line contains the inducible form of Cre (CreERT2) in the astrocyte specific glutamate transporter (GLAST) locus. The fusion of Cre to the ligand binding domain of the modified estrogen receptor (ERT2) is inactive and translocate only upon tamoxifen binding into the nucleus where it can then mediate the recombination.	Mori et al
Uhrf1[tm1a(EUCOMM)Wtsi]	The Uhrf1[tm1a(EUCOMM)Wtsi] mouse line was generated by EUCOMM by using promoterless targeting cassettes for the generation of knockout-first alleles (Skarnes et al., 2011). The KO-first allele is flexible and produces conditional allele (tm1c) upon exposure to site specific recombinase Flp. Further exposure of this conditional allele to another site specific recombinase, Cre then produces the deletion allele (tm1d).	EUCOMM

6.2.1.2 BrdU Administration

To label fast proliferating cells 100mg/kg bodyweight of DNA base analogue 5 bromodeoxyuridine (BrdU) was injected intraperitoneally 1h before sacrifice. BrdU was dissolved at a concentration of 10mg/ml in sterile 0.9 % NaCl solution (Braun) by continuous stirring at 37°C for 2h.

To label slow proliferating stem cells BrdU was given in drinking water at a concentration of 1mg/ ml for two weeks followed by normal drinking water for another two weeks.

6.2.1.3 Tamoxifen Treatment

Tamoxifen (Sigma, T-5648) was dissolved in pre-warmed corn oil (Sigma, C-8267) at a concentration of 20mg/ml by sonicating it for 15 min. Then 50ul of this solution was injected intraperitoneally twice a day for 5 consecutive days to achieve efficient recombination in mice carrying one $GLAST^{CreERT2}$ allele. This solution was kept at 4ºC maximally for 1 month to avoid precipitation.

6.2.1.4 TSP-4 Infusion

Recombinant human Thrombospondin4 (R and D Systems, 2390-TH-050) dissolved in artificial Cerebro Spinal Fluid (aCSF) at a concentration of 100ug/ml or only aCSF was infused at a rate of 250ng/day for 7 days into the lateral ventricle of hGFAP-GFP mice at the coordinates -0.2 (anterioposterior), 1 (mediolateral), 2 (dorsoventral) by miniature implantable osmotic minipumps (Mini Osmotic Pump Model 2001, Alzet; Brain infusion Kit 2, Alzet).

The brain infusion kit and the osmotic pump was assembled and filled with the solution to be delivered according to manufacturer's guidelines and then pumps were kept at 37°C for overnight before implanting into animals. Animals were sacrificed 7days after infusion.

6.2.1.5 Anesthesia and Perfusion

For perfusion, animals were anesthetized by intraperitoneal injection of Ketamin (Ketaminhydrochlorid, 100mg per kg of body weight) and Rompun (Xylazinhydrochlorid, 20mg per kg of body weight) prepared in 0.9 % NaCl solution (Braun). Then they were transcardially perfused first with a preflush of PBS followed by 4 % PFA in PBS. The brains were then removed and post fixed in 4 % PFA overnight.

6.2.2 Methods in Cell Biology

6.2.2.1 Tissue Preparation

For cutting vibratome sections, after post fixation, brains were washed in PBS for a few hours and then embedded in 4% agarose prepared in PBS. After the agarose hardened, brains were cut at a thickness of 70um with the vibratome and collected in PBS. For long term storage, the sections were kept either in PBS including 0.1% sodium azide or in storing solution (see standard solutions and buffers section)

For cutting cryosections, after postfixation, the brains were cryoprotected in 30% sucrose solution prepared in PBS for a few days and then embedded in Tissue-Tek and snap-frozen in dry ice. Frozen brains were then sectioned at a thickness of 20μm at the cryostate and collected on Superfrost glass slides. These slides were kept at -20°C until proceeding with immunohistochemical analyses.

6.2.2.2 Immunostaining

Primary antibodies (see table for the antibody concentrations and companies of the antibodies used) were diluted in 0.1M PBS containing 0.5 % Triton-X-100 and 10 % normal goat serum and sections were incubated with this solution overnight at 4°C. The following day sections were washed in PBS 3 times and then incubated at room temperature for 2 hours with subclass specific secondary antibodies conjugated to a fluorescent dye, diluted also in 0.1M PBS containing 0.5 % Triton-X-100 and 10 % normal goat serum. After several washes in PBS, DAPI was used at a concentration of 0.1μg/ml in PBS to visualize the nuclei by incubating sections for 10 minutes. Then sections were placed by the use of brushes on glass slides, dried shortly and mounted with Aqua Polymount.

Although this general protocol worked for many of the antigens, some antigens required specific retrieval or amplification procedures since they were masked during the tissue preparation or they were weakly expressed. Different retrieval or amplification procedures used in this thesis are summarized below.

6.2.2.2.1   DNA denaturation

Since 5'-bromo-2'-deoxyuridine (BrdU) is incorporated into the DNA, its detection required a special treatment where DNA is denatured. For this, sections were incubated in 2N HCl for 30

min, followed by neutralization of the pH by incubating the sections in 0.1M sodium tetraborate buffer (pH 8.5) for 30min. Afterwards sections were rinsed once in PBS and then incubated in the anti-BrdU antibody at 4°C overnight.

6.2.2.2.2   Microwave heating

In order to retrieve the Ki67 epitope, sections were boiled for 8 min in microwave in 0.01M sodium citrate buffer and then rinsed in PBS a few times before incubation with the primary antibody.

6.2.2.2.3   Tyramide signal amplification

To enhance weak signals or to be able to use antibodies produced in the same species for simultaneous detection of two proteins, tyramide amplification kit from Perkin Elmer was used. Briefly, after washing the sections three times in TNT buffer, endogenous peroxidase activity was quenched by incubating sections in 0,3% H_2O_2 for 30 min. Then sections were washed in TNT buffer again and were incubated with primary antibody diluted in TNB Buffer at 4°C overnight. Next day after several washing steps, sections were incubated with corresponding biotinylated antibody at room temperature for 1 hour, followed by another incubation step with horseradish-peroxidase coupled Streptavidin for another 1 hour. After several washes in TNT buffer, finally the fluorophore tyramides (Fluorescein or Tetramethylrhodamine) diluted 1:100 in the provided amplification buffer were added to the specimens for 7min.

Tyramid Signal Amplification Kit Reagents

Reagent	Content
TNT Buffer	0.1M Tris-HCl (pH 7.5), 0.15M NaCl, 0.005% Tween 20
Blocking Reagent	Milk powder
TNB Buffer	0.1M Tris-HCl (pH 7.5), 0.15M NaCl and Blocking reagent
SA-HRP	Horseradish-peroxidase coupled Streptavidin
Amplification reagent	Fluorescein or Tetramethylrhodamine

6.2.2.3 In *situ* Hybridization

In situ hybridization (ISH) can be divided into 3 parts. (i) generation of plasmids containing cDNA of the mRNAs of interest (described in chapter 6.2.3.7) (ii) in vitro transcription to generate the digoxygenin (DIG)-labeled probes (described in chapter 6.2.3.12) (iii) hybridization of the probe and detection of the mRNA of interest.

ISH was carried out on 70um thick vibratome sections under semi sterile conditions using sterile gloves and pipettes. Hybridization was performed in a sterile Eppendorf tube and the following steps in 24- or 6-well plates.

500ul of hybridization buffer was put in an Eppendorf tube and after adding the RNA probe; the mixture was incubated at 74°C for 4 minutes to separate the RNA strands. Then 3-4 vibratome sections were added to the tube and the hybridization was carried out in a water bath at 65°C overnight. Next day, the washing solution was pre-warmed in a water bath to 65°C and vibratome sections were moved into a 6-well plate containing the pre-warmed washing solution. After incubation of the sections in washing solution twice for 30 minutes, they were moved into wells containing in 1X MABT and incubated in this solution 2X for 30 minutes at room temperature. Then the sections were transferred to 6 well plates containing 500ul of blocking solution and incubated at room temperature for 1 hour. Then the Anti-digoxigenin Fab fragments coupled to alkaline phosphatase (Roche) were diluted 1:2000 in blocking buffer and the vibratome sections were transferred to the next well containing the antibody solution and incubated at 4°C over night. The next day, sections were washed 4 – 5 times in 1X MABT buffer and twice in freshly prepared AP staining buffer. NBT and BCIP (Roche) were added to the AP buffer (3.5μl/ml AP staining buffer) and sections were incubated with this solution until the desired staining intensity was reached. Reaction was stopped by washing the section in autoclaved water.

6.2.2.4 Fluorescence Activated Cell Sorting (FACS)

6.2.2.4.1   Preparation of cells for FACS

WT and hGFAP-GFP animals were anesthetized with ether and killed with cervical dislocation. The brains were then removed and kept in ice cold HBSS+HEPES. The SEZ and the Diencephalon were dissected and put into separate falcon tubes containing 5ml Solution 1 supplemented with 100μl 0.05% Trypsin/EDTA. The tubes were then incubated at 37ºC for

30 minutes and the tissue was mechanically triturated every 15 minutes with a fire polished Pasteur pipette to achieve a proper dissociation of the tissue. After a maximum incubation time of 30 minutes, the enzymatic activity was stopped by adding equal volume of Solution 3 containing 4% BSA and the samples were filtered with a 70μm pore size cell strainer to remove undissociated pieces of tissue.The samples were then centrifuged at 1200rpm for 5 min, the supernatant was removed, and the cell pellet was resuspended in 10ml Solution 2 containing 0.9M sucrose, and centrifuged for 15 min at 2000rpm to get rid of the debris and dead cells in this gradient. The supernatant was again removed, the pellet was resuspended in 2ml ice cold Solution 3 and the resuspended cells were added on top of 13ml Solution 3 and centrifuged at 1500rpm for 7 minutes. The cell pellets obtained from the Diencephalon of hGFAP-GFP animals and from the SEZ and Diencephalon of WT animals were resuspended in neurosphere media to sort cells at the FACS. The cell pellets obtained from the SEZ of hGFAP-GFP animals were resuspended in 500μl staining solution containing 0.02% NaN_3 to continue the staining procedure.

6.2.2.4.2   Immunostaining of cells for FACS

Single cell suspension isolated from the SEZ of hGFAP-GFP animals, was then divided into two tubes and stained either with PE conjugated Prominin1 (1:100) or PE conjugated rat IgG1 K isotype control (1:100) in the staining solution with $NaN_3$for 30 min at 4 °C in the dark. Cells were then washed with staining solution, centrifuged for 5 mins at 1200rpm and the pellet was resuspended in neurosphere media to process for FACS. Immediately before FACS analysis, PI was added 1:1.000 (final concentration, 1μg/ml) to WT cells to determine the proportion of dying cells.

6.2.2.4.3   FACS analysis and sorting

FACSAria (BD) set at purity mode and the appropriate sort rate (below 1000 cells per second for high purity and recovery of cells) was used for sorting of different populations. Compensation was performed for PE and fluorescein isothiocyanate (FITC) since both are excited with a blue laser.Forward scatter–area (FSC-A) and the side scatter–area (SSC-A) gate was used to exclude cell debris and FSC-A and forward scatter–width (FSC-W) gate was used to exclude cell aggregates. Rate of cell death was determined by measuring the

proportion of PI+ cells and all the experiments with cell death rates higher than 5% were discarded

WT, unstained cells were used to set the gate for transgenic hGFAP-GFP and SEZ cells stained with rat IgG1 K isotype control PE were used to set the gate for Prominin1 PE. Then GFP only, Prominin1 only and GFP/Prominin1 double + cells were sorted simultaneously into tubes containing culture medium. After sorting, the cells were centrifuged for 30 minutes at 1000rpm and re-suspended in 100µl of lysis buffer (RLT from QIAGEN with β-mercaptoethanol) for RNA isolation.

6.2.3 Methods in Molecular Biology

6.2.3.1 DNA extraction from tail

In order to maintain the colonies and identify control and mutant animals, mice were genotyped by using the DNA extracted from the tail. To extract DNA, tail biopsies of less than 5mm were taken into 1.5 ml tubes and incubated in 0.5ml lysis buffer overnight at 55 °C. After lysis hair and tissue residues were removed by centrifugation in an Eppendorf centrifuge at maximum speed for 10-20min. Then the supernatant was taken into another tube and DNA was precipitated by adding 0.5ml isopropanol followed by another centrifugation at maximum speed for about 5-7 min. After the supernatant was removed and the pellet was completely dried at room temperature, DNA was dissolved in 300µl ddH$_2$O pH 8 by shaking at 55°C for 1-2 hours.

6.2.3.2 DNA extraction from plasmids

When the DNA was isolated from small scale liquid bacterial cultures QIAGEN Mini Kit was used and when it was isolated from large scale liquid bacterial cultures QIAGEN Maxi Kit was used according to manufacturer's protocol. DNA was resuspended in 50µl or 150-200µl ddH$_2$O depending on use of the Mini or Maxi Kit respectively.

6.2.3.3 RNA extraction

For the generation of in situ probes and for the microarray analysis of Uhrf1 mutant cortices, total RNA was isolated from SEZ and Diencephalon of WT adult mice and from the whole cortical tissue of E14 embryos respectively, using the QIAGEN RNeasy Mini kit according to manufacturer's instructions.

For the confirmation of the microarray data of sorted cell populations by Real Time PCR, around 400.000 events were combined from each sorted population and total RNA was isolated from these sorted cells using the QIAGEN RNeasy Micro kit. Lysis Buffer was supplemented with 1µl of N and P carriers which protect against RNases and surface adsorption in spin column purifications to have a better recovery of small amount of RNA and the rest of the RNA preparation was carried according to manufacturer's protocol.

6.2.3.4 Determination of the concentration and quality of nucleic acids

The concentrations of nucleic acids were determined using the Nanodrop, a spectrophotometer that measures the extinction at 260nm to determine the concentration of nucleic acids and at 280nm to determine the concentration of proteins. The samples that had a E260nm/E280nm ratio between 1.8-2.0 were considered as clean DNA or RNA solutions.

The quality of RNA was further analyzed using the Agilent Bioanalyzer. Agilent Bioanalyzer creates electrophorograms that measure the abundance of ribosomal 5S, 18S, and 28S RNAs. Then it assigns RNA Integrity Number (RIN) that ranges from 1 (reflecting totally degraded RNA) to 10 (reflecting completely intact RNA). For microarray analysis and Real Time PCR only high quality RNA (RIN > 7) samples were used.

6.2.3.5 Genotyping by Polymerase Chain Reaction (PCR)

Reaction mix   2.5µl 10X buffer,

              5µl Q-Solution (Qiagen)

              0.5µl dNTPs,

              1µl each Primer,

              0.2µl Taq Polymerase,

        1.5 µl DNA

              10.7µl H_2O to final volume of 25µl

6.2.3.5.1   Emx1^{Cre} mice

The genotyping protocol of the Emx1^{Cre} mice was adapted from Iwasato et al. 2000.

	94°C	2 min	
	94°C	30 sec	Band size: WT 200bp; transgenic 500bp
35X	65°C	1 min	
	72°C	30 sec	
	72°C	10 min	

6.2.3.5.2 CAG CAT eGFP mice

The genotyping protocol of the CAG CAT eGFP mice was adapted from Nakamura et al. 2006.

	94°C	5 min	
	94°C	30 sec	Band size: 350bp
29X	55°C	30 sec	
	72°C	1 min	
	72°C	10 min	

6.2.3.5.3   hGFAP-GFP mice

The genotyping protocol for the hGFAP-GFP mouse line was adapted from Nolte et al., 2001.

	94°C	2 min	
	94°C	30 sec	
30X	61.5°C	30 sec	Band size: 498bp
	72°C	1 min	
	72°C	5 min	

6.2.3.5.4   Glast^{CreERT2} mice

The genotyping protocol of the Glast^{CreERT2} mice was adapted from Mori et al., 2006.

	94°C	2 min	
	94°C	20 sec	Band size: WT 700bp; recombinant 400bp
35X	55°C	20 sec	
	72°C	30 sec	
	72°C	5 min	

6.2.3.5.5   Uhrf1$^{\text{tm1d(EUCOMM)Wtsi}}$

The genotyping protocol was established according to the protocol received from EUCOMM

95C	5min	
94°C	30 sec	Band size: WT 331bp; recombinant 523bp
65°C	45 sec	
72°C	45sec	
72°C	10 min	

39 X

6.2.3.6 cDNA Synthesis

cDNA synthesis was done either by using the total RNA isolated from the SEZ tissue or by using the total RNA isolated from the sorted cells, using Oligo(dT) primers and the SUPERSCRIPT First Strand Synthesis System (Invitrogen) according to manufacturer's protocol.

6.2.3.7 Real Time PCR (RT-PCR)

To confirm the results obtained from microarray analyses, a quantitative Real Time PCR method was used, using SYBR Green mastermix (Biorad) according to manufacturer's recommendations on a DNA Engine Opticon™ machine (Biorad). GAPDH was used as the housekeeping gene to normalize the target gene's expression and the relative expression was calculated as $E = \frac{1}{2}^{(-\Delta Ct)}$, where Ct is the difference between the threshold of cycle number of GAPDH and the target gene. Primer sequences used for the target genes are given in chapter 6.1.8.3 in materials part.

Conditions for the RT-PCR

	Temp	Duration	Cycle #
Preheating	94°C	15s	1X
Denaturation	94°C	15s	
Annealing	50-60°C	30s	35-40X
Elongation	72°C	30s	

At the end of the elongation step fluorescence of each sample was measured to allow quantification of the RNA.

After amplification a melting curve was obtained by heating at 20°C/seconds to 95°C, cooling at 20°C/seconds to 60°C and slowly heating at 0.1°C/seconds to 98°C with fluorescence data collection at 0.1°C intervals. This melting curve analysis allowed determining melting temperature of primers in order to exclude primer dimers from the analysis.

6.2.3.8 PCR cloning of constructs to generate in situ probes

In order to reduce non-specific binding in products due to the amplification of unexpected primer binding sites, nested PCR was used instead of the standard PCR. Nested PCR involves two sets of primers that are used in two successive runs of PCR and the PCR product from the first amplification serves as a template for the second PCR.

Typically, for the first PCR 40ng of cDNA and for the second (nested) PCR 2µl of the first PCR reaction was used. The PCR was carried out with a total volume of 50µl using in the final mix 1X Fermentas PCR buffer without $MgCl_2$, 1.25mM $MgCl_2$, 0.2µM each primer, 2µM dNTPs and 0.5µl Fermentas Taq-Polymerase under the following conditions:

	Conditions for the first PCR			Conditions for the nested PCR		
	Temp	**Duration**	**Cycle #**	**Temp**	**Duration**	**Cycle #**
Preheating	95°C	20min	1X	95°C	5min	1X
Denaturation	94°C	1min		94°C	1min	
Annealing	48°C	1min	10X	55°C	1min	30X
Elongation	72°C	1min		72°C	1min	
Denaturation	94°C	1min				
Annealing	52°C	1min	20X			
Elongation	72°C	1min				
Final Elongation	72°C	20min	1X	71°C	10min	1X

After successful amplification, the desired product was confirmed by running the samples on 1% agarose gel, and the PCR product was subsequently cloned into pSC –A amp/kan Strata cloning vector that contains T3 and T7 promoter sequences using The StrataClone PCR Cloning Kit according to the manufacturer's protocol.

6.2.3.9 Transformation of the competent bacteria

The chemo-competent E.coli cells were used for the transformation. Cells were first thaw on ice and then 5-200ng of DNA was added to the 100µl cell aliquot and incubated for 20 min on ice. Then the transformation mixture was heat shocked for 45sec at 42 °C, and incubated on ice for another 2 min. 250-900µl of pre-warmed LB medium was added to the transformation reaction mixture and cells were allowed to recover for 1h at 37°C with agitation. Afterwards, different aliquots were plated on LB-ampicillin or LB-kanamycin plates and incubated overnight at 37 °C.

6.2.3.10 Bacterial liquid cultures

For approaches that require small quantities of DNA, 4ml of LB medium and for approaches that require larger quantities of DNA, 200ml of LB medium supplemented with the appropriate antibiotics was inoculated with a single bacterial colony and incubated overnight at 37 °C under vigorous shaking.

6.2.3.11 Restriction Digestion

DNA amount used in the digestion reaction was determined according to the downstream application. A typical reaction for restriction digestion was prepared as follows:

100ng- 10μg	Plasmid DNA
2μl	10X buffer
0.5-3μl	Restriction Enzyme (5-10U)
Σ 20-50μl	H_2O

The digestion mix was incubated in 1.5ml Eppendorf tubes at 37°C or 25°C for 1-2 hours or overnight depending on the enzyme used.

6.2.3.12 Gel Electrophoresis

Appropriate amount of Agarose to prepare 0.8-2 % (w/v) Agarose gel, depending on the size of the nucleic acid of interest, was dissolved in 1X TAE buffer by boiling in a microwave. Then the solution was cooled down, ethidiumbromide (EtBr) was added to a final concentration of 1μg/ml and it was poured into a prepared gel chamber. After the gel solidified, DNA or RNA samples mixed with 6X loading dye and a DNA ladder of appropriate size was loaded and electrophoresis was performed at 100-200V. Then the band patterns of the samples were documented under UV light.

When the DNA analyzed was supposed to be used for downstream applications, the DNA fragments with the right size were cut under UV light (254nm), transferred into an Eppendorf tube and purified using the QIAquick gel extraction kit (Qiagen) according to the manufacturer's protocol.

6.2.3.13 In vitro transcription

For in vitro transcription 1-5μg of ISH plasmid DNA was linearized by overnight digestion in a final volume of 50μl. The linearized DNA was then purified by phenol extraction and in vitro transcription was carried out in a 1.5ml tube by using 1μg DNA, 2μl digoxigenin labelled dNTPs (Roche), 4μl 10X transcription buffer (Stratagene), 1μl RNAse inhibitor (Roche) and 2.5μl of the according RNA Polymerase (T3, T7, Sp6) (Stratagene). The reaction mixture was incubated for 2 hour at 37°C and then 2μl DNAase I was added for 45 min at 37°C to get rid of the residual DNA. RNA was then cleaned with a RNA binding column (Qiagen) and the quality of RNA probe was examined on a gel.

6.2.3.14 Ligation

Insert DNA was generally used in a 5-10 fold excess of vector DNA and a typical reaction for ligation was prepared as follows:

300ng	insert DNA fragment
30ng	vector DNA fragment
2μl	5X T4 DNA Ligase buffer (Invitrogen)
1μl	T4 DNA Ligase (Invitrogen)
Σ 10.0μl	H_2O

6.2.3.15 Sequencing

Before the sequencing the PCR product was cleaned by gel extraction using the QIAquick Gel-Extraction Kit (Qiagen) according to the manufacturer's instructions.

Sequencing PCR reaction was prepared as follows:

0,5μl	Big Dye (contains polymerase)
2,0μl	Big Dye Buffer
10pM	Primer (sense or antisense)
2μl	template DNA

And the sequencing PCR was performed with the following cycling conditions:

	Temp	Duration	Cycle #
Preheating	96°C	1min	1X
Denaturation	96°C	10 sec	
Annealing	50°C	5 sec	35X
Elongation	60°C	4 min	
Final Elongation	4°C	∞	

Finally the PCR reaction was cleaned using DyeEX 2.0 Spin columns (Qiagen) according to the manufacturer's instructions, filled into the sequencing plate and the sequencing was then performed at the Sequencing Core Facility of the Helmholtz Zentrum München.

6.2.3.16 Microarray Analysis

For the analysis of the Uhrf1 mutant cerebral cortices, total RNA was isolated from E14 cortical tissue of 5 mutant and 5 control littermates using the RNeasy Mini kit (Qiagen) according to the manufacturer's instructions with on column digestion of remaining genomic DNA. RNA concentration was measured at the Nanodrop (260nm/280nm ratio), RNA quality was assessed at the Agilent 2100 Bioanalyzer and only high quality RNA (RIN>7) samples were used for microarray analysis

For each microarray analysis 30ng of total RNA was first amplified with Ovation Pico WTA System V2" kit and then labeled with the Encore Biotin Module (Nugen). 2.1μg of amplified cDNA was then hybridized to Affymetrix Gene ST 1.0 arrays according to the manufacturer's instructions.

Expression console (v.1.3.0.187, Affymetrix) was used for quality control and to obtain annotated normalized RMA gene-level data (standard settings including median polish and sketch-quantile normalisation). Statistical analyses were performed by utilizing the statistical programming environment R (R Development Core Team, 2005) implemented in CARMAweb (Rainer et al., 2006).Genewise testing for differential expression was done

employing the limma *t*-test and Benjamini-Hochberg multiple testing correction (FDR<10%). Heatmaps were generated with CARMAweb and cluster dendrograms with R scripts (hclust, agnes, diana). Datasets were filtered for average expression > 50 in mutant and for linear ratios > 1.5X. GO term and pathway enrichment analyses were done with GePS (Genomatix, Germany) or Ingenuity pathway software and significant terms (p<0.05) were determined.

6.2.4 Data Analysis

Stainings were analyzed at an Olympus FV1000 laser-scanning confocal microscope with optical sections of maximum 0.5 − 5μm intervals.

In adult brains recombined cells were identified by GFP immunoreactivity and colocalization with cell type specific antigens was quantified using single optical sections of 70μm thick confocal stacks. Between 4 and 8 brain sections per animal were analyzed and all GFP+ cells along the whole SEZ or DG were counted.

In the embryonic brains, quantifications of PH3+ cells were done across the entire dorsal wall of the cerebral cortex from lateral to medial position and quantifications of Pax6+ cells were performed in 200μm radial stripes.The number of TUNEL+ cells was quantified per area from rostral to caudal regions of the cerebral cortex. All quantifications were performed on images from the dorsal telencephalon using level-matched sections of at least three stage-matched embryos of each genotype, from at least three different litters.

All error bars are presented as standard errors of the mean (± SEM). Statistical significance was tested using student t-test. Data were considered as significant with p<0.05 (*), very significant with p<0.01 (**) and highly significant with p<0.001 (***).

7. Abbreviations

%	percent		**Ctx**	cortex
°C	Degrees Celcius		**Cux1/2**	Cut-Like homeobox 1/2
µg	microgram		**DAPI**	4,6-dasmindino-2-phenylindol
µl	microliter		**DCX**	Doublecortin
µm	micrometer		**dd**	Double distilled
Ara-C	cytosine-β-D-arabinofuranoside		**DG**	Dentate Gyrus
aNSCs	adult neural stem cells		**DIG**	digoxygenin
AJ	Adherens junctions		**Dlx2**	Distal-less homeobox 2
BLBP	Brain lipid binding protein		**Dnmt1**	DNA methytransferase 1
BMP	Bone Morphogenetic Protein		**DMEM**	Dulbecco's Modified Eagel Medium:Nutrient Mixture
bp	base pairs		**DNA**	DeoxyriboNucleic Acid
BrdU	5'-bromo-2'-deoxyuridine		**DP**	Dorsal pallium
BSA	Bovine Serum Albumine		**dpi**	days post-induction
CB	calbindin		**DV**	Dorsal to ventral
CC	Corpus callosum		**E**	Embryonic day
cDNA	complementary DeoxyriboNucleic Acid		**EBSS**	Earle's Balanced Salt Solution
CGE	Caudal Ganglionic Eminence		**ECM**	Extracellular matrix
cKO	Conditional knock out		**EGF**	Epidermal Growth Factor
CNS	Central Nervous System		**EGFR**	Epidermal growth factor receptor
CP	cortical plate		**EM**	Electron microscopy
CR	calretinin		**Emx1/2**	Empty spiracles homeobox 1/2
CSF	cerebrospinal fluid		**EtBr**	Ethidium bromide

FACS	Fluorescence activated cell sorting		**HEPES**	4-(2-Hydroxyethyl)-1-piperazineethanesulfonic acid
FCS	Fetal Calf Serum		**Hes5**	Hairy and enhancer of split 5
FDR	False discovery rate		**het**	heterozygous
FGF	Fibroblast Growth Factor		**HGF**	Hepatocyte growth factor
FITC	fluorescein isothiocyanate		**HRP**	Horseradish-peroxidase
FSC-A	Forward scatter–area		**IgG**	Immunoglobuline G
FSC-W	Forward scatter- width		**INM**	Interkinetic nuclear migration
g	grams		**IP**	Intermediate progenitor
GABA	γ-Aminobutyric acid		**ISH**	In situ hybridization
GCs	Granule cells		**kg**	kilograms
GCL	Granule cell layer		**LeX**	Lewis X
GDNF	Glial cell-derived neurotrophic factor		**LGE**	Lateral Ganglionic Eminence
GE	Ganglionic eminence		**Lhx2**	LIM box 2
GFAP	Glial fibrillary acidic protein		**LP**	Lateral pallium
GFP	Green Fluorescent Protein		**LT-BrdU**	Long term 5'-bromo-2'-deoxyuridine
GJ	Gap junctions		**MABT**	Maleic acid *buffer* containing Tween 20
GLAST	GLutamate ASpartate Transporter		**Mash1**	Mammalian achaete scute homolog-1
GO	Gene ontology		**min**	minute
Gsx1/2	GS homeobox 1/2		**MGE**	Medial Ganglionic Eminence
h	hours		**ML**	Medial to lateral
HAS	Heat-stable antigen		**MP**	Medial pallium
HBSS	Hank's balanced salt solution		**mpi**	months post-induction
HDAC1	Histone deactylase 1		**mRNA**	messenger RNA

NE	Neuroepithelial		**PI**	Propodium iodine
NeuroD1	Neurogenic differentiation 1		**PNA**	peanut agglutinin
ng	nanograms		**PNS**	Peripheral Nervous System
Ngn1/2	Neurogenin 1/2		**Prox1**	Prospero homeobox protein 1
NGS	Normal goat serum		**PV**	parvalbumin
Nkx2.1	NK2 homeobox 1		**RA**	Retinoic Acid
nm	nanometer		**RC2**	Radial glial Cell marker 2
OB	Olfactory bulb		**RCAS**	replication competent avian leukosis
Olig2	Oligodendrocyte lineage transcription factor 2		**RG**	Radial Glia
OPCs	Oligodentrocyte progenitor cells		**RIN**	RNA integrity number
oRG	Outer radial glial		**RMS**	Rostral migratory stream
Pax6	Paired box 6		**RNA**	RiboNucleic Acid
PBS	Phosphate Buffer Saline		**rpm**	revolutions per minute
PCR	Polymerase chain reaction		**RT**	Room temperature
PDGF	*Platelet-derived growth factor*		**RT-PCR**	Real time polymerase chain reaction
PDGFRα	Platelet Derived Growth Factor Receptor α		**s**	seconds
PDL	Poly-D-Lysine		**SDS**	Sodium dodecyl sulphate
PE	Phycoerythrin		**SEM**	Standard error of the mean
PEDF	Pigment epithelium derived factor		**SEZ**	Subependymal zone
Pen/Strep	Penicillin/Streptomycin		**SGZ**	Subgranular zone
PFA	Paraformaldehyde		**Shh**	Sonic Hedgehog
PGCs	Periglomerular cells		**SNPs**	Short neural progenitors
PH3	Phospho-Histone 3		**Sox2**	SRY- related HMG transcription factor 2

Svet1	Subventricular expressed transcript 1		**UV**	UltraViolet light
SVZ	Subventricular zone		**V**	Volts
TAE	Tris Acetate EDTA		**v/v**	volume per volume
TAPs	Transit amplifying progenitors		**VP**	Ventral pallium
Tbr1/2	T-box brain 1/2		**VZ**	Ventricular zone
TF	Transcription factor		**w/o**	without
TGF-alpha	Transforming Growth Factor-Alpha		**w/v**	weight per volume
TSP	Thrombospondin		**Whsc1**	Wolf-Hirschhorn Syndrome Candidate 1
TUNEL	Terminal deoxynucleotidyl transferase (TdT) dUTP Nick-End Labeling		**Wnt**	Wingless
TJ	Tight junctions		**wpi**	weeks post-induction
Uhrf1	Ubiquitin-like, containing PHD and RING finger domains, 1		**wt**	wildtype

8. References

Aaku-Saraste, E., Hellwig, A., & Huttner, W. B. (1996). Loss of occludin and functional tight junctions, but not ZO-1, during neural tube closure--remodeling of the neuroepithelium prior to neurogenesis. *Developmental Biology*, *180*(2), 664–679.

Aaku-Saraste, E., Oback, B., Hellwig, A., & Huttner, W. B. (1997). Neuroepithelial cells downregulate their plasma membrane polarity prior to neural tube closure and neurogenesis. *Mechanisms of Development*, *69*(1-2), 71–81.

Abbady, A.-Q., Bronner, C., Bathami, K., Muller, C. D., Jeanblanc, M., Mathieu, E., … Mousli, M. (2005). TCR pathway involves ICBP90 gene down-regulation via E2F binding sites. *Biochemical Pharmacology*, *70*(4), 570–579.

Abbady, A.-Q., Bronner, C., Trotzier, M.-A., Hopfner, R., Bathami, K., Muller, C. D., … Mousli, M. (2003). ICBP90 expression is downregulated in apoptosis-induced Jurkat cells. *Annals Of The New York Academy Of Sciences*, *1010*, 300–303.

Achour, M., Fuhrmann, G., Alhosin, M., Rondé, P., Chataigneau, T., Mousli, M., … Bronner, C. (2009). UHRF1 recruits the histone acetyltransferase Tip60 and controls its expression and activity. *Biochemical and Biophysical Research Communications*, *390*(3), 523–528.

Adams, J. C., & Lawler, J. (2011). The thrombospondins. *Cold Spring Harbor perspectives in biology*, *3*(10), a009712.

Adolf, B., Chapouton, P., Lam, C. S., Topp, S., Tannhäuser, B., Strähle, U., … Bally-Cuif, L. (2006). Conserved and acquired features of adult neurogenesis in the zebrafish telencephalon. *Developmental Biology*, *295*(1), 278–293.

Akita, K., von Holst, A., Furukawa, Y., Mikami, T., Sugahara, K., & Faissner, A. (2008). Expression of multiple chondroitin/dermatan sulfotransferases in the neurogenic regions of the embryonic and adult central nervous system implies that complex chondroitin sulfates have a role in neural stem cell maintenance. *Stem cells (Dayton, Ohio)*, *26*(3), 798–809.

Alhosin, M., Sharif, T., Mousli, M., Etienne-Selloum, N., Fuhrmann, G., Schini-Kerth, V. B., & Bronner, C. (2011). Down-regulation of UHRF1, associated with re-expression of tumor suppressor genes, is a common feature of natural compounds exhibiting anti-cancer properties. *Journal of experimental clinical cancer research CR*, *30*(1), 41.

Altman, J. (1963). Autoradiographic investigation of cell proliferation in the brains of rats and cats. *The Anatomical record*, *145*(4), 573–591.

Altman, J. (1969). Autoradiographic and histological studies of postnatal neurogenesis. IV. Cell proliferation and migration in the anterior forebrain, with special reference to persisting neurogenesis in the olfactory bulb. *Journal of Comparative Neurology*, *137*(4), 433–457.

Altman, J., & Das, G. D. (1965). Autoradiographic and histological evidence of postnatal hippocampal neurogenesis in rats. *Journal of Comparative Neurology*, *124*(3), 319–335.

Andrews, W. D., Barber, M., & Parnavelas, J. G. (2007). Slit-Robo interactions during cortical development. *Journal of anatomy*, *211*(2), 188–98.

Anton, E. S., Ghashghaei, H. T., Weber, J. L., McCann, C., Fischer, T. M., Cheung, I. D., … Lai, C. (2004). Receptor tyrosine kinase ErbB4 modulates neuroblast migration and placement in the adult forebrain. *Nature Neuroscience*, *7*(12), 1319–1328.

Arima, Y., Hirota, T., Bronner, C., Mousli, M., Fujiwara, T., Niwa, S., … Saya, H. (2004). Down-regulation of nuclear protein ICBP90 by p53/p21Cip1/WAF1-dependent DNA-damage checkpoint signals contributes to cell cycle arrest at G1/S transition. *Genes to cells devoted to molecular cellular mechanisms*, *9*(2), 131–142.

Arita, K., Ariyoshi, M., Tochio, H., Nakamura, Y., & Shirakawa, M. (2008). Recognition of hemi-methylated DNA by the SRA protein UHRF1 by a base-flipping mechanism. *Nature*, 4–6.

Aström, K. E., & Webster, H. D. (1991). The early development of the neopallial wall and area choroidea in fetal rats. A light and electron microscopic study. *Advances in anatomy embryology and cell biology*, *123*, 1–76.

Avvakumov, G. V, Walker, J. R., Xue, S., Li, Y., Duan, S., Bronner, C., … Dhe-paganon, S. (2008). Structural basis for recognition of hemi-methylated DNA by the SRA domain of human UHRF1. *Nature*.

Azari, H., Osborne, G. W., Yasuda, T., Golmohammadi, M. G., Rahman, M., Deleyrolle, L. P., … Reynolds, B. A. (2011). Purification of Immature Neuronal Cells from Neural Stem Cell Progeny. (F. Gelain, Ed.)*PLoS ONE*, *6*(6), 16.

Babbio, F., Pistore, C., Curti, L., Castiglioni, I., Kunderfranco, P., Brino, L., … Bonapace, I. M. (2012). The SRA protein UHRF1 promotes epigenetic crosstalks and is involved in prostate cancer progression. *Oncogene*, (November 2011), 1–10.

Bandtlow, C. E., & Zimmermann, D. R. (2000). Proteoglycans in the developing brain: new conceptual insights for old proteins. *Physiological reviews*, *80*(4), 1267–90.

Barraud, P., Thompson, L., Kirik, D., Björklund, A., & Parmar, M. (2005). Isolation and characterization of neural precursor cells from the Sox1-GFP reporter mouse. *European Journal of Neuroscience*, *22*(7), 1555–1569.

Batista-Brito, R., Close, J., Machold, R., & Fishell, G. (2008). The distinct temporal origins of olfactory bulb interneuron subtypes. *Journal of Neuroscience*, *28*(15), 3966–3975.

Beckervordersandforth, R., Tripathi, P., Ninkovic, J., Bayam, E., Lepier, A., Stempfhuber, B., … Götz, M. (2010). In vivo fate mapping and expression analysis reveals molecular hallmarks of prospectively isolated adult neural stem cells. *Cell stem cell*, *7*(6), 744–58.

Benner, E. J., Luciano, D., Jo, R., Abdi, K., Paez-Gonzalez, P., Sheng, H., … Kuo, C. T. (2013). Protective astrogenesis from the SVZ niche after injury is controlled by Notch modulator Thbs4. *Nature*, *497*(7449), 369–73.

Bergmann, O., Liebl, J., Bernard, S., Alkass, K., Yeung, M. S. Y., Steier, P., … Frisén, J. (2012). The age of olfactory bulb neurons in humans. *Neuron*, *74*(4), 634–9.

Bhide, P. G. (1996). Cell cycle kinetics in the embryonic mouse corpus striatum. *The Journal of comparative neurology*, *374*(4), 506–22.

Bishop, K M. (2000). Regulation of Area Identity in the Mammalian Neocortex by Emx2 and Pax6. *Science*, *288*(5464), 344–349.

Bishop, Kathie M, Rubenstein, J. L. R., & O'Leary, D. D. M. (2002). Distinct actions of Emx1, Emx2, and Pax6 in regulating the specification of areas in the developing neocortex. *Journal of Neuroscience*, *22*(17), 7627–7638.

Blake, S. M., Strasser, V., Andrade, N., Duit, S., Hofbauer, R., Schneider, W. J., & Nimpf, J. (2008). Thrombospondin-1 binds to ApoER2 and VLDL receptor and functions in postnatal neuronal migration. *the The European Molecular Biology Organization Journal*, *27*(22), 3332.

Bolteus, A. J., & Bordey, A. (2004). GABA release and uptake regulate neuronal precursor migration in the postnatal subventricular zone. *Journal of Neuroscience*, *24*(35), 7623–7631.

Bonapace, I. M., Latella, L., Papait, R., Nicassio, F., Sacco, A., Muto, M., … Di Fiore, P. P. (2002). Np95 is regulated by E1A during mitotic reactivation of terminally differentiated cells and is essential for S phase entry. *The Journal of Cell Biology*, *157*(6), 909–14.

Bond, A. M., Bhalala, O. G., & Kessler, J. A. (2012). The dynamic role of bone morphogenetic proteins in neural stem cell fate and maturation. *Developmental neurobiology*, *72*(7), 1068–84.

Bostick, M., Kim, J. K., Estève, P.-O., Clark, A., Pradhan, S., & Jacobsen, S. E. (2007). UHRF1 plays a role in maintaining DNA methylation in mammalian cells. *Science*, *317*(5845), 1760–1764.

Breunig, J. J., Haydar, T. F., & Rakic, P. (2011). Neural stem cells: historical perspective and future prospects. *Neuron*, *70*(4), 614–625.

Brill, M. S., Ninkovic, J., Winpenny, E., Hodge, R. D., Ozen, I., Yang, R., … Götz, M. (2009). Adult generation of glutamatergic olfactory bulb interneurons. *Nature Neuroscience*, *12*(12), 1524–1533.

Brill, M. S., Snapyan, M., Wohlfrom, H., Ninkovic, J., Jawerka, M., Mastick, G. S., … Götz, M. (2008). A dlx2- and pax6-dependent transcriptional code for periglomerular neuron specification in the adult olfactory bulb. *Journal of Neuroscience*, *28*(25), 6439–6452.

Bronner, C. (2011). Control of DNMT1 abundance in epigenetic inheritance by acetylation, ubiquitylation, and the histone code. *Science signaling*, *4*(157), pe3.

Bronner, C., Achour, M., Arima, Y., Chataigneau, T., Saya, H., & Schini-Kerth, V. B. (2007). The UHRF family: oncogenes that are drugable targets for cancer therapy in the near future? *Pharmacology therapeutics*, *115*(3), 419–434.

Brückner, G., & Biesold, D. (1981). Histochemistry of glycogen deposition in perinatal rat brain: importance of radial glial cells. *Journal of Neurocytology*, *10*(5), 749–757.

Buée, L., Hof, P. R., Roberts, D. D., Delacourte, A., Morrison, J. H., & Fillit, H. M. (1992). Immunohistochemical identification of thrombospondin in normal human brain and in Alzheimer's disease. *The American journal of pathology*, *141*(4), 783–788.

Buffo, A., Rite, I., Tripathi, P., Lepier, A., Colak, D., Horn, A.-P., … Götz, M. (2008). Origin and progeny of reactive gliosis: A source of multipotent cells in the injured brain. *Proceedings of the National Academy of Sciences of the United States of America*, *105*(9), 3581–6.

Bulchand, S., Grove, E. A., Porter, F. D., & Tole, S. (2001). LIM-homeodomain gene Lhx2 regulates the formation of the cortical hem. *Mechanisms of Development*, *100*(2), 165–175.

Cáceres, M., Suwyn, C., Maddox, M., Thomas, J. W., & Preuss, T. M. (2007). Increased cortical expression of two synaptogenic thrombospondins in human brain evolution. *Cerebral Cortex*, *17*(10), 2312–2321.

Calaora, V., Chazal, G., Nielsen, P. J., Rougon, G., & Moreau, H. (1996). mCD24 expression in the developing mouse brain and in zones of secondary neurogenesis in the adult. *Neuroscience*, *73*(2), 581–594.

Campbell, K., & Götz, M. (2002). Radial glia: multi-purpose cells for vertebrate brain development. *Trends in Neurosciences*, *25*(5), 235–238.

Capela, A., & Temple, S. (2002). LeX/ssea-1 is expressed by adult mouse CNS stem cells, identifying them as nonependymal. *Neuron*, *35*(5), 865–875.

Cappello, S., Attardo, A., Wu, X., Iwasato, T., Itohara, S., Wilsch-Bräuninger, M., … Götz, M. (2006). The Rho-GTPase cdc42 regulates neural progenitor fate at the apical surface. *Nature neuroscience*, *9*(9), 1099–107.

Cappello, S., Böhringer, C. R. J., Bergami, M., Conzelmann, K.-K., Ghanem, A., Tomassy, G. S., … Götz, M. (2012). A radial glia-specific role of RhoA in double cortex formation. *Neuron*, *73*(5), 911–24.

Cappello, S., Gray, M. J., Badouel, C., Lange, S., Einsiedler, M., Srour, M., … Robertson, S. P. (2013). Mutations in genes encoding the cadherin receptor-ligand pair DCHS1 and FAT4 disrupt cerebral cortical development. *Nature genetics*, *45*(11), 1300–8.

Carlén, M., Meletis, K., Göritz, C., Darsalia, V., Evergren, E., Tanigaki, K., … Frisén, J. (2009). Forebrain ependymal cells are Notch-dependent and generate neuroblasts and astrocytes after stroke. *Nature Neuroscience*, *12*(3), 259–267.

Casanova, M. F., & Trippe, J. (2006). Regulatory mechanisms of cortical laminar development. *Brain Research Reviews*, *51*(1), 72–84.

Castaño, J., Raurell, I., Piedra, J. A., Miravet, S., Duñach, M., & García de Herreros, A. (2002). Beta-catenin N- and C-terminal tails modulate the coordinated binding of adherens junction proteins to beta-catenin. *The Journal of biological chemistry*, *277*(35), 31541–50.

Cayre, M., Strambi, C., & Strambi, A. (1994). Neurogenesis in an adult insect brain and its hormonal control. *Nature*, *368*(6466), 57–59.

Chen, G., Sima, J., Jin, M., Wang, K.-Y., Xue, X.-J., Zheng, W., … Yuan, X.-B. (2008). Semaphorin-3A guides radial migration of cortical neurons during development. *Nature neuroscience*, *11*(1), 36–44.

Chivatakarn, O. (2008). Semaphorin 5A (Sema5A) functions in neocortical development In vivo.

Chojnacki, A. K., Mak, G. K., & Weiss, S. (2009). Identity crisis for adult periventricular neural stem cells: subventricular zone astrocytes, ependymal cells or both? *Nature Reviews Neuroscience*, *10*(2), 153–163.

Chu, J., Loughlin, E. A., Gaur, N. A., SenBanerjee, S., Jacob, V., Monson, C., … Sadler, K. C. (2012). UHRF1 phosphorylation by cyclin A2/cyclin-dependent kinase 2 is required for zebrafish embryogenesis. *Molecular Biology of the Cell*, *23*(1), 59–70.

Citterio, E., Papait, R., Nicassio, F., Vecchi, M., Gomiero, P., Mantovani, R., … Europeo, I. (2004). Np95 Is a Histone-Binding Protein Endowed with Ubiquitin Ligase Activity. *Society*, *24*(6), 2526–2535.

Colak, D., Mori, T., Brill, M. S., Pfeifer, A., Falk, S., Deng, C., … Götz, M. (2008a). Adult neurogenesis requires Smad4-mediated bone morphogenic protein signaling in stem cells. *Journal of Neuroscience*, *28*(2), 434–446.

Colak, D., Mori, T., Brill, M. S., Pfeifer, A., Falk, S., Deng, C., … Götz, M. (2008b). Adult neurogenesis requires Smad4-mediated bone morphogenic protein signaling in stem cells. *The Journal of neuroscience : the official journal of the Society for Neuroscience*, *28*(2), 434–46.

Conover, J. C., Doetsch, F., Garcia-Verdugo, J. M., Gale, N. W., Yancopoulos, G. D., & Alvarez-Buylla, A. (2000). Disruption of Eph/ephrin signaling affects migration and proliferation in the adult subventricular zone. *Nature Neuroscience*, *3*(11), 1091–1097.

Corbin, J. G., Gaiano, N., Machold, R. P., Langston, A., & Fishell, G. (2000). The Gsh2 homeodomain gene controls multiple aspects of telencephalic development.

Development Cambridge England, *127*(23), 5007–20. Corotto, F. S., Henegar, J. A., & Maruniak, J. A. (1993). Neurogenesis persists in the subependymal layer of the adult mouse brain. *Neuroscience Letters*, *149*(2), 111–114.

Corti, S., Nizzardo, M., Nardini, M., Donadoni, C., Locatelli, F., Papadimitriou, D., … Comi, G. P. (2007). Isolation and characterization of murine neural stem/progenitor cells based on Prominin-1 expression. *Experimental Neurology*, *205*(2), 547–562.

Costa, M. R., Ortega, F., Brill, M. S., Beckervordersandforth, R., Petrone, C., Schroeder, T., … Berninger, B. (2011). Continuous live imaging of adult neural stem cell division and lineage progression in vitro. *Development Cambridge England*, *138*(6), 1057–1068.

Crespel, A., Baldy-Moulinier, M., & Lerner Natoli, M. (2004). Neurogenesis in the adult brain: the demise of a dogma and the advent of new treatments. *Revue Neurologique*, *160*(12), 1150–1158.

Curtis, M. A., Kam, M., Nannmark, U., Anderson, M. F., Axell, M. Z., Wikkelso, C., … Eriksson, P. S. (2007). Human neuroblasts migrate to the olfactory bulb via a lateral ventricular extension. *Science*, *315*(5816), 1243–1249.

Cushman, J. D., Maldonado, J., Kwon, E. E., Garcia, A. D., Fan, G., Imura, T., … Fanselow, M. S. (2012). Juvenile neurogenesis makes essential contributions to adult brain structure and plays a sex-dependent role in fear memories. *Frontiers in behavioral neuroscience*, *6*, 3.

Dai, C., Shi, D., & Gu, W. (2013). Negative regulation of the acetyltransferase TIP60-p53 interplay by UHRF1 (ubiquitin-like with PHD and RING finger domains 1). *The Journal of biological chemistry*, *288*(27), 19581–92.

Daskalos, A., Oleksiewicz, U., Filia, A., Nikolaidis, G., Xinarianos, G., Gosney, J. R., … Liloglou, T. (2011). UHRF1-mediated tumor suppressor gene inactivation in nonsmall cell lung cancer. *Cancer*, *117*(5), 1027–1037.

De Marchis, S., Bovetti, S., Carletti, B., Hsieh, Y.-C., Garzotto, D., Peretto, P., … Rossi, F. (2007). Generation of distinct types of periglomerular olfactory bulb interneurons during development and in adult mice: implication for intrinsic properties of the subventricular zone progenitor population. *Journal of Neuroscience*, *27*(3), 657–664.

De Robertis, E. M., Larraín, J., Oelgeschläger, M., & Wessely, O. (2000). The establishment of Spemann's organizer and patterning of the vertebrate embryo. *Nature reviews. Genetics*, *1*(3), 171–81.

DeCarolis, N. A., Mechanic, M., Petrik, D., Carlton, A., Ables, J. L., Malhotra, S., … Eisch, A. J. (2013). In vivo contribution of nestin- and GLAST-lineage cells to adult hippocampal neurogenesis. *Hippocampus*, *23*(8), 708–19.

Dimou, L., Simon, C., Kirchhoff, F., Takebayashi, H., & Götz, M. (2008). Progeny of Olig2-expressing progenitors in the gray and white matter of the adult mouse cerebral cortex.

The Journal of neuroscience : the official journal of the Society for Neuroscience, *28*(41), 10434–42.

Doetsch, F, Caillé, I., Lim, D. A., García-Verdugo, J. M., & Alvarez-Buylla, A. (1999). Subventricular zone astrocytes are neural stem cells in the adult mammalian brain. *Cell*, *97*(6), 703–716.

Doetsch, F, García-Verdugo, J. M., & Alvarez-Buylla, A. (1997). Cellular composition and three-dimensional organization of the subventricular germinal zone in the adult mammalian brain. *Journal of Neuroscience*, *17*(13), 5046–5061.

Doetsch, Fiona, Petreanu, L., Caille, I., Garcia-Verdugo, J. M., & Alvarez-Buylla, A. (2002). EGF converts transit-amplifying neurogenic precursors in the adult brain into multipotent stem cells. *Neuron*, *36*(6), 1021–1034.

Drees, F., Pokutta, S., Yamada, S., Nelson, W. J., & Weis, W. I. (2005). Alpha-catenin is a molecular switch that binds E-cadherin-beta-catenin and regulates actin-filament assembly. *Cell*, *123*(5), 903–15.

Du, Z., Song, J., Wang, Y., Zhao, Y., Guda, K., Yang, S., … Wang, Z. (2010). DNMT1 stability is regulated by proteins coordinating deubiquitination and acetylation-driven ubiquitination. *Science signaling*, *3*(146), ra80.

Emsley, J. G., & Hagg, T. (2003). alpha6beta1 integrin directs migration of neuronal precursors in adult mouse forebrain. *Experimental Neurology*, *183*(2), 273–285.

Eriksson, P. S., Perfilieva, E., Bjork-Eriksson, T., Alborn, A. M., Nordborg, C., Peterson, D. A., & Gage, F. H. (1998). Neurogenesis in the adult human hippocampus. *Nature Medicine*, *4*(11), 1313–1317.

Ernst, A., Alkass, K., Bernard, S., Salehpour, M., Perl, S., Tisdale, J., … Frisén, J. (2014). Neurogenesis in the striatum of the adult human brain. *Cell*, *156*(5), 1072–83.

Eroglu, C. (2009). The role of astrocyte-secreted matricellular proteins in central nervous system development and function. *Journal of cell communication and signaling*, *3*(3-4), 167–176.

Fan, G, Beard, C., Chen, R. Z., Csankovszki, G., Sun, Y., Siniaia, M., … Jaenisch, R. (2001). DNA hypomethylation perturbs the function and survival of CNS neurons in postnatal animals. *The Journal of neuroscience : the official journal of the Society for Neuroscience*, *21*(3), 788–97.

Fan, Guoping, Martinowich, K., Chin, M. H., He, F., Fouse, S. D., Hutnick, L., … Sun, Y. E. (2005). DNA methylation controls the timing of astrogliogenesis through regulation of JAK-STAT signaling. *Development (Cambridge, England)*, *132*(15), 3345–56.

Farley, F. W., Soriano, P., Steffen, L. S., & Dymecki, S. M. (n.d.). Widespread recombinase expression using FLPeR (flipper) mice. *Genesis (New York, N.Y. : 2000)*, *28*(3-4), 106–10.

Felle, M., Joppien, S., Németh, A., Diermeier, S., Thalhammer, V., Dobner, T., … Längst, G. (2011). The USP7/Dnmt1 complex stimulates the DNA methylation activity of Dnmt1 and regulates the stability of UHRF1. *Nucleic Acids Research*, *39*(19), 8355–65.

Feng, J., Chang, H., Li, E., & Fan, G. (2005). Dynamic expression of de novo DNA methyltransferases Dnmt3a and Dnmt3b in the central nervous system. *Journal of neuroscience research*, *79*(6), 734–46.

Feng, J., Fouse, S., & Fan, G. (2007). Epigenetic regulation of neural gene expression and neuronal function. *Pediatric research*, *61*(5 Pt 2), 58R–63R.

Feng, J., Zhou, Y., Campbell, S. L., Le, T., Li, E., Sweatt, J. D., … Fan, G. (2010). Dnmt1 and Dnmt3a maintain DNA methylation and regulate synaptic function in adult forebrain neurons. *Nature neuroscience*, *13*(4), 423–30.

Fietz, S. A., & Huttner, W. B. (2011). Cortical progenitor expansion, self-renewal and neurogenesis-a polarized perspective. *Current Opinion in Neurobiology*, *21*(1), 23–35.

Fischer, J., Beckervordersandforth, R., Tripathi, P., Steiner-Mezzadri, A., Ninkovic, J., & Götz, M. (2011). Prospective isolation of adult neural stem cells from the mouse subependymal zone. *Nature protocols*, *6*(12), 1981–9.

Fode, C., Ma, Q., Casarosa, S., Ang, S.-L., Anderson, D. J., & Guillemot, F. (2000). A role for neural determination genes in specifying the dorsoventral identity of telencephalic neurons. *Genes & Development*, *14*(1), 67–80.

Forni, P. E., Scuoppo, C., Imayoshi, I., Taulli, R., Dastrù, W., Sala, V., … Ponzetto, C. (2006). High levels of Cre expression in neuronal progenitors cause defects in brain development leading to microencephaly and hydrocephaly. *The Journal of neuroscience : the official journal of the Society for Neuroscience*, *26*(37), 9593–602.

Foti, S. B., Chou, A., Moll, A. D., & Roskams, A. J. (2013a). HDAC inhibitors dysregulate neural stem cell activity in the postnatal mouse brain. *International journal of developmental neuroscience : the official journal of the International Society for Developmental Neuroscience*, *31*(6), 434–47.

Foti, S. B., Chou, A., Moll, A. D., & Roskams, A. J. (2013b). HDAC inhibitors dysregulate neural stem cell activity in the postnatal mouse brain. *International journal of developmental neuroscience : the official journal of the International Society for Developmental Neuroscience*, *31*(6), 434–47.

Fouse, S. D., Shen, Y., Pellegrini, M., Cole, S., Meissner, A., Van Neste, L., … Fan, G. (2008). Promoter CpG methylation contributes to ES cell gene regulation in parallel with Oct4/Nanog, PcG complex, and histone H3 K4/K27 trimethylation. *Cell stem cell*, *2*(2), 160–9.

Frauer, C., Hoffmann, T., Bultmann, S., Casa, V., Cardoso, M. C., Antes, I., & Leonhardt, H. (2011). Recognition of 5-Hydroxymethylcytosine by the Uhrf1 SRA Domain. (S. Xu, Ed.)*PLoS ONE*, *6*(6), 8.

Frolova, E., Pluskota, E., Krukovets, I., Burke, T., Drumm, C., Smith, J. D., … Stenina, O. I. (2011). Thrombospondin-4 regulates vascular inflammation and atherogenesis. *Circulation research*, *107*(11), 1313–1325.

Gabay, L., Lowell, S., Rubin, L. L., & Anderson, D. J. (2003). Deregulation of dorsoventral patterning by FGF confers trilineage differentiation capacity on CNS stem cells in vitro. *Neuron*, *40*(3), 485–499

Gadisseux, J. F., & Evrard, P. (1985). Glial-neuronal relationship in the developing central nervous system. A histochemical-electron microscope study of radial glial cell particulate glycogen in normal and reeler mice and the human fetus. *Developmental Neuroscience*, *7*(1), 12–32.

Gal, J. S., Morozov, Y. M., Ayoub, A. E., Chatterjee, M., Rakic, P., & Haydar, T. F. (2006). Molecular and morphological heterogeneity of neural precursors in the mouse neocortical proliferative zones. *The Journal of neuroscience : the official journal of the Society for Neuroscience*, *26*(3), 1045–56.

Garcia, A. D. R., Doan, N. B., Imura, T., Bush, T. G., & Sofroniew, M. V. (2004). GFAP-expressing progenitors are the principal source of constitutive neurogenesis in adult mouse forebrain. *Nature Neuroscience*, *7*(11), 1233–1241.

Garcia, O., Torres, M., Helguera, P., Coskun, P., & Busciglio, J. (2010). A Role for Thrombospondin-1 Deficits in Astrocyte-Mediated Spine and Synaptic Pathology in Down's Syndrome. (M. B. Feany, Ed.)*PLoS ONE*, *5*(12), 12.

Garzotto, D., Giacobini, P., Crepaldi, T., Fasolo, A., & De Marchis, S. (2008). Hepatocyte growth factor regulates migration of olfactory interneuron precursors in the rostral migratory stream through Met-Grb2 coupling. *Journal of Neuroscience*, *28*(23), 5901–5909.

Gleeson, J. G., Lin, P. T., Flanagan, L. A., & Walsh, C. A. (1999). Doublecortin Is a Microtubule-Associated Protein and Is Expressed Widely by Migrating Neurons Brigham and Women ' s Hospital. *Neuron*, *23*(2), 257–271.

Goldman, S. A., & Nottebohm, F. (1983). Neuronal production, migration, and differentiation in a vocal control nucleus of the adult female canary brain. *Proceedings of the National Academy of Sciences of the United States of America*, *80*(8), 2390–2394.

Gonzales-Roybal, G., & Lim, D. A. (2013). Chromatin-based epigenetics of adult subventricular zone neural stem cells. *Frontiers in genetics*, *4*, 194.

Goto, K., Numata, M., Komura, J. I., Ono, T., Bestor, T. H., & Kondo, H. (1994). Expression of DNA methyltransferase gene in mature and immature neurons as well as proliferating cells in mice. *Differentiation; research in biological diversity*, *56*(1-2), 39–44.

Gould, E. (2007). Opinion - How widespread is adult neurogenesis in mammals? *Nature Reviews Neuroscience*, *8*(6), 481–488.

Gould, Elizabeth, Tanapat, P., McEwen, B. S., Flügge, G., & Fuchs, E. (1998). Proliferation of granule cell precursors in the dentate gyrus of adult monkeys is diminished by stress. *Proceedings of the National Academy of Sciences of the United States of America*, *95*(6), 3168–3171.

Götz, M. (2003). Glial cells generate neurons--master control within CNS regions: developmental perspectives on neural stem cells. *The Neuroscientist a review journal bringing neurobiology neurology and psychiatry*, *9*(5), 379–397.

Götz, M., & Huttner, W. B. (2005). The cell biology of neurogenesis. *Nature Reviews Molecular Cell Biology*, *6*(10), 777–788.

Grigoriou, M., Tucker, A. S., Sharpe, P. T., & Pachnis, V. (1998). Expression and regulation of Lhx6 and Lhx7, a novel subfamily of LIM homeodomain encoding genes, suggests a role in mammalian head development. *Development Cambridge England*, *125*(11), 2063–2074.

Gross, C. G. (2000). Neurogenesis in the adult brain: death of a dogma. *Nature Reviews Neuroscience*, *1*(1), 67–73.

Guan, D., Factor, D., Liu, Y., Wang, Z., & Kao, H.-Y. (2013). The epigenetic regulator UHRF1 promotes ubiquitination-mediated degradation of the tumor-suppressor protein promyelocytic leukemia protein. *Oncogene*, *32*(33), 3819–28.

Gumbiner, B. M. (1996). Cell adhesion: the molecular basis of tissue architecture and morphogenesis. *Cell*, *84*(3), 345–57.

Gumbiner, B. M. (2000). Regulation of cadherin adhesive activity. *The Journal of cell biology*, *148*(3), 399–404.

Hack, I., Bancila, M., Loulier, K., Carroll, P., & Cremer, H. (2002). Reelin is a detachment signal in tangential chain-migration during postnatal neurogenesis. *Nature Neuroscience*, *5*(10), 939–945.

Hack, M A, Sugimori, M., Lundberg, C., Nakafuku, M., & Götz, M. (2004). Regionalization and fate specification in neurospheres: the role of Olig2 and Pax6. *Molecular And Cellular Neurosciences*, *25*(4), 664–678.

Hack, Michael A, Saghatelyan, A., De Chevigny, A., Pfeifer, A., Ashery-Padan, R., Lledo, P.-M., & Götz, M. (2005). Neuronal fate determinants of adult olfactory bulb neurogenesis. *Nature Neuroscience*, *8*(7), 865–872.

Hagg, T. (2005). Molecular regulation of adult CNS neurogenesis: an integrated view. *Trends in Neurosciences*, *28*(11), 589–595.

Halfter, W., Dong, S., Yip, Y.-P., Willem, M., & Mayer, U. (2002). A critical function of the pial basement membrane in cortical histogenesis. *Journal of Neuroscience*, *22*(14), 6029–6040.

Hamanoue, M., Matsuzaki, Y., Sato, K.-I., Okano, H. J., Shibata, S., Sato, I., … Okano, H. (2009). Cell surface N-glycans mediated isolation of mouse neural stem cells. *Journal of neurochemistry*, *110*(5), 1575–84.

Hanashima, C., Li, S. C., Shen, L., Lai, E., & Fishell, G. (2004). Foxg1 suppresses early cortical cell fate. *Science (New York, N.Y.)*, *303*(5654), 56–9.

Hartfuss, E., Galli, R., Heins, N., & Götz, M. (2001). Characterization of CNS precursor subtypes and radial glia. *Developmental Biology*, *229*(1), 15–30.

Hashimoto, H., Horton, J. R., Zhang, X., Bostick, M., Jacobsen, S. E., & Cheng, X. (2008). The SRA domain of UHRF1 flips 5-methylcytosine out of the DNA helix. *Nature*, *455*(7214), 826–829.

Haubensak, W., Attardo, A., Denk, W., & Huttner, W. B. (2004). Neurons arise in the basal neuroepithelium of the early mammalian telencephalon. *Proceedings of the National Academy of Sciences of the United States of America*, *101*, 3196–3201.

Heins, N., Malatesta, P., Cecconi, F., Nakafuku, M., Tucker, K. L., Hack, M. A., … Götz, M. (2002). Glial cells generate neurons: the role of the transcription factor Pax6. *Nature neuroscience*, *5*(4), 308–15.

Hermann, A., Gowher, H., & Jeltsch, A. (2004). Biochemistry and biology of mammalian DNA methyltransferases. *Cellular and molecular life sciences : CMLS*, *61*(19-20), 2571–87.

Herrera, D. G., Garcia-Verdugo, J. M., & Alvarez-Buylla, A. (1999). Adult-derived neural precursors transplanted into multiple regions in the adult brain. *Annals of Neurology*, *46*(6), 867–877.

Hirrlinger, J., Scheller, A., Hirrlinger, P. G., Kellert, B., Tang, W., Wehr, M. C., … Kirchhoff, F. (2009). Split-cre complementation indicates coincident activity of different genes in vivo. *PloS one*, *4*(1), e4286.

Hoch, R. V, Rubenstein, J. L. R., & Pleasure, S. (2009). Genes and signaling events that establish regional patterning of the mammalian forebrain. *Seminars in cell developmental biology*, *20*(4), 378–386.

Homayouni, R., Rice, D. S., & Curran, T. (2001). Disabled-1 interacts with a novel developmentally regulated protocadherin. *Biochemical and biophysical research communications*, *289*(2), 539–47.

Hopfner, R, Mousli, M., Jeltsch, J. M., Voulgaris, A., Lutz, Y., Marin, C., … Bronner, C. (2000). ICBP90, a novel human CCAAT binding protein, involved in the regulation of topoisomerase IIalpha expression. *Cancer Research*, *60*(1), 121–128.

Hopfner, Raphael, Mousli, M., Oudet, P., & Bronner, C. (2002). Overexpression of ICBP90, a novel CCAAT-binding protein, overcomes cell contact inhibition by forcing topoisomerase II alpha expression. *Anticancer Research*, *22*(6A), 3165–3170.

Hsieh, J. (2012). Orchestrating transcriptional control of adult neurogenesis. *Genes Development*, *26*(10), 1010–1021.

Hu, L., Li, Z., Wang, P., Lin, Y., & Xu, Y. (2011). Crystal structure of PHD domain of UHRF1 and insights into recognition of unmodified histone H3 arginine residue 2. *Cell research*, *21*(9), 1374–8.

Hutnick, L. K., Golshani, P., Namihira, M., Xue, Z., Matynia, A., Yang, X. W., … Fan, G. (2009a). DNA hypomethylation restricted to the murine forebrain induces cortical degeneration and impairs postnatal neuronal maturation. *Human molecular genetics*, *18*(15), 2875–88.

Hutnick, L. K., Golshani, P., Namihira, M., Xue, Z., Matynia, A., Yang, X. W., … Fan, G. (2009b). DNA hypomethylation restricted to the murine forebrain induces cortical degeneration and impairs postnatal neuronal maturation. *Human molecular genetics*, *18*(15), 2875–88.

Huttner, W. B., & Kosodo, Y. (2005). Symmetric versus asymmetric cell division during neurogenesis in the developing vertebrate central nervous system. *Current Opinion in Cell Biology*, *17*(6), 648–657.

Imayoshi, I., Sakamoto, M., Ohtsuka, T., Takao, K., Miyakawa, T., Yamaguchi, M., … Kageyama, R. (2008). Roles of continuous neurogenesis in the structural and functional integrity of the adult forebrain. *Nature Neuroscience*, *11*(10), 1153–1161.

Iwasato, T., Datwani, A., Wolf, A. M., Nishiyama, H., Taguchi, Y., Tonegawa, S., … Itohara, S. (2000). Cortex-restricted disruption of NMDAR1 impairs neuronal patterns in the barrel cortex. *Nature*, *406*(6797), 726–31.

Jawerka, M., Colak, D., Dimou, L., Spiller, C., Lagger, S., Montgomery, R. L., … Götz, M. (2010a). The specific role of histone deacetylase 2 in adult neurogenesis. *Neuron glia biology*, *6*(2), 93–107.

Jawerka, M., Colak, D., Dimou, L., Spiller, C., Lagger, S., Montgomery, R. L., … Götz, M. (2010b). The specific role of histone deacetylase 2 in adult neurogenesis. *Neuron glia biology*, *6*(2), 93–107.

Jeanblanc, M., Mousli, M., Hopfner, R., Bathami, K., Martinet, N., Abbady, A.-Q., … Bronner, C. (2005). The retinoblastoma gene and its product are targeted by ICBP90: a key mechanism in the G1/S transition during the cell cycle. *Oncogene*, *24*(49), 7337–7345.

Jenkins, Y., Markovtsov, V., Lang, W., Sharma, P., Pearsall, D., Warner, J., … Hitoshi, Y. (2005). Critical Role of the Ubiquitin Ligase Activity of UHRF1, a Nuclear RING Finger Protein, in Tumor Cell GrowthD. (W. Tansey, Ed.)*Molecular Biology of the Cell*, *16*(12), 5621–5629.

Jhas, S., Ciura, S., Belanger-Jasmin, S., Dong, Z., Llamosas, E., Theriault, F. M., … Stifani, S. (2006). Hes6 inhibits astrocyte differentiation and promotes neurogenesis through

different mechanisms. *The Journal of neuroscience : the official journal of the Society for Neuroscience*, *26*(43), 11061–71.

Jin, W., Chen, L., Chen, Y., Xu, S.-G., Di, G.-H., Yin, W.-J., … Shao, Z.-M. (2010). UHRF1 is associated with epigenetic silencing of BRCA1 in sporadic breast cancer. *Breast Cancer Research and Treatment*, *123*(2), 359–373.

Jin, W., Liu, Y., Xu, S., Yin, W., Li, J., Yang, J., & Shao, Z. (2010). UHRF1 inhibits MDR1 gene transcription and sensitizes breast cancer cells to anticancer drugs. *Breast Cancer Research and Treatment*, *124*(1), 39–48.

Kadowaki, M., Nakamura, S., Machon, O., Krauss, S., Radice, G. L., & Takeichi, M. (2007). N-cadherin mediates cortical organization in the mouse brain. *Developmental biology*, *304*(1), 22–33.

Kaneko, N., Kudo, K., Mabuchi, T., Takemoto, K., Fujimaki, K., Wati, H., … Kanba, S. (2006). Suppression of cell proliferation by interferon-alpha through interleukin-1 production in adult rat dentate gyrus. *Neuropsychopharmacology : official publication of the American College of Neuropsychopharmacology*, *31*(12), 2619–26.

Karagianni, P., Amazit, L., Qin, J., & Wong, J. (2008a). ICBP90, a novel methyl K9 H3 binding protein linking protein ubiquitination with heterochromatin formation. *Molecular and Cellular Biology*, *28*(2), 705–717.

Karagianni, P., Amazit, L., Qin, J., & Wong, J. (2008b). ICBP90, a novel methyl K9 H3 binding protein linking protein ubiquitination with heterochromatin formation. *Molecular and cellular biology*, *28*(2), 705–17.

Katoh, K., Yamazaki, R., Onishi, A., Sanuki, R., & Furukawa, T. (2012). G9a histone methyltransferase activity in retinal progenitors is essential for proper differentiation and survival of mouse retinal cells. *The Journal of neuroscience : the official journal of the Society for Neuroscience*, *32*(49), 17658–70.

Kawaguchi, A., Miyata, T., Sawamoto, K., Takashita, N., Murayama, A., Akamatsu, W., … Okano, H. (2001). Nestin-EGFP transgenic mice: visualization of the self-renewal and multipotency of CNS stem cells. *Molecular And Cellular Neurosciences*, *17*(2), 259–273.

Kazanis, I., & ffrench-Constant, C. (2011). Extracellular matrix and the neural stem cell niche. *Developmental neurobiology*, *71*(11), 1006–17.

Kazerounian, S., Yee, K. O., & Lawler, J. (2008). Thrombospondins in cancer. *Cellular and molecular life sciences CMLS*, *65*(5), 700–712.

Kerever, A., Schnack, J., Vellinga, D., Ichikawa, N., Moon, C., Arikawa-Hirasawa, E., … Mercier, F. (2007). Novel extracellular matrix structures in the neural stem cell niche capture the neurogenic factor fibroblast growth factor 2 from the extracellular milieu. *Stem cells (Dayton, Ohio)*, *25*(9), 2146–57.

Kim, H.-J., & Rosenfeld, M. G. (2010). Epigenetic control of stem cell fate to neurons and glia. *Archives of pharmacal research*, *33*(10), 1467–73.

Kim, J. K., Estève, P.-O., Jacobsen, S. E., & Pradhan, S. (2009). UHRF1 binds G9a and participates in p21 transcriptional regulation in mammalian cells. *Nucleic Acids Research*, *37*(2), 493–505.

Kim, S.-Y., Yasuda, S., Tanaka, H., Yamagata, K., & Kim, H. (n.d.). Non-clustered protocadherin. *Cell adhesion & migration*, *5*(2), 97–105.

Kirschenbaum, B., Doetsch, F., Lois, C., & Alvarez-Buylla, A. (1999). Adult subventricular zone neuronal precursors continue to proliferate and migrate in the absence of the olfactory bulb. *Journal of Neuroscience*, *19*(6), 2171–2180.

Knobloch, M., Braun, S. M. G., Zurkirchen, L., von Schoultz, C., Zamboni, N., Araúzo-Bravo, M. J., … Jessberger, S. (2013). Metabolic control of adult neural stem cell activity by Fasn-dependent lipogenesis. *Nature*, *493*(7431), 226–30.

Knoth, R., Singec, I., Ditter, M., Pantazis, G., Capetian, P., Meyer, R. P., … Kempermann, G. (2010). Murine features of neurogenesis in the human hippocampus across the lifespan from 0 to 100 years. (P. Callaerts, Ed.)*PloS one*, *5*(1), e8809.

Kohwi, M., Osumi, N., Rubenstein, J. L. R., & Alvarez-Buylla, A. (2005). Pax6 is required for making specific subpopulations of granule and periglomerular neurons in the olfactory bulb. *Journal of Neuroscience*, *25*(30), 6997–7003.

Kohwi, M., Petryniak, M. A., Long, J. E., Ekker, M., Obata, K., Yanagawa, Y., … Alvarez-Buylla, A. (2007). A subpopulation of olfactory bulb GABAergic interneurons is derived from Emx1- and Dlx5/6-expressing progenitors. *Journal of Neuroscience*, *27*(26), 6878–6891.

Konno, D., Shioi, G., Shitamukai, A., Mori, A., Kiyonari, H., Miyata, T., & Matsuzaki, F. (2008). Neuroepithelial progenitors undergo LGN-dependent planar divisions to maintain self-renewability during mammalian neurogenesis. *Nature Cell Biology*, *10*(1), 93–101.

Kornack, D. R., & Rakic, P. (1999). Continuation of neurogenesis in the hippocampus of the adult macaque monkey. *Proceedings of the National Academy of Sciences of the United States of America*, *96*(10), 5768–5773.

Kretsovali, A., Hadjimichael, C., & Charmpilas, N. (2012). Histone deacetylase inhibitors in cell pluripotency, differentiation, and reprogramming. *Stem cells international*, *2012*, 184154.

Kriegstein, A., & Alvarez-Buylla, A. (2009). The glial nature of embryonic and adult neural stem cells. *Annual review of neuroscience*, *32*, 149–84.

Kriegstein, A. R., & Götz, M. (2003). Radial glia diversity: a matter of cell fate. *Glia*, *43*(1), 37–43.

Kudoh, T., Wilson, S. W., & Dawid, I. B. (2002). Distinct roles for Fgf, Wnt and retinoic acid in posteriorizing the neural ectoderm. *Development Cambridge England*, *129*(18), 4335–4346.

Kuhn, H. G., Dickinson-Anson, H., & Gage, F. H. (1996). Neurogenesis in the dentate gyrus of the adult rat: age-related decrease of neuronal progenitor proliferation. *Journal of Neuroscience*, *16*(6), 2027–2033.

Kuo, C. T., Mirzadeh, Z., Soriano-Navarro, M., Rasin, M., Wang, D., Shen, J., … Jan, Y.-N. (2006). Postnatal deletion of Numb/Numblike reveals repair and remodeling capacity in the subventricular neurogenic niche. *Cell*, *127*(6), 1253–1264.

Lallous, N., Legrand, P., McEwen, A. G., Ramón-Maiques, S., Samama, J.-P., & Birck, C. (2011). The PHD Finger of Human UHRF1 Reveals a New Subgroup of Unmethylated Histone H3 Tail Readers. (M. Gasset, Ed.)*PLoS ONE*, *6*(11), e27599.

Lamb, T. M., & Harland, R. M. (1995). Fibroblast growth factor is a direct neural inducer, which combined with noggin generates anterior-posterior neural pattern. *Development Cambridge England*, *121*(11), 3627–3636.

Lawler, J., Duquette, M., Whittaker, C. A., Adams, J. C., McHenry, K., & DeSimone, D. W. (1993). Identification and characterization of thrombospondin-4, a new member of the thrombospondin gene family. *The Journal of Cell Biology*, *120*(4), 1059–1067.

Levine, A. J., & Brivanlou, A. H. (2007). Proposal of a model of mammalian neural induction. *Developmental Biology*, *308*(2), 247–256.

Li, H. S., Wang, D., Shen, Q., Schonemann, M. D., Gorski, J. A., Jones, K. R., … Jan, Y. N. (2003). Inactivation of Numb and Numblike in embryonic dorsal forebrain impairs neurogenesis and disrupts cortical morphogenesis. *Neuron*, *40*(6), 1105–18.

Li, J., Yin, C., Okamoto, H., Mushlin, H., Balgley, B. M., Lee, C. S., … Zhuang, Z. (2008). Identification of a novel proliferation-related protein, WHSC1 4a, in human gliomas. *Neuro-oncology*, *10*(1), 45–51.

Liauw, J., Hoang, S., Choi, M., Eroglu, C., Choi, M., Sun, G., … Steinberg, G. K. (2008). Thrombospondins 1 and 2 are necessary for synaptic plasticity and functional recovery after stroke. *Journal of cerebral blood flow and metabolism official journal of the International Society of Cerebral Blood Flow and Metabolism*, *28*(10), 1722–1732.

Lien, W.-H., Klezovitch, O., Fernandez, T. E., Delrow, J., & Vasioukhin, V. (2006). alphaE-catenin controls cerebral cortical size by regulating the hedgehog signaling pathway. *Science (New York, N.Y.)*, *311*(5767), 1609–12.

Lim, D. A., Tramontin, A. D., Trevejo, J. M., Herrera, D. G., García-Verdugo, J. M., & Alvarez-Buylla, A. (2000). Noggin antagonizes BMP signaling to create a niche for adult neurogenesis. *Neuron*, *28*(3), 713–726.

Liu, X., Hashimoto-Torii, K., Torii, M., Ding, C., & Rakic, P. (2010). Gap junctions/hemichannels modulate interkinetic nuclear migration in the forebrain precursors. *The Journal of neuroscience : the official journal of the Society for Neuroscience*, *30*(12), 4197–209.

Liu, X., Wang, Q., Haydar, T. F., & Bordey, A. (2005). Nonsynaptic GABA signaling in postnatal subventricular zone controls proliferation of GFAP-expressing progenitors. *Nature Neuroscience*, *8*(9), 1179–1187.

Lois, C., & Alvarez-Buylla, A. (1994). Long-distance neuronal migration in the adult mammalian brain. *Science*, *264*(5162), 1145–1148.

Lois, C., García-Verdugo, J. M., & Alvarez-Buylla, A. (1996). Chain migration of neuronal precursors. *Science*, *271*(5251), 978–981.

Lu, Z., & Kipnis, J. (2010). Thrombospondin 1--a key astrocyte-derived neurogenic factor. *The FASEB journal official publication of the Federation of American Societies for Experimental Biology*, *24*(6), 1925–1934.

Lugert, S., Basak, O., Knuckles, P., Haussler, U., Fabel, K., Götz, M., … Giachino, C. (2010). Quiescent and active hippocampal neural stem cells with distinct morphologies respond selectively to physiological and pathological stimuli and aging. *Cell stem cell*, *6*(5), 445–456.

Lugert, S., Vogt, M., Tchorz, J. S., Müller, M., Giachino, C., & Taylor, V. (2012). Homeostatic neurogenesis in the adult hippocampus does not involve amplification of Ascl1(high) intermediate progenitors. *Nature communications*, *3*(1), 670.

Luo, J., Shook, B. A., Daniels, S. B., & Conover, J. C. (2008). Subventricular zone-mediated ependyma repair in the adult mammalian brain. *Journal of Neuroscience*, *28*(14), 3804–3813.

Luskin, M. B. (1993). Restricted proliferation and migration of postnatally generated neurons derived from the forebrain subventricular zone. *Neuron*, *11*(1), 173–189.

Lysko, D. E., Putt, M., & Golden, J. A. (2011). SDF1 regulates leading process branching and speed of migrating interneurons. *The Journal of neuroscience : the official journal of the Society for Neuroscience*, *31*(5), 1739–45.

Ma, D. K., Bonaguidi, M. A., Ming, G.-L., & Song, H. (2009). Adult neural stem cells in the mammalian central nervous system. *Cell Research*, *19*(6), 672–682.

Ma, D. K., Marchetto, M. C., Guo, J. U., Ming, G., Gage, F. H., & Song, H. (2010). Epigenetic choreographers of neurogenesis in the adult mammalian brain. *Nature neuroscience*, *13*(11), 1338–44.

Ma, H., Chen, H., Guo, X., Wang, Z., Sowa, M. E., Zheng, L., … Shi, Y. (2012). M phase phosphorylation of the epigenetic regulator UHRF1 regulates its physical association

with the deubiquitylase USP7 and stability. *Proceedings of the National Academy of Sciences of the United States of America*, *109*(13), 4828–33.

MacDonald, J. L., & Roskams, A. J. (2008). Histone deacetylases 1 and 2 are expressed at distinct stages of neuro-glial development. *Developmental dynamics : an official publication of the American Association of Anatomists*, *237*(8), 2256–67.

Machon, O., van den Bout, C. J., Backman, M., Kemler, R., & Krauss, S. (2003). Role of β-catenin in the developing cortical and hippocampal neuroepithelium. *Neuroscience*, *122*(1), 129–143.

Mallamaci, A., Muzio, L., Chan, C. H., Parnavelas, J., & Boncinelli, E. (2000). Area identity shifts in the early cerebral cortex of Emx2-/- mutant mice [see comments]. *Nature Neuroscience*, *3*(7), 679–686.

Marín, O., Yaron, A., Bagri, A., Tessier-Lavigne, M., & Rubenstein, J. L. (2001). Sorting of striatal and cortical interneurons regulated by semaphorin-neuropilin interactions. *Science (New York, N.Y.)*, *293*(5531), 872–5.

Meilinger, D., Fellinger, K., Bultmann, S., Rothbauer, U., Bonapace, I. M., Klinkert, W. E. F., … Leonhardt, H. (2009). Np95 interacts with de novo DNA methyltransferases, Dnmt3a and Dnmt3b, and mediates epigenetic silencing of the viral CMV promoter in embryonic stem cells. *EMBO Reports*, *10*(11), 1259–1264.

Menn, B., Garcia-Verdugo, J. M., Yaschine, C., Gonzalez-Perez, O., Rowitch, D., & Alvarez-Buylla, A. (2006). Origin of oligodendrocytes in the subventricular zone of the adult brain. *Journal of Neuroscience*, *26*(30), 7907–7918.

Mercier, F., Kitasako, J. T., & Hatton, G. I. (2002). Anatomy of the brain neurogenic zones revisited: fractones and the fibroblast/macrophage network. *Journal of Comparative Neurology*, *451*(2), 170–188.

Merkle, F. T., Mirzadeh, Z., & Alvarez-Buylla, A. (2007). Mosaic organization of neural stem cells in the adult brain. *Science*, *317*(5836), 381–384.

Methot, L., Hermann, R., Tang, Y., Lo, R., Al-Jehani, H., Jhas, S., … Stifani, S. (2013). Interaction and antagonistic roles of NF-κB and Hes6 in the regulation of cortical neurogenesis. *Molecular and cellular biology*, *33*(14), 2797–808.

Ming, G., & Song, H. (2005). Adult neurogenesis in the mammalian central nervous system. *Annual Review of Neuroscience*, *28*(March), 223–250.

Ming, G.-L., & Song, H. (2011). Adult neurogenesis in the mammalian brain: significant answers and significant questions. *Neuron*, *70*(4), 687–702.

Mirzadeh, Z., Merkle, F. T., Soriano-Navarro, M., Garcia-Verdugo, J. M., & Alvarez-Buylla, A. (2008). Neural stem cells confer unique pinwheel architecture to the ventricular surface in neurogenic regions of the adult brain. *Cell stem cell*, *3*(3), 265–278.

Miyata, T, Kawaguchi, A., Okano, H., & Ogawa, M. (2001). Asymmetric inheritance of radial glial fibers by cortical neurons. *Neuron*, *31*(5), 727–741.

Miyata, Takaki, Kawaguchi, A., Saito, K., Kawano, M., Muto, T., & Ogawa, M. (2004). Asymmetric production of surface-dividing and non-surface-dividing cortical progenitor cells. *Development Cambridge England*, *131*(13), 3133–3145.

Møllgård, K., Balslev, Y., Lauritzen, B., & Saunders, N. R. (1987). Cell junctions and membrane specializations in the ventricular zone (germinal matrix) of the developing sheep brain: a CSF-brain barrier. *Journal of Neurocytology*, *16*(4), 433–444.

Molyneaux, B. J., Arlotta, P., Menezes, J. R. L., & Macklis, J. D. (2007). Neuronal subtype specification in the cerebral cortex. *Nature reviews. Neuroscience*, *8*(6), 427–37.

Montgomery, R. L., Hsieh, J., Barbosa, A. C., Richardson, J. A., & Olson, E. N. (2009). Histone deacetylases 1 and 2 control the progression of neural precursors to neurons during brain development. *Proceedings of the National Academy of Sciences of the United States of America*, *106*(19), 7876–81.

Mori, T., Buffo, A., & Götz, M. (2005). The novel roles of glial cells revisited: the contribution of radial glia and astrocytes to neurogenesis. *Current Topics in Developmental Biology*, *69*(05), 67–99.

Mori, T., Tanaka, K., Buffo, A., Wurst, W., Kühn, R., & Götz, M. (2006). Inducible gene deletion in astroglia and radial glia--a valuable tool for functional and lineage analysis. *Glia*, *54*(1), 21–34.

Mori, T., Yuxing, Z., Takaki, H., Takeuchi, M., Iseki, K., Hagino, S., … Wanaka, A. (2004). The LIM homeobox gene, L3/Lhx8, is necessary for proper development of basal forebrain cholinergic neurons. *European Journal of Neuroscience*, *19*(12), 3129–3141.

Moser, M., Binder, O., Wu, Y., Aitsebaomo, J., Ren, R., Bode, C., … Patterson, C. (2003). BMPER, a novel endothelial cell precursor-derived protein, antagonizes bone morphogenetic protein signaling and endothelial cell differentiation. *Molecular and cellular biology*, *23*(16), 5664–79.

Mousli, M., Hopfner, R., Abbady, A.-Q., Monté, D., Jeanblanc, M., Oudet, P., … Bronner, C. (2003). ICBP90 belongs to a new family of proteins with an expression that is deregulated in cancer cells. *British Journal of Cancer*, *89*(1), 120–127.

Murase, S., & Horwitz, A. F. (2002). Deleted in colorectal carcinoma and differentially expressed integrins mediate the directional migration of neural precursors in the rostral migratory stream. *Journal of Neuroscience*, *22*(9), 3568–3579.

Murciano, A., Zamora, J., López-Sánchez, J., & Frade, J. M. (2002). Interkinetic nuclear movement may provide spatial clues to the regulation of neurogenesis. *Molecular And Cellular Neurosciences*, *21*(2), 285–300.

Muto, M., Kanari, Y., Kubo, E., Takabe, T., Kurihara, T., Fujimori, A., & Tatsumi, K. (2002). Targeted disruption of Np95 gene renders murine embryonic stem cells hypersensitive to DNA damaging agents and DNA replication blocks. *The Journal of Biological Chemistry*, *277*(37), 34549–34555.

Muzio, L., & Mallamaci, A. (2003). Emx1, emx2 and pax6 in specification, regionalization and arealization of the cerebral cortex. *Cerebral Cortex*, *13*(6), 641–647.

Nady, N., Lemak, A., Walker, J. R., Avvakumov, G. V, Kareta, M. S., Achour, M., … Dhe-Paganon, S. (2011). Recognition of multivalent histone states associated with heterochromatin by UHRF1 protein. *The Journal of Biological Chemistry*, *286*(27), 24300–24311.

Nakamura, T., Colbert, M. C., & Robbins, J. (2006). Neural crest cells retain multipotential characteristics in the developing valves and label the cardiac conduction system. *Circulation research*, *98*(12), 1547–54.

Ng, K. L., Li, J.-D., Cheng, M. Y., Leslie, F. M., Lee, A. G., & Zhou, Q.-Y. (2005). Dependence of olfactory bulb neurogenesis on prokineticin 2 signaling. *Science*, *308*(5730), 1923–7.

Nguyen, L., Malgrange, B., Breuskin, I., Bettendorff, L., Moonen, G., Belachew, S., & Rigo, J.-M. (2003). Autocrine/paracrine activation of the GABA(A) receptor inhibits the proliferation of neurogenic polysialylated neural cell adhesion molecule-positive (PSA-NCAM+) precursor cells from postnatal striatum. *Journal of Neuroscience*, *23*(8), 3278–3294.

Nguyen-Ba-Charvet, K. T., Picard-Riera, N., Tessier-Lavigne, M., Baron-Van Evercooren, A., Sotelo, C., & Chédotal, A. (2004). Multiple roles for slits in the control of cell migration in the rostral migratory stream. *Journal of Neuroscience*, *24*(6), 1497–1506.

Ninkovic, J., Mori, T., & Götz, M. (2007). Distinct modes of neuron addition in adult mouse neurogenesis. *Journal of Neuroscience*, *27*(40), 10906–10911.

Ninkovic, J., Steiner-Mezzadri, A., Jawerka, M., Akinci, U., Masserdotti, G., Petricca, S., … Götz, M. (2013). The BAF complex interacts with Pax6 in adult neural progenitors to establish a neurogenic cross-regulatory transcriptional network. *Cell stem cell*, *13*(4), 403–18.

Noctor, S C, Flint, A. C., Weissman, T. A., Dammerman, R. S., & Kriegstein, A. R. (2001). Neurons derived from radial glial cells establish radial units in neocortex. *Nature*, *409*(6821), 714–20.

Noctor, Stephen C, Martínez-Cerdeño, V., Ivic, L., & Kriegstein, A. R. (2004). Cortical neurons arise in symmetric and asymmetric division zones and migrate through specific phases. *Nature Neuroscience*, *7*(2), 136–144.

Noctor, Stephen C, Martínez-Cerdeño, V., & Kriegstein, A. R. (2007). Contribution of intermediate progenitor cells to cortical histogenesis. *Archives of Neurology*, *64*(5), 639–642.

O'Leary, D. D. M., Chou, S.-J., & Sahara, S. (2007). Area patterning of the mammalian cortex. *Neuron*, *56*(2), 252–69.

O'Shea, K. S., Liu, L. H., Kinnunen, L. H., & Dixit, V. M. (1990). Role of the extracellular matrix protein thrombospondin in the early development of the mouse embryo. *The Journal of Cell Biology*, *111*(6 Pt 1), 2713–2723.

O'Shea, K. S., Rheinheimer, J. S., & Dixit, V. M. (1990). Deposition and role of thrombospondin in the histogenesis of the cerebellar cortex. *The Journal of Cell Biology*, *110*(4), 1275–1283.

Ortega, F., Costa, M. R., Simon-Ebert, T., Schroeder, T., Götz, M., & Berninger, B. (2011). Using an adherent cell culture of the mouse subependymal zone to study the behavior of adult neural stem cells on a single-cell level. *Nature protocols*, *6*(12), 1847–59.

Ortega, F., Gascón, S., Masserdotti, G., Deshpande, A., Simon, C., Fischer, J., … Berninger, B. (2013). Oligodendrogliogenic and neurogenic adult subependymal zone neural stem cells constitute distinct lineages and exhibit differential responsiveness to Wnt signalling. *Nature cell biology*, *15*(6), 602–13.

Paez-Gonzalez, P., Abdi, K., Luciano, D., Liu, Y., Soriano-Navarro, M., Rawlins, E., … Kuo, C. T. (2011). Ank3-dependent SVZ niche assembly is required for the continued production of new neurons. *Neuron*, *71*(1), 61–75.

Papait, R., Pistore, C., Grazini, U., Babbio, F., Cogliati, S., Pecoraro, D., … Bonapace, I. M. (2008). The PHD domain of Np95 (mUHRF1) is involved in large-scale reorganization of pericentromeric heterochromatin. (Y. Zheng, Ed.)*Molecular Biology of the Cell*, *19*(8), 3554–3563.

Papait, R., Pistore, C., Negri, D., Pecoraro, D., Cantarini, L., & Bonapace, I. M. (2007). Np95 is implicated in pericentromeric heterochromatin replication and in major satellite silencing. *Molecular biology of the cell*, *18*(3), 1098–106.

Paratcha, G., Ibáñez, C. F., & Ledda, F. (2006). GDNF is a chemoattractant factor for neuronal precursor cells in the rostral migratory stream. *Molecular And Cellular Neurosciences*, *31*(3), 505–14.

Pastrana, E., Cheng, L.-C., & Doetsch, F. (2009). Simultaneous prospective purification of adult subventricular zone neural stem cells and their progeny. *Proceedings of the National Academy of Sciences of the United States of America*, *106*(15), 6387–6392.

Patthey, C., & Gunhaga, L. (2014). Signaling pathways regulating ectodermal cell fate choices. *Experimental cell research*, *321*(1), 11–6.

Pilz, G.-A., Shitamukai, A., Reillo, I., Pacary, E., Schwausch, J., Stahl, R., … Götz, M. (2013). Amplification of progenitors in the mammalian telencephalon includes a new radial glial cell type. *Nature communications*, *4*, 2125.

Pinto, L., & Götz, M. (2007). Radial glial cell heterogeneity--the source of diverse progeny in the CNS. *Progress in Neurobiology*, *83*(1), 2–23.

Puelles, L., Kuwana, E., Puelles, E., Bulfone, A., Shimamura, K., Keleher, J., … Rubenstein, J. L. (2000). Pallial and subpallial derivatives in the embryonic chick and mouse telencephalon, traced by the expression of the genes Dlx-2, Emx-1, Nkx-2.1, Pax-6, and Tbr-1. *Journal of Comparative Neurology*, *424*(3), 409–438.

Purushothaman, A., Sugahara, K., & Faissner, A. (2012). Chondroitin sulfate "wobble motifs" modulate maintenance and differentiation of neural stem cells and their progeny. *The Journal of biological chemistry*, *287*(5), 2935–42.

Qin, W., Leonhardt, H., & Spada, F. (2011). Usp7 and Uhrf1 control ubiquitination and stability of the maintenance DNA methyltransferase Dnmt1. *Journal of Cellular Biochemistry*, *112*(2), 439–444.

Rajakumara, E., Wang, Z., Ma, H., Hu, L., Chen, H., Lin, Y., … Shi, Y. (2011). PHD finger recognition of unmodified histone H3R2 links UHRF1 to regulation of euchromatic gene expression. *Molecular Cell*, *43*(2), 275–284.

Ramírez-Castillejo, C., Sánchez-Sánchez, F., Andreu-Agulló, C., Ferrón, S. R., Aroca-Aguilar, J. D., Sánchez, P., … Fariñas, I. (2006). Pigment epithelium-derived factor is a niche signal for neural stem cell renewal. *Nature Neuroscience*, *9*(3), 331–339.

Regad, T., Bellodi, C., Nicotera, P., & Salomoni, P. (2009). The tumor suppressor Pml regulates cell fate in the developing neocortex. *Nature neuroscience*, *12*(2), 132–40.

Reynolds, B. A., & Weiss, S. (1992). Generation of neurons and astrocytes from isolated cells of the adult mammalian central nervous system. *Science*, *255*(5052), 1707–10.

Rhee, K.-D., Yu, J., Zhao, C. Y., Fan, G., & Yang, X.-J. (2012). Dnmt1-dependent DNA methylation is essential for photoreceptor terminal differentiation and retinal neuron survival. *Cell death & disease*, *3*, e427.

Richards, L. J., Kilpatrick, T. J., & Bartlett, P. F. (1992). De novo generation of neuronal cells from the adult mouse brain. *Proceedings of the National Academy of Sciences of the United States of America*, *89*(18), 8591–5.

Rietze, R. L., Valcanis, H., Brooker, G. F., Thomas, T., Voss, A. K., & Bartlett, P. F. (2001). Purification of a pluripotent neural stem cell from the adult mouse brain. *Nature*, *412*(6848), 736–739.

Risher, W. C., & Eroglu, C. (2012). Thrombospondins as key regulators of synaptogenesis in the central nervous system. *Matrix biology journal of the International Society for Matrix Biology*, *31*(3), 170–7.

Robel, S., Berninger, B., & Götz, M. (2011). The stem cell potential of glia: lessons from reactive gliosis. *Nature reviews. Neuroscience*, *12*(2), 88–104.

Rothbart, S B, Dickson, B. M., Ong, M. S., Krajewski, K., Houliston, S., Kireev, D. B., … Strahl, B. D. (2013). Multivalent histone engagement by the linked tandem Tudor and PHD domains of UHRF1 is required for the epigenetic inheritance of DNA methylation. *Genes Development*, *27*(11), 1288–1298.

Rothbart, Scott B, Krajewski, K., Nady, N., Tempel, W., Xue, S., Badeaux, A. I., … Strahl, B. D. (2012). Association of UHRF1 with methylated H3K9 directs the maintenance of DNA methylation. *Nature structural & molecular biology*, *19*(11), 1155–60.

Rubenstein, J. L. R. (2011). Annual Research Review: Development of the cerebral cortex: implications for neurodevelopmental disorders. *Journal of child psychology and psychiatry, and allied disciplines*, *52*(4), 339–55.

Sabatino, L., Fucci, A., Pancione, M., Carafa, V., Nebbioso, A., Pistore, C., … Colantuoni, V. (2012). UHRF1 coordinates peroxisome proliferator activated receptor gamma (PPARG) epigenetic silencing and mediates colorectal cancer progression. *Oncogene*, (January), 1–12.

Sadler, K. C., Krahn, K. N., Gaur, N. A., & Ukomadu, C. (2007). Liver growth in the embryo and during liver regeneration in zebrafish requires the cell cycle regulator, uhrf1. *Proceedings of the National Academy of Sciences of the United States of America*, *104*(5), 1570–1575.

Saghatelyan, A., De Chevigny, A., Schachner, M., & Lledo, P.-M. (2004). Tenascin-R mediates activity-dependent recruitment of neuroblasts in the adult mouse forebrain. *Nature Neuroscience*, *7*(4), 347–356.

Sanai, N., Nguyen, T., Ihrie, R. A., Mirzadeh, Z., Tsai, H.-H., Wong, M., … Alvarez-Buylla, A. (2011). Corridors of migrating neurons in the human brain and their decline during infancy. *Nature*, *478*(7369), 382–6.

Sawamoto, K., Wichterle, H., Gonzalez-Perez, O., Cholfin, J. A., Yamada, M., Spassky, N., … Alvarez-Buylla, A. (2006). New neurons follow the flow of cerebrospinal fluid in the adult brain. *Science*, *311*(5761), 629–32.

Schmidt-Supprian, M., & Rajewsky, K. (2007). Vagaries of conditional gene targeting. *Nature immunology*, *8*(7), 665–8.

Schuurmans, C., & Guillemot, F. (2002). Molecular mechanisms underlying cell fate specification in the developing telencephalon. *Current Opinion in Neurobiology*, *12*(1), 26–34.

Sen, G. L., Reuter, J. A., Webster, D. E., Zhu, L., & Khavari, P. A. (2010). DNMT1 maintains progenitor function in self-renewing somatic tissue. *Nature*, *463*(7280), 563–7.

Seri, B., García-Verdugo, J. M., McEwen, B. S., & Alvarez-Buylla, A. (2001). Astrocytes give rise to new neurons in the adult mammalian hippocampus. *Journal of Neuroscience*, *21*(18), 7153–7160.

Shahbazian, M. D., & Grunstein, M. (2007). Functions of site-specific histone acetylation and deacetylation. *Annual review of biochemistry*, *76*, 75–100.

Sharif, J., Muto, M., Takebayashi, S., Suetake, I., Iwamatsu, A., Endo, T. A., … Koseki, H. (2007). The SRA protein Np95 mediates epigenetic inheritance by recruiting Dnmt1 to methylated DNA. *Nature*, *450*(7171), 908–12.

Shen, Q., Wang, Y., Kokovay, E., Lin, G., Chuang, S.-M., Goderie, S. K., … Temple, S. (2008). Adult SVZ stem cells lie in a vascular niche: a quantitative analysis of niche cell-cell interactions. *Cell stem cell*, *3*(3), 289–300.

Shihabuddin, L. S., Horner, P. J., Ray, J., & Gage, F. H. (2000). Adult spinal cord stem cells generate neurons after transplantation in the adult dentate gyrus. *The Journal of neuroscience : the official journal of the Society for Neuroscience*, *20*(23), 8727–35.

Shimamura, K., Martinez, S., Puelles, L., & Rubenstein, J. L. (1997). Patterns of gene expression in the neural plate and neural tube subdivide the embryonic forebrain into transverse and longitudinal domains. *Developmental Neuroscience*, *19*(1), 88–96.

Shitamukai, A., Konno, D., & Matsuzaki, F. (2011). Oblique radial glial divisions in the developing mouse neocortex induce self-renewing progenitors outside the germinal zone that resemble primate outer subventricular zone progenitors. *Journal of Neuroscience*, *31*(10), 3683–3695.

Shoukimas, G. M., & Hinds, J. W. (1978). The development of the cerebral cortex in the embryonic mouse: an electron microscopic serial section analysis. *The Journal of comparative neurology*, *179*(4), 795–830.

Siegenthaler, J. A., Tremper-Wells, B. A., & Miller, M. W. (2008). Foxg1 haploinsufficiency reduces the population of cortical intermediate progenitor cells: effect of increased p21 expression. *Cerebral cortex (New York, N.Y. : 1991)*, *18*(8), 1865–75.

Simon, C., Götz, M., & Dimou, L. (2011). Progenitors in the adult cerebral cortex: cell cycle properties and regulation by physiological stimuli and injury. *Glia*, *59*(6), 869–81.

Singh, R. P., Shiue, K., Schomberg, D., & Zhou, F. C. (2009). Cellular epigenetic modifications of neural stem cell differentiation. *Cell transplantation*, *18*(10), 1197–211.

Sirko, S., Behrendt, G., Johansson, P. A., Tripathi, P., Costa, M., Bek, S., … Götz, M. (2013). Reactive glia in the injured brain acquire stem cell properties in response to sonic hedgehog. [corrected]. *Cell stem cell*, *12*(4), 426–39.

Sirko, S., von Holst, A., Weber, A., Wizenmann, A., Theocharidis, U., Götz, M., & Faissner, A. (2010). Chondroitin sulfates are required for fibroblast growth factor-2-dependent

proliferation and maintenance in neural stem cells and for epidermal growth factor-dependent migration of their progeny. *Stem cells (Dayton, Ohio)*, *28*(4), 775–87.

Skarnes, W. C., Rosen, B., West, A. P., Koutsourakis, M., Bushell, W., Iyer, V., … Bradley, A. (2011). A conditional knockout resource for the genome-wide study of mouse gene function. *Nature*, *474*(7351), 337–42.

Snapyan, M., Lemasson, M., Brill, M. S., Blais, M., Massouh, M., Ninkovic, J., … Saghatelyan, A. (2009). Vasculature guides migrating neuronal precursors in the adult mammalian forebrain via brain-derived neurotrophic factor signaling. *The Journal of neuroscience : the official journal of the Society for Neuroscience*, *29*(13), 4172–88.

Spalding, K. L., Bergmann, O., Alkass, K., Bernard, S., Salehpour, M., Huttner, H. B., … Frisén, J. (2013). Dynamics of hippocampal neurogenesis in adult humans. *Cell*, *153*(6), 1219–27.

Spassky, N., Merkle, F. T., Flames, N., Tramontin, A. D., García-Verdugo, J. M., & Alvarez-Buylla, A. (2005). Adult ependymal cells are postmitotic and are derived from radial glial cells during embryogenesis. *Journal of Neuroscience*, *25*(1), 10–18.

Stancik, E. K., Navarro-Quiroga, I., Sellke, R., & Haydar, T. F. (2010). Heterogeneity in ventricular zone neural precursors contributes to neuronal fate diversity in the postnatal neocortex. *The Journal of neuroscience : the official journal of the Society for Neuroscience*, *30*(20), 7028–36.

Stenina, O. I., Topol, E. J., & Plow, E. F. (2007). Thrombospondins, their polymorphisms, and cardiovascular disease. *Arteriosclerosis thrombosis and vascular biology*, *27*(9), 1886–1894.

Stoykova, A., Treichel, D., Hallonet, M., & Gruss, P. (2000). Pax6 modulates the dorsoventral patterning of the mammalian telencephalon. *Journal of Neuroscience*, *20*(21), 8042–8050.

Suh, H., Consiglio, A., Ray, J., Sawai, T., D'Amour, K. A., & Gage, F. H. (2007). In vivo fate analysis reveals the multipotent and self-renewal capacities of Sox2+ neural stem cells in the adult hippocampus. *Cell stem cell*, *1*(5), 515–528.

Sussel, L., Marin, O., Kimura, S., & Rubenstein, J. L. (1999). Loss of Nkx2.1 homeobox gene function results in a ventral to dorsal molecular respecification within the basal telencephalon: evidence for a transformation of the pallidum into the striatum. *Development Cambridge England*, *126*(15), 3359–3370.

Takahashi, H., & Liu, F.-C. (2006). Genetic patterning of the mammalian telencephalon by morphogenetic molecules and transcription factors. *Birth defects research. Part C, Embryo today : reviews*, *78*(3), 256–66. Takahashi, T., Misson, J. P., & Caviness, V. S. (1990). Glial process elongation and branching in the developing murine neocortex: a qualitative and quantitative immunohistochemical analysis. *Journal of Comparative Neurology*, *302*(1), 15–28.

Takahashi, T., Nowakowski, R. S., & Caviness, V. S. (1996). Interkinetic and migratory behavior of a cohort of neocortical neurons arising in the early embryonic murine cerebral wall. *Journal of Neuroscience*, *16*(18), 5762–5776.

Takeichi, M. (2007). The cadherin superfamily in neuronal connections and interactions. *Nature reviews. Neuroscience*, *8*(1), 11–20.

Tan, S.-L., Nishi, M., Ohtsuka, T., Matsui, T., Takemoto, K., Kamio-Miura, A., … Kageyama, R. (2012). Essential roles of the histone methyltransferase ESET in the epigenetic control of neural progenitor cells during development. *Development (Cambridge, England)*, *139*(20), 3806–16.

Tavazoie, M., Van Der Veken, L., Silva-Vargas, V., Louissaint, M., Colonna, L., Zaidi, B., … Doetsch, F. (2008). A specialized vascular niche for adult neural stem cells. *Cell stem cell*, *3*(3), 279–288.

Tien, A. L., Senbanerjee, S., Kulkarni, A., Mudbhary, R., Goudreau, B., Ganesan, S., … Ukomadu, C. (2011). UHRF1 depletion causes a G2/M arrest, activation of DNA damage response and apoptosis. *The Biochemical journal*, *435*(1), 175–185.

Tittle, R. K., Sze, R., Ng, A., Nuckels, R. J., Swartz, M. E., Anderson, R. M., … Gross, J. M. (2011). Uhrf1 and Dnmt1 are required for development and maintenance of the zebrafish lens. *Developmental Biology*, *350*(1), 50–63.

Toresson, H., Potter, S. S., & Campbell, K. (2000). Genetic control of dorsal-ventral identity in the telencephalon: opposing roles for Pax6 and Gsh2. *Development Cambridge England*, *127*(20), 4361–4371.

Tucker, R. P., Adams, J. C., & Lawler, J. (1995). Thrombospondin-4 is expressed by early osteogenic tissues in the chick embryo. *Developmental dynamics an official publication of the American Association of Anatomists*, *203*(4), 477–490.

Unoki, M, Daigo, Y., Koinuma, J., Tsuchiya, E., Hamamoto, R., & Nakamura, Y. (2010). UHRF1 is a novel diagnostic marker of lung cancer. *British Journal of Cancer*, *103*(2), 217–222.

Unoki, M, Kelly, J. D., Neal, D. E., Ponder, B. A. J., Nakamura, Y., & Hamamoto, R. (2009). UHRF1 is a novel molecular marker for diagnosis and the prognosis of bladder cancer. *British Journal of Cancer*, *101*(1), 98–105.

Unoki, Motoko, Nishidate, T., & Nakamura, Y. (2004). ICBP90, an E2F-1 target, recruits HDAC1 and binds to methyl-CpG through its SRA domain. *Oncogene*, *23*(46), 7601–7610.

Ventura, R. E., & Goldman, J. E. (2007). Dorsal radial glia generate olfactory bulb interneurons in the postnatal murine brain. *Journal of Neuroscience*, *27*(16), 4297–4302.

Wang, Chengkun, Shen, J., Yang, Z., Chen, P., Zhao, B., Hu, W., … Cao, C. (2011). Structural basis for site-specific reading of unmodified R2 of histone H3 tail by UHRF1 PHD finger. *Cell research*, *21*(9), 1379–82.

Wang, Congmin, Liu, F., Liu, Y.-Y., Zhao, C.-H., You, Y., Wang, L., … Yang, Z. (2011). Identification and characterization of neuroblasts in the subventricular zone and rostral migratory stream of the adult human brain. *Cell research*, *21*(11), 1534–50.

Wang, F., Yang, Y.-Z., Shi, C.-Z., Zhang, P., Moyer, M. P., Zhang, H.-Z., … Qin, H.-L. (2012). UHRF1 promotes cell growth and metastasis through repression of p16(ink^{4}a) in colorectal cancer. *Annals of surgical oncology*, *19*(8), 2753–62.

Wang, X., Tsai, J.-W., LaMonica, B., & Kriegstein, A. R. (2011). A new subtype of progenitor cell in the mouse embryonic neocortex. *Nature Neuroscience*, *14*(5), 555–561.

Weigmann, A., Corbeil, D., Hellwig, A., & Huttner, W. B. (1997). Prominin, a novel microvilli-specific polytopic membrane protein of the apical surface of epithelial cells, is targeted to plasmalemmal protrusions of non-epithelial cells. *Proceedings of the National Academy of Sciences of the United States of America*, *94*(23), 12425–12430.

Weinandy, F., Ninkovic, J., & Götz, M. (2011). Restrictions in time and space--new insights into generation of specific neuronal subtypes in the adult mammalian brain. *European Journal of Neuroscience*, *33*(6), 1045–1054.

Willaime-Morawek, S., Seaberg, R. M., Batista, C., Labbé, E., Attisano, L., Gorski, J. A., … Van Der Kooy, D. (2006). Embryonic cortical neural stem cells migrate ventrally and persist as postnatal striatal stem cells. *The Journal of Cell Biology*, *175*(1), 159–168.

Wodarz, A., & Huttner, W. B. (2003). Asymmetric cell division during neurogenesis in Drosophila and vertebrates. *Mechanisms of Development*, *120*(11), 1297–1309.

Wojcik-Stanaszek, L., Gregor, A., & Zalewska, T. (2011). Regulation of neurogenesis by extracellular matrix and integrins. *Acta neurobiologiae experimentalis*, *71*(1), 103–12.

Wu, H., Coskun, V., Tao, J., Xie, W., Ge, W., Yoshikawa, K., … Sun, Y. E. (2010). Dnmt3a-dependent nonpromoter DNA methylation facilitates transcription of neurogenic genes. *Science (New York, N.Y.)*, *329*(5990), 444–8.

Wurst, W., & Bally-Cuif, L. (2001). Neural plate patterning: upstream and downstream of the isthmic organizer. *Nature Reviews Neuroscience*, *2*(2), 99–108.

Xie, S., Jean, J., & Qian, C. (2012). UHRF1 Double Tudor Domain and the Adjacent PHD Finger Act Together to Recognize K9me3-Containing Histone H3 Tail. *Journal of Molecular Biology*, *415*(2), 318–28.

Yamada, S., Pokutta, S., Drees, F., Weis, W. I., & Nelson, W. J. (2005). Deconstructing the cadherin-catenin-actin complex. *Cell*, *123*(5), 889–901.

Yan, F., Tan, X.-Y., Geng, Y., Ju, H.-X., Gao, Y.-F., & Zhu, M.-C. (2011). Inhibition effect of siRNA-downregulated UHRF1 on breast cancer growth. *Cancer biotherapy radiopharmaceuticals*, *26*(2), 183–189.

Yang, P., Guo, L., Duan, Z. J., Tepper, C. G., Xue, L., Chen, X., … Chen, H.-W. (2012). Histone methyltransferase NSD2/MMSET mediates constitutive NF-κB signaling for cancer cell proliferation, survival, and tumor growth via a feed-forward loop. *Molecular and cellular biology*, *32*(15), 3121–31.

Yoshida, M., Suda, Y., Matsuo, I., Miyamoto, N., Takeda, N., Kuratani, S., & Aizawa, S. (1997). Emx1 and Emx2 functions in development of dorsal telencephalon. *Development Cambridge England*, *124*(1), 101–111.

Young, K. M., Fogarty, M., Kessaris, N., & Richardson, W. D. (2007). Subventricular zone stem cells are heterogeneous with respect to their embryonic origins and neurogenic fates in the adult olfactory bulb. *Journal of Neuroscience*, *27*(31), 8286–8296.

Yun, K., Potter, S., & Rubenstein, J. L. (2001). Gsh2 and Pax6 play complementary roles in dorsoventral patterning of the mammalian telencephalon. *Development Cambridge England*, *128*(2), 193–205.

Zhang, J., Gao, Q., Li, P., Liu, X., Jia, Y., Wu, W., … Wong, J. (2011). S phase-dependent interaction with DNMT1 dictates the role of UHRF1 but not UHRF2 in DNA methylation maintenance. *Cell Research*, *21*(12), 1723–39.

Zhang, Y., & Hu, W. (2012). NFκB signaling regulates embryonic and adult neurogenesis. *Frontiers in biology*, *7*(4).

Zhao, Y., Marín, O., Hermesz, E., Powell, A., Flames, N., Palkovits, M., … Westphal, H. (2003). The LIM-homeobox gene Lhx8 is required for the development of many cholinergic neurons in the mouse forebrain. *Proceedings of the National Academy of Sciences of the United States of America*, *100*(15), 9005–9010.

Zhou, Q., Dalgard, C. L., Wynder, C., & Doughty, M. L. (2011). Histone deacetylase inhibitors SAHA and sodium butyrate block G1-to-S cell cycle progression in neurosphere formation by adult subventricular cells. *BMC neuroscience*, *12*(1), 50.

Zimmermann, D. R., & Dours-Zimmermann, M. T. (2008). Extracellular matrix of the central nervous system: from neglect to challenge. *Histochemistry and cell biology*, *130*(4), 635–53.

9. Curriculum Vitae

PERSONAL DETAILS

Date of birth   : 02.06.1985

Gender   : Female

Nationality   : Turkish

EDUCATION

2007–present — International Max Planck Research School for Molecular and Cellular Life Sciences (IMPRS-LS) and Graduate School of Systemic Neurosciences (GSN-LMU), Munich, Germany

2003 – 2007 — Middle East Technical University (METU), Faculty of Art and Sciences, Turkey. Bc.S in Molecular Biology and Genetics

ACADEMIC POSITIONS

2013 July – present — Postdoctoral Fellow, Molecular Biology and Genetics Department, Koc University, Istanbul, Turkey. (Asst. Prof. Gulayse Ince-Dunn's Lab)

2008 – 2013 June — Graduate Student, Helmholtz Zentrum Munchen German Research Center for Environmental Health (GmbH) Institute of Stem Cell Research, Neuherberg, Germany. (Prof. Dr. Magdalena Götz's Lab)

2005 – 2007 — Undergraduate Research Student, Middle East Technical University, Ankara, Turkey. (Prof. Dr. Vasıf Hasırcı's Lab)

2006 June – 2006 Sep	Research Trainee, University of California, LosAngales, David Geffen School of Medicine, Los Angales, USA. (Prof. Dr. Yi Eve Sun's Lab)
2006 Jan – 2006 March	Research Trainee, Max-Planck Institute of Biophysical Chemistry, Department of Genes and Development, Gottingen, Germany. (Prof. Dr. Gregor Eichele's Lab)

PUBLICATIONS

Beckervordersandforth R, Tripathi P, Ninkovic J, **Bayam E**, Lepier A, Stempfhuber B, Kirchhoff F, Hirrlinger J, Haslinger A, Lie DC, Beckers J, Yoder B, Irmler M,Götz M. (2010) In vivo fate mapping and expression analysis reveals molecular hallmarks of prospectively isolated adult neural stem cells. Cell Stem Cell. 2010 Dec 3; 7(6):744-58.

POSTER PRESENTATIONS

Bavarian Research Association for Neural Stem Cells, ForNeuroCell II Meeting, Munich, 2013.Title: The role of Uhrf1 in adult and embryonic neurogenesis.

8th FENS Forum of Neuroscience Satellite Event - Regulation of adult neurogenesis: from epigenetics to behavior, Barcelona, 2012. Title: The role of Uhrf1 in adult neurogenesis in Subependymal Zone and Dentate Gyrus

International Society for Stem Cell Research (ISSCR) Annual Meeting, San Francisco, 2010. Title: Prospective Isolation of Adult Mouse Neural Stem Cells Reveals New Insights into Their Identity and Factors Regulating Neural Stem Cell Fate and Renewal

10. Affidavit

Eidesstattliche Versicherung/Affidavit

Hiermit versichere ich an Eides statt, dass ich die vorliegende Dissertation
"Transcriptome analysis of adult neural stem cells and functional analysis of novel candidate genes TSP-4 and Uhrf1" selbstständig angefertigt habe, mich außer der angegebenen keinerweiteren Hilfsmittel bedient und alle Erkenntnisse, die aus dem Schrifttum ganz oderannähernd übernommen sind, als solche kenntlich gemacht und nach ihrer Herkunft unterBezeichnung der Fundstelle einzeln nachgewiesen habe.

I hereby confirm that the dissertation "Transcriptome analysis of adult neural stem cells and functional analysis of novel candidate genes TSP-4 and Uhrf1" is the result of my own work and that I have only used sources or materials listed and specified in the dissertation.

München, 24.04.2014
Munich, 24.04.2014   Efil Bayam

List of Contributions

The following people contributed materials or raw data to this work.

Asst. Prof. Dr. Cagla Eroglu kindly provided the TSP-4 null and heterozygous brains used for the analysis of neurogenesis upon TSP-4 deletion (Fig.16-18). **PD. Dr. Frank Zaucke** kindly provided the TSP-4 antibody (used in Fig.14) and **Dr. Fabio Spada** and **Asst. Prof. Dr. Ian Marc Bonapace** kindly provided the Uhrf1 antibody (used in Fig 21-23, 26, 35-37). **Dr. Christiane Simon** provided the injured brain sections used for the analysis of Uhrf1 protein after injury (Fig.23). **Emily Violette Baumgart** performed amplification of RNAs and preparation of cDNAs for hybridization of Uhrf1 heterozygous and cKO samples to Affymetrix Gene ST 1.0 arrays and **Dr. Martin Irmler** performed the analysis of microarray data upon Uhrf1 deletion in the developing cerebral cortex (Fig.47 and Tables 1-2).

Munich, 24.04.2014

Efil Bayam   Prof. Dr. Magdalena Götz